

ISSN 1028-2335

*№1*  
*(146)*  
**2025**

# ТЕОРІЯ І ПРАКТИКА МЕТАЛУРГІЇ

## THEORY AND PRACTICE OF METALLURGY

Ювілейний випуск. 100 років кафедри  
Електрометалургії ім. академіка М. І. Гасика



# ТЕОРІЯ І ПРАКТИКА МЕТАЛУРГІЇ

*№1*  
*(146)*  
2025

НАУКОВО-ВИРОБНИЧИЙ ЖУРНАЛ

Видається з березня 1997 року  
Виходить 4 рази на рік

**Засновники:** Український державний університет науки і технологій  
Відділення матеріалознавства та металургії  
Академії інженерних наук України

**Видавець:** Український державний університет науки і технологій

Дніпро  
2025

# THEORY AND PRACTICE OF METALLURGY

*No. 1*  
*(146)*  
2025

SCIENTIFIC AND PRODUCTION JOURNAL

Issued since March 1997  
Released 4 times a year

**Founders:** Ukrainian State University of Science and Technologies  
Department of Materials Science and Metallurgy  
Of the Academy of Engineering Sciences of Ukraine

**Publisher:** Ukrainian State University of Science and Technologies

Dnipro  
2025

Журнал зареєстровано в Національній раді України з питань телебачення і радіомовлення як друковане медіа. Рішення № 924 від 28.09.2023. Ідентифікатор медіа: R30-01392.

Наказом Міністерства освіти і науки України №157 від 09.02.2021 р. журнал включено до категорії «Б» переліку наукових фахових видань України за спеціальностями:

133 – Галузеве машинобудування;

136 – Металургія;

161 – Хімічні технології

## РЕДАКЦІЙНА КОЛЕГІЯ

**Головний редактор – Пройдак Ю.С.**, д.т.н., проф., Український державний університет науки і технологій, Україна

**Заступник головного редактора – Камкіна Л.В.**, д.т.н., проф., Український державний університет науки і технологій, Україна

**Баюл К.В.**, д.т.н., проф., Інститут чорної металургії ім. З. І. Некрасова НАН України, Україна

**Білодіденко С.В.**, д.т.н., проф., Український державний університет науки і технологій, Україна

**Єрємін О.О.**, д.т.н., проф., Український державний університет науки і технологій, Україна

**Зайчук О.В.**, д.т.н., проф., Український державний університет науки і технологій, Україна

**Засельський В.Й.**, д.т.н., проф., Державний університет економіки і технологій, Україна

**Малий Є.І.**, д.т.н., проф., Український державний університет науки і технологій, Україна

**Сухий К.М.**, чл.-кор. НАН України, д.т.н., проф., Український державний університет науки і технологій, Україна

**Сігарьов Є.М.**, д.т.н., проф., Дніпровський державний технічний університет, Україна

**ZhouHua J.**, Doctor of Technical Sciences, Professor, School of Metallurgy, Northeastern University, Liaoning, China

**Karbowniczek M.**, Professor, Dept. of Metal Engineering and Industrial Computer Science, AGH University of Science & Technology, Krakow, Poland

**Gasik M.M.**, Doctor of Technical Sciences, Professor, Aalto University Foundation, Espoo, Finland

**Sladkovskiy A.V.**, Doctor of Technical Sciences, Professor, Poland

**Stovpchenko G.P.**, Doctor of Technical Sciences, Professor, Tianjin Heavy Industry research and Development Co, Ltd, Tianjin, China

**Medovar L.B.**, Doctor of Technical Sciences, Professor, Tianjin Heavy Industry research and Development Co, Ltd, Tianjin, China

**Lezhnev S.N.**, Doctor of Technical Sciences, Professor, Rudny Industrial Institute, Rudny, Kazakhstan

**Volkova O.**, Technische Universität Bergakademie Freiberg, Freiberg, Germany

Матеріали публікуються мовою оригіналу та ліцензуються відповідно до [Creative Commons Attribution 4.0 International \(CC BY 4.0\)](https://creativecommons.org/licenses/by/4.0/).

Автори зберігають авторські права на опубліковані статті та надають видавцеві невиключне право на публікацію статті з посиланням на нього, як на оригінального видавця, у разі повторного використання, а також на розповсюдження статті у будь-якій формі та на будь-яких носіях.

Автори можуть укладати окремі додаткові договори про невиключне поширення опублікованої статті (наприклад, розміщення її в інституційному репозитарії або публікація в книзі) із зазначенням її первинної публікації в цьому журналі з обов'язковим зазначенням doi статті.



The Journal is registered as a print media outlet by the National Council of Television and Radio Broadcasting of Ukraine. Decision No. 924, dated September 28, 2023. Media Identifier: R30-01392.

By the order of the Ministry of Education and Science of Ukraine No. 157 from 09.02.2021 p. the journal is included in category "B" of the list of scientific professional publications of Ukraine, by specialties:

133 - Industry engineering;  
136 - Metallurgy;  
161 - Chemical technologies

#### EDITORIAL BOARD

**Editor in Chief – Proidak Yu.S.**, D. Sc. (Tech.), Professor, Ukrainian State University of Science and Technologies, Ukraine

**Deputy Editor-in-Chief – Kamkina L.V.**, D. Sc. (Tech.), Professor, Ukrainian State University of Science and Technologies, Ukraine

**Baiul K.V.**, D. Sc. (Tech.), Professor, Iron and Steel Institute of Z. I. Nekrasov National Academy of Sciences of Ukraine, Ukraine

**Bilodidenko S.V.**, D. Sc. (Tech.), Professor, Ukrainian State University of Science and Technologies, Ukraine

**Yeromin O.O.**, D. Sc. (Tech.), Professor, Ukrainian State University of Science and Technologies, Ukraine

**Zaichuk O.V.**, D. Sc. (Tech.), Professor, Ukrainian State University of Science and Technologies, Ukraine

**Zaselskyi V.Y.**, D. Sc. (Tech.), Professor, State University of Economics and Technologies, Ukraine

**Malyi E.I.**, D. Sc. (Tech.), Professor, Ukrainian State University of Science and Technologies, Ukraine

**Sukhyi K.M.**, Corresponding Member of the National Academy of Sciences of Ukraine, D. Sc. (Tech.), Professor, Ukrainian State University of Science and Technologies, Ukraine

**Siharov Ye.M.**, D. Sc. (Tech.), Professor, Dniprovskiy State Technical University, Ukraine

**ZhouHua J.**, Doctor of Technical Sciences, Professor, School of Metallurgy, Northeastern University, Liaoning, China

**Karbowiczek M.**, Professor, Dept. of Metal Engineering and Industrial Computer Science, AGH University of Science & Technology, Krakow, Poland

**Gasik M.M.**, Doctor of Technical Sciences, Professor, Aalto University Foundation, Espoo, Finland

**Sladkovskiy A.V.**, Doctor of Technical Sciences, Professor, Poland

**Stovpchenko G.P.**, Doctor of Technical Sciences, Professor, Tianjin Heavy Industry research and Development Co, Ltd, Tianjin, China

**Medovar L.B.**, Doctor of Technical Sciences, Professor, Tianjin Heavy Industry research and Development Co, Ltd, Tianjin, China

**Lezhnev S.N.**, Doctor of Technical Sciences, Professor, Rudny Industrial Institute, Rudny, Kazakhstan

**Volkova O.**, Technische Universität Bergakademie Freiberg, Freiberg, Germany

Articles are published in their original language and licensed under [Creative Commons Attribution 4.0 International \(CC BY 4.0\)](https://creativecommons.org/licenses/by/4.0/).

Authors retain copyright of the published papers and grant to the publisher the non-exclusive right to publish the article, to be cited as its original publisher in case of reuse, and to distribute it in all forms and media.

Authors can enter the separate, additional contractual arrangements for non-exclusive distribution of the published paper (e.g., post it to an institutional repository or publish it in a book), with an indication of its primary publication in this journal and the mandatory indication of the article's doi.

*Sukhyy K.M., Proidak Yu.S.*

## On the 100th Anniversary of the Department of Electrometallurgy

*Сухий К.М., Проїдак Ю.С.*

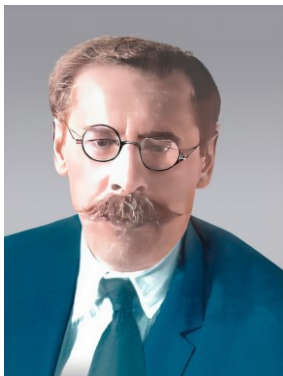
### До 100-річчя кафедри електрометалургії

**Abstract.** The article reflects the origin and development of the electrometallurgical industry in Ukraine. The emphasis is placed on the role of the Department of Electrometallurgy at the Dnipro Metallurgical Institute in this process. The Department of Electrometallurgy was established in 1925. This was facilitated by the leading role of scientists, professors, doctors of technical sciences Telnyi S. I., Khytryk S. Y., Hasyk M. I., who made a significant contribution to the development of the electrometallurgical industry in Ukraine and the training of highly qualified specialists. In the article, the key stages of formation and development of electrometallurgy have been outlined, and the crucial role of scientists and teachers of the Department has been stated.

**Key words:** electrometallurgy of steel and ferroalloys, abrasive and carbon-containing materials, non-ferrous metallurgy.

**Анотація.** В статті висвітлено походження та розвиток електрометалургійної галузі в Україні. Акцент зроблено на ролі кафедри електрометалургії Дніпровського металургійного інституту в цьому процесі. Кафедра електрометалургії була заснована у 1925 році. Цьому сприяла провідна роль вчених, професорів, докторів технічних наук Тельного С.І., Хитрика С.І., Гасика М.І., які зробили значний внесок у розвиток електрометалургійної промисловості України та підготовку висококваліфікованих фахівців. В статті окреслено ключові етапи становлення та розвитку електрометалургії, а також визначено вирішальну роль вчених і викладачів кафедри.

**Ключові слова:** електрометалургія сталі та феросплавів, абразивні та вуглецевмісні матеріали, кольорова металургія.



Telnyi S.I.



Khytryk S.Y.



Hasyk M.I.

The Department of Electrometallurgy was organized as part of the Katerynoslav Mining School.

At the opening of the school in 1899, its faculty numbered 13 members. It should be noted that in the early years of the Katerynoslav Higher Mining School there were no departments as such, in the school there were two divisions – Mining and Factory – where the so-called cabinet system of education was implemented [1]. Mykhailo Oleksandrovych Pavlov, a graduate of the St. Petersburg Mining Institute and a metallurgical engineer, was invited to serve as Head of the Factory Department of the school and the full professor

of metallurgy. By that time, he had established himself as a highly qualified and creative specialist.

Before that, he had been sent to a number of European enterprises to study industrial experience. In 1893, he visited Berlin, Paris, London, Milan, Venice and Vienna and familiarized himself with the work of Swedish metallurgical plants. This trip significantly enriched M.A. Pavlov as an engineer and metallurgical specialist.

Thus, M. A. Pavlov laid the foundation for metallurgical education in Katerynoslav and in Ukraine as a whole [2]. From the very first years of training specialists, the school paid great attention to chemical



education, realizing that metallurgy was high-temperature chemistry.

In 1900, the board of the school elected the renowned scientist P. H. Rubin as the head of the metallurgy cabinet.

At the beginning of 1905, he was appointed as Acting Extraordinary Professor. He gave lectures on pig iron metallurgy, fuels, non-ferrous metallurgy, and metallography, as well as supervised graduates' theses.

As part of the steel metallurgy course in 1917, a section on electrometallurgy was introduced, focusing on metal smelting in electric arc furnaces. Stepan Ivanovych Telnyi was the founder of this course and the first lecturer. He graduated from the Factory division in 1914 and was retained as a scholarship holder to continue his research work. Under his active involvement and guidance, an electrometallurgical laboratory was established, where he, together with Professor H. Ye. Yevreinov developed the first electric steelmaking furnace with a rotating voltaic arc. In 1920, he was appointed Assistant Professor of this department, and from January 1, 1925 he became a Professor and head of the first in the country Department of Electrometallurgy. It should be said that at that time there was no research on the application of electricity in metallurgy for metal smelting in the country at all, so S. I. Telnyi is rightfully considered the founder of the national scientific school of electrometallurgy.

The first records of electric steelmaking in Ukraine date back to 1913. The Novokonstantynivka and Makiivka steel plants each had one electric furnace with a capacity of 0.5 tons.

The introduction of electric steelmaking gave impetus to the development of electric furnace construction in various regions of the Russia of that time. Ukrainian scientists were at the forefront of this process, including the first head of the Department of Electrometallurgy at the Dnipro Metallurgical Institute, Doctor of Technical Sciences, Professor, Honored Worker of Science and Technology Stepan Ivanovych Telnyi (1890-1962).

His 1914 diploma project on electrometallurgy was awarded a prize by the Council of the Mining Institute, which decided to retain S. I. Telnyi at the Department of Metallurgy to prepare him for teaching and research as a professor's scholarship holder. Already in those years, the young scientist demonstrated his wide range of knowledge. In 1914, together with Professor of Chemistry L. V. Pisarzhevskiy, he published an article on electrochemistry entitled "Electrolytic Method of Obtaining Solid Iodine from Solution." Later, S. I. Telnyi devoted himself to the development of electrometallurgical furnaces, which was greatly facilitated by a research trip to the Kyiv Polytechnic Institute (KPI), where he worked under the supervision of Professor V. P. Izhevskiy.

Such rapid career growth was facilitated by outstanding scientific achievements. In 1919, the first arc steelmaking furnaces designed by H. S. Yevreinov and S. I. Telnyi were installed in the Katerynoslav

railway workshops and at the metallurgical plant in Katerynoslav. The results of the furnaces' operation were successful.

As noted in the book "The Development of Electrothermal Engineering," S. I. Telnyi's idea attracted attention of many scientists, along with L. I. Morozenskiy's invention of a device for arc control and simultaneous metal stirring. On this basis, in the 1940s, devices for electromagnetic stirring of liquid metal in electric furnaces were developed in Sweden, which were used for several decades to equip most large arc furnaces.

The staff of the Department was gaining recognition within the scientific community, and new young engineers joined the Department. In 1924, the Central District Electrotechnical Trust established a group at the Kharkiv Electromechanical Plant to organize the production of domestic electric furnaces, headed by electrometallurgist L. I. Aronov and designer A. P. Ionov. In the history of electrothermal technology development, 1925 was marked as the year of creation of the first industrial electric steelmaking furnace designed by L. I. Aronov and A. P. Ionov with a transformer capacity of 2000 kW and a capacity of 250 kg, which was characterized by more advanced technical solutions compared to foreign models. In 1926, the German company AEG purchased licenses from the State Electrotechnical Trust for the right to construct such furnaces in Europe.

Starting from 1925, the need arose for rapid development of steel electrometallurgy and its quality basis, the electro-ferroalloy industry. In the early 20s, there were only a few ferroalloy furnaces with a capacity of 280-1000 kV-A for the production of ferrosilicon and ferrochromium, so there was a need to further develop the domestic ferroalloy industry.

At this time, in 1926, Spirydon Yosypovych Khytryk (1895-1980), the future patriarch of the Ukrainian scientific school of ferroalloy production, Honored Worker of Science and Technology of the Ukrainian SSR, Professor, Doctor of Technical Sciences, graduated from the Mining Institute with a degree in Electrometallurgy of Steel and Ferroalloys.

For his excellent academic performance and successful defense of his diploma project in electrometallurgy, after graduating from the institute in 1926, S. Y. Khytryk was invited to take the position of assistant at the Department of Electrometallurgy at the Dnipropetrovsk Mining Institute. In connection with the separation of the metallurgical faculty of the Dnipropetrovsk Mining Institute into an independent multidisciplinary Dnipropetrovsk Metallurgical Institute (DMetI) in 1930, S. Y. Khytryk transferred to DMetI initially as an assistant and then as an associate professor at the Department of Electrometallurgy. At the same time, he was engaged in extensive social and scientific work. From 1932, he worked for eight years in the editorial office of the journals "Robochyi Metalurh", "Domez" and "Theory and Practice of Metallurgy" as a scientific secretary, deputy editor, and editor-in-chief. Notably, the journal "Theory and Practice of Metallurgy" is the

oldest scientific publication of the Ukrainian metallurgical industry, having been published since 1928.

In 1930, Mykola Makarovych Chuyko, a graduate of the Minsk Polytechnic Institute, joined the Department and later became a leading scientist in the field of steel electrometallurgy. At that time, S. I. Telnyi was appointed Dean of the Metallurgical Faculty and a design consultant at Dnipro Industrial Complex, and the Department of Electrometallurgy became a truly national center for training electrometallurgical specialists.

Graduates of the Department of Electrometallurgy of DMetI stood at the origins of the formation and development of domestic electrometallurgy, including the Ukraine's first electrometallurgical enterprises – Dniprostal (now Dneprospeysstal) and a ferroalloy plant in Zaporizhzhia.

In 1925, a group of metallurgists working on the problem of Dniprobud as part of a commission headed by I. H. Oleksandrov put forward a project to organize and construct a ferroalloy plant in Zaporizhzhia (formerly Oleksandrivsk) utilizing the low-cost electricity from the Dnipro hydroelectric power station.

Since 1928, and more specifically with the construction of the Dnipro hydroelectric power station, the steel and ferroalloys industry began to emerge as an independent sub-industry. During the first five-year plan (1928-1932), two electric arc steelmaking furnaces were put into operation at the Dneprostal plant (since 1939, Dneprospeysstal, Zaporizhzhia), along with two ore-reduction ferroalloy electric furnaces at Zaporizhzhia Ferroalloy Plant.

The first foundation of Dniprostal (now Dneprospeysstal, Zaporizhzhia) was laid on April 22, 1931, and on October 10, 1932, on the day of the ceremonial opening of the Dnipro hydroelectric power station, the first smelting was produced using Dnipro power.

From the first years of the plant's operation, the scientific research conducted by the Department and its graduates has been related to the development of various steel grades, improvement of existing technological processes, development of theoretical foundations and deepening of the theory of deoxidation, refining, and alloying of a wide range of electrometallurgical steels. An outstanding metallurgical scientist, Doctor of Technical Sciences, Professor M. M. Chuyko was always at the head of most of these developments. His contribution to the formation and development of Ukrainian electric steelmaking science and technology is invaluable. The beginning of his scientific career coincided with the first years of operation of the first Ukrainian specialized steel production plant – Dneprospeysstal. M. M. Chuyko dedicated nearly his entire life to the establishment and development of scientific research and the improvement of technological processes at this enterprise.

Other electrothermal production facilities were established on the basis of the Dnipro hydroelectric power station. In 1932, the construction of the Dnipro Aluminum Plant, consisting of three plants – an

alumina plant, an electrolytic plant, and an electrode plant with alumina from its own production – continued at a rapid pace. At that time, the electrode plant produced its first products – anodes, coal blocks and anode paste – in October 1933. In June of the same year, Dnipro Aluminum Plant was launched without the participation of foreign specialists.

The invaluable contribution of the Department of Electrometallurgy to the development of scientific foundations, the design, implementation and improvement of electrothermal equipment and technological processes for the production of a wide range of special electric steels and various types of ferroalloys, as well as the training of electrometallurgical engineers for almost the entire country, was widely recognized by the scientific community. Notably, the Department of Electrometallurgy played a leading role in the establishment of the Ukrainian scientific school of electrometallurgy, which led to the scientific and professional growth of its leading members.

In 1932, S. I. Telnyi was appointed Deputy Director for Research at DMetI, and in 1934 he became Deputy Director for Academic Work, the positions he held until 1939, while also managing the Department of Electrometallurgy. In 1936, by the decision of the Higher Attestation Commission, S. I. Telnyi was awarded the academic title of Professor, and in 1937, without defending his dissertation, he was awarded the degree of Candidate of Technical Sciences. S. Y. Khytryk defended his Candidate's dissertation in 1936 and in the same year he was awarded the academic title of Associate Professor of the Department of Electrometallurgy. In 1939, M. M. Chuyko defended his Candidate's dissertation and was also elected to the position of Associate Professor.

The pre-war period was marked by the rapid development of the electrometallurgy of steel and ferroalloys worldwide. The country was ranked first in the world in the production of electric steel and ferroalloys (1940), and this is due in no small part to the scientists and faculty of the Department of Electrometallurgy of the DMetI. Between 1924 and 1941, about 200 electrometallurgical engineers were trained, who successfully worked in the most responsible positions in ministries, factories, research, design, and educational institutes.

The Great Patriotic War (1941-1945) was a severe trial for the entire Ukrainian people. Nearly all major plants were evacuated to the east, along with some of the highly skilled engineers and skilled workers in the leading smelting specialties.

Between July and October 1941, all the equipment of the ferroalloy plant and Dneprospeysstal was evacuated from Ukraine. This equipment was used to put into operation electric steelmaking and rolling mills in the east, and in 1942, the ferroalloy production facility was put into operation.

Serving as Deputy Head of the Technical Department, S. Y. Khytryk headed all research work on improving the technology for producing ferrochrome, silicochrome, and ferrosilicon. For the first time, the technology was developed for producing low-carbon

ferrochrome by blowing ferrochrome with air in a converter, for producing ferrotungsten from domestic ores, as well as for creating alloys so necessary for the front and victory.

During this period, M. M. Chuyko headed the electrometallurgical laboratory at the plant and lectured at the Siberian Metallurgical Institute, while also leading research on the development and improvement of armor steel production technology for tanks. S. Y. Khytryk and M. M. Chuyko were awarded high governmental awards for their wartime efforts.

After the liberation of Dnipropetrovsk from the German occupation in October 1943, the DMetl began to revive, with the Department of Electrometallurgy as one of its main divisions.

In October 1943, after the liberation of Zaporizhzhia, work began on the restoration of the Zaporizhzhia Ferroalloy Plant. As early as August 1944, the plant organized calcium carbide smelting for construction and reconstruction work at enterprises in Zaporizhzhia, Donbas, and Kryvyi Rih. By 1950, the production of electric steel and ferroalloys reached the pre-war level. The era of rapid development of Ukraine's industrial potential began, and new processes and materials were created, in the development of which the Department of Electrometallurgy played a significant role [3].

In January 1944, S. Y. Khytryk was appointed Acting Head of the Department of Electrometallurgy. Based on the results of ongoing research, S. Y. Khytryk developed the theory of energy and material balance in ferroalloy electric smelting, the theory of vacuum refining of chromium alloys, and introduced and implemented the technology of vacuum treatment of liquid ferrochrome in a ladle at leading industrial plants. These achievements allowed him to successfully defend his Doctoral Dissertation in 1953. In 1954, he was awarded the degree of Doctor of Technical Sciences and the title of Professor at the Department of Electrometallurgy. From 1953 to 1962, working as Vice-Rector for Research at the DMetl, S. Y. Khytryk dedicated significant efforts to the establishment and advancement of science at the institute, while remaining Head of the Department of Electrometallurgy [4].

The development of the nuclear industry required the creation of new structural materials, which in many cases are based on chromium steels and alloys with exceptionally low carbon content and minimum permissible content of harmful impurities (S and P) and gases (N<sub>2</sub> та H<sub>2</sub>). The Department was prepared to meet that challenge. Research was conducted in two areas – vacuum treatment of chromium alloys in liquid and solid states. The second direction particularly captivated the young scientist Mykhailo Ivanovych Hasyk, the future academician of the National Academy of Sciences of Ukraine, Professor, Doctor of Technical Sciences, future Head of the Department of Electrometallurgy. At the beginning of the 60s (1962-1964), the Department's research staff included about 60 researchers and engineers.

The rapid growth of scientific potential could not but affect the Department's research outcomes, expanding its scientific interests and the scope of application of the accumulated scientific experience. A special group was created at the Department to deal with classified topics on the production of ultra-low-carbon chromium steels for pipe assortment [5].

M. I. Hasyk played a leading role in the scientific substantiation and search for alternative materials to replace bauxite in the domestic abrasive industry and alumina production. At the same time, he continued to work on the theoretical aspects of solid-phase refining of ferrochrome; established regularities between the maximum carbon content, metal oxidation levels and the degree of removal of harmful impurities and gases; developed technological regulations for a three-stage process; provided initial data for the creation of a unique vacuum processing unit and supervised its creation, development and industrial implementation. He achieved significant success in obtaining high-quality super-refined chromium-based alloys used in the nuclear industry.

Summarizing the obtained results, M. I. Hasyk defended his doctoral dissertation in 1968, and a year later, in 1969, he was awarded the academic title of Professor at the Department of Electrometallurgy.

Electric steelmaking production was becoming increasingly predominant in specialized metallurgical plants and heavy and medium engineering plants, such as Kharkiv Malyshev Plant, Novo-Kramatorsk Machine-Building Plant, Nikopol Pivdennotrubnyi Plant, Dnipropetrovsk Pipe Rolling Plant, Sumy Oil and Gas Pipe Plant, Kremenchuk Steel Plant, Kryvyi Rih Central Ore Repair Plant, Dnipropetrovsk Switch Plant, Kramatorsk Energomashspetsstal Plant, and others.

Due to shifts in the structure of smelted steel and in the methods of its production, as well as an increase in the share of low-alloy and alloy steels, it became necessary to expand the production of ferroalloys. For this reason, it was decided to construct two ferroalloy plants in Ukraine – the Stakhanov Ferroalloy Plant, for the production of ferrosilicon of various grades, and the Nikopol Ferroalloy Plant, for the production of manganese alloys.

The Department of Electrometallurgy at DMetl gained a reputation as one of the country's largest centers for research and personnel training in the field of electrothermal production. It established close scientific ties and conducted joint research with the Georgian Polytechnic Institute and the Institute of Metallurgy of the Academy of Sciences of the Georgian SSR. Highly appreciating the scientific achievements, they sent their students to the department for scientific internships and theoretical experiments. The department became an all-Union training highly hub for highly qualified electrometallurgical specialists.

Young scientists from Kazakhstan came to the Department to test their research, receive evaluations on its value and significance, and obtain recommendations for their dissertation defenses.



At that time, the construction of one of the world's largest ferroalloy plants, the Nikopol Ferroalloy Plant, began.

For Ukraine, which has globally significant manganese ore reserves, the decision to construct a manganese ferroalloy plant in the Nikopol manganese ore deposit area was a strategic one.

Head of the Department, Professor, Doctor of Technical Sciences Khytryk S. Y. was present at the historic groundbreaking ceremony. Acknowledging scientific merits of the Department, the State Committee for Science and Technology and the Ministry of Higher and Secondary Specialized Education issued a decree in 1966 to establish a Problem Ferroalloy Laboratory at the Department of Electrometallurgy of the DMetI to solve the scientific problems of the plant. At that time, it was the only laboratory in the country equipped with the latest research equipment and electric furnace capacities, such as an X-ray microanalyzer "Cameca", X-ray structural analysis unit, electron microscopes, Balzers gas analysis unit for steel, automated volumetric and gravimetric analysis systems, viscosity and electrical conductivity measurement setups for oxide melts, laboratories for chemical analysis, petrographic and metallographic studies; three electric arc furnaces with a capacity of 0.5 to 1.5 tons, a plasma furnace, a high-frequency induction furnace, vacuum furnaces and other equipment that ensures the implementation of the full metallurgical cycle.

In 1973, Professor, Doctor of Technical Sciences M. I. Hasyk was elected Head of the Department of Electrometallurgy of the DMetI.

The diversity of scientific issues and interests that M. I. Hasyk had to delve into broadened his horizons, allowed him to critically assess the state of a particular scientific issue at the time and eventually transfer this experience to the Department. In 1973, the Department of Electrometallurgy, together with the Problem Ferroalloy Laboratory, had 214 members, including 5 doctors and 32 candidates of technical sciences. At that time, the structuring of scientific research began to emerge with the formation of separate creative groups headed by doctors and candidates of science, professors and associate professors.

In order to assess the contribution of the Department's scientists to the formation and development of the Nikopol Ferroalloy Plant, it is necessary to note the uniqueness of electric furnace melting units, which had no analogues in the world at that time, the scale and breadth of the range of manganese ferroalloys produced by the plant [6].

For the first time in the world, the plant installed a domestic rectangular closed electric ore-reducing furnace with a capacity of 63,000 kV-A, a bath size of 22×10m, and 6 self-heating electrodes measuring 2.8×0.9 m. This unique unit, which resembles a 25-meter swimming pool in size, smelted up to 310 tons of ferrosilicon manganese and ferromanganese per day, while other electric furnaces at that time melted no more than 90-100 tons per day. However, the development of the technology for the production of manganese alloy production in these furnaces and the improvement of their reliability were a serious challenge for the Ukrainian electric ferroalloy industry and, above all, for the staff of the plant and the Department of Electrometallurgy of the DMetI, from which they came out with honor, further enhancing their scientific credibility in the country and in the world [7].

The achievements of the Department in developing new and improving existing technological processes are due to the high theoretical and professional training of its graduates, the effective work of the postgraduate and doctoral programs at the Department of Electrometallurgy. This is evidence that over the years, the Department's educational and research work has been constantly improving in line with contemporary requirements. Currently, training is conducted under such educational and professional programs as Electrometallurgy of Steel and Ferroalloys, Special Metallurgy and Non-Ferrous Metallurgy, with 152 undergraduate and 200 postgraduate students enrolled in the department. Over the 100 years of its existence, the department has trained more than 2,500 broad-profile specialists in cross-industry areas and specialties, 140 candidates and 25 doctors of technical sciences, many of whom received state and international awards and grants.

## References

1. Rubin, P. G. (Ed.). (1909). *Historical Sketch of the Emergence of the Ekaterinoslav Higher Mining School and its Activities During the First Decade (1899-1909)*. Typographic Publishing of the Provincial Zemstvo
2. Myronenko, M. (2025). *Figures: Essays about scientists*. Lira
3. Isaenko, N. (1949). Joyful results. *Dniprovsk pravda*, (256(2590)).
4. Taran-Zhovnir, Y.M. (Ed.). (1999). *State Metallurgical Academy of Ukraine: History of the formation of the university and the development of its scientific and pedagogical schools*. Porohy
5. *National Metallurgical Academy of Ukraine in Names (Encyclopedic reference)*. (2008). ART PRESS
6. Hryshchenko, S. H. (2022). Modern trends in the development of the world and Ukrainian ferroalloy industry. *Theory and practice of metallurgy*, (2(133)), 5-8.

Отримано редколегією / Received by the editorial board: 11.11.2024  
Прийнято до друку / Accepted for publication: 20.02.2025

Gasik M. M.

## Microwave processing of materials in metallurgy

Гасик М.М.

## Мікрохвильова обробка матеріалів у металургії

**Abstract.** The application of microwave technology in minerals processing and metallurgy is getting interest as it allows non-conventional treatment of depleted resources and has positive environmental and economic impact. Microwave processing provides rapid and selective heating with energy efficiency, in contrast to traditional methods. This work analysis some basic features of this technology and shows examples of modelling and experimental study of hybrid microwave treatment of oxide materials, highlighting differences in achievable temperatures and heating times. The model for experimental hybrid microwave furnace with cavity resonating in  $TM_{012}$  mode at 2.45 GHz with 2 kW power has been implemented in COMSOL software and tested on heating of zirconia samples with SiC based susceptor. Electric field and temperature distributions have been simulated and heating rate variations analysed in different positions of the cavity. Results of the analysis are discussed together with the potential use of microwave technology in ore treatment, mineral processing, smelting and carbothermic reduction. This technology has a very good potential in enhancing metal recovery, reducing energy consumption, and improving processing, but this requires understanding about how different materials reacts with microwaves and how the furnaces have to be optimized for a better sustainability.

**Key words:** microwave, mineral, applications, modelling, heating, reduction.

**Анотація.** Застосування мікрохвильових технологій у переробці мінералів та в металургії викликає інтерес, оскільки дозволяє нетрадиційну обробку виснажених ресурсів та має позитивний екологічний та економічний вплив. Мікрохвильова обробка забезпечує швидкий та селективний нагрів з високою енергоефективністю, на відміну від традиційних методів. У цій роботі проаналізовано деякі основні особливості цієї технології та наведено приклади моделювання та експериментального дослідження гібридної мікрохвильової обробки оксидних матеріалів, висвітлюючи відмінності в досяжних температурах та часі нагріву. Модель експериментальної гібридної мікрохвильової печі з резонатором, що резонує в режимі  $TM_{012}$  на частоті 2.45 ГГц з потужністю 2 кВт, була реалізована в програмному забезпеченні COMSOL та протестована на нагріванні зразків цирконію з використанням суцетора на основі SiC. Були змодельовані розподіли електричного поля та температури, а також проаналізовані зміни швидкості нагріву в різних положеннях резонатора. Результати аналізу обговорюються разом з потенційним використанням мікрохвильової технології в обробці руд, переробці мінералів, виплавці та карботермічному відновленні. Ця технологія має дуже хороший потенціал у підвищенні вилучення металів, зниженні споживання енергії та покращенні процесів, але це вимагає розуміння того, як різні матеріали реагують на мікрохвилі та як печі повинні бути оптимізовані для кращої стійкості.

**Ключові слова:** мікрохвилі, мінерал, застосування, моделювання, нагрів, відновлення.

**Introduction.** Microwave technology operating in a frequency range of 300 MHz to 300 GHz, where frequencies of 915 MHz and 2.45 GHz being most commonly used [1]. In a high-frequency microwave field, polar molecules become polarized and oscillate at high frequencies along with the alternating electromagnetic field, resulting in the rapid oscillation of molecules and interactions between them. This converts the lost electromagnetic energy into thermal energy in the material [1, 2], so the dielectric loss factor is one of the key parameter in feasibility of this method for high temperature heating. In a simplified form, the power absorbed by a unit volume of medium from microwaves is proportional to frequency ( $f$ , Hz), real part of dielectric permittivity ( $\epsilon'$ ), loss factor ( $\tan \delta$ ) and to squared electric-field strength ( $E$ , V/cm) inside the material:

$$P = 2\pi f \cdot \epsilon_0 \cdot \epsilon' \cdot \tan \delta \cdot |E|^2 \quad (1)$$

where  $\epsilon_0 = 8.854 \cdot 10^{-14}$  F/cm is the permittivity of the vacuum. The dielectric loss is dependent on material properties, frequency and temperature so the heating might become more accelerating (thermal runaway) or

retarded with time when the composition of the material changes.

**Literature analysis.** Due to essential features of microwave processing, it has considerable potential in minerals processing, hydro- and pyrometallurgy, as it may present substantial energy savings [2]. Microwave heating differs fundamentally from conventional methods, quickly penetrating materials and interacting with their molecular and crystalline structures [1]. This interaction causes molecular vibration and frictional heating, making it more efficient than conduction heating [1-3]. This especially enables microwave processing in ore treatment, particularly for difficult to recovered minerals and high-value products (rare metals, precision metals) due their efficiency and environmental benefits [1].

In Table 1 it is seen that most of transition metals oxides and sulphides are very good microwave absorbers and can be heat very rapidly. Carbon can be heat very fast and this enables extremely rapid reduction to produce metals, as other oxides remain at lower



temperatures. Carbothermic microwave reduction demonstrates that microwave heating can initiate chemical reactions at lower temperatures, impacting the reduction mechanism significantly. It was reported [3] that the highest temperatures were obtained with

carbon and most of the metal oxides like NiO, MnO<sub>2</sub>, Fe<sub>3</sub>O<sub>4</sub>, Co<sub>2</sub>O<sub>3</sub>, CuO and WO<sub>3</sub>. Metal powders and some metal halides also heated well; gangue such as quartz, calcite and feldspar do not heat up [3].

Table 1. Microwave heating effect at 2.45 GHz on particulate solids with the time needed to reach the indicated temperatures [2-4].

Substance	Heating time, min	T °C	Substance	Heating time, min	T °C
Al	6	577	MgO	40	1300
Al <sub>2</sub> O <sub>3</sub>	24	1900	MnO	6	113
C	0.2	1000	MnO <sub>2</sub>	6	1287
CaCO <sub>3</sub>	7	61	MoO <sub>3</sub>	0.46	750
CaO	40	200	MoS <sub>2</sub>	0.1	900
Co	3	697	Ni	1	384
Co <sub>3</sub> O <sub>4</sub>	3	1290	Ni <sub>2</sub> O <sub>3</sub>	3	1300
Cr <sub>2</sub> O <sub>3</sub>	7	130	NiO	6.3	1305
CuO	4	800	PbO	13	900
CuS	5	600	TiO <sub>2</sub>	8.5	79
Fe	7	768	UO <sub>2</sub>	0.1	1100
Fe <sub>2</sub> O <sub>3</sub>	6	1000	V <sub>2</sub> O <sub>5</sub>	11	714
Fe <sub>3</sub> O <sub>4</sub>	0.5	500	Zr	6	462
FeS	6	800	ZrO <sub>2</sub>	4	63

Yoshikawa et al. [5] have investigated the microwave carbo-thermal reduction reaction of nickel oxide. When NiO particles and graphite are used, 100% metallic Ni is produced after only a few minutes by microwave heating. The reduction reaction is highly effective under microwave magnetic field irradiation. Several studies have shown that the reduction of Fe, Sc and Mg oxides is effective under microwave irradiation, demonstrating that the energy efficiency of microwave irradiation is higher [6]. Another example is for manganese carbonate ores, which are becoming an increasingly important potential source of manganese, and the calcination and agglomeration of these ores by microwave irradiation has been investigated [7] where under optimal microwave conditions sintering temperatures of >1500 °C were achieved to product manganosite (MnO) and hausmannite (Mn<sub>3</sub>O<sub>4</sub>) with the sinter strengths comparable to those of conventionally processed materials.

In terms of industrial implementation [3] a metallurgical microwave reduction process could save 15-50% over a conventional operation. Microwave assisted carbothermic reduction on ilmenite concentrate mixed with lignite powder and CaCO<sub>3</sub> it was and confirmed that the reduction rate of metal oxide by microwave heating was faster than by conventional heating [3].

Rapid heating of ore minerals in a microwave transparent matrix generates thermal stress of sufficient magnitude to create micro-cracks along mineral boundaries, which improves reaction kinetics, grinding and leaching efficiency [3, 8]. The rapid volumetric heating by microwave treatment results in differential expansion and contraction of different mineral phases, creating internal stresses weakening the ore's structure which become more brittle and easier to grind, reducing the energy requirements for comminution [1]. In practice, it was demonstrated that microwave pretreatment of sulphide ores resulted in a reduction of up

to 30% in grinding energy requirements [8]. The preferential heating of specific mineral phases can improve the liberation of valuable minerals from gangue components, increasing the overall recovery rate.

However, microwave processing in metallurgy requires proper investment in microwave generators and furnaces with specific design to ensure that the heat generation and distribution is optimal for the selected material. This dictates that more information about materials properties (especially dielectric permittivity and loss factor) vs. temperature, frequency and materials size need to be studied. This could be achieved in experimental facilities.

**Objectives of this work.** The goal of this work is to highlight potential of microwave applications in metallurgy and to demonstrate experimental and calculation methods for a better understanding how microwave power and heat are generated and distributed inside the materials.

**Materials and methods.** An experimental hybrid 2 kW, 2.45 GHz mono-mode (TM<sub>012</sub>) microwave furnace was set up in Aalto University, Finland (Fig. 1).

The "hybrid" functionality of the microwave cavity comes from the use of SiC susceptor which can be placed around the sample in the case the material is weakly interacting with the microwave radiation at the beginning. Because SiC is a very good absorber, it starts heating first to provide radiative heating to the sample, which, upon increasing temperature, starts to couple with microwaves. In this case indirect heating share decreases, which also can lead to inverse temperature gradient (specimen becomes hotter inside than outside). For demonstration zirconia was used as test material which is known poorly coupled with microwaves at low temperatures but better at higher temperatures.

For calculation of the microwave power and heat distribution COMSOL Multiphysics software was used

with two coupled modules, radiofrequency and heat transfer. First the magnitude of the electromagnetic field in the whole cavity must be evaluated and consecutively the heat generation by this field in the material can be calculated. This first step is based on Maxwell equations [9] where the cavity (item 1 in Fig. 1) is modelled in 3D for a harmonic propagation mode. The second step deploys standard Fourier heat transfer equation with added source due to absorption of the microwave power [4, 9]. This 3D model of the cavity and specimen is shown in Fig. 2.

**Results and discussion.** An example of calculated electrical field distribution in the cavity is shown in Fig. 3. The red zones correspond to maximal field strength (in this case 18 kV/m) and indicate the position where the specimen would be optimally located. As by the Eq. (1), this can lead to the maximum power which is proportional to square of the field strength. In the case of zirconia, magnetic component is also present but its contribution to heating is much less [2, 3].

Temperature in the specimen as measured from its top depends on the input power and time. Figure 4 shows that temperatures over 1273K can be reached

in less than 3 min when the input power exceeds 1.5 kW. In the SiC susceptor, very high heating rates (up to 2000 K/min) are spotted already after 1 min of heating, decreasing to 30-50 K/min after 5-10 min. However, at that point heating of the susceptor itself is almost zero because now zirconia sample starts to couple with the microwaves and the heating focus shifts into the sample [4].

The model developed allows proper simulation of the heating process and can be used to experimentally test the properties of different materials behavior in these conditions without explicit knowledge of their dielectric permittivity function. These results, as well as in earlier studies, show that in many cases temperature in the interior of the material could be much higher than at the surface and significant improvements in heat transfer can be achieved for materials, such as oxides which poor thermal conductivity limits conventional heat [2]. The energy densities in microwave systems can be relatively high and can lead to very high internal heating rates, especially at the beginning of the process which is difficult to achieve with conventional furnaces.

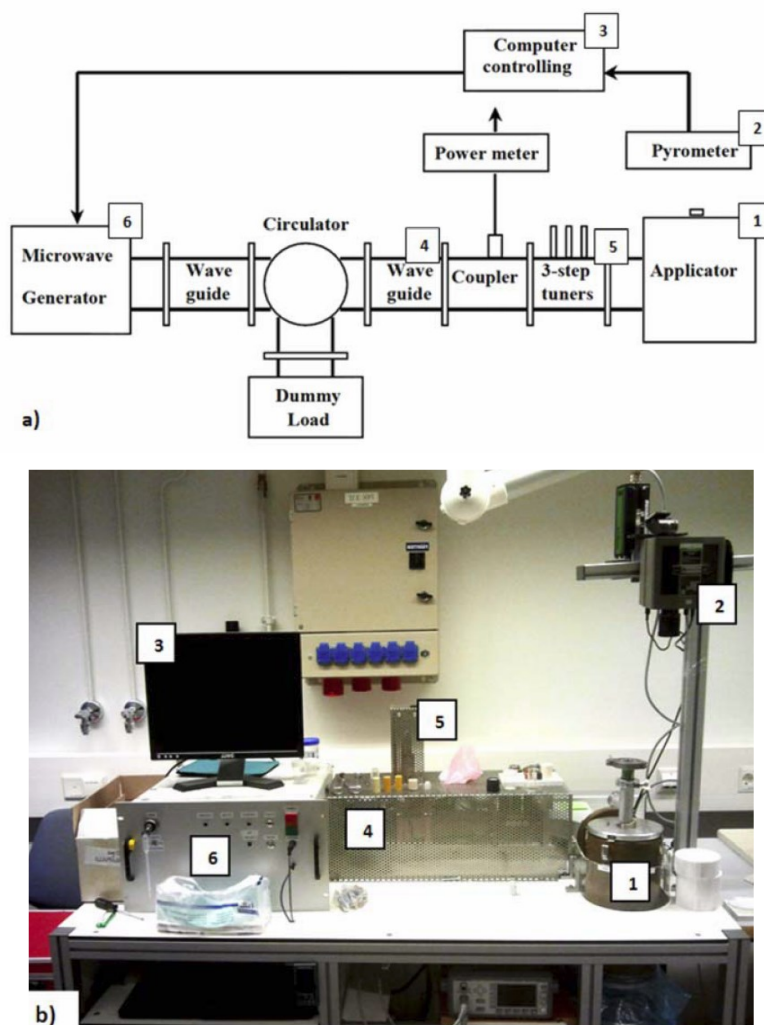


Fig. 1. The scheme (a) and overall view (b) of experimental 2 kW hybrid microwave furnace: 1 – the cavity with the sample, 2 – two-way optical pyrometer, 3 – control system, 4 – waveguide, 5 – microwave tuners, 6 – generator [4].

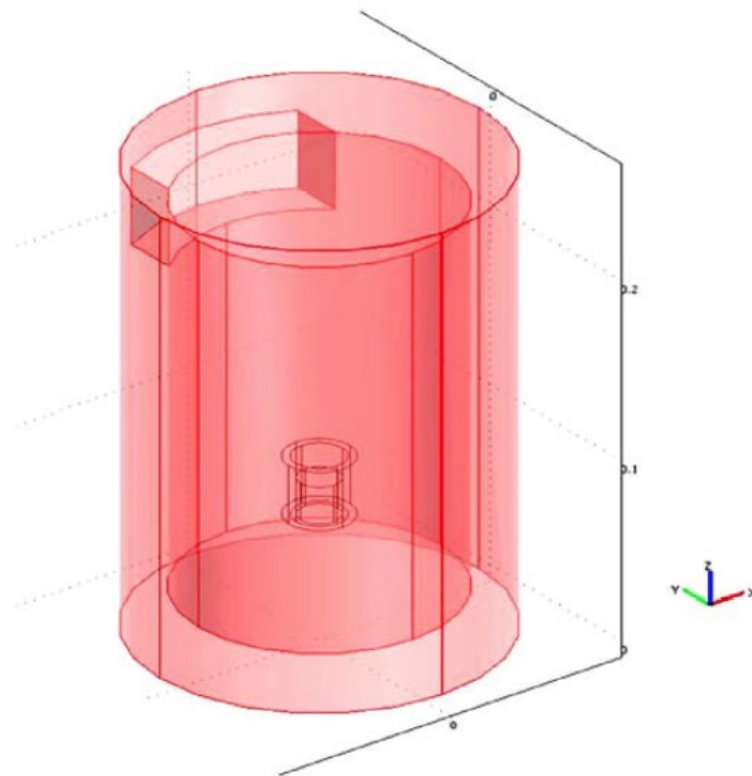


Fig. 2. The COMSOL model of the microwave furnace cavity (dimensions in m) and the specimen position.

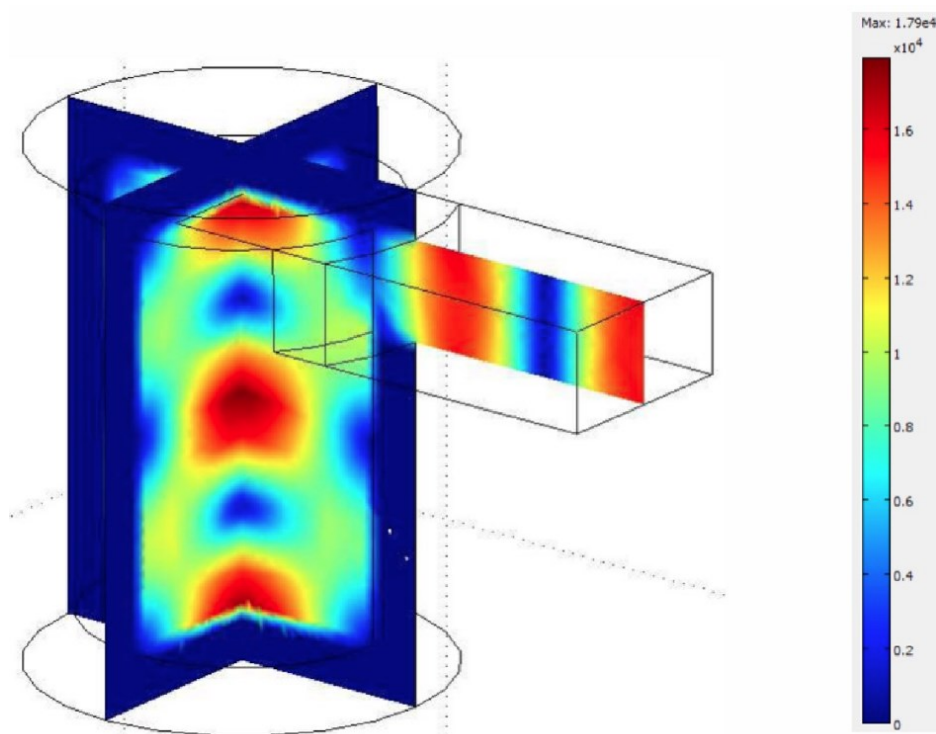


Fig. 3. Calculated electrical field strength (V/m) in the waveguide and cavity for 1.2 kW input at 2.45 GHz in  $TE_{10}$  mode.



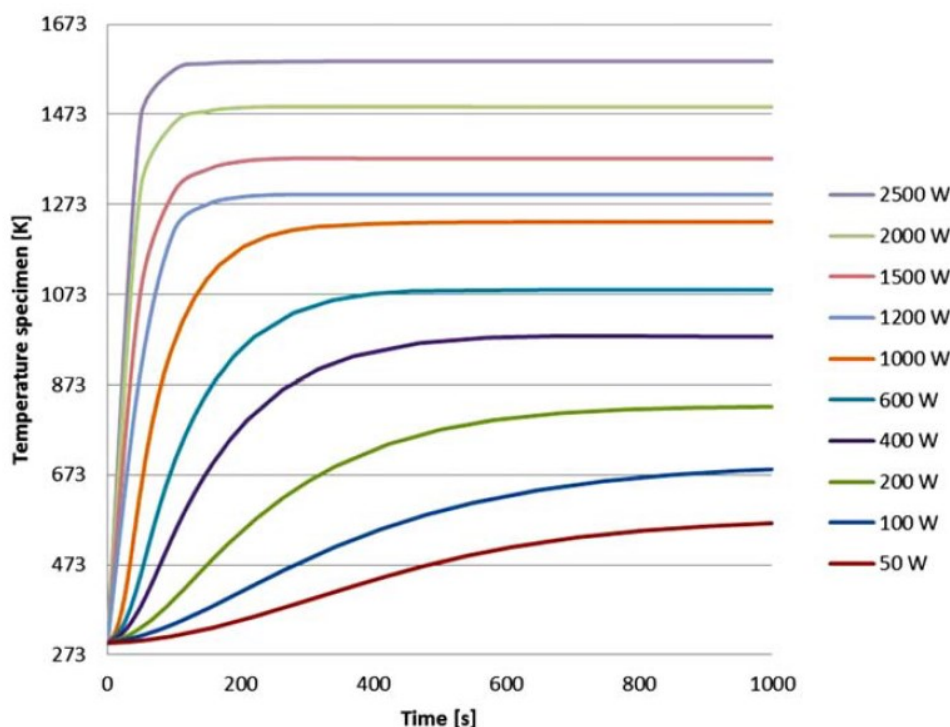


Fig. 4. Calculated temperatures of the specimen vs. time and input power.

The microwaves energy source is relatively clean and easily controlled, facilitating continuous processing, minimizing the amount of off-gas and also the amount of dust particles. This improves working conditions in microwave processes to be far more superior to those in conventional processes, promoting both endothermic and exothermic reactions as well as synthesis [2, 10]. Selective heating can be attained – for example when heating manganese carbonate ore,  $\text{CaCO}_3$  component would remain much colder (Table 1) as major heat generation will be in the manganese phase.

**Conclusions.** Microwave technology in mineral metallurgy presents a progressive and efficient approach to ore processing, aligning with the industry's need for innovation and sustainability [1,2]. Despite

that microwave energy is more expensive than electricity, the efficiency of microwave heating is often much higher than conventional heating and overcomes this costs differences, especially when high-value materials are being recovered. The practical applications of microwave treatment (ores processing, reduction, drying) have demonstrated significant improvements in process efficiency, energy consumption, and environmental impact [2, 3] and it is evident that microwaves could achieve effects such as inverse heating and rapid effect with a higher cost-efficiency. Among challenges required for successful implementation of the technique are still more fundamental understanding of microwaves interaction with different minerals as well as analysis of kinetics of the processes.

### References

1. Chen, J., Li, X., Gao, L., Guo, S., & He, F. (2024). Microwave treatment of minerals and ores: heating behaviours, applications, and future directions. *Minerals*, 14(3), 219. <https://doi.org/10.3390/min14030219>
2. Horikoshi, S., Schiffmann, R. F., Fukushima, J., & Serpone, N. (2018). *Microwave chemical and materials processing*. Springer Nature. <https://doi.org/10.1007/978-981-10-6466-1>
3. Koleini, S.M.J., & Barani, K. (2012). Microwave heating applications in mineral processing. In W. Cao (Ed.). *The development and application of microwave heating*. (pp. 79-104). InTech Open. <https://doi.org/10.5772/45750>
4. Lapauw, T. (2013). Assessing the electromagnetic field effects during microwave sintering. [M. Sc. Thesis, Katholieke Universiteit Leuven, Belgium]
5. Yoshikawa, N., Ishizuka, E., Mashiko, K., & Taniguchi, S. (2007). Carbon reduction kinetics of NiO by microwave heating of the separated electric and magnetic fields. *Metall. Mater. Trans. B*, 38, 863–868. <https://doi.org/10.1007/s11663-007-9093-7>
6. Fujii, S., Yamamoto, M., Haneishi, N., Tsubaki, S., Fukushima, J., Takizawa, H., & Wada, Y. (2021). Reduction of metal oxides using thermogravimetry under microwave irradiation. *AIP Advances*, 11, 065207. <https://doi.org/10.1063/5.0050907>
7. Amankwah, R.K., & Pickles, C.A. (2005). Microwave calcination and sintering of manganese carbonate ore. *Canadian Metall. Quart.*, 44(2), 239–248. <https://doi.org/10.1179/cmqu.2005.44.2.239>
8. Kingman, S. W. (2006). Recent developments in microwave processing of minerals. *Intern. Mater. Rev.*, 51(1), 1-12. <https://doi.org/10.1179/174328006X79472>

9. Gasik, M. M., Gasik, M. I., Petrov, B. F., Kutuzov, S. V., Urazlina, O. Yu., & Derkach, V. V. (2006). Computer modelling and industrial implementation of single-stage calcination of anthracite in electrocalcinators. *Metall. Mining Industry. Ukraine*, (3), 27-30
10. Pickles, C.A. (2009). Microwaves in extractive metallurgy: part 2 - a review of applications. *Mineral. Eng.*, 22(13), 1112–1118. <https://doi.org/10.1016/j.mineng.2009.02.014>
11. Nissinen, T., Kiros, Y., Gasik, M., & Leskelä, M. (2003).  $\text{MnCo}_2\text{O}_4$  preparation by microwave-assisted route synthesis (MARS) and the effect of carbon admixture. *Chem. Mater.*, 15(26), 4974–4979. <https://doi.org/10.1021/cm031093x>

Отримано редколегією / Received by the editorial board: 03.12.2024

Прийнято до друку / Accepted for publication: 20.02.2025

**Jiang ZhouHua, Yang Ce, Zhu HongChun, Lu HongBin**  
**The-state-Art of steelmaking technology based on hydrogen metallurgy**

**Сучасний стан технології виробництва сталі  
на основі водневої металургії**

**Abstract.** This paper puts forward the viewpoint that "hydrogen steelmaking" replaces "oxygen steelmaking", and summarizes and evaluates the research status of "hydrogen steelmaking". Hydrogen metallurgy steelmaking has unique advantages in energy saving, consumption reduction and product quality improvement. On the one hand, hydrogen has a highly efficient melting effect, which can effectively reduce the energy consumption of steelmaking. "Hydrogen" in plasma state has the characteristics of high temperature and high thermal conductivity, which can be used as a highly efficient heat source to realize the melting of charge and heating of steel, and has been applied in steelmaking processes such as EAF, converter and tundish. Blowing gaseous "Hydrogen" can accelerate the homogenization in the composition and temperature, and the movement of hydrogen bubbles can be adhered to the non-metallic inclusions which can be accelerated to float out. At the same time, hydrogen reacts with oxygen in the liquid steel to release a large amount of heat, which improves the thermodynamic and kinetic conditions of the melt pool reaction. In addition, "Hydrogen" can inhibit oxidation and reduce the loss of Cr, Mn and other alloying elements by creating a reducing atmosphere. On the other hand, "Hydrogen" has a non-polluting refining effect that significantly improves the cleanliness of the steel. Based on the high activity and high reducibility of "Hydrogen", "Hydrogen" can effectively remove impurity elements such as O, C, N, S and P in steel, especially "Hydrogen" in plasma state, which can directly react with the impurity elements to generate  $H_2O$ ,  $CH_4$ ,  $NH_3$ ,  $H_2S$  and  $PH_3$  and other gaseous products that are easy to be volatilized and removed, so as to avoid the formation of non-metallic inclusions, and to realize the highly efficient and high-cleanliness steelmaking with "zero inclusions". Therefore, the development of a new generation of green, near-zero carbon, "zero inclusion" and pollution-free steelmaking process using "hydrogen" instead of "carbon" will accelerate the green, high-quality, and sustainable development of the steel industry.

**Key words:** hydrogen metallurgy, steelmaking, hydrogen plasma, melting, refining, green and low-carbon.

**Анотація.** У статті висувається точка зору, що "водневе виробництво сталі" замінює "кисневе виробництво сталі", а також узагальнюється та оцінюється стан досліджень "виробництва сталі з використанням водню". Воднева металургія сталі має унікальні переваги в енергозбереженні, зменшенні споживання та покращенні якості продукції. З одного боку, водень має високоефективний плавильний ефект, який може ефективно зменшити енергоспоживання при виробництві сталі. "Водень" у плазмовому стані характеризується високою температурою та високою теплопровідністю, що може бути використано як високоефективне джерело тепла для реалізації плавки шихти та нагріву сталі, і вже застосовується в сталеплавильних процесах, таких як електродугові печі, конвертери та проміжні ковші. Продування газоподібним "воднем" може прискорити гомогенізацію хімічного складу та температури, а рух водневих бульбашок може сприяти прилипанню неметалевих включень, що прискорює їхнє спливання. Водночас, водень реагує з киснем у рідкій сталі, виділяючи велику кількість тепла, що покращує термодинамічні та кінетичні умови реакції розплаву. Крім того, "водень" може пригнічувати окислення та зменшувати втрати Cr, Mn та інших легуючих елементів шляхом створення відновлювальної атмосфери. З іншого боку, "водень" має ефект рафінування без забруднення, що значно покращує чистоту сталі. Завдяки високій активності та високій відновлювальній здатності "водню", "водень" може ефективно видаляти домішкові елементи, такі як O, C, N, S та P зі сталі, особливо "водень" у плазмовому стані, який може безпосередньо реагувати з домішковими елементами, утворюючи  $H_2O$ ,  $CH_4$ ,  $NH_3$ ,  $H_2S$  та  $PH_3$  та інші газоподібні продукти, які легко випаровуються та видаляються, щоб уникнути утворення неметалевих включень та реалізувати високоефективне та високочисте виробництво сталі з "нульовими включеннями". Таким чином, розробка нового покоління зелених, майже безвуглецевих, "безвключних" та екологічно чистих сталеплавильних процесів з використанням "водню" замість "вуглецю" прискорить зелений, високоякісний та сталий розвиток сталеливарної промисловості.

**Ключові слова:** воднева металургія, виробництво сталі, воднева плазма, плавка, рафінування, зелений та низьковуглецевий.

## 1. Introduction

In 2023, the output of crude steel in China was 1.019 billion tons, accounting for more than half of the global total, with remarkable achievements [1, 2]. Steel industry is characterized by resource-intensive and energy-intensive. Currently, carbon emissions account for about 16% of China's total, and it is the largest

carbon emission industry in the manufacturing industry [1, 3, 4]. Under the "dual-carbon" strategy, the iron and steel industry is the main battlefield of the industrial green development, and the problems of excessive carbon emissions have to be solved urgently to promote the green and healthy development of the iron and steel industry [3, 6, 7]. On the other hand, it is

© Jiang ZhouHua – School of Metallurgy, State Key Laboratory of Digital Steel, Northeastern University, Liaoning, China  
Yang Ce, Zhu HongChun, Lu HongBin – School of Metallurgy, Northeastern University, Liaoning, China



This is an Open Access article under the CC BY 4.0 license <https://creativecommons.org/licenses/by/4.0/>

necessary to strengthen the research and development and industrialization of key high-end steel to solve the problem of improving the quality of key materials required for the development of high-end manufacturing industry [4, 8]. Therefore, the green and high-quality development is the main theme of the future development of the steel industry, and the active development of a new generation of green near-zero carbon steel production process will effectively solve the ecological environment pollution, product quality instability and other problems, thus boosting the high-quality sustainable development of the steel industry.

In the traditional iron and steel metallurgy process, the ironmaking process is "carbon metallurgy" which uses carbon as reducing agent and heat source, while the steelmaking process is "oxygen steelmaking" which uses oxygen as oxidant to remove impurities such as carbon, silicon and phosphorus in the hot metal. A large amount of greenhouse gas  $\text{CO}_2$  is produced in the process of iron and steel making. At the same time, in the later stage of steelmaking, aluminum and other deoxidizing agents must be used to deoxidize and produce a large number of  $\text{Al}_2\text{O}_3$  non-metallic inclusions to pollute the liquid steel, leading to a decline in the performance of steel materials. Green hydrogen is regarded as the key to a carbon-free economy, with the advantages of wide sources, high thermal efficiency, high energy density, clean and renewable, etc. The application of "hydrogen" in iron and steel production is expected to solve the problems that have long restricted the green, high-quality and sustainable development of steel industry [2, 7, 9, 10]. At present, hydrogen-metallurgy ironmaking technology such as hydrogen-rich blast furnace and hydrogen-based shaft furnace reduction is a hot research and development in the world, and some technologies have been applied in industrialization, which can reduce the carbon emission of ironmaking process by more than 50% [2, 7, 11]. At the same time, hydrogen metallurgy iron product (for example, the direct reduction iron - DRI) have the advantages of low content of harmful impurity elements and low carbon content, and is one of the best

iron source materials for the production of high clean steel [7, 12]. However, the current theoretical research and technical development of hydrogen metallurgy are mainly concentrated in the ironmaking field, and there are few reports in the steelmaking field. So, could the theory and technology of hydrogen metallurgy be applied to the field of steelmaking, replace the traditional "oxygen steelmaking", and fully open up a new generation of green near-zero carbon steel production process based on hydrogen metallurgy? The author thinks that this is a major issue to promote the green, high-quality and sustainable development of the steel industry.

This paper reviews the theory, technology research and application status of "hydrogen steelmaking", and puts forward a new generation of green near-zero carbon steel production process, aimed at promoting the green, high-quality and sustainable development of the steel industry.

## 2. The role of hydrogen in the steelmaking process

In the steelmaking process, hydrogen acts in two main forms: gaseous and plasma, each demonstrating distinct characteristics:

(1) Gaseous: Hydrogen is a monomer formed by the element hydrogen, with the chemical formula  $\text{H}_2$ , which is the lowest molecular weight substance in nature and is also recognized as one of the most environmentally friendly energy sources. As an emerging strategic energy source, hydrogen has the advantages of abundant sources, high thermal efficiency, high energy density, clean use and renewability [2, 7, 9-10].

(2) Plasma state: Hydrogen exists in the form of hydrogen molecules in its natural state. With the increasing energy contained in hydrogen molecules, they gradually transition to the "plasma state" [13-14]. There are various forms of hydrogen molecules in this transition to the plasma state, including molecular  $\text{H}_2$  (ground state  $\text{H}_2$  and excited state  $\text{H}_2^*$ ), atomic state  $\text{H}$  (ground state  $\text{H}$  and excited state  $\text{H}^*$ ),  $\text{H}^+$ ,  $\text{H}_2^+$ ,  $\text{H}_3^+$ , and  $e^-$ . In terms of reduction potential, the hierarchy is as follows:  $\text{H}^+ > \text{H}_2^+ > \text{H}_3^+ > \text{H} > \text{H}_2$ , as shown in Fig. 1 [14-16].

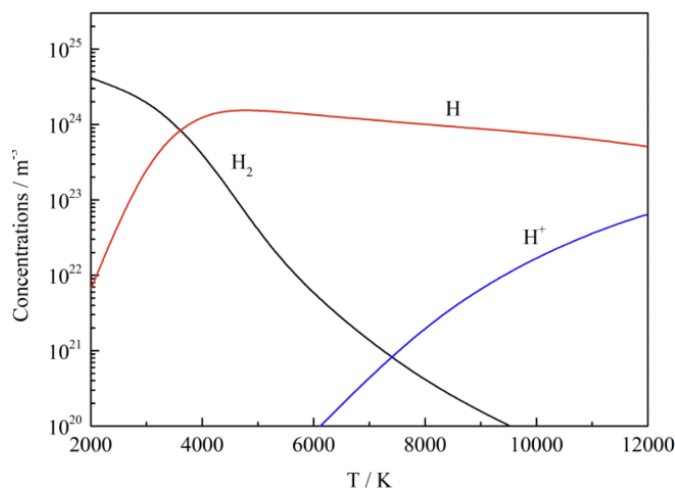


Fig. 1. Equilibrium composition of hydrogen at different temperatures at one atmospheric pressure.

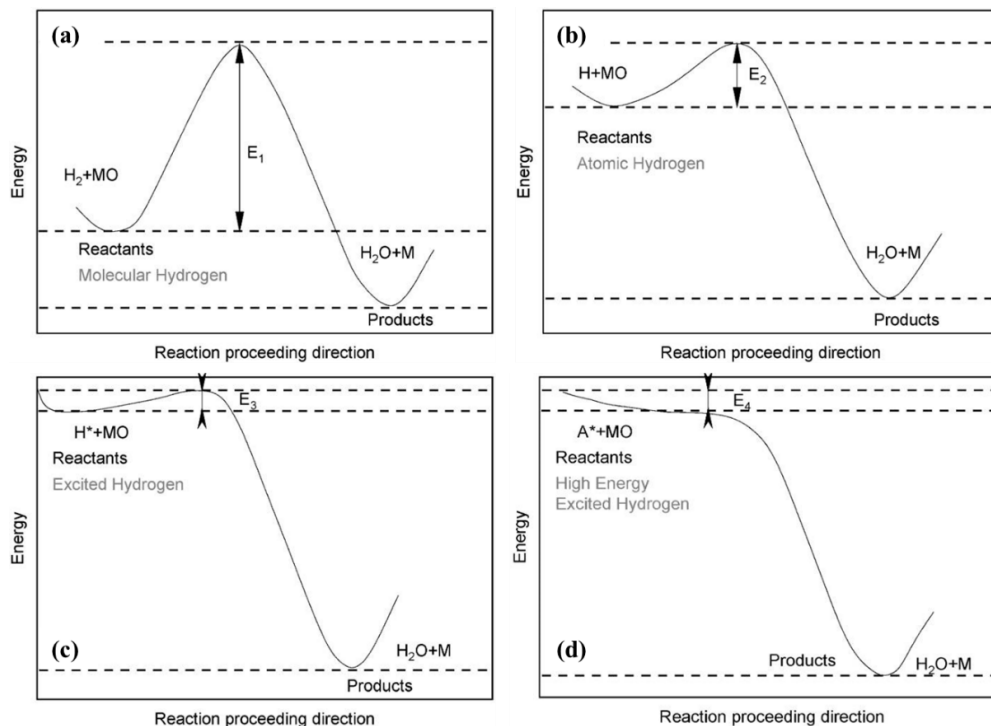


Fig. 2. The activation energy of the reaction of different types of hydrogen with metal oxides (a) Molecular hydrogen; (b) Atomic hydrogen; (c) Excited hydrogen; (d) High energy excited hydrogen.

Based on the variance in reduction potential, the trend of the reaction between various hydrogen forms and metal oxides differs. Fig. 2 illustrates the schematic diagram of activation energies of different forms of hydrogen reacting with metal oxides, in which the activation energies are respectively  $E_1 > E_2 > E_3 > E_4$  from the largest to the smallest. It can be seen that the closer hydrogen is to the final ionization state, the lower the activation energy of reducing metal oxides, and the easier the reaction will be [15].

In summary, the two forms of "hydrogen" in the steelmaking process have dual functions. Firstly, the reaction between "hydrogen" and metal oxide releases a significant amount of heat, which rapidly melts the charge and heats the liquid steel. In particular, hydrogen in plasma state has the characteristics of higher temperature and greater heat transfer efficiency, which can be directly used as a heat source to quickly heat the charge or liquid steel. Secondly, due to its high

reducibility, especially hydrogen in plasma state, hydrogen can efficiently remove impurity elements such as O and S from the steel. This helps prevent the formation of non-metallic inclusions that could pollute the liquid steel and enables high clean steel smelting. Additionally, hydrogen has the potential to replace common injection gases like argon and nitrogen to stir liquid steel and accelerate mixing within the melt pool.

### 3. The Smelting effect of "hydrogen"

#### 3.1. The heating effect of "hydrogen"

The heating effect of "hydrogen" is a process in which hydrogen or hydrogen-containing gas is dissociated into plasma to form a high-temperature hydrogen plasma torch, which is used as a high-temperature heat source to achieve rapid melting of the charge or precise temperature control of liquid steel [13, 17]. At present, plasma heating technology has been applied in EAF, converter and tundish equipment. The system diagram is shown in Fig. 3 [18-20].

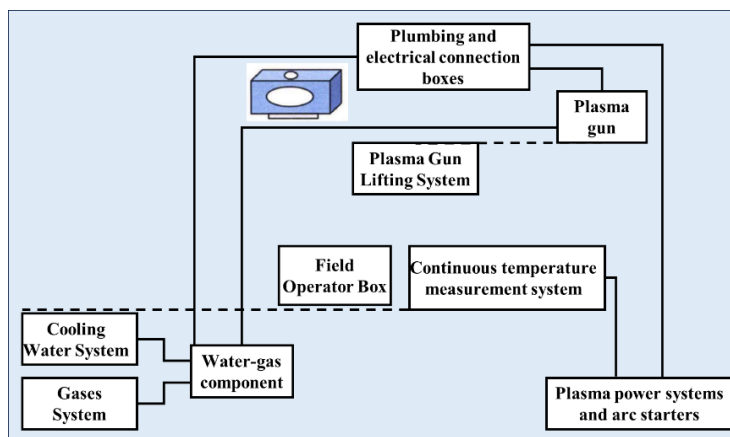


Fig. 3. Schematic diagram of the plasma heating system equipment for tundish.



The results show that the temperature in the plasma torch center increases from 10417 K to 11660 K when 5% hydrogen is added into argon. When 5% hydrogen is added to nitrogen, the temperature can be increased from 10789 K to 11254 K, and the larger the proportion of hydrogen, the higher the central temperature of the jet, and the faster the heating rate of the molten pool [17]. Taking a 100 kg multifunctional DC ladle furnace as an example, the heating rate of the molten pool is faster than that of the solid electrode by

injecting Ar-H<sub>2</sub> mixture into the molten pool through the hollow graphite electrode. The higher the proportion of H<sub>2</sub> in the mixed gas, the faster the heating rate of the molten pool [21]. In addition, hydrogen-containing gas CH<sub>4</sub> also has efficient heating effect, but the heating efficiency does not increase with the increase of CH<sub>4</sub> concentration. When 95%Ar-5%CH<sub>4</sub> is blown into the molten pool, the heating rate is the largest, as shown in Fig. 4 [22].

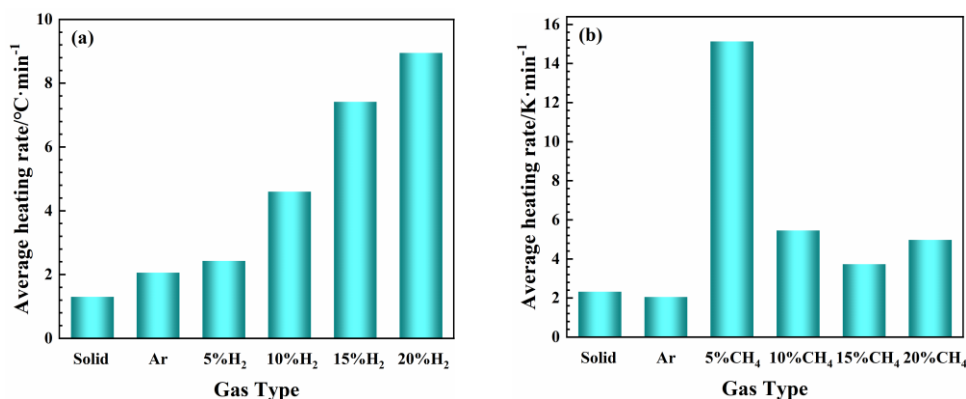


Fig. 4 Influence of hydrogen containing gas on melt pool heating rates: (a) H<sub>2</sub>; (b) CH<sub>4</sub>.

In actual production, according to the characteristics of steel and metallurgical quality requirements, reasonable selection of heating power and time, and other process parameters to control the heating efficiency of hydrogen plasma can not only meet the requirements of melting heating rate and end temperature [13, 23], but also effectively reduce the loss of refractory materials and improve the service life of smelting equipment [24]. In addition, hydrogen plasma torch has the characteristics of high impact force, which can not only improve the fluidity of liquid steel and accelerate the floating of inclusions, but also increase the temperature of slag layer and reduce the viscosity of slag layer, so as to improve the adsorption capacity of slag layer to inclusions, and help improve the cleanliness of liquid steel [25]. However, at this stage, plasma heating also has some problems, such as expensive equipment, short service life, difficult arc-starting, and electromagnetic radiation generated by plasma heating process has great interference on weak current systems [26].

### 3.2. The Stirring Effect of "Hydrogen"

Gas injection is a commonly used method to enhance metallurgical reactions in the steelmaking process [27-31]. It serves to stir the liquid steel, promoting homogenization of its composition and temperature, as well as facilitating the formation of small bubbles that accelerate the removal of impurities. Hydrogen injection not only creates smaller and more dispersed bubbles for enhanced stirring, but also generates significant chemical heat by reacting with dissolved oxygen or blown oxygen in the molten steel [27, 32-34]. Additionally, hydrogen can aid in decarbonization and contribute to low-oxygen or no-oxygen smelting in converters, thereby reducing carbon emissions [27, 34]. Furthermore, it provides a reducing atmosphere that

inhibits over-oxidation and minimizes loss of metal elements during steelmaking. Any residual hydrogen dissolved in the molten steel can be effectively removed during subsequent vacuum refining processes without compromising final product quality (Fig. 5 (a)) [16, 33-35]. Taking production data from Pangang Group Xichang Steel & Vanadium Co., Ltd. 210-ton converter as an example [35], at an blowing intensity of 0.1 m<sup>3</sup>·min<sup>-1</sup>·t<sup>-1</sup>, hydrogen injection yields an extra 16174.72 kJ compared to argon injection (Fig. 5 (b)) and increases scrap charging ratio by 8.17% (Fig. 5 (c)). Moreover, higher bottom-blowing intensities correspond to greater extra calorific value and scrap charge ratios; CO<sub>2</sub> emission reductions also correlate with increased hydrogen intensity at the bottom blow (Fig. 5 (d)).

The practice has demonstrated that hydrogen blowing can effectively address the issues of "insufficient temperature" and "slag dilution" in the AOD converter smelting process of high manganese stainless steel based on its advantages in efficient stirring, rapid heating, and providing a reducing atmosphere. Specific measures are outlined as follows [36].

During the first decarburization stage (Fig. 6 (a)), to prevent the potential hazards of hydrogen and oxygen reacting and causing explosions, they are separately injected into the converter from the side. The reaction between hydrogen and oxygen generates a significant amount of heat within the converter, while unreacted hydrogen is completely consumed by the top-blown oxygen, effectively raising the temperature of molten steel without relying on carbon and reducing carbon emissions. Additionally, blown hydrogen can facilitate the reduction of hexavalent chromium in slag, thereby improving chromium recovery rates.

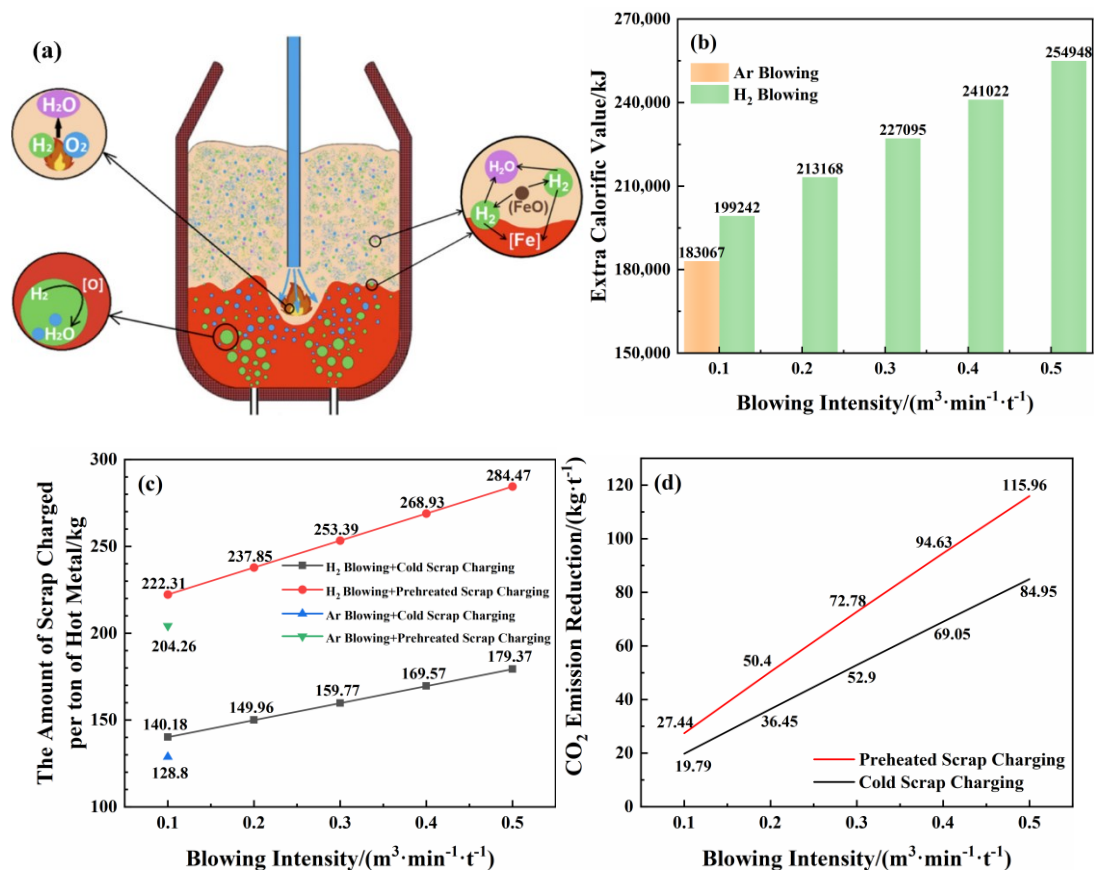


Fig. 5. Metallurgical effects of hydrogen blowing in converter: (a) Metallurgical behavior of hydrogen in the converter; (b) Extra calorific value; (c) Scrap charge; (d) CO<sub>2</sub> emission reduction.

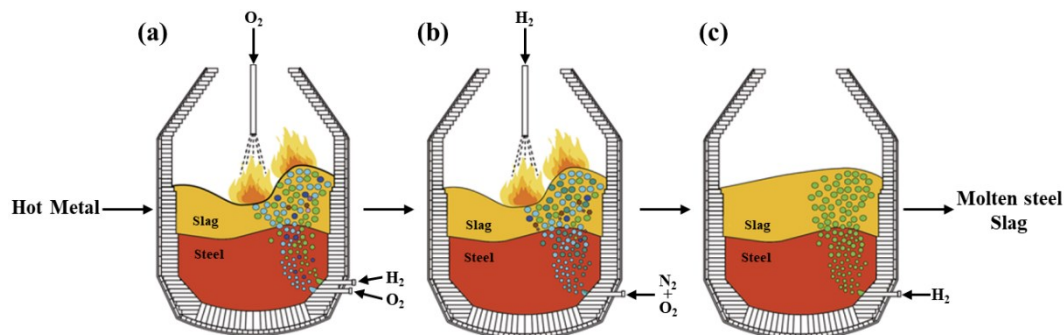


Fig. 6. Schematic diagram of hydrogen blowing smelting of high manganese stainless steel: (a) The first decarburization stage; (b) The second decarburization stage; (c) The reduction stage.

During the second decarburization stage (Fig. 6 (b)), oxygen and nitrogen blown into the converter from the side enhance the decarburization process; any remaining oxygen is eliminated by reacting with hydrogen from the top, generating heat and sustaining the molten steel temperature.

During the reduction stage (Fig. 6 (c)), hydrogen is injected into the side to intensify mixing within the molten pool for more uniform composition and temperature of molten steel as well as promote reduction reactions.

In summary, hydrogen injection in the steelmaking process not only further strengthens the stirring effect and improves the kinetic conditions of steelmaking; but also will react with the dissolved oxygen in the molten

steel and the oxygen sprayed, release a lot of heat, maintain or increase the temperature of the molten steel, and improve the thermodynamic conditions of steelmaking. The dissolved hydrogen is subsequently removed by vacuum degassing without affecting the metallurgical quality of the steel.

#### 4. The refining effect of "hydrogen"

Hydrogen, especially hydrogen in plasma state, has extremely high chemical activity and reducibility, and can react quickly with impurity elements such as O, N, S and P and C in liquid steel to generate gas products that are easily removed by vacuum (Fig. 7 [37]), to avoid the formation of non-metallic inclusions contaminating the molten steel due to the addition of deoxidizers and slag-making agent, and the increase

of oxygen in the molten steel due to oxygen blowing and decarburization. The green, near-zero-carbon, high-clean steel smelting with “less oxygen or non-oxygen” and “zero inclusions” is realized [37-44]. A small

amount of dissolved hydrogen in steel can be reduced to very low levels ( $1 \times 10^{-6}$ ) by means of vacuum degassing, thus completely eliminating adverse effects such as hydrogen embrittlement [33-34].

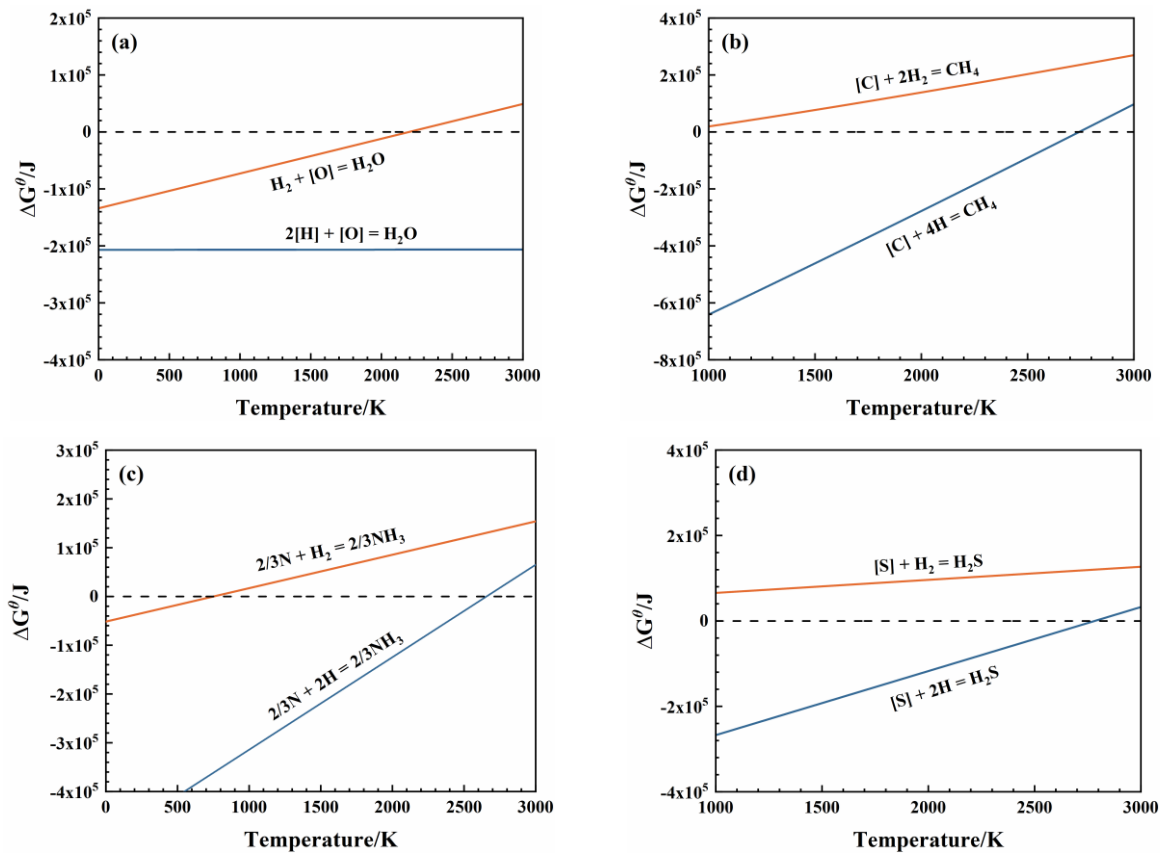


Fig. 7. Gibbs free energy of the reaction of “hydrogen” with impurity elements in steel: (a) Hydrogen-oxygen reaction; (b) Hydrogen-carbon reaction; (c) Hydrogen-nitrogen reaction; (d) Hydrogen-sulfur reaction.

#### 4.1. “Hydrogen” deoxidation

As we all know, high oxygen content is the cause of large-size inclusions in steel. The traditional deoxidation methods are difficult to completely remove inclusions [45]. Hydrogen reacts with dissolved oxygen in the molten steel to produce water, which can directly discharge the molten steel and effectively reduce the oxygen content in the steel [36, 46-48]. At the same time, the injection of gaseous hydrogen into the liquid

steel can also stir the liquid steel to strengthen mass transfer, increase the diffusion rate of dissolved oxygen to the interface between hydrogen bubble and liquid steel, and improve the kinetic conditions of hydrogen deoxidation [27, 33-34]. However, with the refining process, the driving force of dissolved oxygen mass transfer to the hydrogen bubble-liquid steel interface decreases, and the deoxidation rate and hydrogen utilization rate both decrease, as shown in Fig. 8 [49].

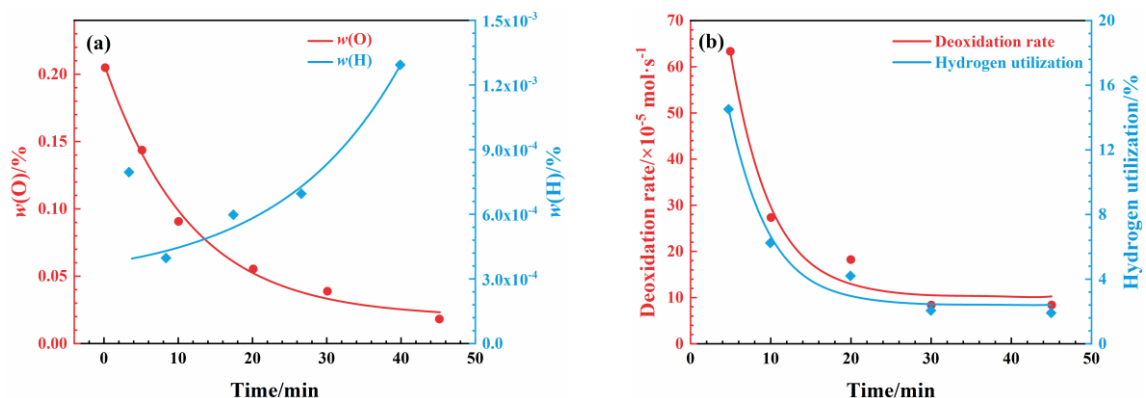
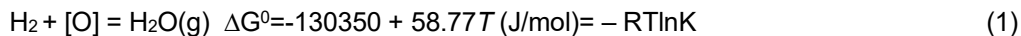


Fig. 8. Effect of hydrogen blowing time on the rate of deoxidation and hydrogen utilization: (a) Oxygen and hydrogen content in steel; (b) Deoxidation rate and hydrogen utilization rate.

In the process of hydrogen deoxidation, due to the low solubility of hydrogen in molten steel, the atomic hydrogen deoxidation reaction is limited, and the deoxidation is mainly controlled by the reaction rate of molecular hydrogen and dissolved oxygen. The molecular

hydrogen deoxidation reaction equation is shown in (1) and (2). It can be seen that when the steelmaking temperature is constant, hydrogen deoxidation is controlled by  $P_{H_2O}/P_{H_2}$ , and it is independent of the [H] content in steel and pressure [49-50].



$$[\%O] = \frac{P_{H_2O}}{P_{H_2}} \frac{1}{f_O \cdot K} \quad (2)$$

Although hydrogen deoxidation is not affected by pressure, when the C content in steel is high and the environmental pressure is low, the carbon-oxygen reaction product CO continues to be discharged from the molten steel, resulting in the carbon-oxygen reaction continuing, and the deoxidation means is transformed into carbon deoxidation. When carbon deoxidation is dominant, the tiny bubbles formed by blowing hydrogen can provide a nucleation interface for CO, adsorb CO and discharge molten steel, and cooperatively promote deoxidation [46, 49-50].

Therefore, by controlling the pressure and promoting the alternating deoxidation of carbon and hydrogen, high purity steel smelting can be achieved, the specific steps are shown in Fig. 9 [50]:

(1) In the late stage of converter smelting, [C%] is low and [O] is excessive in steel. At the same time of hydrogen blowing deoxidation, the hydrogen bubble can provide the carbon-oxygen reaction interface and reduce the nucleation resistance, and the carbon-

oxygen reaction products are removed with the hydrogen bubble floating up, as shown in Fig. 9 (a);

(2) Tapping and ladle bottom blowing  $H_2$ . Without an external oxygen source, [C] has competitive deoxidation with  $H_2$ , and carbon and hydrogen deoxidation is carried out alternately. As in (1), the  $H_2$  bubbles can provide reaction interfaces and reduce nucleation resistance, and the reaction products can discharge out of the molten pool via the  $H_2$  bubbles, as shown in Fig. 9 (b);

(3) Before vacuum refining, adding sufficient amount of carbon powder, carbon deoxidation capacity is enhanced and dominant, and the deoxidation product CO is removed by floating into the hydrogen bubble, as shown in Fig. 9 (c);

(4) In the vacuum treatment stage, high vacuum leads to carbon deoxidation capacity is stronger than hydrogen, only C can complete deep deoxidation, while dissolved hydrogen in steel is also removed at this stage, as shown in Fig. 9 (d).

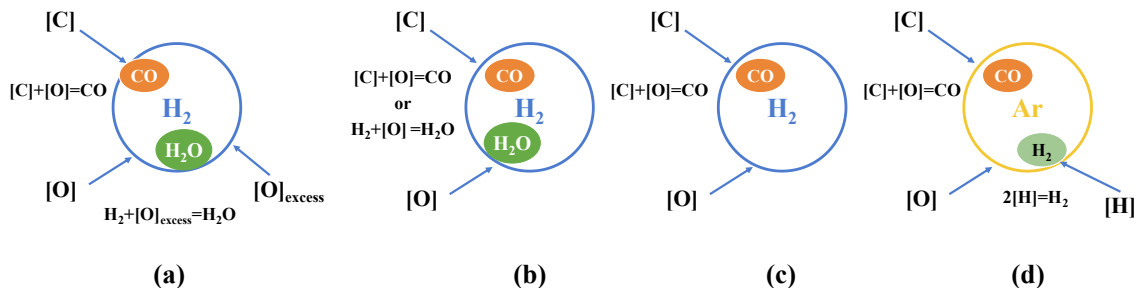


Fig. 9. Method of smelting high-clean steel in converter: (a)  $H_2$  bottom blowing at the later stage of converter smelting; (b) Tapping and ladle bottom blowing  $H_2$ ; (c) Adding carbon powder into ladle; (d) RH vacuum treatment.

Based on the characteristics of high-efficiency hydrogen deoxidation and the easy floating of hydrogen bubbles, the "micro-hydrogen bubble" refining technology has been developed. Due to its simple operation and remarkable deoxidation and inclusion removal effects, it has attracted more attention [30-31, 51-53]. The specific technical route is as follows: First, a large amount of hydrogen or hydrogen-containing gas is injected into the liquid steel for refining, which in addition to efficient deoxidation, while the dissolved hydrogen in steel reaches more than  $8 \times 10^{-6}$ ; After that, in the vacuum refining process, the dissolved hydrogen in steel is vacuumed to form tiny bubbles (1 mm) with inclusions as heterogeneous nucleation points, which

are carried and adhered to the inclusions to float to the slag for removal. In addition, the generated hydrogen bubble reduces the nitrogen partial pressure and strengthens the nitrogen removal effect of the liquid steel. Practice has proved that the micro-hydrogen bubble refining effect is obvious,  $w(O) \leq 20 \times 10^{-6}$ ,  $w(H) \leq 2 \times 10^{-6}$ ,  $w(N) \leq 60 \times 10^{-6}$  in steel, and the cleanliness has been significantly improved, as shown in Fig. 10 [51]. To sum up, the key of the micro-hydrogen bubble method is to improve the solubility of hydrogen in molten steel, and pressure metallurgy can be used to increase the amount of hydrogen dissolved in molten steel in the actual production [54-55].

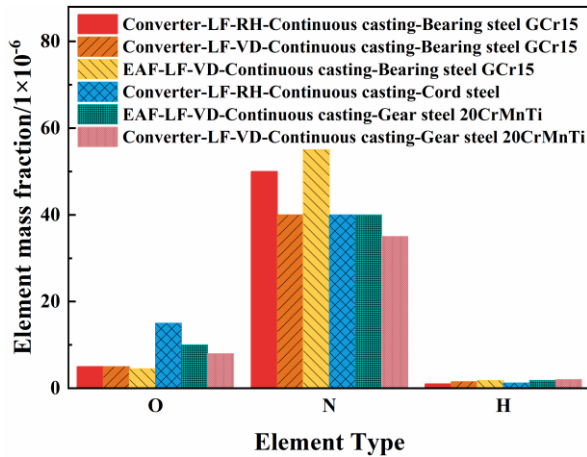


Fig. 10. Effect of micro hydrogen bubble method on the content of O, N and H elements in steel.

The above analysis is not difficult to see that after hydrogen deoxidation, the oxygen content in steel is still high, and the deep deoxidation effect is poor. The activation energy of hydrogen plasma and oxygen in steel is lower, and the deoxidation reaction is easier to carry out [37]. Therefore, hydrogen plasma has the potential of deep deoxidation. Take the deoxidation of hydrogen plasma based on argon-hydrogen mixture as an example, as shown in Fig. 11 [40-41].

Hydrogen plasma deoxidation is mainly divided into two stages, namely: 1) rapid deoxidation stage, the deoxidation rate is fast, and the oxygen content in liquid iron is rapidly reduced to a low level; 2) In the deep deoxidation stage, the deoxidation rate is slow, and the minimum oxygen content after deoxidation can be below  $5 \times 10^{-6}$ . The deoxidation rate and limit of the whole hydrogen plasma deoxidation process increase significantly with the increase of the concentration of

hydrogen plasma particles, the lowest can be about  $1 \times 10^{-6}$ , with strong deoxidation capacity and no other types of inclusions generated.

In addition, hydrogen-containing reducing gases such as  $\text{CH}_4$  and liquefied petroleum gas also have deoxidation capacity [45, 56-59]. In steelmaking environment,  $\text{CH}_4$  can be decomposed into C and  $\text{H}_2$  ( $\text{CH}_4 = \text{C} + 2\text{H}_2(\text{g})$ ), and then react with [O] in steel, deoxidation products ( $\text{CO}$  and  $\text{H}_2\text{O}$ ),  $\text{H}_2$  and undecomposed  $\text{CH}_4$  can be removed by floating up with bubbles. Studies have shown that [56], at  $1600^\circ\text{C}$ ,  $\text{CH}_4$  has a significant deoxidation effect, and can be used as an initial deoxidizer to deoxidize liquid steel, as shown in Fig. 12. Similarly, hydrogen-containing reducing gases such as liquefied petroleum gas will decompose at high temperatures to generate C and  $\text{H}_2$  for deoxidation refining of liquid steel [59].

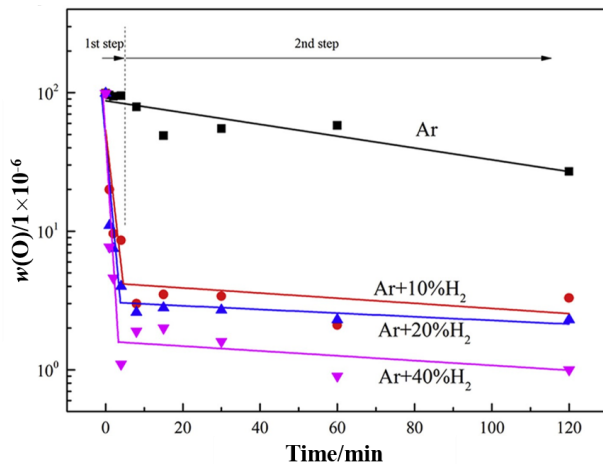


Fig. 11. Oxygen content trend with time in hydrogen plasma melting process.

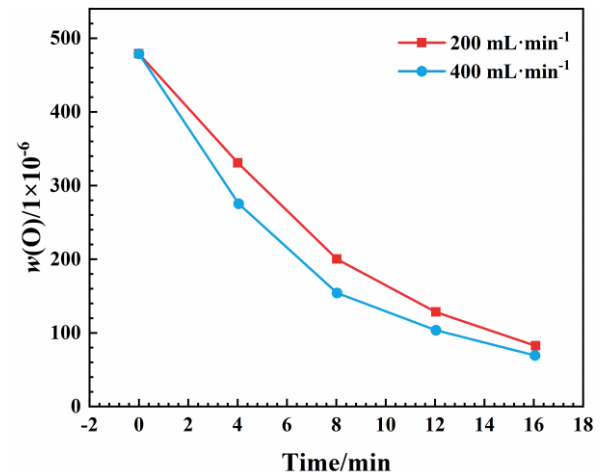


Fig. 12. Oxygen mass fraction of molten steel during  $\text{CH}_4$  deoxidation.

#### 4.2. "Hydrogen" decarbonization

Carbon is an important element that affects the mechanical and corrosion properties of steel, and is one of the most concerned indexes in steelmaking process. At present, oxygen blowing is one of the most common way for decarbonization, but it will increase  $\text{CO}_2$  emissions and lead to a substantial increase in oxygen in steel, which greatly increases the difficulty of

deoxidation in subsequent refining processes and increases the proportion of large-size harmful non metallic inclusions in steel [60]. Therefore, it is very difficult to achieve high purity smelting by this refining method. It is found that carbon in steel is extremely difficult to react with gaseous hydrogen at steelmaking temperature, but it is very easy to react with hydrogen in plasma state to generate  $\text{CH}_4$  gas and directly discharge liquid



steel. While decarbonizing and controlling carbon, there is no residue of inclusions polluting liquid steel and “zero” CO<sub>2</sub> emission, as shown in Fig. 7(b) [37-38, 43, 61].

Because metal plasma guns are expensive and difficult to be maintained, hydrogen plasma is currently formed in the refining process mainly through the dissociation of hydrogen or hydrogen-containing gases by hollow graphite electrode plasma guns. The use of graphite electrode will cause carbonization of liquid steel to a certain extent and increase carbon content [25, 62]. Carbonization only occurs at low carbon

content in the steel, and the greater the concentration of hydrogen plasma particles in plasma, the weaker the carbonization phenomenon and the smaller the carburization degree. For example, the proportion of hydrogen increases from 10% to 20%, and the carbonization rate of molten steel decreases from  $3.73 \times 10^{-6}/\text{min}$  to  $3.1 \times 10^{-6}/\text{min}$ , as shown in Fig. 13 (a) [63]. When the carbon content of molten steel is high, the hydrogen plasma decarburization effect is very significant and is completely unaffected by carbonization, as shown in Fig. 13 (b) [38].

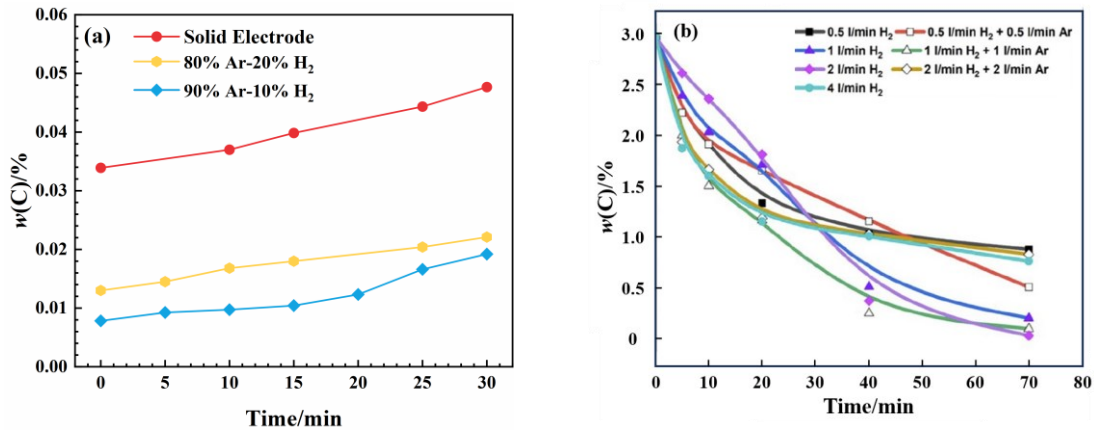


Fig. 13. Effect of hydrogen plasma on C content in steel: (a) Low carbon steel; (b) High carbon steel.

Although gaseous hydrogen cannot directly decarbonize steel, compared with argon, blowing hydrogen is more likely to form small dispersed bubbles, which can provide a nucleating interface for CO, adsorb CO and discharge liquid steel, accelerate the reaction of carbon residue and oxygen in steel, and further reduce the content of C in liquid steel [46, 49-50], as shown in Fig. 14.

In summary, “hydrogen” has excellent decarbonization ability, especially hydrogen plasma, can achieve deep decarbonization, but under low carbon conditions, the degree of decarbonization is affected by plasma gun material and hydrogen plasma particle concentration, etc. In actual production, it is necessary

to rationally optimize the production process according to the carbon content requirements of steel grades.

#### 4.3. “Hydrogen” denitrification

Similar to decarbonization, nitrogen in steel cannot be removed by reacting with gaseous hydrogen to form gaseous products at steelmaking temperature, as shown in Fig. 7 (c) [37]. However, the small dispersed bubbles formed by blowing hydrogen increase the interface reaction area and promote the diffusion of nitrogen in steel to the hydrogen bubble interface to form nitrogen, thus reducing the N content in steel [51]. Nitrogen in liquid steel can be reduced to 0.002% by injecting hydrogen at normal pressure, as shown in Fig. 15 [49].

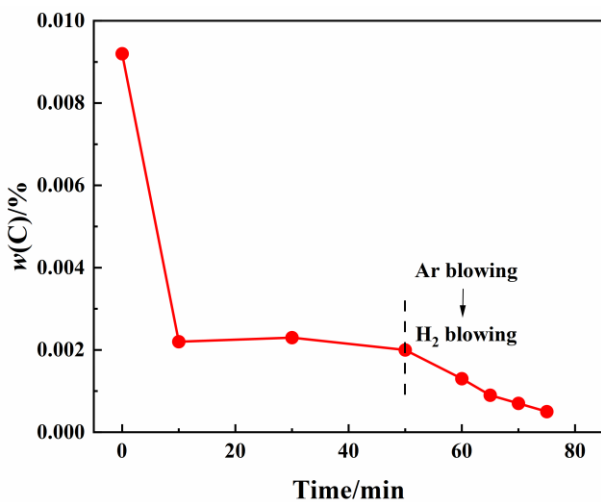


Fig. 14. Effect of hydrogen blowing on the C content in steel.

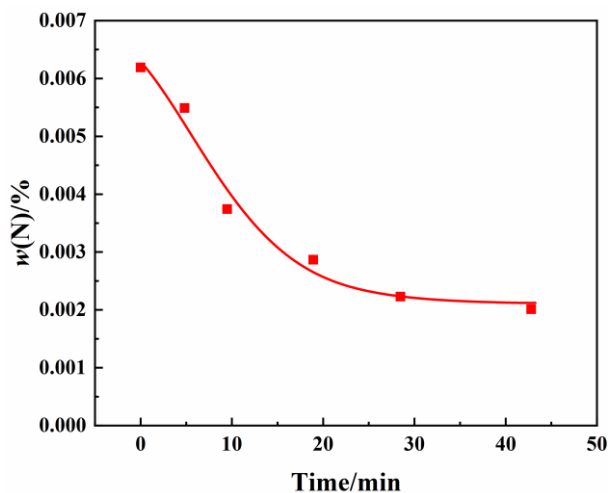


Fig. 15. Variation of elemental N content in steel with time.

In contrast, hydrogen plasma can easily react with [N] in steel to generate  $\text{NH}_3$ , which can discharge liquid steel and effectively reduce the N content in steel. Therefore, in EAF smelting, ladle refining, VOD refining or RH refining, hydrogen can be added to argon/nitrogen to form hydrogen-containing plasma to achieve

efficient nitrogen removal [43, 64]. In addition, the use of hydrogen-containing reduction gas such as  $\text{CH}_4$  instead of hydrogen to dissociate hydrogen plasma also has the effect of nitrogen removal, as shown in Table 1 [19, 42, 65-66].

Table 1. Examples of changes in nitrogen content in plasma melted steel.

Experimental equipment	Alloy Melt	Gas	Effect of nitrogen removal
20 kVA DC Electric Arc Furnace	Pure Iron	$\text{Ar-N}_2\text{-H}_2$	Compared to $\text{Ar-N}_2$ , $w(\text{N})$ decreases in $\text{Ar-N}_2\text{-H}_2$
150 kg Electric Arc Furnace (Two AC Plasma Torches)	Molten Steel	90%Ar-10%H <sub>2</sub>	$w(\text{N})$ decreases to $1 \times 10^{-4}$
		95%Ar-5%CH <sub>4</sub>	$w(\text{N})$ decreases to $15 \times 10^{-6}$
2 ~ 5 kg Crucible (Plasma Furnace with Single Plasma Torch)	Stainless Steel	Ar-H <sub>2</sub>	$w(\text{N}) < 0.05\%$
	Pure Iron		$w(\text{N})$ reduced from 0.05% to 0.015%
	25%Cr-Fe		$w(\text{N})$ reduced from 0.11% to 0.065%
150 kg Plasma Furnace	Carbon Saturated Low Alloy Steel	CH <sub>4</sub>	$w(\text{N})$ reduced from 0.21% to 0.15%
	Low Alloy Steel	Kerosene	$w(\text{N})$ reduced from 0.18% to 0.11%
Plasma Arc Melting Furnace	Pure Iron	Ar-1%H <sub>2</sub>	$w(\text{N})$ can be reduced to $2 \sim 3 \times 10^{-6}$
		Ar-5%H <sub>2</sub>	$w(\text{N})$ can decrease to as low as $1 \times 10^{-6}$

#### 4.4. "Hydrogen" desulphurization

At present, slagging desulphurization and addition of desulphurization agents are the most commonly used desulphurization methods, but the desulphurization efficiency of such methods is relatively low, and sulfide inclusions are easily formed, which deteriorates the mechanical properties of materials. In contrast, hydrogen desulfurization produces  $\text{H}_2\text{S}$  gas, which can directly exclude liquid steel without inclusion residue, and can realize ultra-low sulfur steel smelting [37-39, 41]. Like hydrogen decarbonization and nitrogen, gaseous hydrogen cannot react with sulfur in steel, as shown in Fig. 7 (d) [37]. However, the fine dispersed hydrogen bubbles formed by blowing hydrogen not only increase the content of dissolved hydrogen in steel, but also accelerate the reaction of sulfur with the locally dissolved hydrogen, and the reaction product  $\text{H}_2\text{S}$  can be removed with the hydrogen bubbles to achieve desulfurization. However, when the sulfur content of molten steel is low, the desulfurization effect of hydrogen injection is extremely limited [46, 49], as shown in Fig. 16 (a). In contrast, hydrogen plasma desulfurization has a more significant effect, similar to hydrogen plasma deoxidation, and the degree and rate of desulfurization are greatly improved with the increase of hydrogen plasma particle concentration, as shown in Fig. 16 (b) [39, 41].

#### 4.5. "Hydrogen" dephosphorization

For most types of steel, the high content of phosphorus in steel is very easy to cause serious

segregation in the solidification process of steel, thus reducing the impact performance of steel and deteriorating the service performance of steel, so it is necessary to remove phosphorus as much as possible in the smelting process [67]. Commonly used dephosphorization methods such as lime powder blowing will seriously erode the furnace lining and seriously deteriorate the safety of the furnace lining [68]. In contrast, hydrogen plasma can react with phosphorus in steel to generate  $\text{PH}_3$  gas and directly discharge liquid steel, which can control phosphorus in steel at a lower level, as shown in Fig. 17 [38]. However,  $\text{PH}_3$  will decompose into P and  $\text{H}_2$  in a high temperature environment, so it is necessary to reasonably control the smelting temperature, refining time and vacuum degree during the dephosphorization of hydrogen plasma to prevent the "phosphorus return" of liquid steel.

In summary, "hydrogen" can react with impurity elements such as O, C, N, S and P in steel to generate gaseous products, achieve high efficiency, less slag and "zero inclusions" pollution-free refining, in which plasma hydrogen can be deeply refined, and can completely avoid the oxygen decarbonization process, and greatly reduce the  $\text{CO}_2$  emissions of smelting processes such as electric arc furnace and converter. At the same time, the cleanliness of the liquid steel is greatly improved. Therefore, "hydrogen" refining will be an important refining way for the preparation of green high-quality high-end special steel in the future.

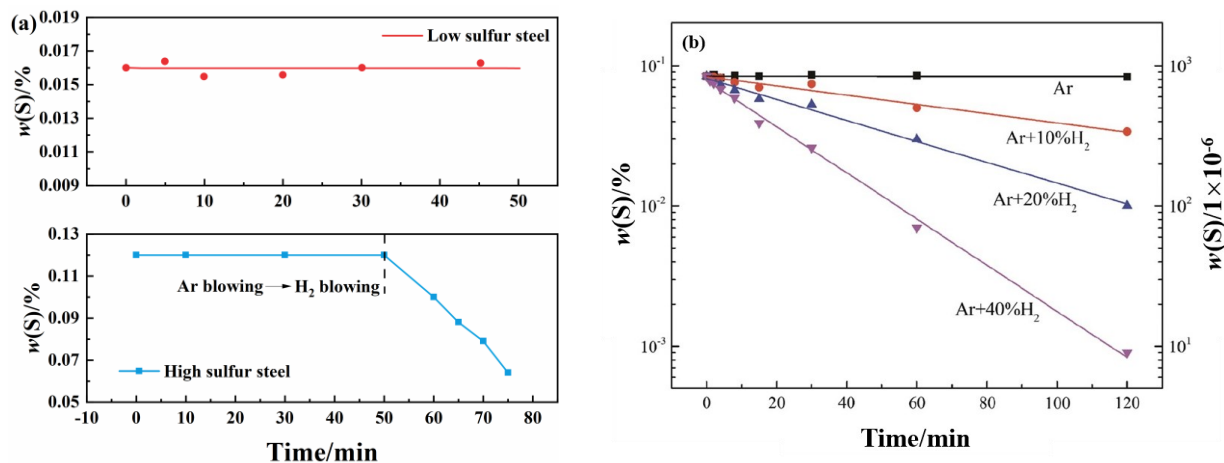


Fig. 16. Effect of "hydrogen" on the S content of steel: (a) Hydrogen; (b) Hydrogen plasma.

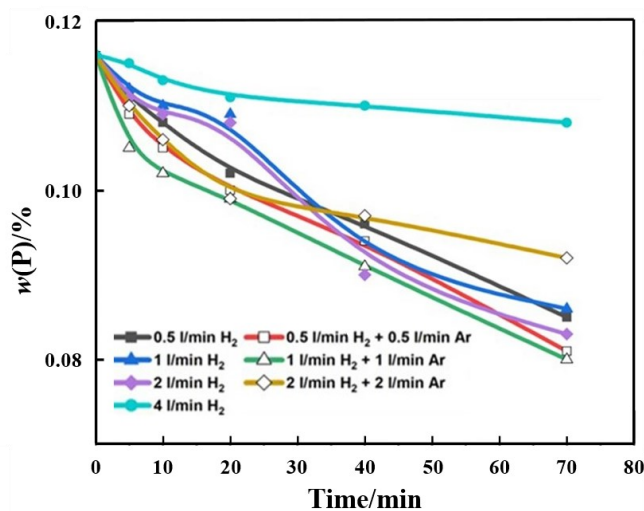


Fig. 17. Effect of hydrogen plasma on the P content of steel.

### 5. Prospects for a new generation of hydrogen metallurgy steelmaking processes

"Hydrogen" is the clean energy with the greatest development potential in the 21st century, and it is the best substitute for coal and other fossil fuels [9, 10]. The use of "hydrogen" in the process of steelmaking has outstanding advantages, which can not only achieve rapid melting and high-clean refining, but also significantly reduce  $CO_2$  emissions in the process of steelmaking [27, 34-35]. Under the background of the implementation of the environmental protection strategy, the steel preparation process has gradually evolved into three categories: "BF-BOF" process, "Scarp-EAF" process, "DRI-EAF" process. Among them, the "DRI-EAF" process has the natural properties of low carbon and even zero carbon, and its  $CO_2$  emission reduction ability is obvious to all. At present, hydrogen metallurgy mainly focuses on the ironmaking process, as shown in Table 2 [2, 69], and there are few reports on the theoretical research and production application of hydrogen metallurgy steelmaking. Therefore, hydrogen metallurgy through the entire iron and steel metallurgy production process is the development direction to promote the green, high-quality and

sustainable development of the iron and steel industry.

Therefore, based on the outstanding advantages of hydrogen metallurgy steelmaking, which is characterized by green, low carbon, rapid melting and high efficiency and high cleanliness refining, a new generation of green and near-zero carbon steel production process with hydrogen plasma electric furnace and hydrogen plasma refining furnace as the core is proposed (Fig. 18). Its core includes low carbon ironmaking, low carbon and low oxygen steelmaking and "zero inclusion" pollution-free refining and other hydrogen metallurgy technologies. The main processes include:

1. The use photovoltaic, wind power and other clean energy power (green electricity) to produce hydrogen by water electrolysis (green hydrogen);
2. Using hydrogen-rich gas such as pure hydrogen, natural gas and petrochemical waste hydrogen as reducing agent, low carbon or no carbon pure DRI is produced by hydrogen-based shaft furnace;
3. The use of green electric furnace (hydrogen plasma furnace) [43] and pollution-free refining furnace [44] (hydrogen plasma ladle refining furnace) to achieve near-zero carbon emission steelmaking;

4. Through continuous casting and rolling, the required steel was produced; Some high-end special steels adopt the new generation of gradient ultrafast cooling mold casting and controlled atmosphere

electroslag remelting and other special metallurgical technologies, and then produce high-end special steel products that meet the requirements through forging and heat treatment.

Table 2 Research status and objectives of hydrometallurgy

Project Sponsor	Project name/Key technology	Goals/Achievements
Europe	ULCOS	CO <sub>2</sub> emission are reduced by 50%
Japan	COURSE50	Hydrogen is used as a reducing agent to reduce carbon emissions by 10%
Korea	COOLSTAR	Direct reduced iron is produced by hydrogen reduction
Austrian	H2FUTURE	To produce hydrogen by electrolysis of water, the hydrogen yield is 1200 cm <sup>3</sup> /h
German	Thyssenkrupp hydrogen-based ironmaking experiment	Hydrogen production from electrolyzed water for the reduction of iron ore and steelmaking, with the aim of achieving a 30% reduction in carbon emissions by 2030 and zero carbon emissions by 2050
Sweden	HYBRIT	Electrolysis of water to produce hydrogen and use of hydrogen to produce direct reduced iron
US	MIDREX	Using hydrogen volume fraction exceeds 50% of the reducing gas preparation of iron oxide
China Baowu Steel Group Corporation	Hydrogen-rich carbon cycle in blast furnace, Hydrogen reduction and Hydrogen production technology of nuclear energy, etc.	Carbon peak by 2023, carbon reduction by 30% by 2035, and carbon neutrality by 2050
HBIS	Energiron-ZR (zero reforming) technology replaces carbon metallurgy, and hydrogen metallurgy research agreements are signed with all parties	Construction of 1.2 million tons of hydrogen metallurgy project, 70% of hydrogen used for the production of direct reduced iron
Angang Steel Group Limited	Wind power + photovoltaic power - electrolytic water hydrogen production - hydrogen metallurgy technology	Total carbon emissions by 2035 will be 30% lower than peak
Baogang Group	Carrying out research on low-carbon metallurgical technologies and industrialized applications	Photovoltaic hydrogen production - Pipeline transport of hydrogen - green hydrogen metallurgy
JISCO	The Hydrogen Metallurgy Research Institute was established, and the demonstration base of "Coal-based hydrogen metallurgy + Dry grinding and dry separation of iron from Jiusteel" was built	Founded "coal-based hydrogen metallurgy theory" and "Shallow hydrogen metallurgy magnetization roasting theory"
Zhongjin Taihang Mining Co., LTD	Coke oven gas dry reforming reduction + PERED shaft furnace process combination	Hydrogen-based direct reduced iron project with an annual output of 300000 t
Jianlong Group	Hydrogen-based melting reduction smelting high purity cast iron and development of hydrogen-rich melting reduction CISP new process	Annual CO <sub>2</sub> emissions are reduced by 112000 t
Nippon Steel Group	Hydrogen was extracted by producing ethylene acetate symbiotic product from natural gas	It is planned to produce 50 t of direct reduced iron per year
Jinnan Steel	Blast furnace hydrogen-rich injection	Hydrogen injection in 2000 m <sup>3</sup> blast furnaces

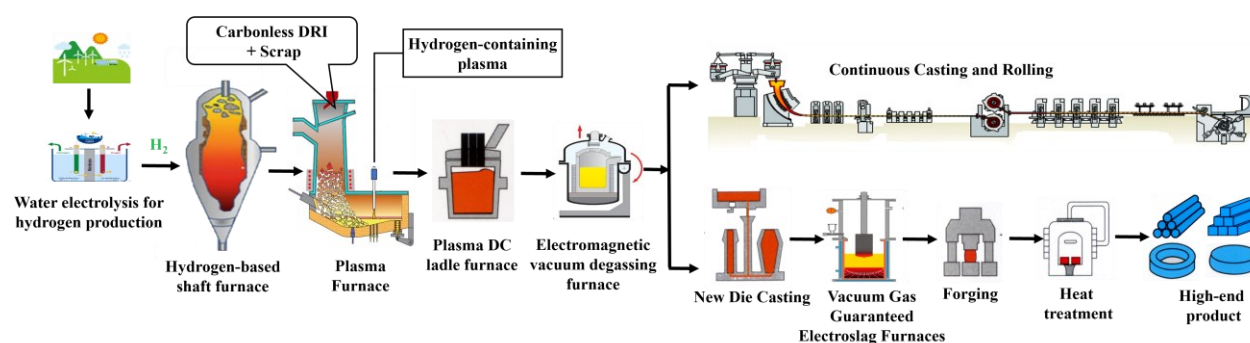


Fig. 18. New-generation ferrous metallurgical process with zero-carbon hydrometallurgy.

Fig. 19 shows the comparison between the new process and the traditional process. It can be seen from the figure that the oxygen content in the traditional process is reduced to a very low level after the iron-making stage, but it is significantly increased in the stage of oxygen blowing and decarburization in steelmaking. The deoxidizing agent such as aluminum needs to be added for subsequent deoxidation, and the deoxidizing products pollute the liquid steel as non-metallic inclusions. It will eventually lead to a decrease in the cleanliness of the liquid steel. In contrast, in the whole new process, the oxygen content has been in a continuously decreasing state, the steelmaking process basically does not need to deoxidize or use pollution-free hydrogen plasma deoxidize, and the steel is basically free of inclusions, so ultra-high clean steel can be manufactured. In terms of the change of the carbon content, the carbon content of hot metal in the traditional process of ironmaking stage reaches about 4.5%, and in the steelmaking stage, a large amount of oxygen is blown to decarbonize, resulting in a large amount of carbon consumption, and the CO<sub>2</sub> emission per ton of steel is as high as 1.8 t. The new process

uses hydrogen reduction, and the whole process only needs to add an appropriate amount of carbon to the liquid steel according to the target carbon content of the steel grade, without the decarbonization process, that is, to achieve near zero CO<sub>2</sub> emissions. In terms of temperature, compared with the traditional process, the temperature in the ironmaking stage of the new process is significantly reduced, and the temperature in the steelmaking stage is also reduced. From the perspective of solid waste gas emission, the slag amount of the new process in the ironmaking stage is only 1/5 of the traditional process, and the slag amount in the steelmaking stage is only 1/10 of the traditional process. Therefore, compared with the traditional BF-BOF process, the new process has a remarkable effect on energy saving and emission reduction. It is estimated that the new process will reduce CO<sub>2</sub> emissions by more than 95%, reduce oxygen consumption by more than 95%, save energy by 30-50%, shorten production cycle by more than 50%, reduce cost by 30-50%, reduce nitrogen content in steel by 10-50%, reduce oxygen content by 10-50%, and reduce non-metallic inclusions by 50-90%.

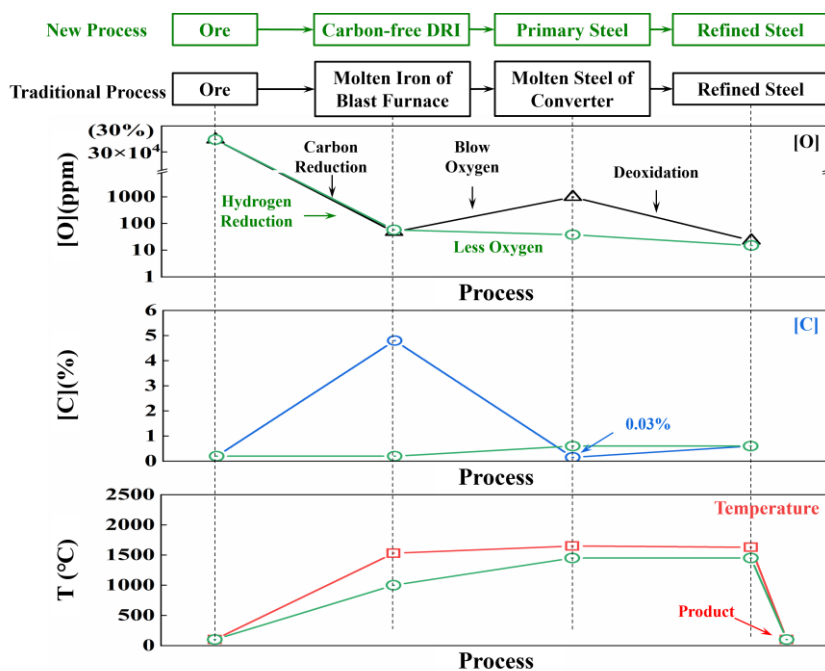


Fig. 19. Comparison of oxygen content, carbon content and temperature in the new process with the traditional blast furnace-converter long process.

The development of the above-mentioned innovative new processes is one of the important ways for China to accelerate the implementation of green development and upgrade the quality of steel products. Therefore, strongly develop the basic theoretical research of hydrogen metallurgy steelmaking, develop key equipment such as new green electric furnace (hydrogen plasma electric furnace) and pollution-free refining furnace (hydrogen plasma ladle refining furnace), and develop an innovative new steelmaking technology characterized by "hydrogen steelmaking" instead of "oxygen steelmaking". It will effectively solve important problems such as ecological environmental

pollution and unstable product quality in the steel industry, so as to promote the green, high-quality and sustainable development of the iron and steel industry.

## 6. Conclusion and prospect

"Hydrogen steelmaking" replacing the traditional "oxygen steelmaking" is an innovative theory and technology in the current steelmaking field, overcoming the theory and key technologies of hydrogen metallurgy steelmaking, and fully opening up a new generation of green near-zero carbon steel production process based on hydrogen metallurgy, which is an important means to promote the green, high-quality and sustainable development of China's iron and steel industry



and implement the goal of “double carbon” and “high-quality development”.

(1) Hydrogen plasma has the advantages of high temperature and high thermal conductivity, and can be used as an efficient heat source to achieve rapid melting of charge or precise temperature control of liquid steel, which has been preliminarily applied in steelmaking processes such as EAF, converter and tundish.

(2) The injection of hydrogen can promote the homogenization of the composition and temperature of the molten steel, and the hydrogen bubble can adhere to non-metallic inclusions during the floating process, and the “hydrogen” can also react with dissolved oxygen and sprayed oxygen to release a lot of heat, improving the thermodynamic and kinetic conditions of the molten pool reaction.

(3) “Hydrogen” can create a reducing atmosphere, which can inhibit the over-oxidation of liquid steel,

reduce the iron loss in the steelmaking process, and the loss of other metal elements such as Cr and Mn.

(4) “Hydrogen” can efficiently remove impurities such as O, C, N, S and P, especially hydrogen plasma, which can directly generate highly volatile gas products such as H<sub>2</sub>O, CH<sub>4</sub>, NH<sub>3</sub>, H<sub>2</sub>S and PH<sub>3</sub>, to avoid the formation of non-metallic inclusions, and achieve “zero inclusions” of high cleanliness steelmaking, which is the development direction of future steelmaking technology.

(5) A new generation of green near-zero carbon steel production process based on hydrogen metallurgy is the key to accelerate the green, high-quality and sustainable development of China's iron and steel industry and the implementation of the goal of “double carbon” and “high-quality development”, and is currently a major issue in the field of iron and steel metallurgy.

### References

1. Lu, L. J., Wang, F., Wang, H. F., Qiu, J., & Ping, X. D. (2024). *J. Iron Steel Res*, 36(2), 150-162
2. Tong, S., Ai, L. Q., Hong, L. G., Zhou, M. J., & Yuan, Y. P. (2023). *Mater. Rep*, 37(23), 117-124
3. Y, J., Xu, L., Liu, Z. P., & Chen, H. Z. (2022). *China Metall*, 32(4), 1-8
4. Wang, Z., Xiao, L. J., & Gan, Y. (2024). *Mater. Rep*, 38(03), 101-107
5. Li, X. (2022). *China Plant Engineering*, (4), 1
6. Yang, Z. W., Yu, J. B., Zhang, Y. F., Wang, J., & Ren, Z. M. (2023). *China Metall*, 33(12), 31-41
7. Lu, L. J., Wang, F., Wang, H. F., Qiu, J., & Ping, X. D. (2024). *Iron & Steel*, 59(03), 183-196
8. Zhang, S. C., Jiang, Z. H., Li, H. B., Zahng, W., Li, G. P., & Fan, G. W. (2019). *J. Iron Steel Res*, 31(2), 132-144
9. Okolie, J. A., Patra, B. R., Mukherjee, A., Nanda, S., Dalai, K., & Kozinski, A. (2021). *Int. J. Hydrogen Energy*, 46(13), 8885-8905
10. Liu, W., Zuo, H., Wang, J., Xue, Q. G., Ren, B. L., & Yang, F. (2021). *Int. J. Hydrogen Energy*, 46(17), 10548-10569
11. Zhao, Z. L. (2023). *Sustainable Mining and Metallurgy*, 39(5), 1-8
12. Yu, Y., Wang, F., Qi, Y. H., Zheng, A. J., & Li, Y. (2024). *J. Iron Steel Res*, 36(3), 283-298
13. Wu, G. Y., & Dai, Y. N. (1998). *J. Kunming Univ. Sci. Technol., Sci. Technol*, (3), 110-117+122
14. Zhang, Y. W., Ding, W. Z., Guo, S. Q., & Hu, X. K. (2004). *Shanghai Met*, (4), 17-20
15. Zarl, M. A., Farkas, M. A., & Schenk, J. (2020). *Metals*, 10(10), 1394
16. Ding, C. Y., Xue, S., Chang, R. D., Jiang, F., & Long, H. M. (2024). *J. Iron Steel Res*, 36(05), 568-579
17. Hu, M. L., Li, Z. X., Wei, J. G., Wei, X. G., & Wu, Z. H. (1985). *Mater. Prot*, (4), 2-5
18. Tang, H. Y., Liu, J. W., Wang, K. M., Xiao, H., & Li, A. W. (2021). *Acta Metall. Sin*, 57(10), 1229-1245
19. Zhang, H. S. (2010). PhD Thesis, *Northeastern University*
20. Ye, M. L. (2020). PhD Thesis, *University of Science and Technology Beijing*
21. Zhang, H. S., Zhan, D. P., Jiang, Z. H., Chen, Z. P., & Shen, H. J. (2009). *Ind. Heat*, 38(5), 10-13
22. Zhan, D. P., Zhang, H. S., Jiang, Z. H., Gong, W., Li, H. B., & Chen, Z. P. (2011). *Adv. Mater. Res*, 402, 142-146
23. Wan, T. J., Yuan, Z. F., Fan, Y. S., & Xin, C. (1991). *Iron Steel Vanadium Titanium*, (3), 75-79
24. Chen, K. Y., Chang, L. Z., & Wang, J. J. (2015). *Wide and Heavy Plate*, 21(5), 38-43
25. Li, J. S., Wang, C., Chen, Y. F., Yang, S. F., Liu, W., Bai, Y., Huang, Y. C., & Sun, Y. (2024). *Special Steel*, 45(1), 1-11
26. Mao, B., Tao, J. M., & Jiang, T. X. (2008). *Continuous Casting*, (5), 4-8
27. Liu, J. H., Pan, Y. K., He, Y., Zhang, J., Yan, B. J., & Deng, Z. Q. (2022). *China*, CN113337669B, 2022
28. Zheng, S. G., & Zhu, M. Y. (2008). *Iron & Steel*, (6), 25-29
29. Xue, Z. L., Wang, Y. F., Wang, L. T., Li, Z. B., & Zhang, J. W. (2003). *Acta Metall. Sin*, (4), 431-434
30. Liu, J. H., Zhang, J., & Li, K. W. (2017). *Steelmaking*, 33(2)(2017), 1-9+14
31. Li, K. W., Liu, J. H., Zhang, J., & Shen, S. B. (2017). *Metall. Trans. B*, 48(4), 2136-2146
32. Liu, J. H., Zhang, S., & He, Y. (2022). *China*, CN113621759B
33. He, Y., Xu, H., Liu, J. H., Zhang, J., Yan, B. J., & Deng, Z. Q. (2022). *China*, CN113373277B
34. He, Y., Liu, J. H., Zhang, J., Yan, B. J., & Deng, Z. Q. (2022). *China*, CN113355477B
35. Liu, J. H., Peng, H. B., He, Y., Yang, X. D., Xu, H., & You, D. L. (2022). *Metals*, 12(10), 1633
36. Xu, H., Liu, J. H., He, Y., & Liu, H. B. (2023). *Clean Technol. Environ. Policy*, 25(7), 2377-2391
37. Kumar, R., Saha, A. K., & Mandal, A. K. (2023). *Can. Metall. Q*, 62(2), 383-395
38. Kumar, R., Saha, A. K., Malik, K. N., & Mandal, A. K. (2023). *JOM*, 75(12), 5667-5675
39. Guo, X. L., Yu, J. B., Zhang, Y. J., Li, X., Wang, J., Liao, H. L., & Ren, Z. M. (2018). *Metall. Trans. B*, 49(6), 2951-2955
40. Guo, X. L., Yu, J. B., Zhang, Y. J., Liu, L., Liao, H. L., & Ren, Z. M. (2018). *Int. J. Hydrogen Energy*, 43(27), 12153-12157
41. Guo, X. L. (2019). PhD Thesis, *Shanghai University*

42. Mimura, K., Saito, K., & Isshiki, M. (1999). *Jpn. Inst. Met.*, 63(9), 1811-1190
43. Jiang, Z. H., Zhu, H. C., Lu, H. B., Yao, C. L., Zheng, Y. J., Zhang, S. C., & Zheng, L. C. (2023). *China*, CN115679036A
44. Jiang, Z. H., Zhu, H. C., Lu, H. B., Yao, C. L., Zheng, Y. J., Zhang, S. C., & Zheng, L. C. (2024). *China*, CN115595401B
45. Xing, W., Ni, H. W., Zhang, H., & He, H. Y. (2009). *The Chinese Journal of Process Engineering*, 9(S1), 443-447
46. Makarov, M. A., & Aleksandrov, A. A. (2009). *Russ. Metall.*, (2), 95-99
47. Cao, L., Zhu, L. G., Guo, Z. H., & Qiu, G. X. (2023). *Ironmaking & Steelmaking*, 50(4), 360-369
48. Liu, Y., Lu, Y. C., Wang, H. B., Zhu, Z. Y., Zhao, J., Wang, Z. M., Ma, C. W., Li, H. B., Wang, Y. L., Liu, B. S., Hao, N., Hu, X. T., Kuai, D. S., Xie, C. H., & Liu, G. L. (2022). *China*, CN114058785A
49. Xing, W., Ni, H. W., Zhang, H., He, H. Y., Cheng, R. J., & Xu, B. (2009). *The Chinese Journal of Process Engineering*, 9(S1), 234-237
50. Cao, L., Zhu, L. G., & Guo, Z. H. (2023). *J. Iron Steel Res. Int.*, 30(1), 1-20
51. Liu, J. H., Zhang, J., He, Y., Ding, H., & Deng, Z. Q. (2018). *China*, CN106086315B
52. Liu, J. H., Zhang, S., He, Y., & Zhang, J. (2020). *China*, CN110592322B
53. Zhang, J., He, Y., Liu, J. H., Yan, B. J., Zhang, S., & Li, W. (2019). *Vacuum*, 168, 108803
54. Ren, Z. M., Li, X. F., Guo, X. L., Hou, Y., & Yu, J. B. (2019). *China*, CN105779699B
55. Zhang, J. (2020). PhD Thesis, *University of Science and Technology Beijing*
56. Chen, W., Wang, J. J., Chang, L. Z., Peng, C. S., & Meng, L. P. (2017). *Continuous Casting*, 42(2), 48-53
57. Meng, Y. Y., Wang, J. J., Zhou, L., Peng, C. S., & Meng, L. P. (2013). *Chinese Society for Metals, Steelmaking Division*, 406-412
58. Xing, W. (2009). PhD Thesis, *Wuhan University of Science and Technology*
59. Wang, H. J., Wang, J. J., Meng, Y. Y., Chang, L. Z., & Zhou, L. (2015). *The Chinese Journal of Process Engineering*, 37(3), 286-291
60. Xu, K. D. (2009). *Acta Metall. Sin.*, 45(3), 257-269
61. Oh, J. M., Roh, K. M., & Lim, J. W. (2016). *Int. J. Hydrogen Energy*, 41(48), 23033-23041
62. Wang, C., Pan, G. P., Yang, C. Z., Zhang, J., & Zhao, P. (1997). *Iron & Steel*, (9), 21-24
63. Zhan, D. P., Zhang, H. S., Jiang, Z. H., Gong, W., & Chen, Z. P. (2011). *Adv. Mater. Res.*, 239-242, 2361-2364
64. Wei, G. S., Li, X., Zhu, R., Xu, G. Y., Li, C., Chang, H., Feng, C., & Su, R. F. (2023). *China*, CN116356119B
65. Neuschütz, D., & Spirin, D. (2003). *Steel Res. Int.*, 74(1), 19-25
66. Neuschütz, D., & Spirin, D. (2004). *Chinese Society for Metals, German Iron and Steel Institute*, 8
67. Zhao, B., Zhang, N., Peng, G. H., Wang, C. Y., Wu, W., & Wei, W. (2023). *Special Steel*, 44(2), 52-55
68. Dong, K., Wang, C. Y., Zhu, R., Liu, R. Z., Ren, X., & Liu, W. J. (2023). *Iron & Steel*, 58(8), 13-24
69. Zhang, X. Y., Jiao, K. X., Zhang, J. L., & Ziyu, G. (2021). *J. Cleaner Prod.*, 306, 127259

Отримано редколегією / Received by the editorial board: 11.12.2024

Прийнято до друку / Accepted for publication: 20.02.2025

*Gryshchenko S.G., Proidak Yu.S., Ponomarenko R.V., Kravchenko A.P.,  
Kalenkov O.F., Kudriavtsev S.L.*

## Ukrainian steel and ferroalloys in 2022-2024: how russian aggression has impacted on the work of the country's metallurgical industry

*Грищенко С.Г., Пройдак Ю.С., Пономаренко Р.В., Кравченко А.П.,  
Каленков О.Ф., Кудрявцев С.Л.*

## Українська сталь та феросплави у 2022-2024 роках: як російська агресія вплинула на роботу металургійної промисловості країни

**Abstract.** This article analyzes the state of the Ukrainian metallurgical industry, particularly steel and ferroalloy production, between 2022 and 2024, emphasizing the significant impact of the full-scale russian aggression. It highlights the industry's successes in 2021, when growth in steel and ferroalloy production was driven by favorable market conditions. The consequences of the russian invasion are detailed, including territorial occupation, infrastructure destruction, challenges with logistics and raw materials, and a shortage of qualified personnel, which led to a threefold reduction in steel production in 2022 and a substantial decline in ferroalloy output. Statistical data for 2022-2024 is presented, showing a gradual recovery in steel production volumes and a continued decrease in ferroalloy production, even leading to plant shutdowns in the fourth quarter of 2023. Special attention is given to the measures undertaken by Ukrainian enterprises to adapt to the new circumstances, including reorienting towards alternative raw material sources and optimizing electrotechnological regimes. The systemic problems facing the industry are highlighted: proximity to conflict zones, high electricity tariffs, personnel shortages, and logistical difficulties. In the context of Ukraine's European integration and its commitment to "green metallurgy," the prospects for the recovery and development of the domestic metallurgical sector are discussed, including projects for direct reduced iron and "green" steel production. Ukraine's potential to become a key supplier of "green" metallurgical raw materials for Europe is underscored.

**Key words:** Ukrainian metallurgy, russian aggression, steel production, ferroalloys, decarbonization, green metallurgy, recycled materials.

**Анотація.** У статті проаналізовано стан української металургійної промисловості, зокрема виробництва сталі та феросплавів, у період з 2022 по 2024 роки, наголошуючи на значному впливі повномасштабної російської агресії. Висвітлено успіхи галузі у 2021 році, коли зростання виробництва сталі та феросплавів було обумовлено сприятливими ринковими умовами. Детально описано наслідки російського вторгнення: окупацію територій, руйнування інфраструктури, проблеми з логістикою та сировиною, а також дефіцит кваліфікованого персоналу, що призвело до трикратного скорочення виробництва сталі у 2022 році та значного падіння виробництва феросплавів. Наведено статистичні дані за 2022-2024 роки, демонструючи поступове відновлення обсягів виробництва сталі та скорочення виробництва феросплавів, аж до зупинки заводів у четвертому кварталі 2023 року. Особливу увагу приділено заходам, вжитим українськими підприємствами для адаптації до нових умов, включаючи переорієнтацію на альтернативні джерела сировини та оптимізацію електротехнологічних режимів. Висвітлено системні проблеми галузі: близькість до зони бойових дій, високі тарифи на електроенергію, нестача кадрів та логістичні труднощі. У контексті європейської інтеграції України та курсу на "зелену металургію" обговорюються перспективи відновлення та розвитку вітчизняної металургії, включаючи проекти з виробництва відновленого заліза та "зеленої" сталі. Підкреслюється потенціал України стати ключовим постачальником "зеленої" металургійної сировини для Європи.

**Ключові слова:** українська металургія, російська агресія, виробництво сталі, феросплави, декарбонізація, зелена металургія, вторинна сировина.

In April 2025, the centennial of the establishment of the Department of Electrometallurgy of the Ukrainian State University of Science and Technology (at the time of its establishment - the Dnipropetrovsk Metallurgical Institute) will be celebrated. It will not be an exaggeration to say that it was the Department of Electrometallurgy, for many of us - the "alma mater", that became the founder of the world-famous school of Ukrainian electrometallurgy, the educator of a galaxy

of many thousands of ferroalloy and electric steelmakers who held and hold leading positions at industry enterprises, the developer of many highly efficient technological processes of world class. Congratulating our native department on its anniversary, we sincerely wish to continue to firmly hold the banner of domestic electrometallurgical science in our hands, which is especially important now, in the difficult conditions in which the metallurgical industry of Ukraine found itself

© Gryshchenko S. G. - Chairman of the Board of the Ukrcolormet Association,  
Proidak Yu.S. - d.t.s., profesor Ukrainian State University of Science and Technology,  
Ponomarenko R.V. - Nikopol Ferroalloy Plant,  
Kravchenko A.P. - JSC Zaporozhye Ferro Alloys Plant,  
Kalenkov O.F., - Association UKRMETALURGPROM,  
Kudriavtsev S.L. - Ukrainian Association of Ferroalloy Manufacturers



This is an Open Access article under the CC BY 4.0  
license <https://creativecommons.org/licenses/by/4.0/>

with the beginning of large-scale Russian aggression in February 2022.

We will begin our analysis of the work with 2021 - the last pre-war year for our country. As is known, in 2021, global steel production in the world increased by 3.7% compared to 2020 - to 1.95 billion tons. 2021 was also successful for Ukrainian metallurgists - favorable conditions in external markets and high demand for rolled steel in the domestic market (due to the active phase of the "Great Construction") contributed to the growth of production indicators. Compared to the previous year, steel production in Ukraine in 2021 increased by 3.6% - to 21.4 million tons. Ukraine was in the top twenty world steel producers.

The production of ferroalloys of all types (ferrosilicomanganese, high-carbon ferromanganese, metallic manganese, ferrosilicon) in the pre-war 2021 also increased and amounted to 858.7 thousand tons, which corresponds to 115% compared to the previous year 2020.

The full-scale Russian aggression has caused, along with other losses for Ukraine, a crisis situation in the metallurgy industry. The occupation of part of the territory in eastern Ukraine, where the main metallurgical facilities are located, constant shelling and destruction, disruptions in the supply of raw materials and energy resources, disruption of logistics routes for the export of finished products due to the blockade of sea ports, and the loss of qualified personnel during mobilization have led to a three-fold reduction in steel

production and a reduction in steel production. In 2022, Ukrainian metallurgists produced only 6.4 million tons of steel (29.9% compared to the previous year, including Mariupol plants in January-February 2022), of which more than half (3.4 million tons) fell on the pre-war first two months of the year. In 2023, global steel production amounted to 1.851 billion tons (-0.1% compared to 2022). In Ukraine, this indicator amounted to 6.228 million tons (+26.9% compared to the previous year), respectively, the volume of finished rolled products increased to 5.372 million tons (+31.2%). Depending on the enterprise, or rather, the region of its location, the utilization of pig iron, steel and rolled products in 2023 ranged from 20% to 70%. It should be noted that a significant part of the production capacities (over 60%) of the MMC of Ukraine is located in the temporarily occupied territory.

Ferroalloy production in 2022 also decreased significantly - to 537.9 thousand tons, which corresponds to 62.6% of the previous year's level. This trend took place and intensified in 2023: ferroalloy production was only 43.9% compared to the previous year. In the fourth quarter of 2023, Ukrainian ferroalloy plants were forced to completely stop production activities.

With what indicators did the metallurgical industry of Ukraine end 2024? Let us recall that according to the World Steel Association, global steel production in 2024 decreased by 0.9% compared to 2023 - to 1.839 billion tons. This is evidenced by the global ranking of steel-producing countries [1], Fig. 1.

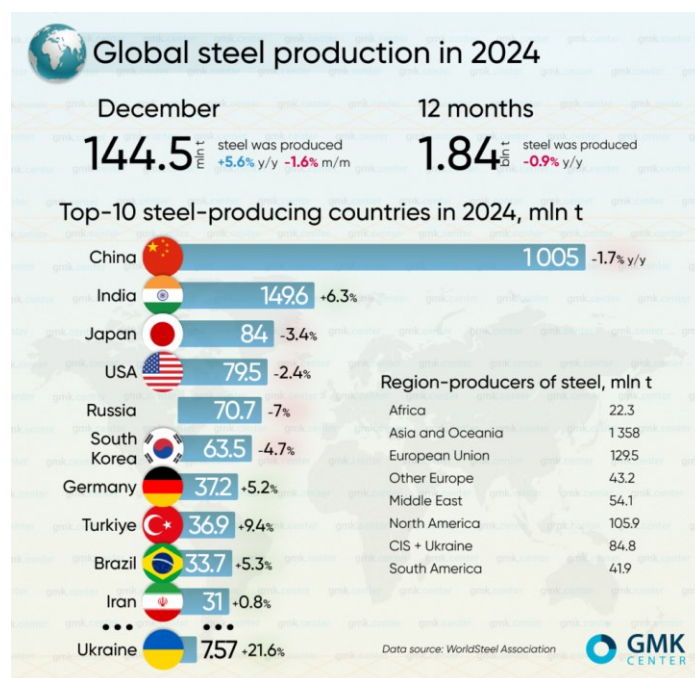


Fig. 1. Global steel production in 2024.

The top ten steel producing countries in 2024 according to World Steel include: China – 1.005 billion tons (-1.7% y/y); India – 149.6 million tons (+6.3%); Japan – 84 million tons (-3.4%); USA – 79.5 million tons (-2.4%); Russia – 70.7 million tons (-7%); South Korea – 63.5 million tons (-4.7%); Germany – 37.2 million

tons (+5.2%); Turkey – 36.9 million tons (+9.4%); Brazil – 33.7 million tons (+5.3%); Iran – 31 million tons (+0.8%).

Steel production in Ukraine in 2024 amounted to 7.57 million tons (+21.6% compared to the previous year 2023), thus the country took 24th place in the

global ranking of steel producers. In order not to return to statistics, we note that in the first 2 months of 2025, steel production in Ukraine amounted to 1.183 million tons (+9.9% compared to the corresponding period in

2024); in the world ranking, Ukraine has been in 20th place since the beginning of this year.

The current situation in the ferroalloy industry looks as follows (Fig. 2).



Fig. 2. Production output at enterprises of the ferroalloy industry of Ukraine in 2022-2024, thousand tons.

The industry resumed its work in April-May last year after the above-mentioned forced shutdown in the fall of 2023. According to the results of 2024, Ukrainian ferroalloy enterprises reduced production by 49.4% compared to 2023 - only to 108.2 thousand tons. By type of ferroalloys, production decreased as follows last year: silicomanganese - by 45%, to 104.2 thousand tons; ferromanganese - by 66.5%, to 3.6 thousand tons. The output of ferrosilicon (calculated at 45%) and other ferroalloys amounted to only 0.12 thousand tons and 0.28 thousand tons, respectively. The production of metallic manganese and manganese concentrate was not carried out last year.

Significantly, more than 4.5 times in 2024, the export of Ukrainian ferroalloys was reduced - to 77.3 thousand tons from 344.2 thousand tons in 2023 [2].

The temporary occupation of the territory of the Luhansk and Donetsk regions by the aggressor required metallurgical and ferroalloy enterprises to radically reorient the raw material base to replace the lost permanent suppliers. First of all, it was necessary to resolve the issue of using alternative reducing agents, which were previously produced from coking coal of the Donetsk basin. In cooperation with coke and chemical industry enterprises, the main parameters and specifics of using coke of various brands from new suppliers for smelting the entire range of ferroalloys were worked out, including such requirements for the quality of reducing agents as CRI, CRS and electrical resistance.

Similar work was carried out on limestones used in

blast furnace and ferroalloy charges and for lime production. Alternative sources of limestone have been found, including dolomitized, high- and low-phosphorus for various types of cast iron and ferroalloys. The technology of calcining limestones of a new composition and macrostructure in shaft furnaces has been developed, improving the quality of the produced lime while simultaneously increasing the service life of the lining of the calcining furnaces from 1-2 years to 3 years.

The types of iron-containing raw materials used in ferrosilicon smelting have been expanded; in particular, steel shavings have been replaced with other materials containing reduced iron and minimal impurities.

Increased attention has been paid to the processing of previously accumulated slags from ferrosilicon smelting using products for remelting. Technologies for casting this alloy into thin ingots in a mold with a reduced depth on a carousel-type casting machine have been mastered, which has reduced losses in the form of metal beads. Losses of commodity alloys in the process of product fractionation have been reduced. Due to these and other measures, the consumption of the ore part of the raw material containing manganese, in the form of agglomerate and ore, has been reduced by 15-20%, carbon reducing agents by 10-15%, and electricity by 13-15%.

In conditions of periodic power outages, optimal electrotechnological modes of ferroalloy smelting have been worked out with regulation of the use of electric furnace capacities - reduction or complete cessation of energy consumption in the time intervals of the



greatest daily deficit of electricity and its maximum cost.

The above-described measures have allowed to stabilize the situation in the MMC to a certain extent, but unfortunately, the so-called systemic current issues remain unresolved. The current problems of metallurgical and ferroalloy enterprises are as follows [2]:

- a larger share of enterprises that remained in the territory controlled by Ukraine are located mainly in the zone of direct active hostilities or in adjacent regions, with all the inherent risks for equipment and personnel;
- metallurgical and, above all, ferroalloy enterprises are suffering greatly from high electricity tariffs. Electricity prices for industrial consumers in Ukraine are now often several times higher than in developed European countries. In addition, industry pays 100% of the prepayment for electricity for the next month. For enterprises, this means significant frozen working capital, and if there is no electricity for two days after another shelling, no one will compensate for these losses;
- there is a constant shortage of production personnel due to constant mobilization and departure of employees to safer areas;
- logistical problems that MMC enterprises constantly face. There is an increase in the cost of port cargo handling operations in the ports of "Great Odessa". A transition to annual transportation along the Danube is possible, but the tariffs there are even more expensive due to the increase in the burden of railway freight transportation and the low volume of vessel loading.

We very much hope that the development of the domestic metallurgical and ferroalloy industries is included in the pool of state interests. To support the sector, the authorities must, first of all, resolve the situation with the rise in energy prices and in general for the services of the so-called "natural monopolists". Otherwise, our industry will simply disappear, and Ukraine will not have its own production of metallurgical products and ferroalloys.

In the difficult realities of martial law, the main efforts of the industry are aimed at preserving and maximizing the use of production capacities. But it is already obvious that a radical revision of all previously developed programs and plans for technical re-equipment and development of the industry will be required, based on new conditions and guided by new principles. It is necessary to focus not only on the restoration of facilities destroyed by the war, but also to take into account all the latest achievements of world metallurgy, world and European standards in the field of energy efficiency and environmental friendliness, minimizing the use of raw materials and waste-free production, and producing high-quality products based on the requirements of metal-consuming industries, primarily the construction and defense industries. This approach is embedded in the Concept of the program for the revival of domestic metallurgy in the post-war period, which is currently being developed by the associations of Ukrainian MMCs together with industry and

academic scientific institutions and universities.

When developing this document, Ukrainian scientists and manufacturers take into account global and European trends in the development of the so-called "green metallurgy." Let us recall that green metallurgy is a set of measures aimed at reducing carbon dioxide emissions in steel production. According to the European Green Deal, this level should be reduced by 80% by 2050 - to 250 kg of emissions per ton of steel [3].

Even before the Russian invasion, the export-oriented Ukrainian industry was actively planning for the "green" modernization of production. This was facilitated by several factors: Ukraine's obligations under the Association Agreement with the EU, the high requirements of the European market for the environmental friendliness of products, and the pressure of the Ukrainian public, which does not want to put up with the depressing state of the natural environment in industrial cities.

In the pre-war years, the share of spending on environmental protection measures in the total volume of capital investments of mining and metallurgical companies increased from 39.8% in 2017 to 53.8% in 2020. And the share of "environmental" investments in the entire industry in the total volume of investments and expenditures on environmental protection in industry increased, according to the State Statistics Service, from 41.1% to 54.8%, that is, the lion's share of all pre-war investments is environmental investments.

The war changed everything, and not only in Ukraine. The Ukrainian events became an additional factor that influenced the decline in industrial production in the world. Restrictions on gas supplies by Russia caused an energy crisis, rising food prices and global inflation. The World Bank predicts an annual increase in consumer prices of up to 8.8%; inflation in the eurozone, according to the European Commission, will be 7.6%, and in the EU - 8.3%. High energy prices negatively affect European industry, and the need to change energy import routes causes an imbalance in supply chains.

The taxonomy has changed: Europe had to include nuclear energy and natural gas in the taxonomy as fuels that contribute to the transition to a carbon-free economy. It has become obvious that abandoning fossil fuels is not so easy. Investments in their development are growing, which means emissions in the extraction process will decrease more slowly.

However, the EU's overall policy of moving away from fossil fuels has remained unchanged. Moreover, Russia's gas blackmail has convinced Europe of the correctness of the chosen path. We quote the decision of the European Commission: "Modernisation and decarbonisation of energy-intensive industries must be a top priority. The European Green Deal aims to create new markets for climate-neutral and year-round products such as steel, cement and basic chemicals. To lead this change, Europe needs new industrial processes and cleaner technologies to reduce costs and increase market readiness. The Commission will support breakthrough clean steel technologies leading to

a zero-carbon steel production process. The EU ETS Innovation Fund will help to deploy other large-scale innovation projects to support clean products in all energy-intensive sectors."

All these decisions also concern the Ukrainian metallurgy, taking into account the acceleration of Ukraine's European integration with the EU: on June 23, 2022, Ukraine acquired the status of a candidate for membership in the European Union and now we will have to accelerate reforms in order, including in the environmental sphere, to truly enter the European family.

A number of environmental programs have been developed in Ukraine, which are included in the draft National Recovery Plan of Ukraine, including projects in the metallurgical industry. The developers of the Recovery Plan intend to join the chain of added value of "green" steel: increase the production of DR-class pellets, ensure the production of direct reduction iron and hot-briquetted iron, including using H<sub>2</sub>, and produce "green" steel in electric arc furnaces. The total approximate cost of metallurgical projects is \$5.8 billion. This includes private and public investments. It is expected that most of the investment will come from private players after the introduction of competitive interest rates, war zone insurance and measures to improve the business environment.

To address these issues, we need to develop relations between European and Ukrainian companies in the metallurgical sector in the post-war period and would like to present some ideas on the possibility of developing these relations. We have always held the opinion that Ukraine needs to integrate its metallurgical industry with Europe for the following reasons:

- Ukraine is an important part of Europe – territorially, historically, even being a part of the European geological structure and is working on a strategic plan for full economic integration with the European Union; the metallurgical industry should be part of this integration;

- Ukraine has large resources of metallurgical raw materials, which allows it to produce semi-finished products necessary for the metallurgical industry of Europe;

- Ukraine, like Europe, does not have sufficient natural gas resources along with coal. At the same time, the metallurgical sector, as is known, is a large consumer of natural gas and coal using traditional technologies. Europe has begun to phase out that part of the metallurgical industry that is heavily dependent on gas and coke used in blast furnaces and has begun to switch to electric arc furnaces that do not require the latter. Ukraine should also adhere to this policy, producing semi-finished products for European steel production: direct reduction iron pellets (DRI Pellets), hot briquetted iron (HBI);

- Europe is working on the development of "green energy" resources in various sectors, including the metallurgical sector, and has recently launched a new program for the production of iron pellets using such a renewable energy source as hydrogen. Ukraine has great potential for the production of "green energy", including hydrogen, and has reserves of iron ore of a certain quality; thus, Ukraine will be able to effectively participate in this program and integrate with Europe.

Specialists of MMC-Center [4] have made calculations that indicate the best positions of Ukrainian metallurgy to become major suppliers of "green" metallurgical raw materials, to ensure a "green" transition to Europe. According to these calculations, Ukrainian producers have the opportunity to increase steel production by 2035 to 15 million tons at a capacity utilization level of 80%, including 6.0 million tons of steel - using low-carbon technology.

Maintaining and developing ties with the world metallurgical and ferroalloy community, Ukrainian metallurgists will continue to look for ways to stabilize the situation, first of all - to stop Russian aggression, and in this regard we count on the active assistance and support of our foreign colleagues.

## References

1. Kolisnychenko, V. (2024). *Results of the work of the metallurgical industry of Ukraine in 2024*. GMK center. <https://gmk.center/ua/infographic/ukrainska-metalurgiya-dosyagla-pika-u-2024-roci-shho-dali/>
2. Hryhorenko, Yu. (2019). *Executive Director of UkrFA - on the results of the ferroalloy industry and its prospects*. GMK center. <https://gmk.center/ua/interview/sergij-kudryavcev-eksport-ferosplaviv-do-turechchini-skorotiv-sya-na-40/>
3. Kybovska, A., Berdyskykh, A. (2022). *Invasion into the future - how Russian aggression jeopardized the prospects of "green" modernization of Ukrainian industry*. Delo.ua. <https://delo.ua/ru/industry/vtorzenie-v-budushhee-kak-rossiyskaya-agressiya-postavila-pod-ugrozu-perspektivy-zelenoi-modernizacii-ukrainskoi-promyslennosti-405845/25.10.2022>
4. Zinchenko, S. (2024). *"Green" transformation of the EU steel industry in 2025-2030 and prospects for Ukrainian metallurgy*. GMK center. [https://gmk.center/wp-content/uploads/2024/12/2024\\_UKR\\_Green-Steel-Transform\\_25-35.pdf](https://gmk.center/wp-content/uploads/2024/12/2024_UKR_Green-Steel-Transform_25-35.pdf)

Отримано редколегією / Received by the editorial board: 17.01.2025  
Прийнято до друку / Accepted for publication: 20.02.2025

Karbowniczek M.

## Some aspects in the electric arc steelmaking production

### Деякі аспекти у виробництві сталі в електродугових печах

**Abstract.** The electric arc furnace (EAF) is the initial aggregate and the key point in many carbon steel and in most stainless-steel melting plants. In the article new solutions in construction, technology, operations and control, used in modern steelmaking plant, will be presented. On literature background the results of author's investigation in electric steelmaking area will be showed. Special attention will be paid on the foaming slag technology used for thermal efficiency increase which means a low cost operation. New elaborated and patented method of stainless-steel slag foaming technology will be described. With slag foaming is connected the optimization procedure concern on minimum the electrical energy consumption and tap-to-tap time. Industrial application in this area will be presented. As a separate chapter the solution in environmental protection during EAF production will be described.

**Key words:** EAF, foaming slag, electrical energy, steelmaking.

**Анотація.** Електродугова піч (ЕДП) є початковим агрегатом та ключовим елементом на багатьох підприємствах з виплавки вуглецевої сталі та на більшості підприємств з виплавки нержавіючої сталі. У статті представлені нові рішення в конструкції, технології, експлуатації та управлінні, що використовуються на сучасному сталеплавильному заводі. На основі літературних джерел показані результати власних досліджень автора в галузі електрометалургії. Особливу увагу приділено технології спінювання шлаку, яка використовується для підвищення теплової ефективності, що означає низьку собівартість роботи. Описано новий розроблений та запатентований метод технології спінювання шлаку при виробництві нержавіючої сталі. Зі спінюванням шлаку пов'язана процедура оптимізації щодо мінімізації споживання електричної енергії та часу плавки. Представлено промислове застосування спінювання шлаку. Окремим розділом описано рішення щодо захисту навколишнього середовища під час виробництва в ЕДП.

**Ключові слова:** ЕДП, спінений шлак, електрична енергія, виробництво сталі.

#### 1. Introduction

The electric arc furnace (EAF) is used to steel production about one hundred years. Meantime from simply construction and not complicated production technology to present state of art the furnace was continuously developed. Nevertheless the modern furnace is still based on the classical formulation, enough close to the original idea, obviously technologically and economically improved to make the EAF faster and more efficient.

Steel is currently produced using a two-stage technology. During the first stage liquid metal bath is obtained in the steelmaking furnace (the electric arc furnace as well as the oxygen converter). During the second stage the metal bath is subjected to refinement in the process of the off-furnace steel metallurgy (also known as the ladle metallurgy). The aim of the refinement is to obtain a chemical composition and metallurgical quality which are appropriate for the produced grade of steel. The goal is also to obtain the temperature which would enable proper casting.

The electric furnace steelmaking has been increased continuously in recent years, except last year. This trend is friendly for the environment if one considers that the EAF route facilitates the recycling of steel scrap, the conservation of resources, and the reduction of CO<sub>2</sub> emissions from steelmaking. Among the available tools for metal bath creating, the electric arc

furnace seems the highest flexibility with respect to the selection of charge materials and their structure. This particular feature of the EAF allows to select the most convenient charge mix which is less dependent on the level of the market price fluctuations. The feasibility of using steel scrap, DRI and hot metal in a range of 0 – 100% has been already confirmed by a large number of existing installations.

The developments in electric steel making show the big steps to reach the today's high standard. Importance was the competition to the established AC electric arc furnaces with high transformer performance (SUHP furnaces) by the direct current DC arc furnaces. With these furnaces the repercussion in the mains voltage, the electrode consumption and the noise emission was reduced remarkably. The DC electric arc furnace operates with just one graphite electrode in the roof operating as the cathode, and a bottom anode in the bottom.

Process modeling is often used for the observation and control of the EAF process. Online process models allow the calculation of values incapable of measurement like the actual liquid and solid steel and slag mass in the furnace or the permanent monitoring of the actual mean temperature of the liquid steel.

Two particular solutions to modern electric arc furnace steelmaking are presented below.



## 2. The foaming slag technology

Since many years the foaming slag practice in the EAF is well established in low alloyed steel production. It improves thermal efficiency of the melting, lowers refractory and electrode consumptions, and provides a stable arcing at lower noise level. Good foaming effect is attainable by suitable slag viscosity strongly affected by iron oxide content in the slag as well as permanent iron oxidation and iron oxide reduction by injected oxygen and carbon into the metal bath and slag, respectively. In case of high alloyed steels with high chromium content the preconditions for slag foaming effect are diametrical different. Oxygen injected into the steel produces mainly chromium oxide with totally different properties in comparison with iron oxide, it changes significantly the slag viscosity. The solubility of chromium oxide in the slag is considerable weaker in comparison with that of iron oxide at the same thermal and basicity conditions. Also the reduction of chromium oxide by carbon does not attain such intensity as the reduction of iron oxide. The gas generation is poor. The oxygen/carbon injection technique in the high chromium alloyed steel production is due to the chemical and physical conditions evidently hazardous and

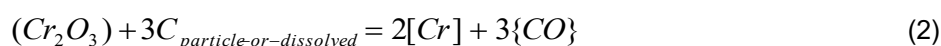
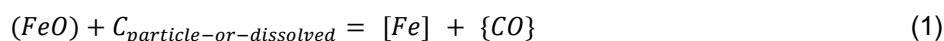
difficult in operation. The risk of uncontrolled oxidation of chromium is pronounced, resulting in high chromium losses and poor foaming.

The novel technology distinguishes principal from the conventional one, which uses injection of oxygen and carbon via manipulator lances. The new technique bases on the reduction of iron and chromium oxide by carbon as well as on the thermal dissociation of lime stone contained in a small dimensioned briquette. Specific density of the briquettes is assorted to have value between slag and metal. Its introduction into the melt causes placing exactly on the slag and metal boundary - optimal place for the requested gas generated reaction.

### 2.1. Idea of slag foaming formation

Two factors define the foamy slag formation: the foaming material with the corresponding reacting components, which produce gaseous products, and the slag viscosity dependent on the chemistry and temperature. A liquid slag is for the foam formation a prerequisite.

The principal reaction that creates gas bubbles in the slag is the reduction of iron and chromium oxides are given by the following stoichiometry:



The reaction (1) in carbon steelmaking is the principle and iron oxide is the major component in the slag. When the slag viscosity is suitable for sustaining foam, then the simple carbon injection into the slag causes the foaming effect. Other situation is in case of stainless steel slag. The major components are CaO, SiO<sub>2</sub> and Cr<sub>2</sub>O<sub>3</sub>. The SiO<sub>2</sub> is a fluxing component, while the Cr<sub>2</sub>O<sub>3</sub> stiffens the slag. Due to the higher chromium affinity to oxygen the Cr<sub>2</sub>O<sub>3</sub> generation takes place preferentially in comparison with FeO. Therefore it is important to control the chromium oxide content and the slag basicity, responsible for the viscosity, which constrains gas bubbles to temporary detainment in the slag layer.

The bubble forming phenomenon is a process of formation new surface area by the mechanical force resolved by reaction gas. In the presented technology this gas is effective for the reduction reaction of metal oxides by carbon taking place in a briquette or pellet introduced into the metal bath. Buoyancy forces of bubbles crack the slag surface saturating temporarily the top layer to create the foam. With a sustained gas flow coming from the reacting briquettes the population of the bubble aggregation as foam continues to grow. As a consequence of it, the height of the foam layer increases. Importance for such mechanism is the optimal placing of the briquettes to get the maximum foaming effectiveness. It is the boundary between the slag layer and liquid metal. With the control of the briquette density, corresponding to the range between that of slag and metal (3-7 t/m<sup>3</sup>) such placing is always reachable. The foam height increases with the increase of

the gas flow rate; it is directly proportional to the foaming material rate.

Fig. 1 illustrates the principle of the slag foaming.

### Theoretical considerations and laboratory tests

The aim of this laboratory experiment was to establish adequate forms and chemical compositions of the materials for effective foaming of high chromium oxide slag. The materials were supposed to contain iron oxide scales, carbon carriers, and high-carbon ferrochromium as weighting agent as well as possibly calcium carbonate as additional producer of gas for foaming process. As to the form of the foaming materials either briquettes or pellets of different sizes were considered. Furthermore, the research study was carried out by making laboratory heats, sampling metal and slag phases for chemical analysis in order to optimize the foam ability.

In the first stage of the work, the most promising materials for foaming were selected based on theoretical considerations. A model for computation of the specific densities of the foaming mixtures was applied.

In the second stage of the work, the foaming mixtures were prepared in forms of briquettes and pellets of different sizes. A number of 40 heats were performed in a laboratory arc furnace to investigate the impact of various parameters on the height and stability of the generated foams [1].

In the third stage, the experimentally obtained results were analysed and the final conclusions and technological recommendations as to the optimal conditions for the slag foaming were established.

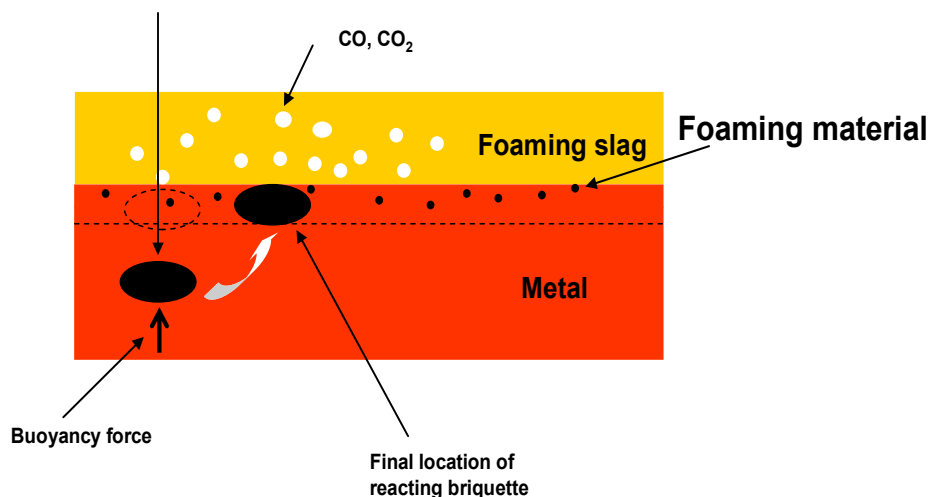


Figure 1. Principle of foaming slag formation by briquette.

Results indicate that the highest foamability was obtained for the pellets of a 8-10 mm diameter, while the lowest for those of a 2-5 mm diameter. The effect is due to the fact that small pellets do not sink through the slag layer down but float up to the slag surface. The phenomenon is caused by the interfacial tension forces at the pellet/liquid slag boundary. While floating on the slag surface, the bubbles formed in the pellets do not go into the slag layer but go into the ambient atmosphere. For pellets, the foaming time was lower than this for briquettes. It can be explained by the kind of their structure. Briquettes which are compressed materials have lower porosity. Decreased contact surface with liquid slag causes slower heat transfer, slower reduction of the iron oxides in the briquettes and in consequence lower gas rate. Only briquettes were selected for industrial examination.

#### Industrial tests

On the base of the above described laboratory test the industrial test of foamy slag at high Cr-oxide in an EAF was carried out to prove its industrial functionality as well as viability. The EAF-AC with the capacity between 25-35t and transformer of 32 MVA is designed for pre-metal production of austenitic and ferritic steel grades in common operation with the down stream operating 80t AOD-L and MRP-L converters.

The test being integrated into the current production consisted of 45 austenitic and 15 ferritic heats. The test procedure distinguishes from the normal operation,

where oxygen is blown during the whole super heating period. The reason of such procedure was to separate the oxygen effect on the carbon and metal oxidation, additional generation of CO bubbles, as well as impact effect of the gas stream. Several heats were tested under normal operational conditions.

As the test results show, the foaming of a  $\text{Cr}_2\text{O}_3$  rich EAF slag is a difficult but under controlled slag conditions possible task. Results of this industrial test confirm the correct recipe of the foaming material and the optimal reacting place of the briquettes. Further experiences of the test show also dependences between the initial slag amount and its foamability. Intensive gas development in combination with the slag mass and the desired low viscosity allows slag generations with sufficient height for complete cover of the electric arcs. The optimal initial slag amount fluctuates in the range 68-72 kg/t<sub>steel</sub>. Fig. 2 illustrates areas of slag composition after briquette additions. It can be seen, that the most slags were good reduced. The average residual  $\text{Cr}_2\text{O}_3$  in the slag was indicated by 4,2%. Also the basicity in the range 1,3-1,35 was established as optimal. This part of the slag system must be considered to be the optimum area. The viscosity is in this part low, however, partly undissolved lime and higher  $\text{Cr}_2\text{O}_3$  content increases the viscosity. Fig.3 illustrates a typical slag height development of a AISI 304 heat. The slag heights were measured with a reference to the electrode diameter.

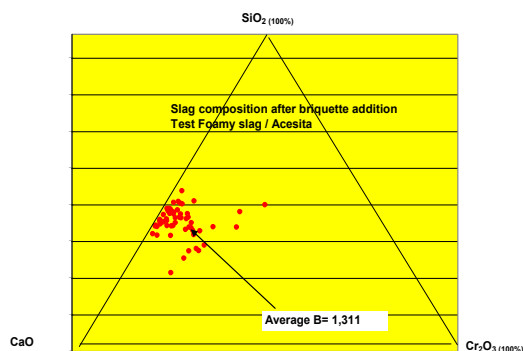


Figure 2. Standardized slag diagram.

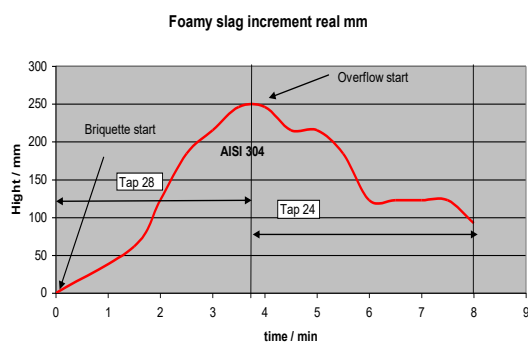


Figure 3. Slag height course.



As the curve shows, after approx. 2 minutes the slag reached the adequate height suitable for the electric arc cover. During the next 4 minutes this level was established, leaving the required range after 4 – 5 minutes. It should be mentioned, that since the 3.5 minutes an overflow of the slag through the furnace door was observed. The slag mass was relating to this continuous reduction until a stable level was reached. It was observed in other tests with oxygen blowing, that the oxygen stream support in the receipt of the foaming layer. In view on the electrode consumption the foamy slag has an undisputed significance.

All tests demonstrate that the new foaming slag technology for stainless steelmaking in EAF which is carried out by foaming materials containing scale, carbon and ballast materials, introduced into the furnace in briquettes form with a special defined density and in combination with a controlled slag viscosity implicates sufficient foaming quality and its height. The slag height is controllable by intensity and duration of additions.

### 3. The optimisation of the electric energy consumption in the EAF

The aim of steel production in the arc furnace is obtaining the liquid metal bath from the scrap metal as quickly as possible and using as low costs as possible. The structure and the construction of the furnace is subordinate to the aim. So it is the technological method of running the process. The technology of the process encompasses proper preparation and loading of the charge materials (scrap, slag forming materials, carburizing materials) as well as their melting by means of electric energy transformed into heat in the electric arc. The optimal control of the work of an arc furnace with the alternating current is a complex process due to the quantity and variety of the working parameters. Many physical phenomena as well as chemical reactions take place during the melting process.

Their precise mathematical description does not seem possible. At the same time the competition at the steel market requires the furnace to work economically which is tantamount to a decrease in production costs. It is impossible to optimize the furnace work in a way that would decrease the costs and produce high quality steel in a universal way at the same time. Different producers apply different methods of controlling the production costs.

Therefore, an attempt has been made to optimize the demand for electric energy used in the production process in the arc furnace. The used energy is one of the most important components of the production costs. If one plans such parameters of the furnace that would optimize the use of energy, the costs will go down.

#### 3.1. The concept of the model

Many physical and chemical phenomena, which take place during the steel melting process in the electric arc furnace, can be presented by means of the physical and chemical models describing these phenomena. One of such phenomena is calculating the demand for electric energy. Preparing a model of electric energy demand will enable the optimisation of the electric energy consumption. So far many models used in industrial practice have been described in literature [2-5]. The most often used methods included the method of selecting the equation's form and determining the factors. The use of modelling based on the physical chemistry of the process is a difficult task on account of a large amount of simultaneous physical and chemical phenomena requiring a complex mathematical description. Therefore, an attempt was made to use a method based on the calculus of probability. The genetic algorithm method was used in order to identify the available statistical equations describing the use of electric energy in the arc furnace (Figure 4).

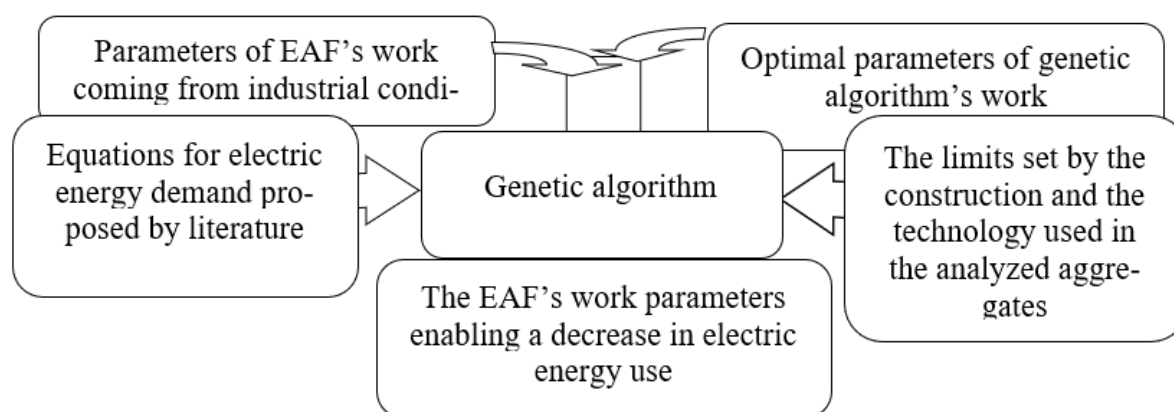


Figure 4: A schematic diagram of the proposed model

#### 3.2. The obtained results

Elaborated software was used to calculate such factors of the melting process that would ensure minimal demand for the electric energy. The obtained results were compared with minimal, maximal and medium values from the actual real melts.

The developed software AGEAF was used to calculate the optimal demand for electric energy in the steelmaking process in the electric arc furnace. The real parameters describing the steelmaking process with values ranging from the minimal to maximal values were used as the entry data. The values of the

parameters were established according to the AGEAF algorithm in order to obtain minimal demand for electric energy. The energy was calculated by mean of different equations, detailed described in literature [6].

The obtained results, as an example, and average values for the real melting processes are shown in Table 1.

Table 1. The average values from real melts and the obtained factor values which enabled minimal energy consumption and which were calculated the AGEAF software use.

Factor's name	Average values of real melts	Predicted values			
		Equation a	Equation b	Equation c	Equation d
Calculated value of the electric energy demand, kWh/Mg	396	294	273	293	285
Weight of metallic charge, Mg metallicznego, Mg	157	151	145	153	159
Weight of melted metal, Mg	140	145	148	149	152
Weight of remaining metal, Mg	10	6.2	4.6	7.6	3.0
Slag weight, Mg	10	10	10	10	10
Oxygen used for the process, m <sup>3</sup> /Mg <sup>3</sup> /Mg	33	33,5	35	32	34
Gas used for the process, m <sup>3</sup> /Mg	3.4	2.8	2.15	3.5	4.9
Temperature of the metal bath before tapping, °C	1609	1609	1609	1609	1609
Tap to tap time, min	52	58	53	55	61
Time of energy consumption by the furnace, min	40	35	40	44	42

\* - detailed description of equations (a) ÷ (d) is included in literature [6]

The minimal demand for electric energy calculated on the basis of equations is in each case smaller than that for the real melting processes. Consequently, it is possible to select such values of particular factors that would lower the demand for electric energy. The analysis of particular values of different factors led to the conclusion that equation (b) best reflects the real working conditions of the investigated arc furnace. In order to optimize the demand for energy, it is advised to use the above mentioned equation. As can be seen from the data in Table 2, the calculated values of particular factors are different from the average values from real melting processes. The smallest difference that can be noticed is that in the time from one melt to another and the biggest difference is that in the melted metal weight. Such results show that the time from one melt

to another has the biggest influence on the energy demand. The factor showing the biggest difference from the average real value has the least significance when it comes to energy demand. Similar relations were obtained as far as other analyzed equations are concerned.

The analysis of the results shows that the quality of the database used for optimizing the energy demand is not the best. It can be said that the minimal and maximal values used in optimizing the energy demand were coincidental to a large extent. That is why theoretical minimal and maximal values of particular factors were assumed. They were prepared on the basis of the furnace's construction parameters and technological data and are shown in Table 2.

Table 2. Theoretical parameters for the optimization process in AGEAF software for the furnace.

Factor's name	Values	
	Minimal	Maximal
Weight of the metallic charge, Mg	140	165
Weight of melted metal, Mg	120	162
Weight of remaining metal, Mg	0	10
Slag weight, Mg	8	12
Oxygen used for the process, m <sup>3</sup> /Mg	0	50
Gas used for the process, m <sup>3</sup> /Mg	0	10
Temperature of the metal bath before tapping, °C	1590	1610
Tap to tap time, min	45	55
Time of energy consumption by the furnace, min	35	45
DRI weight	0	5
HBI weight	0	5

AGEAF software was again used to calculate the electric energy demand on the basis of minimal and maximal values from Table 2. The results are presented in Table 3. The results show that the calculated value of optimal, i.e. minimal, demand for energy assessed on the basis of equations (a) ÷ (d) differs

depending on the equation. The smallest value was obtained in the case of equations (a) and (d). Higher values were obtained in the case of equations (b) and (c). It means that for such working conditions it is good to use equations (a) and (d).

Table 3. The factor values which enabled minimal energy consumption and which were calculated by the AGEAF software use.

Factor's name	Predicted values			
	Equation a	Equation b	Equation c	Equation d
calculated value of electric energy demand, kWh/Mg	297	349	350	298
Weight of the metallic charge, Mg	144	151	159	150
Weight of melted metal, Mg	141	146	147	142
Weight of remaining metal, Mg	8	4.9	9.0	7.7
Slag weight, Mg	10	10	10	10
Oxygen used for the process, m <sup>3</sup> /Mg	42,36	32	32,9	40
Gas used for the process, m <sup>3</sup> /Mg	3.8	2.7	8.2	7.3
Temperature of the metal bath before tapping, °C	1600	1600	1600	1600
Tap to tap time, min	52,9	50	52	46,5
Time of energy consumption by the furnace, min	38	37,6	38	38
DRI weight	–	4,47	–	2,65
HBI weight	–	1	–	2

\* - detailed description of equations (a) ÷ (d) is included in literature [6]

The values of the factors which cause the optimal energy consumption show that it is recommended to work on the melting technology. It is recommended to develop such technologies that would use those factors that make the energy demand optimal.

#### 4. Conclusions

Steel is sometimes produced using a two-stage technology. During the first stage liquid metal bath is obtained in the steelmaking furnace but during the second stage the metal bath is subjected to refinement in the process of the ladle metallurgy. Among the available tools for metal bath creating, the electric arc furnace seems the highest flexibility with respect to the selection of charge materials and their structure. This particular feature of the EAF allows to select the most

convenient charge mix. Process modeling is often used for the observation and control of the EAF process. Online process models allow the calculation of values incapable of measurement like the actual liquid and solid steel and slag mass in the furnace or the permanent monitoring of the actual mean temperature of the liquid steel.

Two particular solutions to modern electric arc furnace steelmaking are presented in the article:

the foaming slag technology used in case of high alloyed steels with high chromium content and

the developed software used to calculate the optimal demand for electric energy in the steelmaking process in the electric arc furnace.

#### References

1. Reichel, J., et al. (2008). *9<sup>th</sup> European Electric Steelmaking Conference*, Krakow, Poland
2. Adams, W., Alameddine, S., Bowman, B., Lugo, N., Paegle, S., & Stafford, P. (2001). *Proc. 59<sup>th</sup> Electric Arc Furnace Conference*, Phoenix Arizona
3. Camdali, U., Tunc, M., & Karakaş, A. (2003). *Energy Conversion and Management*, 44, 961
4. Köhle, S. (1999). *Recent improvements In modelling energy consumption of electric arc furnaces*, Düsseldorf, Germany
5. Pfeifer, H., & Kirschen, M. (2002). *Electric Steelmaking Conference*, Venice, Italy
6. Czaplá, M., et al. (2008). *9<sup>th</sup> European Electric Steelmaking Conference*, Krakow, Poland

Отримано редколегією / Received by the editorial board: 15.11.2024  
Прийнято до друку / Accepted for publication: 20.02.2025

Stovpchenko G.P., Medovar L.B.

## Decarbonisation challenges for steelmaking and scrap recycling role

Стовпченко Г.П., Медовар Л.Б.

### Проблеми декарбонізації металургії та роль переробки металобрухту

**Abstract.** This article discusses the challenges the steelmaking industry faces in striving to achieve competitive alternatives and potential solutions in response to the imperatives of decarbonization and zero-waste manufacturing. Expanding scrap recycling is a logical practical solution that the steel industry must pursue to effectively reduce its carbon emissions amidst its current structure. One of the steps towards achieving this is by utilizing alternative scrap sources to enhance iron recovery. The Recovery Slagged Scrap (RSS) from steelmaking includes metal pieces covered by low-conductive slag, which changes its melting behaviour. Analysis of trials results has shown that adding RSS to BOF iron-bearing charge mix can speed up the formation of primary slag and at proper consumption does not pose technological difficulties. Utilizing RSS as a coolant or slag-forming addition may improve the melting process and provide cost reduction of a charge mix for a steelmaking facility.

**Key words:** decarbonization, steelmaking, scrap recycling, iron recovery.

**Аноатація.** В статті обговорюються виклики, з якими стикається металургійна промисловість у прагненні досягти конкурентоспроможних альтернатив та потенційних рішень у відповідь на імперативи декарбонізації та безвідходного виробництва. Розширення переробки металобрухту є логічним практичним рішенням, до якого має прагнути сталеливарна промисловість для ефективного зменшення викидів вуглецю в умовах її нинішньої структури. Одним із кроків до досягнення цього є використання альтернативних джерел брухту для підвищення відновлення заліза. Відновлений шлаковий брухт (RSS) зі сталеливарного виробництва включає металеві шматки, покриті низькопровідним шлаком, що змінює його поведінку при плавленні. Аналіз результатів випробувань показав, що додавання RSS до залізовмісної шихти кисневого конвертера може прискорити утворення первинного шлаку і при належній витраті не створює технологічних труднощів. Використання RSS як охолоджувача або шлакоутворюючої добавки може покращити процес плавлення та забезпечити зниження собівартості шихти для сталеливарного підприємства.

**Ключові слова:** декарбонізація, виробництво сталі, переробка металобрухту, відновлення заліза.

#### Introduction: state-of-the art of CO<sub>2</sub> emission in today's steelmaking routes

Steelmaking is one of the energy- and CO<sub>2</sub>-intensive branches of the modern industry [1,2]. Every average ton of crude steel (1,882.6 bln ton production in 2024) is accompanied by around 1.85 tons of CO<sub>2</sub>, summarising 7-8% of global emissions.

Throughout all stages of metals' raw excavating, preparation, and processing, there are both direct and indirect emissions of greenhouse gases, including CO<sub>2</sub>. Direct emissions include methane at coal mining, coke gas at coke burning, and exhaust gases from the reduction and burning of carbon-bearing components (at sintering and pellets roasting, blast furnace (BF) or direct reduction iron (DRI) gas- and coal-fed units, and steel melting in oxygen converters (BOF) and electric arc furnaces (EAF)) and CO<sub>2</sub> at limestone and magnesite calcination. Indirect emissions come from energy used for all these and downstream technological processes and transportation. Not less problem for further sustainable growth of steelmaking is the considerable amount of raw materials needed annually: iron ore – 2.4 bln ton [1, 2]; coal – 1.1 billion tons; lime (dolime)

140-160 mln t [3]; and magnesite – 18 - 27 mln t (for refractory lining and mixtures [4]).

The focus of steelmaking over the past decade has shifted towards the development of low-carbon and carbon-free technologies. The leading steel manufacturers form Global Low-Carbon Metallurgical Innovation Alliance [5] making strides towards a low-carbon future [6] and have taken up the challenge to achieve carbon neutrality in 2050 to meet the Paris Agreement on climate change targets. Ferrous metallurgy's CO<sub>2</sub> emissions are expected to fall 30% by 2050 compared to 2021 levels [7] and the main challenge is efficiently remove carbon from iron reduction processes.

The main source of CO<sub>2</sub> emissions is ironmaking dates back to prehistoric times, when mainly only carbon and flame were available for iron reduction from metal-bearing ores. To someone without knowledge of the features of the optimal conditions for the realisation of variety of physicochemical processes of reduction and refining in steel production, the procedures may seem paradoxical and illogical. In the traditional blast furnace-oxygen converter tandem, a large amount of carbon is first used to produce pig iron and its content in the metal is increased to almost 4%, and then it is

© Stovpchenko G.P. – Doctor of Technical Sciences, Professor, Tianjin Heavy Industry research and Development Co, Ltd, Tianjin, China;

Medovar L.B. – Doctor of Technical Sciences, Professor, Tianjin Heavy Industry research and Development Co, Ltd, Tianjin, China



This is an Open Access article under the CC BY 4.0 license <https://creativecommons.org/licenses/by/4.0/>

removed using oxygen, which was removed from the ore on the first stage. Nevertheless, the blast furnace (BF) is still the most efficient unit of carbothermic reduction of iron. Furthermore, the downstream Basic Oxygen Furnace (BOF) process converting an iron into steel is also very attractive, being energy efficient due to the exothermic oxidation of carbon, silicon, and iron during oxygen blowing, eliminating the need for external heat sources.

It should be mentioned that the GHG emission from today's steelmaking routes (t CO<sub>2</sub>/t steel) is sufficiently different [8,9]: BF followed by BOF produces 2.33; natural gas-based DRI followed by EAF – 1.37; and EAF with 100% scrap – 0.68 (based on 2022 calculation), that defines last option to be the mainstream vector. To cut CO<sub>2</sub> emissions, the ironmaking route must be fundamentally transformed (by eliminating carbon as reductant) or added by installations capturing CO<sub>2</sub> from exhaust gases.

Specific strategies and technologies employed by steel manufacturers may vary depending on factors such as energy consumption conditions and developing technological improvements [10] market constraints and regional regulations.

We do not discuss in detail the most ambitious scenario of the global transfer to electrolytic hydrogen as reducer and fuel, which, like the direct electrolysis of iron, can provide genuinely carbon-free metallurgy since there is yet to be enough energy capacity for such transition worldwide. Nevertheless, the concept of green hydrogen electrolysis is promising for its potential as a clean and renewable energy carrier and power grid stability balancing in spite that its large-scale production remaining economically challenging [11-13].

Currently, most hydrogen production is achieved through steam methane reforming, which utilizes

natural gas. This method gives "blue" hydrogen that is cheaper but results in carbon dioxide emissions that should be accounted for steel making it "grey" (not fully "green"). The challenges include the need for extensive infrastructure for hydrogen production, transportation, and storage, and the overall economics of the process.

Small-scale pilot projects and demonstration plant have successfully produced molten iron by iron oxide electrolysis (MOE) [14-16] using renewable energy, but these projects face constraints when it comes to scaling up production to meet significant volumes of demand and the high cost of renewable energy technologies. As renewable energy technologies become more cost-effective and efficient, the economic viability of large-scale projects is expected to improve and open pathways for implementing technological advancements for traditional and future industrial routes.

### The nowadays challenges of basic oxygen steelmaking industry

A significant share of today's steelmaking ecosystem consists of the energy-efficient but carbon-intensive BF/BOF route, which changing for any other facilities would have far-reaching effects on steel customers. For example, In the EU in 2020, more than half of the steel produced (56%) was made via the primary BF/BOF route and the other 44% through the recycling route using EAF [17]. In China, which produces half of all world steel, abandoning the BF/BOF route favouring EAF is most challenging because BOF steel share is almost nine times higher than that produced in EAF (10.9%).

Besides, only scrap recycling is not enough source to meet the growing steel demand. Global consumption of ferrous scrap in 2022 was 610 million tons, nearly 32%wt of raw materials, for 1.95 billion tons of total crude steel production (Figure 1).

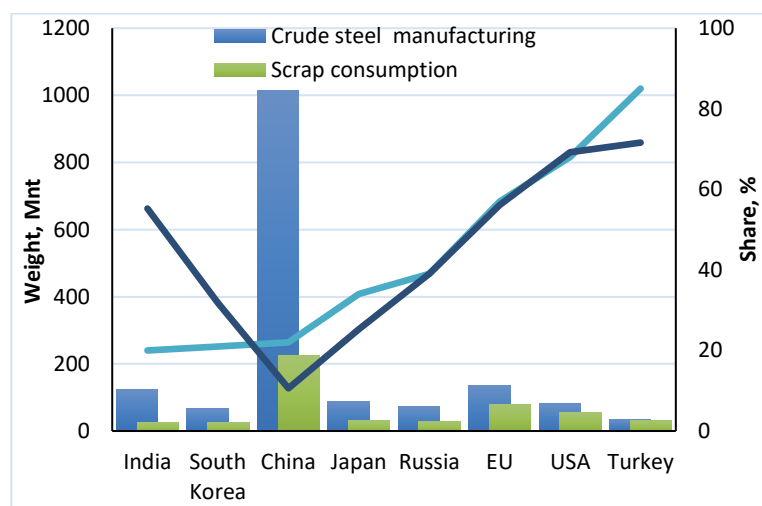


Figure 1. Scrap share and main performances of steelmaking by countries (2022).

The most developed and commercially proven pathway to decarbonization is the EAF route involving alternative iron-bearing charge materials and efficiency-increasing techniques - scrap preheating, waste heat recycling and clean materials using. The possibility for the near future is to use proven

steelmaking routes [18-20] together with existing infrastructure and technologies (Figure 2) combined with Carbon Capture Utilisation and Storage (CCUS) [20-22].

In our opinion, renewable electricity, minimized carbon and maximized hydrogen involvement as fuel



wherever possible, and Carbon Capture Utilisation and Storage (CCUS) technologies are effective pathways to low-CO<sub>2</sub> and fossil-free steelmaking, which will be

implemented in the nearest future. CCUS-equipped production is already a reality [21,22], which should be but not jet scale-up to big industrial capacities.




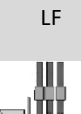
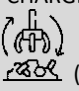
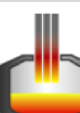


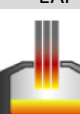



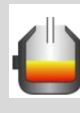
	Main raw material	Iron reduction	Hot metal	Steelmaking unit	Secondary metallurgy	CO <sub>2</sub> emission	Future improvements
Actual	Iron ore Coke Scrap (up	BF 	Pre-treatment  De-S /De-P	BOF 	LF 	2,33	Circular carbon Biomass reductants Hydrogen injection Carbon capture and usage
	SOLID CHARGE -Scrap up to 100%  (+pig iron+DRI)			EAF 	VD/VOD 	0,68	Clean electricity
Future	High-grade iron ore Methane/Hydrogen Scrap Clean electricity	DRI – CH <sub>4</sub>  DRI unit - H <sub>2</sub>		EAF 		1,37  Near Zero	Clean electricity Hydrogen to iron ore reduction
	Low-grade iron ore Hydrogen reduction Clean electricity	DRI unit – CH <sub>4</sub>  DRI unit- H <sub>2</sub>	Smelting in SAF-type smelter 	BOF 		Sufficient reduction	Circular carbon Carbon capture and usage

Figure 2. Flow diagrams of main eventual routes of steelmaking

Integrated steel mills with BF-BOF are now elaborating strategies to change existing flow charts with more sustainable options. Despite the enormous investments needed, some producers have already decided to replace BF with DRI facilities. The direct reduced iron manufacture is now considered crucial to near-zero emission steel, and DRI involvement is foreseen for both BOF and EAF finals. However, the BOF process is inefficient with only solid iron-bearing charge mix and, therefore, an intermediary smelter became necessary to melt DRI and feed BOF by hot metal. Thus, well-developed and widely used in the ferroalloys industry, submerged arc furnaces (SAF) are good candidates for liquid metal supply to BOF.

Nevertheless, the tandem of DRI and EAF units is today's most recognized alternative to the traditional BF-BOF route, which rather not survive without equipping by CCUS.

Another common concern is the raw materials quality worsening: recirculated steel scrap accumulates tramp elements, and high-grade ores availability and iron content in DRI concentrates are shrinking, increasing the range of harmful and ballast components as well. DRI's residual gangues (having a high content of silica oxide) will increase lime and flux consumption.

Besides, replacing both graphite electrodes and magnesium-carbon lining in EAF with other materials will fundamentally change existing practices.

Modern EAFs use a single-slag process with scrap melting intensification by oxygen blowing and bath mixing by neutral gas purging for ordinary semi-finished product manufacturing for further secondary metallurgy processing. High-performance electric arc furnaces are equipped with powerful transformers (0.7 - 1.5 MVA/t), wall gas-oxygen burners system and door manipulators with oxygen lance. Slag foaming by injection of carbonaceous powders (10-15 kg/t) with the simultaneous blowing of oxygen (30-60 nm<sup>3</sup>/t) accompanies by CO<sub>2</sub> emission but gives substantial gains: exothermic reaction heat (chemical energy), arcs shielding to better energy transfer to metal bath and additional power from CO afterburning reducing overall energy consumption on 10-30 kWh/t despite of more slag-forming additives; fewer metal losses due to part of iron oxides reduction from slag; nitrogen absorption decreases by 10-20 ppm (to a level of about 30 ppm for conventional semi-product).

The best available practice of high-performance 100-120 t EAF demonstrates specific electricity consumption of 310-360 kWh/ton due to up to 45% of the total heat input from chemical energy sources and mixing a bath, the heat duration - tap-to-tap time (TTT) reaches 34-45 minutes [last record 2023 was at Badische stahl werke [23], which is approaching but less than the indicators for oxygen converters, which besides have larger volumes. Increasing the metal

bath diameter reduces the efficiency of wall burners that lowering productivity. That means more EAFs will be necessary to balance the productivity of replacing BOFs.

Thus, there are several challenges connected with BOF replacement by EAF. Increasing EAF operational tap weight to 200-350 tons requires installing transformers of colossal capacity. If we take norms of 0.7 – 1.5 MVA/t nowadays, their power will reach 150-600 MVA. The problem is that units will introduce significant disturbance and imbalance in the electrical distribution grids.

The entire range of existent iron-bearing charge involvement and phasing out carbon in EAF require drastic changes in the already well-optimized technology. Today electric arc furnaces can use various types of initial charge mix: scrap metal - up to 100%, liquid iron - up to 40%, and direct reduced iron - up to 100%, providing the most ecology and cost-efficient steelmaking process emitting much less CO<sub>2</sub> than the BF/BOF route. Steel scrap is the original raw material to melt in EAFs, and operation with other charge components both the DRI and or iron is less efficient because requires changes in technology and, in the ideal case, in the EAF design:

- both DRI and iron usage accompanied by bigger volumes of forming slags because of high silicon in their composition, which should be removed from metal and bound with lime additives;
- blowing of high carbon and silica iron melt accompanied by the temperature increase requires coolants (scrap, DRI, lime) that also leads to the same problem with slag handling. Moreover, molten iron usage does not align with decarbonization (as discussed above).

Another essential task is prioritizing the circularity of basic oxygen steelmaking (both from BOF and EAF) by-products, such as basic oxygen steelmaking slag (further BOS), through iron recycling. For every ton of crude steel produced is accompanied in average with 150-250 kg of slag. The composition of BOF/EAF slag typically consists of 85-90% mineral components, which are complex oxides of calcium, silicon, aluminium, manganese, iron, and calcium and manganese sulfides, and 10-15% metallic phase, made up of droplets and beads of various sizes and shapes. While BF slags are fully utilised in cement production and road

construction good for other applications the steelmaking slags (both from BOF and EAF) is more challenging to reuse in the same fields due to the high content of metal oxides (iron, manganese, chromium and others (depending on the particular shop), metallic particles of various size and undissolved lime [24-29].

The extraction of metal pieces and particles of various fractions (usually to less than 1 mm) is the primary stage of today's way of solid steelmaking slag reuse that involves mineral processing technologies. Recovery slagged Scrap (RSS) gained from cooled steelmaking slags are specific materials with metal and slag parts. The annual formation of RSS worldwide can be estimated at 29 - 43 mln tons that cannot be neglected, and this resource can be effectively used in steelmaking, reducing demands for primary raw. For these reasons, this article gives a mathematical simulation of RSS melting and the results of its use in BOF shop.

### **Some results and consideration on Recovery Slagged Scrap (RSS) involving in steelmaking**

In this study, the results of industrial batches of Recovery Slagged Scrap (RSS) is presented as the prospective way of CO<sub>2</sub> emission reduction and approach to zero-waste manufacturing. RSS (fraction 20-200 mm) was obtained from a specialized crushing and screening complex that processes slags from Ukrainian steelmaking plant (BOF producing semi-product of low-alloy steel grades). Cooled slags discharged from slag pots were crushed by a falling load with collecting of largest parts of Recovery Slagged Scrap (RSS). The rests were crashed further and classifying with undergoing de-slagging on a tumbling drum with further beneficiation (gravity, size, and magnetic separation) and further classification into batches. The metal part has the same composition as that of averaged semi-product of the shop, and the slag part chemistry is the same as a final refining slag in the steelmaking unit. The slag shares on the surface of RSS depended on its pieces' size and shape and made about 5% in weight (12-15 %vol) on average for fractions 20-200 mm from the slag of the BOF shop. The slag-free metal surface of scrap pieces is covered by a 1-2 mm thick iron oxides layer (Figure 3).



Figure 3. The appearance of bulk RSS in fraction 20-200 mm (a) and separate piece (b) - 85 mm in length.

The slag part of RSS was a hardened stone-like substance with 2.8-3.6 basicity ( $\Sigma(\text{CaO} + \text{MgO}) / \Sigma\text{SiO}_2$  and FeO content 17-22 wt%. The main components content was determined by X-ray fluorescence method according Ukrainian standard DSTU 3564-97. The slag part is similar to the composition of the high basicity refining slag at the end of BOF melt ( $\text{CaO}/\text{SiO}_2 > 2.8$ ; CaO 45-60 wt%;  $\text{SiO}_2$  13-18 wt%; FeO 15-25wt%; MgO 4-8 wt%;) that is consistent with many previous researches [24, 28-30]. The bulk density was defined as simple dividing a mass (4.5-5 tons) of RSS scrap (20-200 mm) on scrap pan volume ( $3 \text{ m}^3$ ) that gave the bulk density value in the range 1500-1600  $\text{kg}/\text{m}^3$ .

Metal part chemical composition was determined by standard spectral analysis according to ASTM E415-21. Elements content it deviated from piece to piece, but average total alloying elements is less than 1 wt%, sulphur and phosphorus contents are in the limits for ordinary structural steels (no more than 0, 04% for both).

Because of sufficient oxide layer on the RSS surface (both slags or oxides), its melting mechanism is different from conventional scrap with a clean surface. At low melt flow velocity, RSS pieces melting time is close to ordinary scrap pieces. At higher rates that are typical for high-intensive steelmaking processes, the melting time of RSS pieces can increase. Faster melting of RSS occurs due to low melting points and low thermal conductivity of slag, reducing the period of frozen shell formation preceding the kinetic stage of melting. The importance of the period of frozen shell was formation shown by research [31], where it takes almost 50% of the total melting time of DRI, and the thickness of this shell increases by increasing the initial particle size. The discovered patterns also coincide with the conclusion made for scrap melting controlled by carbon mass transfer at 1573–1723 K that the relative contribution of parameters is the following: mixing power > bath temperature > specific surface area > carbon content [32].

This approach can enhance RSS technology in steelmaking units. Since RSS screens heat transfer to the lower layers of charge it is not recommended to put it above of another scrap grades that should be compelled at loading profile composing. To prevent sticking of RSS in big pieces it should be charged over the entire area of a steelmaking unit bath. Faster melting of the charge mix containing RSS and induction of primary slag due to the participation of scrap slag in slag formation, which made it possible to reduce the consumption of lime and fluorspar without deteriorating desulfurization conditions. However, in this case, it is necessary to take into account the specifics of the RSS composition and, probably, a change in the loading technology and intermediate slag removal be required to prevent an increase in the content of impurities but this reduces the productivity of the converter.

The early formation of slag via dissolving lime is a crucial factor for reducing iron burning losses, efficient melt refining and lining protection at oxygen blowing in both BOF and EAF [27, 33,34]. Due to relatively low

melting point and high content of FeO the RSS's slag part contributes in early appearance of liquid slag and increasing its basicity ( $\text{CaO}/\text{SiO}_2$ ) supporting dephosphorization and desulphurization. The positive effect of BOF's slag reuse in various periods of melting is well known - slag can act as fluxing agent intensifying lime dissolution and slag formation, as BOF's bath cooler while and after blowing and as a thickener for the final slag before tapping to reduce its ingress into the ladle and for lining slagging. The RSS's slag cover performs the same functions increasing primary slag volume, basicity and speed-up lime dissolution [33-36].

Content of elements in RSS is close to a final product that is good for any processing unit. RSS extracted from BOF slag of steelmaking plant producing semi-product of low alloyed steels fully meets these requirements since deviations of semi-product composition are quite narrow, besides several heats' slags can be averaged in one batch.

In the BOF steelmaking process, two types of slags are formed: slags of the initial melting period - primary slags with a high (up to 50 wt%) iron content (represented by FeO and  $\text{Fe}_2\text{O}_3$  oxides and metal beads) and low basicity. Such slags are discharges after the initial refining period completion and in principle can be stored and processed separately for utilisation for other purpose; -the final slags from the production of low-carbon steel contain a lower amount of iron (see above) but have higher basicity value (up to 4 units). A small part of the final slag enters the steel-pouring ladle together with the semi-product, and after casting, a conglomerate of the final slag and metal residues is formed, containing the maximum content of metallic iron.

In BOF the oxygen blowing of hot metal is accompanied by the release of a large amount of heat, which most often is absorbed by scrap having closest in composition to the semi-finished product produced from the unit in compare with other alternative iron coolers (hard iron, direct reduced iron, sinter or pellets, iron ore lumps), limestone or lime. Replacing scrap by any of these materials has its positive and negative aspects, affecting the chemical composition of semi-product, slag foaming, tap temperature and refractory wear [36].

Based on our analysis of BOF shop statistics, we found that using RSS resulted in copper, nickel, and chromium content in steel that was 1.6-2.0 times higher, while purchased steel scrap had content that was 3-4 times higher compared to metalized pellets. Thus, the composition of iron-bearing charge should be controlled to keep satisfactory level of impurities.

RSS using as a coolant does not entail changes in the BOF melt technology but has the same advantages as using of main materials of BOF charge - scrap and lime: slag part acts as a fluxing agent in helping to form refining slag early facilitating the removal of impurities and promoting better steel cleanliness and scrap is scrap – nothing to say more.

Performed analysis shown that there are no obstacles that are associated with technological difficulties and environmental safety since the scrap is used in the

same unit. RSS is easily sorted into various fractions and has quite a stable chemical composition. For high-quality steel melting RSS can be mixed with DRI to reduce and keep a competitive product cost.

The RSS extracted from slags from EAF working on 100% scrap contents more tramp elements, which removal in the steelmaking processes is inefficient or impossible (non-ferrous metals Cu, Sn, Ni, Cr, V, W and As, Sb). This reason in an EAF the addition of own RSS should be limited by 10-20 % (preliminary). Another reason is that residual slag on the surface of RSS has low electric conductivity; thus, thick layers of charged RSS will deteriorate arcing in the EAF. As in the case of BOF, RCC should not be loaded on top of another scrap charge. The usage of RSS in EAF charge mix can accelerate slag forming that lowers energy consumption and refractory wear.

Very preliminary the RSS fraction for EAF should be reduced to 20- 100 mm (instead of upper size 200 mm for BOF) to prevent problem with arcing because of low conductivity of slag covered its surface. Nevertheless, it seems that the allowable amount of RSS in the low-alloy steelmaking is limited primarily by increase in total volume of slag. When the RSS originates from fresh slags of the BOF shop working with stable composition of semi-product the amount of phosphorus and sulphur in the slag part is not critical. On contrary, the high basicity BOF slags contain a certain amount of lime this is one more argument to RSS recycling in steelmaking units.

Another case is steelmaking shops producing of high alloy and stainless steel, where the slags composition varied from heat to heat and content of alloying elements in both RSS slag and metal parts can be sufficiently different depending of the ordered grade. RSS from such slags is even more valuable because of high content of alloying elements, and it is important to carefully classify slags on several grades and process them separately to assure stable chemical composition.

The following RSS classification from semi-product for low alloy steel manufacturing can be recommended basing on experimental trials and literature data [30,35,36] scrap of fraction 0-10 mm having a slag content of more than 10% wt. can be and usually is utilized

in the sinter charge. Meanwhile, scrap measuring 10-120 mm and with a slag content of 5-10%wt is used in the blast furnace charge. Scrap measuring 20-200 mm with less than 5% slag content fit to using in steelmaking units. The optimal steps for RSS classification and use can differ from plant to plant, depending on processing facilities and the exploited steelmaking process but found peculiarities of RSS melting allow improve charging practice of basic oxygen steelmaking (both BOF and EAF) and resulting performances. Any case the widening of RSS reuse in steelmaking will increase iron recycling efficiency and became a small brick in a basement of carbon-neutral and zero-waste steel production.

### Conclusion

Decarbonization is a challenge and a possibility for steelmaking simultaneously, being a chance to check new approaches and technologies and improve existing technological routes in between which EAF is the most prospective.

Technological scenario for different steelmaking shops can depend on iron-bearing charge conditions and availability of hydrogen and renewable reductants and fuels.

In our opinion, it is not rational to pursue zero-carbon steelmaking because carbon is the most effective and inexpensive hardener, reducing agent, fuel and integral part of refractories, electrodes, and casting mixtures. Today there are no practical solutions to completely exclude carbon from composition of both steel grades and essential metallurgical materials. Nevertheless, all possibilities where carbon can be efficiently replaced by another reductant or electricity should be widely implemented.

The alternative scrap involvement confirms lime consumption decreasing with the same value of desulphurization as it was predicted by improvements in slag formation and better dissolution of lime due to action of slag part of RSS.

RSS internal recycling in both BOF and EAF can contribute to the iron recovery ratio, lower costs of iron-bearing charge mix and is a step toward zero-waste steelmaking.

### References

1. *December 2024 crude steel production and 2024 global crude steel production totals*. Worldsteel.org. <https://worldsteel.org/media/press-releases/2025/december-2024-crude-steel-production-and-2024-global-totals>
2. *Iron Ore Mining Market Analysis by Reserves, Production, Assets, Demand Drivers and Forecast to 2030*. GlobalData. <https://www.globaldata.com/store/report/iron-ore-mining-market-analysis>
3. Manocha, S., & Ponchon, F. (2018). Management of Lime in Steel. *Metals*, 8(9), 686. <https://doi.org/10.3390/met8090686>
4. *The European Magnesite/Magnesia Industry: enabler in the transition to a low-carbon economy*. (2020). Euromines. [https://www.euromines.org/files/euromines\\_magnesite-decarbonisation\\_297x210mm\\_fin.pdf](https://www.euromines.org/files/euromines_magnesite-decarbonisation_297x210mm_fin.pdf)
5. *2021 Global Low-carbon Metallurgy Innovation Forum*. WorldSteel Association. <https://worldsteel.org/media-centre/industry-member-news/2021-member-news/baowu-organises-2021-global-low-carbon-metallurgical-alliance-conference/>
6. *Making strides towards a low-carbon future*. Nature.com. <https://www.nature.com/articles/d42473-023-00009-8>
7. Hoffmann, C., Van Hoey, M., & Zeumer, B. (2020). Decarbonization challenge for steel. McKinsey&Company website. <https://www.mckinsey.com/industries/metals-and-mining/our-insights/decarbonization-challenge-for-steel/>
8. *World Steel in Figures 2024*. Worldsteel.org

9. *Iron and Steel Technology Roadmap*. (2020). International Energy Agency. [https://iea.blob.core.windows.net/assets/eb0c8ec1-3665-4959-97d0-187ceca189a8/Iron\\_and\\_Steel\\_Technology\\_Roadmap.pdf](https://iea.blob.core.windows.net/assets/eb0c8ec1-3665-4959-97d0-187ceca189a8/Iron_and_Steel_Technology_Roadmap.pdf)
10. Birat, J.-P., Lorrain, J.-P., & de Lassat, Y. (2009). The "CO<sub>2</sub> tool": CO<sub>2</sub> emissions & energy consumption of existing & breakthrough steelmaking routes. *Revue de Métallurgie*, 9, 325-336
11. *The potential of hydrogen for decarbonising steel production*. Europa.eu. [https://www.europarl.europa.eu/Reg-DATA/etudes/BRIE/2020/641552/EPRS\\_BRI\(2020\)641552\\_EN.pdf](https://www.europarl.europa.eu/Reg-DATA/etudes/BRIE/2020/641552/EPRS_BRI(2020)641552_EN.pdf)
12. Younas, M., Shafique, S., Hafeez, A., Javed, F., & Rehman, F. (2022). An Overview of Hydrogen Production: Current Status, Potential, and Challenges. *Fuel*, 316, 123317
13. Gabriel, K. S., El-Emam, R. S., & Zamfirescu, C. (2022). Technoeconomics of large-scale clean hydrogen production – A review. *International Journal of Hydrogen Energy*, 47(72), 30788-30798
14. Sadoway, D. R. (1991). Electrochemical Processing of Refractory Metals. *Journal of Metals*, 43(7), 15-19
15. Allanore, A. (2015). Features and challenges of molten oxide electrolytes for metal extraction. *J Electrochem Soc*, 162, E13–E22
16. Allanore, A., Yin, L., & Sadoway, D. R. (2013). A new anode material for oxygen evolution in molten oxide electrolysis. *Nature*, 497, 353–357
17. Joint Research Centre. (2022). *EU climate targets: how to decarbonise the steel industry*. [https://joint-research-centre.ec.europa.eu/jrc-news-and-updates/eu-climate-targets-how-decarbonise-steel-industry-2022-06-15\\_en](https://joint-research-centre.ec.europa.eu/jrc-news-and-updates/eu-climate-targets-how-decarbonise-steel-industry-2022-06-15_en)
18. Voraberger, B., Wimmer, G., Dieguez Salgado, U., Wimmer, E., Pastucha, K., & Fleischanderl, A. (2022). Green LD (BOF) Steelmaking – Reduced CO<sub>2</sub> Emissions via Increased Scrap Rate. *Metals*, 12(3), 466. <https://doi.org/10.3390/met12030466>
19. Fan, Z., & Friedmann, S. J. (2021). Low-carbon production of iron and steel: Technology options, economic assessment, and policy. *Joule*, 5(4), 829-862
20. Wimmer, G., Voraberger, B., Kradel, B., & Fleischanderl, A. (2022). Breakthrough Pathways to Decarbonize the Steel Sector. *Mitsubishi Heavy Industries Technical Review*, 59(4), 1-7. <https://www.mhi.co.jp/technology/review/pdf/e594/e594120.pdf>
21. Metals Magazine. <https://magazine.primetals.com/2022/12/12/steelanol-market-ready-carbon-capture-and-utilization-technology/>
22. Benavides, K., Gurgel, A., Morris, J., et al. (2024). Mitigating emissions in the global steel industry: Representing CCS and hydrogen technologies in integrated assessment modelling. *International Journal of Greenhouse Gas Control*, 131, 103963. <https://doi.org/10.1016/j.ijggc.2023.103963>
23. Website. [www.bse-kehl.de](http://www.bse-kehl.de)
24. Yang, J., Firsbach, F., & Sohn, I. (2022). Pyrometallurgical processing of ferrous slag "co-product" zero waste full utilization: A critical review. *Resources, Conservation and Recycling*, 178, 106021. <https://doi.org/10.1016/j.resconrec.2021.106021>
25. Das, B., Prakash, S., Reddy, P. S. R., & Misra, V. N. (2007). An overview of utilization of slag and sludge from steel industries. *Resources, Conservation and Recycling*, 50(1), 40-57. <https://doi.org/10.1016/j.resconrec.2006.05.008>
26. Branca, T. A., Colla, V., Algermissen, D., Granbom, H., Martini, U., Morillon, A., Pietruck, R., & Rosendahl, S. (2020). Reuse and Recycling of By-Products in the Steel Sector: Recent Achievements Paving the Way to Circular Economy and Industrial Symbiosis in Europe. *Metals*, 10, 345. <https://doi.org/10.3390/met10030345>
27. Li, Z., Li, J., Spooner, S., & Seetharaman, S. (2022). Basic Oxygen Steelmaking Slag: Formation, Reaction, and Energy and Material Recovery. *Steel Research Int.*, 93, 2100167. <https://doi.org/10.1002/srin.202100167>
28. Yi, H., Xu, G., Cheng, H., Wang, J., Wan, Y., & Chen, H. (2012). An Overview of Utilization of Steel Slag. *Procedia Environmental Sciences*, 16, <https://doi.org/10.1016/j.proenv.2012.10.108>
29. Andrés-Vizán, S. M., Villanueva-Balsera, J. M., Álvarez-Cabal, J. V., & Martínez-Huerta, G. M. (2020). Classification of BOF Slag by Data Mining Techniques According to Chemical Composition. *Sustainability*, 12, 3301. <https://doi.org/10.3390/su12083301>
30. Sheremet, V. A., Kekukh, A. V., Orel, G. A., Kostenko, G. P., Brodskij, A. S., Mukhachev, A. A., Stovpchenko A. P., & Romanenko, I. V. (2004). Efficiency of using the small size metal particles from slag dumps. *Stal*, (6), 34-36
31. González, O. J. P., Ramírez-Argáez, M. A., & Conejo A. N. (2010). Mathematical Modeling of the Melting Rate of Metallic Particles in the Electric Arc Furnace, *ISIJ Int.*, 50 (1), 9–16
32. Gao, M., Gao, J. T., Zhang, Y. L., & Yang, S. F. (2021). Evaluation and Modeling of Scrap Utilization in the Steelmaking Process. *JOM*, 73, 712–720. <https://doi.org/10.1007/s11837-020-04529-2>
33. Kitamura Sh. (2017). Dissolution Behavior of Lime into Steelmaking Slag. *ISIJ International*, 57(10), 1670-1676. <https://doi.org/10.2355/isijinternational.ISIJINT-2017-109>
34. Martinsson, J., Glaser, B. & Sichen, D. (2018). Lime Dissolution in Foaming BOF Slag. *Metallurgical and Materials Transactions B*, 49. <https://doi.org/10.1007/s11663-018-1421-6>
35. Kumar, S. D., Prasad, G., Ghorui, P. K. & Ranjan, M. (2008). Coolant strategies for BOF steelmaking, *Ironmaking & Steelmaking*, 35(7), 539-544. <https://doi.org/10.1179/174328108X335159>
36. Yi, H., Xu, G., Cheng, H., Wang, J., Wan, Y., & Chen, H. (2012). An Overview of Utilization of Steel Slag. *Procedia Environmental Sciences*, 16. <https://doi.org/10.1016/j.proenv.2012.10.10>

Отримано редколегією / Received by the editorial board: 16.01.2025

Прийнято до друку / Accepted for publication: 20.02.2025



**Shevchenko D.V., Ovcharuk A.M., Gladkih V.A., Bezugliy A.V., Nikolenko A.V.**  
**Research of the ore reducing furnaces electrical modes**  
**for ferronickel production**

**Шевченко Д.В., Овчарук А.М., Гладких В.А., Безуглий А.В., Ніколенко А.В.**  
**Дослідження електричних режимів рудовідновлювальних печей**  
**для виробництва феронікелю**

**Abstract.** The paper presents the results of a study of the electrical modes of ferronickel furnaces OTF-1 and OTF-2 at the Pobuzhsky ferronickel plant. It was found that the furnaces operate in arcless mode. An asymmetrical voltage mode is observed: electrode casing - under, which indicates an unbalanced mode of the furnace. As a result of measurements, a significant transfer of power was detected in the area of the electrical circuit of the 4th, 5th, 6th electrodes. An analysis of the electrical mode of a 48 MVA round ferronickel furnace in the city of Hua-Hua (China) showed that the use of a furnace transformer without a voltage booster and an autotransformer makes it possible to provide the necessary electrical mode of ferronickel furnaces. An analysis of the electrical mode of a 90 MVA round ferronickel furnace in Guatemala showed the possibility of operating these furnaces in a combined mode, i.e. in the presence of an electric arc, which is controlled by the resistance of the electrodes and the power ratio in the electric arc and slag.

**Key words:** ferronickel, ore thermal furnace, electric mode, mathematical modeling, six-electrode furnace.

**Анотація.** У роботі представлено результати дослідження електричних режимів феронікелевих печей OTF-1 та OTF-2 на Побузькому феронікелевому заводі. Встановлено, що печі працюють у бездуговому режимі. Спостерігається асиметричний режим напруги, що свідчить про незбалансований режим роботи печі. В результаті вимірювань виявлено значну передачу потужності в зоні електричного кола 4-го, 5-го, 6-го електродів. Аналіз електричного режиму круглої феронікелевої печі потужністю 48 МВА у місті Хуа-Хуа (Китай) показав, що використання пічного трансформатора без підсилювача напруги та автотрансформатора дозволяє забезпечити необхідний електричний режим феронікелевих печей. Аналіз електричного режиму круглої феронікелевої печі потужністю 90 МВА в Гватемалі показав можливість роботи цих печей у комбінованому режимі, тобто за наявності електричної дуги, яка контролюється опором електродів та співвідношенням потужності в електричній дузі та шлаку.

**Ключові слова:** феронікель, руднотермічна піч, електричний режим, математичне моделювання, шести-електродна піч.

## Introduction

The main quantity of ferroalloys is produced in three-electrode and six-electrode ore reduction furnaces. Round three-electrode furnaces, which are symmetrical not only in geometry, but also creates a symmetrical load on the network, have become widespread. Along with this, six-electrode furnaces with round and rectangular electrodes are also used in industry. If a lot of research has been carried out on round three-electrode furnaces, their optimal modes for various alloys have been determined, then on rectangular furnaces, there are few such researches and it is still not clear how the current is distributed in the working space of the furnace and what electrical mode is optimal. To study this issue, we developed an electrical model of a furnace, where the internal resistance of a section of the electrical circuit was determined by the internal resistance of ammeters. To solve this problem, the widespread computer program Electronic Workbench 5.12 was used.

## Theoretical and Experimental Researches

As six-electrode furnace is a powerful consumer of a symmetrical three-phase network, then the circuit for connecting consumers of each phase is equivalent to an open triangle, and the source voltage of each phase is distributed among the half-phases [1]. To determine the role of the metal in the electrical circuit of the furnace and the distribution of current in the bath, the first model does not have grounding in half phases. Despite the symmetry in voltage between the half-phases of phases A and B, the current between them is about 7% of the phase current (Fig. 1). As a result, the current between half-phases increases. Thus, this model makes it possible to estimate the current distribution in the furnace with a sufficient degree of accuracy.

Based on theoretical assumptions, the electrical modes of two six-electrode furnaces OTF-1 and OTF-2 of the Pobuzhsky ferronickel plant were studied. During the research, it was found that the hearth of the furnace bath is grounded with the workshop structures. In

© Shevchenko D.V. – postgraduate student, Ukrainian State University of Science and Technologies;  
Ovcharuk A.M. – Doctor of Technical Sciences, Professor, Ukrainian State University of Science and Technologies;  
Gladkih V.A. – Doctor of Technical Sciences, Professor, Ukrainian State University of Science and Technologies;  
Bezugliy A.V. – Senior lecturer, Ukrainian State University of Science and Technologies;  
Nikolenko A.V. – Head of department, Candidate of Technical Sciences, Associate Professor, Ukrainian State University of Science and Technologies



This is an Open Access article under the CC BY 4.0 license <https://creativecommons.org/licenses/by/4.0/>

While analyzing the measuring complex of furnaces OTF-1 and OTF-2, it was found that in the source circuit of each phase there are two sections of the circuit of the so-called half-phases. The furnace control system ensures the symmetry of each half-phase in current, voltage and power. It is believed that the symmetry of these parameters ensures optimal operation

With the advent of a metal equivalent, the voltage symmetry between sources is broken, but remains the same between half-phases (Fig. 2).



#	U <sub>IA</sub>	U <sub>IB</sub>	U <sub>IC</sub>	U <sub>ao</sub>	U <sub>ox</sub>	U <sub>Bo</sub>	U <sub>Oy</sub>	U <sub>Co</sub>	U <sub>Oz</sub>	U <sub>e1</sub>	U <sub>e2</sub>	U <sub>e3</sub>	U <sub>e4</sub>	U <sub>e5</sub>	U <sub>e6</sub>
1	388	390	373	253	202	257	255	271	271	249	194	248	252	264	268
2	348	375	367	262	218	252	260	272	274	260	216	257	255	268	261

#	U <sub>fA</sub>	U <sub>fB</sub>	U <sub>fC</sub>	U <sub>ao</sub>	U <sub>ox</sub>	U <sub>Bo</sub>	U <sub>oy</sub>	U <sub>co</sub>	U <sub>oz</sub>	U <sub>e1</sub>	U <sub>e2</sub>	U <sub>e3</sub>	U <sub>e4</sub>	U <sub>e5</sub>	U <sub>e6</sub>
1	447	355	434	236	222	272	227	205	320	225	219	255	227	202	303
2	466	374	407	240	192	263	268	320	243	219	181	201	202	325	235

As shown by measurements between 3<sup>rd</sup> and 4<sup>th</sup>, and especially between 5<sup>th</sup> and 6<sup>th</sup> electrodes, the voltage of the secondary winding of the transformer of phases B and C significantly exceeded, which

indicates the transfer of power from adjacent phases using a magnetic field. A large voltage between the electrodes of adjacent phases indicates a significant current between the electrodes of adjacent phases. The unbalance of the voltages measured in the electrode-under section indicates an unbalanced power distribution (Fig. 3 – 6).

The calculations showed that the power losses for the first and second modes of OTF-1 were 751.8 kW and 861.6 kW, respectively, taking into account losses in the transformer - 1303.1 kW and 1412.9 kW [3].

OTF-2 is characterized by artificial current unbalance, power transfer between phases B and C, as well as losses on a short network that are greater than on OTF-1 - in total they were 1534.7 kW and 1484.3 for the first and second measurements, taking into account losses in the transformer - 2089.7 kW and 2039.3 kW.

The measured voltage between the electrodes and the hearth confirms the unbalance of power introduced across the half-phases.

Measurements showed the presence of a current between adjacent phases, which for a symmetrical mode is more than 10% of the electrode current, i.e. it

is impossible to assume that in a six-electrode furnace the phase circuits are autonomous.

After processing the measurement results of the electrical mode, a mathematical model of a six-electrode ferronickel furnace was compiled, taking into account power transfer. The resistance of sections of the electrical circuit was represented by the internal resistance of the current meters. There is no nonlinear element in the furnace circuit - an electric arc. The model shows complete symmetry in phases. The transfer of energy by the magnetic field of adjacent phases is represented by additional sources of EMF for phases B and C. The electrode currents of phases B and C are higher than phase A. The current in the upper horizons of the furnace is 50% of the electrode current. The current between adjacent phases is 15% of the electrode current. Noteworthy is the large voltage unbalance in the half-phases between the electrode casing and the furnace hearth - and this means that there is an unbalance of the power introduced into the furnace in half-phases. The voltages between the electrode casings, measured on an operating furnace, are close in value to those obtained from the mathematical model.

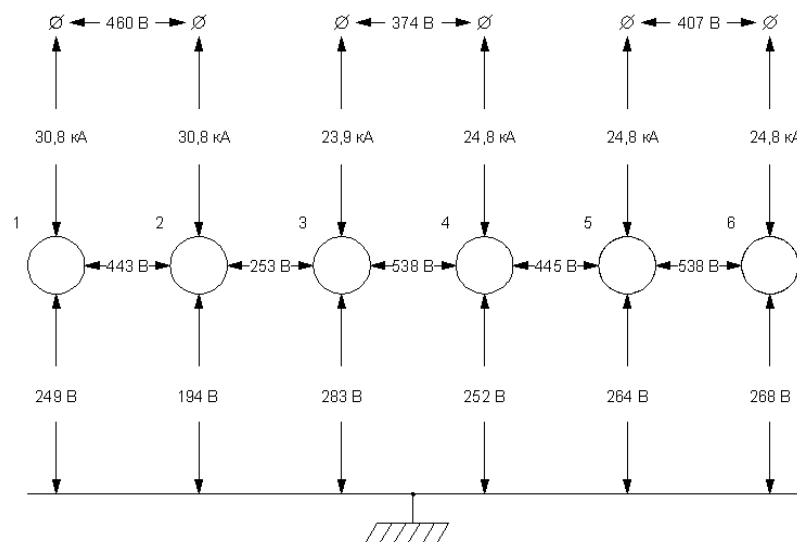


Fig. 3. Voltage measurement scheme OTF-1.

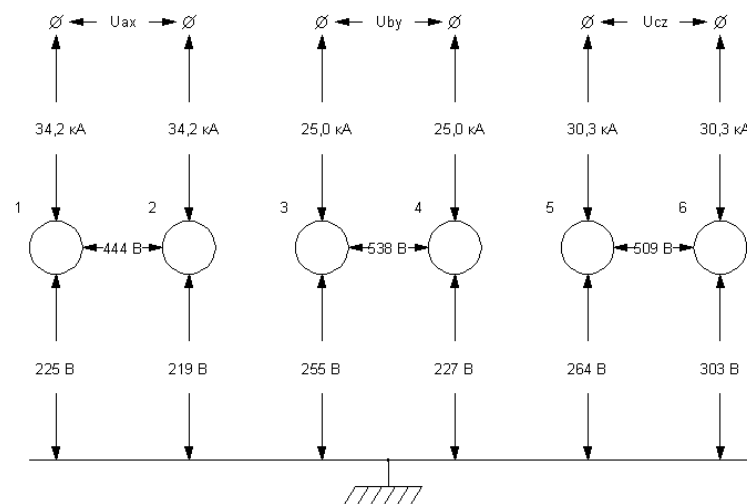


Fig. 4. Voltage measurement scheme OTF-2.

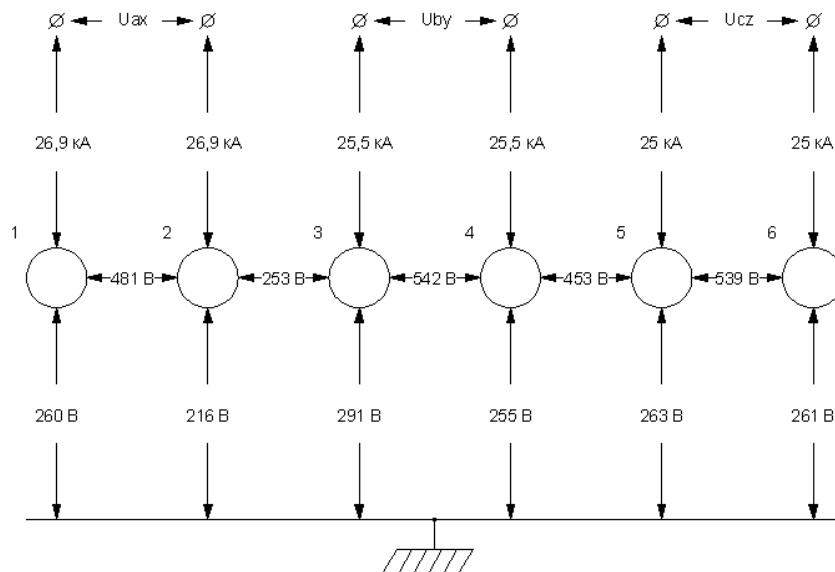


Fig. 5. Voltage measurement scheme OTF-1.

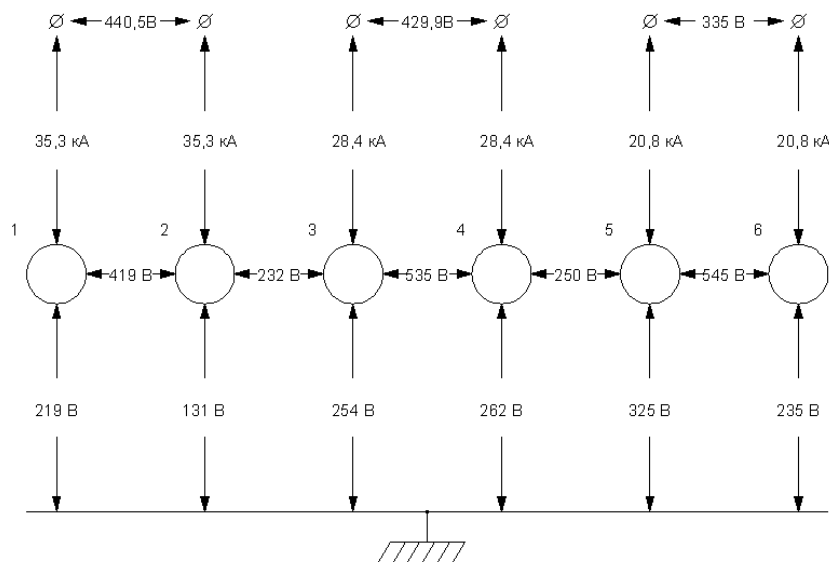


Fig. 6. Voltage measurement scheme OTF-2.

Using a mathematical model, the electrical mode was analyzed by half-phases of a six-electrode ferro-nickel furnace (Fig. 7).

Based on the data obtained from the measurement results at OTF-1 and OTF-2 and the mathematical model, proposals were made that make it possible to increase the accuracy of measurements and ensure symmetrical operation of the furnaces.

Thus, based on numerous measurements of the electrical operating modes of six-electrode furnaces OTF-1 and OTF-2, it was established:

- furnaces operate in resistance mode and the main amount of energy is released in the upper horizons of the furnace;
- furnaces producing ferronickel from oxidized nickel ores are characterized by arcless operation;
- significant power transfer was noted in phases B and C. This indicates an asymmetric operating mode of the furnaces, which causes an increase in the voltage between electrodes 3-4 and 5-6, respectively;

- the potential of the OTF-2 measuring complex differs from the furnace feed potential by 2-3 V.

Round three-electrode furnaces are powered by a three-phase alternating current network, which is provided by single-phase and three-phase furnace transformers. In the second case, the short network is asymmetrical and power transfer is observed. With single-phase transformers, a short network can be symmetrical. Under these conditions, it becomes possible to work at different stages in phases. This generates an equalizing current in the triangle circuit. Its magnitude is not controlled by anyone, and given the triangle switching on the electrodes, this current, passing between the cheeks of adjacent phases, can cause overheating of the electrode casing, disrupt the mode of its formation and subsequently break. Therefore, it is unacceptable to work at different stages on phases. In such furnaces, it is easy to control their electrical mode using the third harmonic, indicating the presence of an arc.

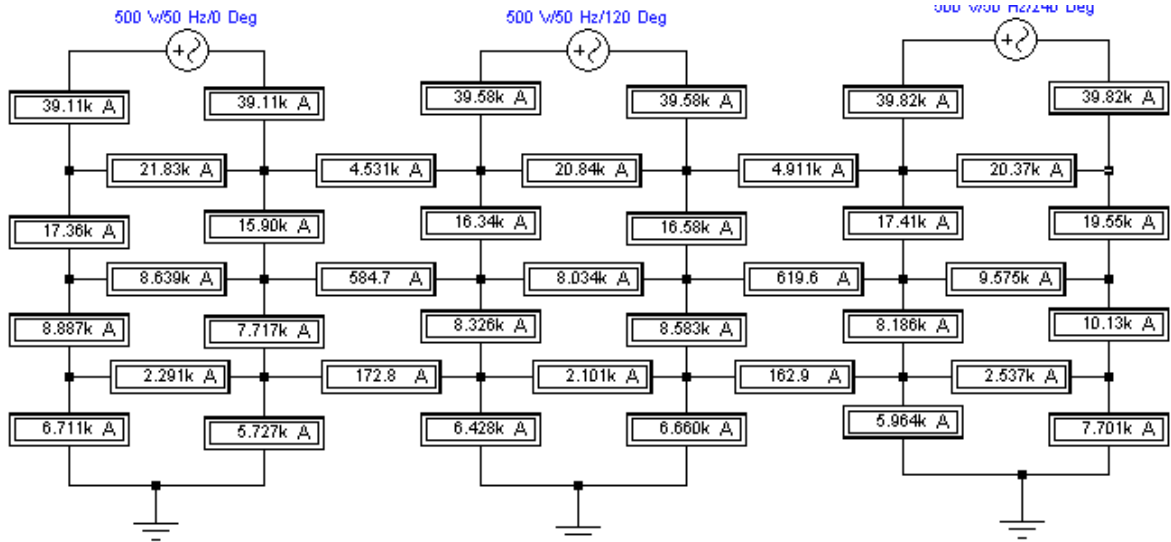


Fig. 7. Mathematical model of the electrical mode of a six-electrode OTF.

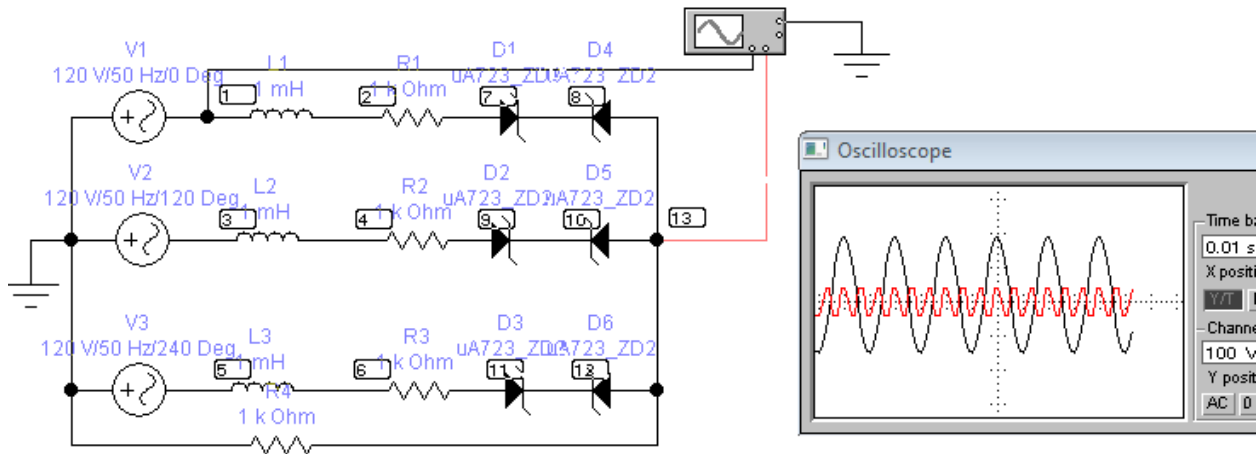


Fig. 8. Electrical diagram of a three-electrode furnace research.

As already noted, three-electrode arc furnaces create a symmetrical load on the network. To compensate for reactive power, longitudinal or transverse compensation is used. With longitudinal compensation, the inductive reactance of a short network can be compensated to a large extent, while the  $X_L/R$  condition of continuous arc burning is violated, which limits the power input into the furnace. Therefore, a transverse compensation scheme is mainly used. Furnaces operating at low  $\cos \varphi$  provide conditions for continuous arc burning. Traditionally, furnaces were equipped with

furnace units, where, in addition to the furnace transformer, booster transformers and autotransformers were used. In one of the projects of a ferronickel plant in China, a furnace transformer without a booster transformer was proposed. The secondary winding of each phase consisted of 4 windings for a current of 10000 A. Switching of these windings is carried out using jumpers.

The technical characteristics of the ore-thermal round furnace with a capacity of 48 MVA are given in table 3.

Table 3. Technical characteristics of the ore-thermal round furnace with a capacity of 48 MVA.

Parameters	Unit	Meaning
Furnace power	MVA	48
Transformer rated power	MVA	16
Number of transformers	—	3
Primary voltage	kV	110
Limits of secondary line voltage when connecting secondary windings in series	V	800-340
Limits of secondary line voltage with parallel connection of secondary windings	V	400-170
Number of transformer stages	—	24



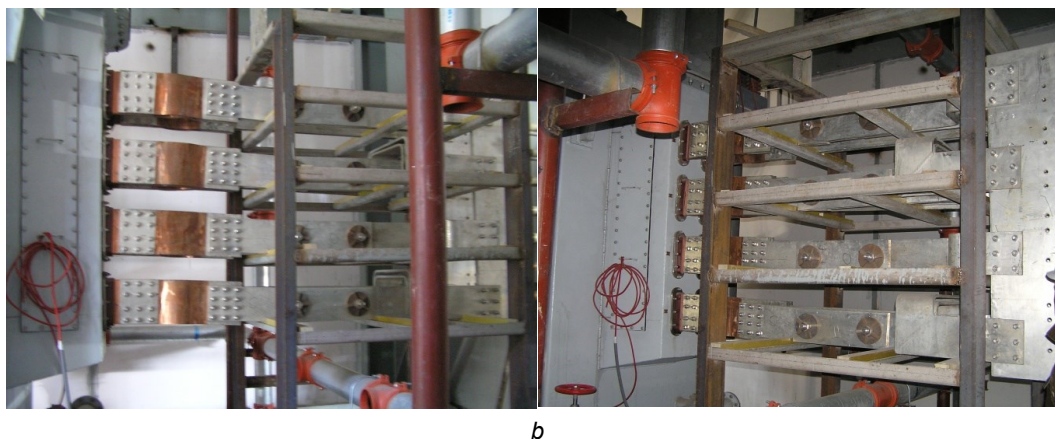
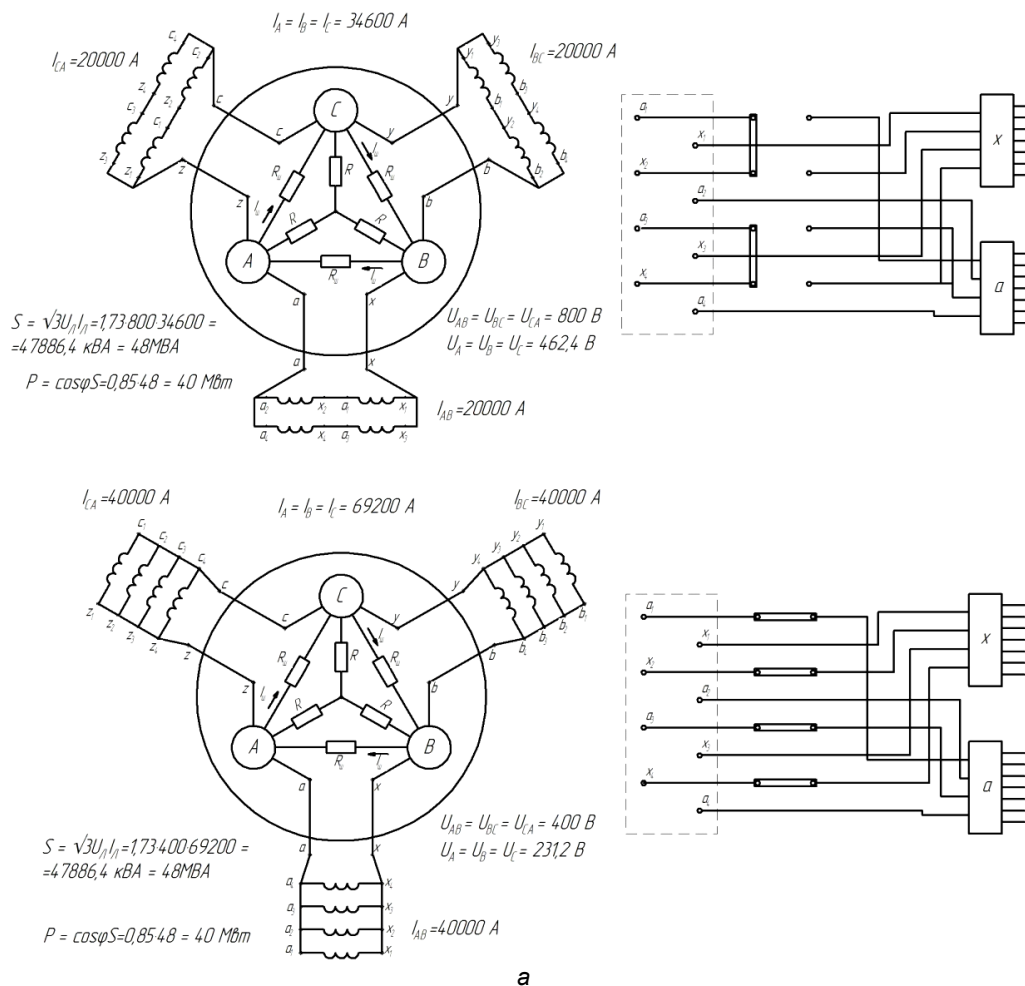


Fig. 9. Short network switching: a – diagram; b – general view.

As indicated in the characteristics, the furnace has 3 single-phase transformers of 16 MVA each.

The project envisaged the use of nickel-containing raw materials with various physical and chemical properties in the processing process. In this regard, the furnace transformer must have a wide range of voltage adjustment of the secondary winding with a high utilization rate of the installed power of the transformer.

We have thoroughly worked out the theoretical basis for solving this problem. The existing method of increasing the cross-section of the secondary winding at several subsequent stages compared to the first one

does not provide a solution to the problem. In our case, it was necessary to solve this problem by changing the voltage of the secondary winding of the furnace by 50%. A split-phase circuit was proposed, consisting of 4 secondary windings designed for a current of 10 kA with their subsequent switching, which ensures a minimum number of switching elements and a minimum switching current. To solve this problem, a non-standard arrangement of the terminals of the secondary windings of the transformer was proposed, which was successfully implemented by the Chinese transformer manufacturer (Sinosteel company) based on a patent

of Ukrainian specialists [4]. During switching process 4 secondary windings were connected in parallel, which provided a phase current of 40 kA and an electrode current of 69.2 kA. The circuit was assembled with 4 jumpers in 10 kA circuits with a linear voltage of 400 V. The second switching mode provides for pairwise series-parallel connection of secondary windings. Switching is carried out by two jumpers in a 10 kA

current circuit (Fig. 9).

With this switching, the linear voltage of the secondary winding is 800 V at a rated phase current of 20 kA, and the electrode current of 34.6 kA. Feeding substation with deep input 110 kV (Fig. 10). The 110 kV current supply to the furnace units is carried out through modern measuring and switching devices.

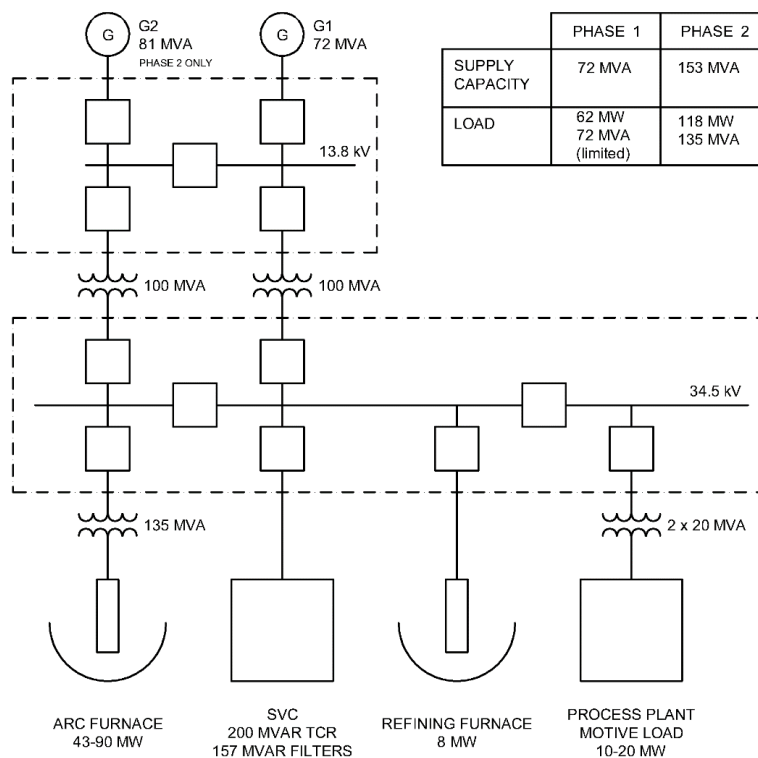


Fig. 10. Furnace power supply diagram.

With the help of hydraulics bypass and move the electrodes happens. During the period of operation of the furnace, switching devices and other components of the electrical circuit showed reliable operation and efficient operation of the furnace at optimal electrical parameters for conducting the process on nickel-containing raw materials with various physical and chemical properties.

The ore-thermal furnace (OTF) at the ProNico plant (Guatemala) is a round furnace designed for smelting cinder with a nominal power of 90 MW [5]. The three-transformer 45 MVA furnace is designed to melt 180 tons of cinder per hour at a furnace power of 90 MW, with a specific hearth power of approximately 400 kW/m<sup>2</sup> and a power utilization factor of 0,85 under load. A summary of the design parameters of the furnace section is given in Table 4.

Controlling the electrical mode of the furnace is in changing the following parameters [6]:

- current on the electrodes ( $I_{el}$ ) – depends on the voltage on the electrodes. As the resistance increases, the current decreases and vice versa;
- voltage on the electrodes ( $U_{el}$ ) – depends on the supply voltage on the high side (5.52 kV, 11 kV,

17.25 kV, 34.5 kV), the connection diagram of the furnace transformer windings (Y or  $\Delta$ ), and the position of the voltage step switch (1-35).

The current and voltage on the electrodes determine the power by phase and the total power of the furnace (Fig. 11).

The choice of electrical mode under different conditions is shown at Fig. 12-15.

The resistance at the electrodes ( $R_{el}$ ) determines the position of the working end of the electrode in relation to the slag surface (Fig. 16) and the ratio of the power (or heat) generated in the arc to the power released in the slag bath due to the resistance of the slag.

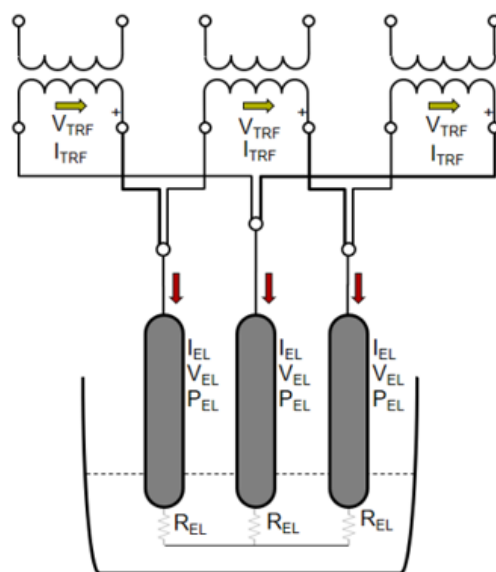
The resistance or electrical conductivity of the slag depends on its composition ( $k$  – electrical conductivity, 1/Ohm·cm):

$$\ln(k) = -4,45 + 9,152 \cdot \text{FeO} + 5,34 \cdot (\text{CaO} + \text{MgO}) \text{ at } 1500^\circ\text{C}$$

As can be seen from the equation, MgO and especially FeO increases electrical conductivity or reduces resistance. It is also known that SiO<sub>2</sub> and Al<sub>2</sub>O<sub>3</sub> increase the resistance of the slag.

Table 4. Parameters of round OTF.

Parameter	Unite	Operation with one tubular rotary furnace	Operation with two tubular rotary furnace
Furnace power	MW	45	90
Melting of the cinder	t/h	90	180
Cinder temperature	°C	850-900	
Total electricity consumption (per 1 ton of cinder)	kW·h/t	520	480
Furnace diameter (inside the casing)	m	18	
Furnace diameter (inside the lining)	m	16,9	
Furnace operating mode		Half-arc	Arc
Hearth area	m <sup>2</sup>	225	
Specific power of the hearth	kW/m <sup>2</sup>	200	400
Bath specific power	kW/m <sup>2</sup>	200	130
Bath resistance for 1 electrode	mOhm	6	12
Electrode current strength	kA	45	45
Characteristics of electrodes	3 Soderberg electrodes – 2 m in diameter		
Transformer rated power	MBA	135	
Transformer rated current	kA	60	
Metal release temperature	°C	1525	
Temperature of the liquid phase of the metal	°C	1450	
Slag release temperature	°C	1600	
Temperature of the liquid phase of the slag	°C	1550	
Metal production rate	t/h	4,1	9,7
Metal release frequency	pcs/day	2,1	5
Slag production rate	t/h	64,6	158,3
Dust generation rate	t/h	0,9	
Exhaust gas volume	nm <sup>3</sup> /h	14385	35970
Flue gas temperature	°C	750-850	



$$V_{EL} = \frac{V_{TRF}}{\sqrt{3}}$$

$$I_{EL} = \frac{V_{EL}}{R_{EL}} = \frac{V_{TRF}}{\sqrt{3} \times R_{EL}}$$

$$P_{EL} = V_{EL} \times I_{EL}$$

3 ELECTRODES ARE CONDUCTING

$$P_{FNC} = 3 \times P_{EL}$$

Fig. 11. Schematic diagram of the connection of furnace transformers and electrodes.

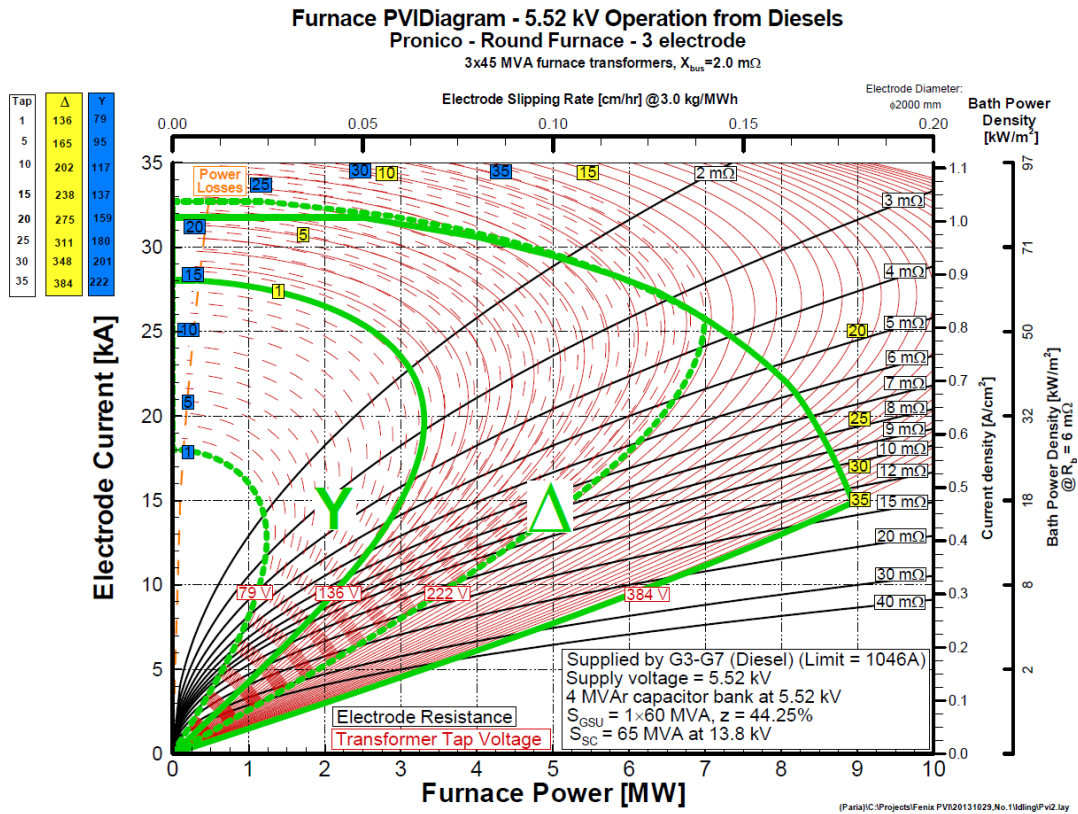


Fig. 12. 5.52 kV Operation on diesel generation.

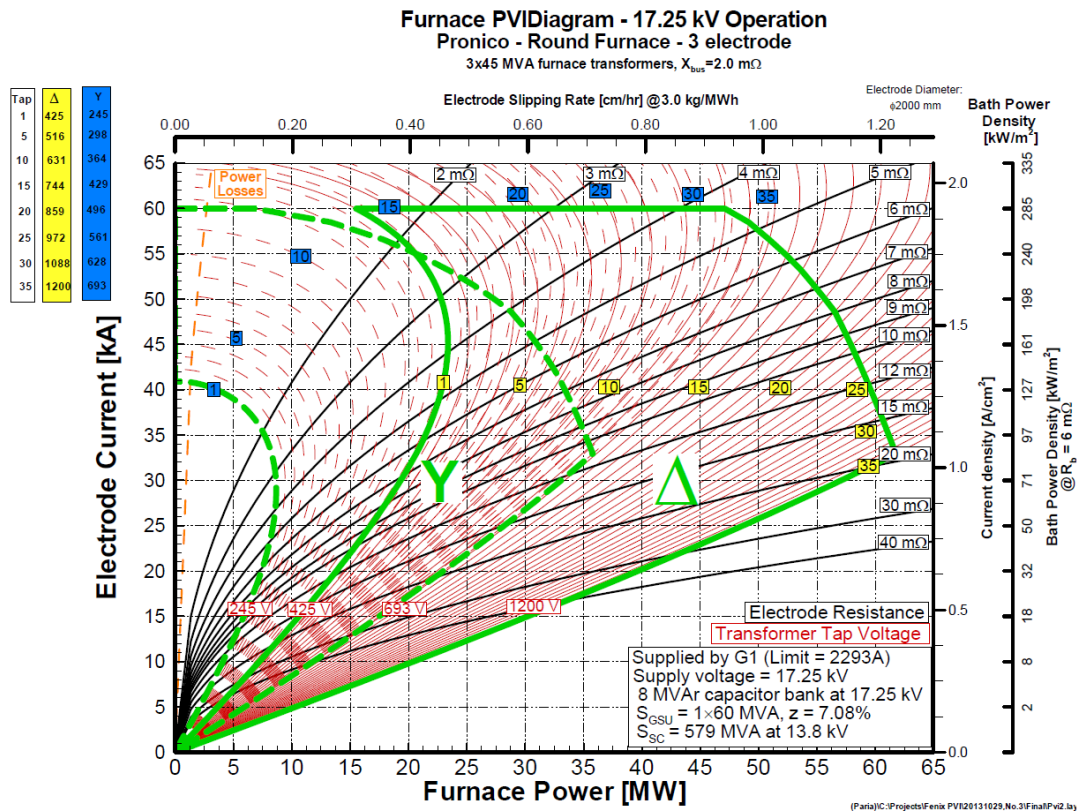


Fig. 13. 17,25 kV Operation on one turbogenerator.



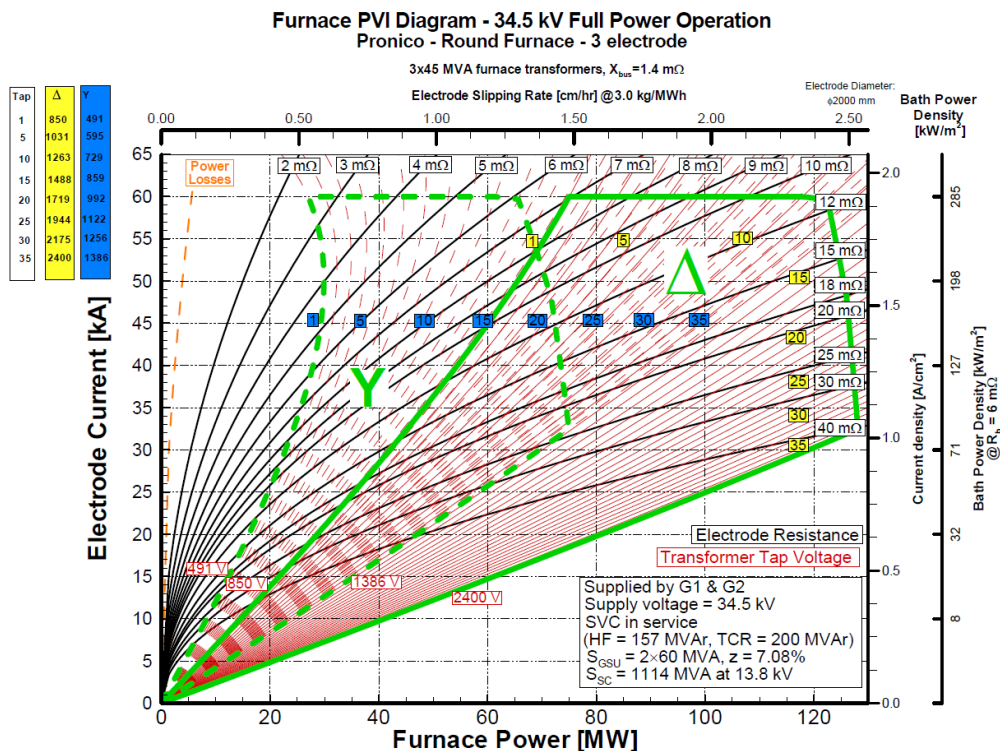
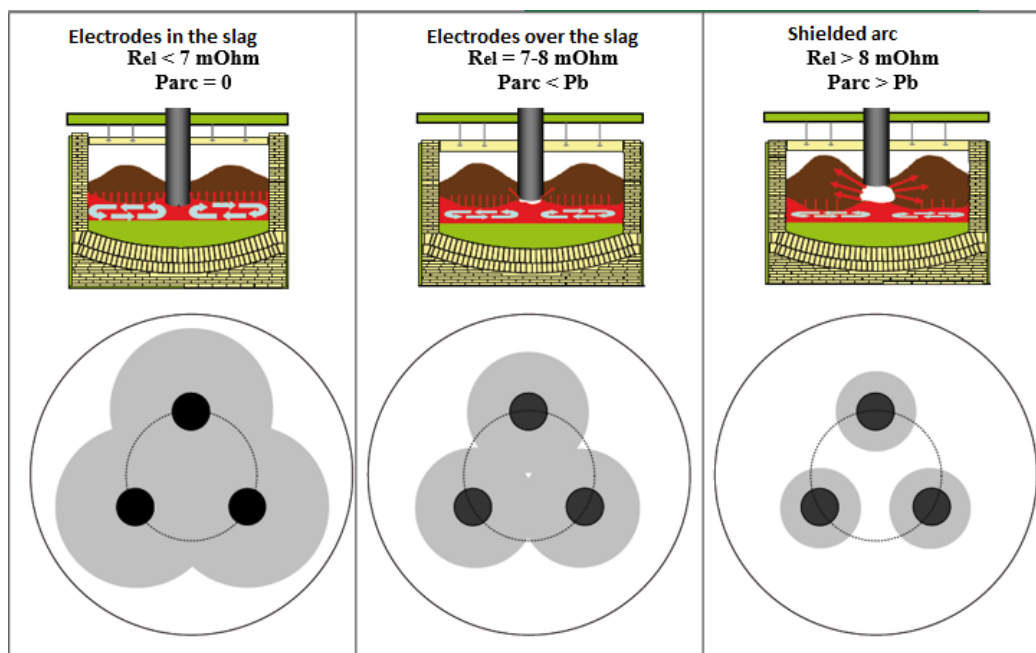


Fig. 14. 34,5 kV Operation on two turbogenerators.

Fig. 15. Area of active melting zone depending on  $R_{\text{el}}$ ,  $P_{\text{arc}}$  and  $P_b$ .

The total power released in the furnace consists of the power released in the arc ( $P_{\text{arc}}$ ) and the power released in the slag bath ( $P_b$ ). The ratio  $P_{\text{arc}} / P_b$  is an important technological parameter. Insufficient power of the slag bath  $P_b$  will lead to low slag temperature, more viscous slag and difficulties with its release. Too high a power of the slag bath will increase the thermal load on the lining of the furnace walls, due to the increased temperature of the slag (increased overheating), and will lead to more intense mixing of

the slag in the furnace (wear of the lining and high heat losses).

The resistance value on the electrodes ( $R_{\text{el}}$ ) is determined by the furnace operator depending on the target ratio  $P_{\text{arc}} / P_b$ . As the resistance value increases, the penetration of the electrodes into the slag decreases (or the distance from the end of the electrode to the surface of the slag increases), and the area of the active melting zone of the slag bath changes.



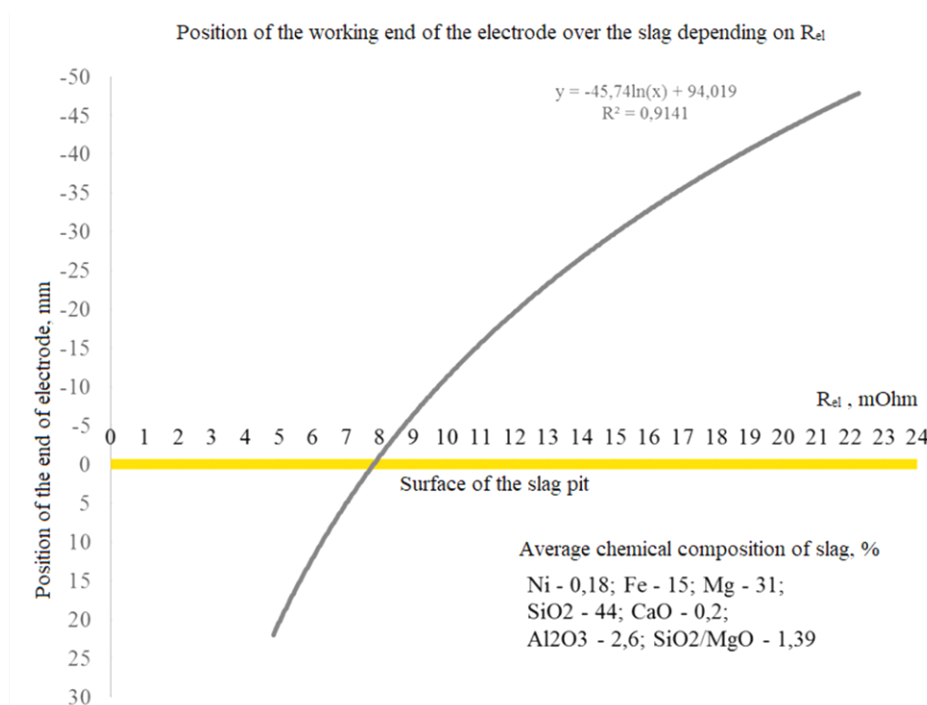
Fig. 16. Position of the working end of the electrode depending on  $R_{el}$ .

Table 5. Operating modes and electrical parameters of the OTF

Operating mode	Power, MW	$R_{el}$ , mOhm	Average $P_{arc} / P_b$
Idling	<7	3-10	0
Warming up	7-20	7-14	1,4
Normal operation	20-30	10-16	1,7
Normal operation	30-40	12-18	2,0
Normal operation	40-50	15-20	2,3
Normal operation	50-60	18-22	2,7
Normal operation	>60	>18	>2,9

Table 6. Electric mode of the furnace in 24 hours

Parameter	One-time parameter	Parameter range for 24 hours
P [MW]	84	79-87,0
P [MW] one phase	28	16,6-49,9
cos $\varphi$	0,91	0,58-0,95
I [kA]	43,7	16,6-54,5
U [V]	664,3	450-1204
Stage	13	12-15
Electrode bypass [mm]	575,5	126-835
Active resistance R [mOhm]	15,7	9,2-87,3

## Conclusions

Electrical parameters of ore reduction furnaces with a capacity of 46-90 MW with a rectangular (six-electrode) and round (three-electrode) bath are characterized by a significant difference in the distribution of electric current in the bath of smelting units - in

rectangular furnaces there is a power imbalance in the half-phases, and in round furnaces - on the electrodes when operating at different phase voltages. The authors of the current paper are working to improve the electrical parameters of ore reduction furnaces and develop new sources of their energy supply.

## References

1. Bezugliy, A. V., Nikolenko, A. V., Shevchenko, D. V., Ovcharuk, A. N., Kuvaev, V. Iu., Bezugly, V. A., & Zamkovoy, O. V. (2021). Improvement of the Process of Conducting Arc-Free Ferronickel Melting in a Six-Electrode Furnace. In *Proceedings of the 16<sup>th</sup> International Ferro-Alloys Congress (INFACON XVI) 2021*.
2. Bepalov, O. L., Bezugliy, A. V., Solokha, V. K., Nikolenko, A. V., Gasik, M. I., Ovcharuk, A. N., Kuvaev, V. Iu., Patyaka, V. A., Bezugliy, V. A., & Zamkovoy, O. V. (2018). Symmetry of electric operating modes of three-phase

electric arc furnaces according to harmonic spectrum. In *INFACON XV – Proceedings of the 15<sup>th</sup> International Ferro-Alloys Congress, 25-28 February, 2018, Cape Town, South Africa. Vol. 1. Ferroalloys.* (pp. 247-252). SAIMM Publications, Johannesburg

3. Bezugliy, V. A., Bezugliy, A. V., Sokolov, K. D., Nikolenko, A. V., Zamkovoy, O. V., Ovcharuk, A. N., Kuvaev, V. Iu., & Patyaka, V.A. (2018). Research of electrical parameters of operation of three-phase ore reduction furnaces of increased power. In *Materials of the International Scientific and Technical Conference VIII "Key aspects of the development of the electrometallurgical industry", Kyiv, Ukraine, April the 19-20, 2018* (pp. 61-71)
4. Bezugliy, A. V., Sadovnyk, Iu. V., & Lysakov, A. V. (2008). *The method of regulating the electrical mode of an ore-thermal furnace.* (Patent No. 33283 Ukraine). <https://sis.nipo.gov.ua/uk/search/detail/315412/>
5. Shevchenko, D. V., Anderson, B., Wikston, J., & Kadar, L. (2015). Furnace Power Supply Requirements for a High Powered Smelting Furnace. *Proceedings of the Fourteenth Ferroalloys Congress Energy efficiency and environmental friendliness are the future of the global Ferroalloy industry*, 649-657
6. Sherstobitov, A., Pershin, D., Avdeev, A., Polyenetsky, S., Elksnis, Y., Sedighy, M., & Shen, D. (2020). 90 MW 3 Electrode Furnace with an Electrically Islanded Power Plant Utilizing SPLC, SVC Electrical Efficiency and Stable Operation in Shielded Arc. *Proceedings of the 59<sup>th</sup> Conference of Metallurgists, COM 2020.* The Canadian Institute of Mining, Metallurgy and Petroleum

Отримано редколегією / Received by the editorial board: 10.12.2024

Прийнято до друку / Accepted for publication: 20.02.2025

Zaselskyi V.Y., Popolov D.V.

**Laboratory studies on the effect of vibro-impact action  
of the screening surface on the main technological indicators  
of metallurgical raw material screening**

Заселський В.Й., Пополов Д.В.

**Дослідження впливу віброударної дії просіювальної поверхні  
на основні технологічні показники грохочення  
металургійної сировини**

**Abstract.** The article presents the results of a study on the effect of vibro-impact action of the screening surface on the main technological indicators of metallurgical raw material screening. The screening process is one of the key technological operations in the preparatory processes of metallurgical production, as it directly influences the quality of raw material fractionation and process productivity. The issue of screen aperture clogging significantly limits the efficiency of screening, leading to a decrease in the quality of prepared charge and an increase in energy costs. The purpose of the study is to investigate the effect of vibro-impact action of the screening surface on aperture clogging and the productivity indicators of metallurgical raw material screening. To achieve this goal, a laboratory model of a vibratory screener was developed, allowing for the simulation of various vibration modes of the box and studying their impact on the raw material screening process. The research methodology included a series of experiments with varying amplitude and angular frequency of box oscillations, analysis of the results using mathematical statistics methods, and the construction of mathematical models of the dependence of transportation productivity and clogging coefficient on vibration parameters. Experiments were conducted for two types of screening surfaces – fixed and freely laid, which allowed for assessing the impact of vibro-impact loads on screen aperture self-cleaning. The results showed that maximum transportation productivity is achieved at a forced oscillation amplitude of  $2 \cdot 10^{-3}$  m and an acceleration of  $28 \dots 32$  m/s<sup>2</sup>. At the same time, the clogging coefficient significantly decreases at an amplitude of  $1.8 \dots 2.2 \cdot 10^{-3}$  m and an oscillation frequency of  $94.2 \dots 102$  s<sup>-1</sup>. The constructed mathematical models allow predicting changes in the technological parameters of the process depending on the dynamic characteristics of the box and assist in selecting optimal operating modes for vibratory screeners. The scientific novelty of the work lies in determining the effect of vibro-impact action on the efficiency of metallurgical raw material screening and forming new approaches to reducing screen surface clogging. The practical significance of the study is due to the possibility of using the obtained results to modernize existing screeners and develop new designs with improved technological characteristics, which will contribute to enhancing the efficiency of preparatory processes in metallurgical production.

**Key words:** screening, vibro-impact action, screening surface, productivity, clogging, metallurgical raw materials, mathematical modeling.

**Анонція.** У статті представлено результати дослідження впливу віброударної дії просіювальної поверхні на основні технологічні показники грохочення металургійної сировини. Процес грохочення є однією з ключових технологічних операцій у підготовчих процесах металургійного виробництва, оскільки безпосередньо впливає на якість фракціонування сировини та продуктивність процесу. Проблема забивання отворів сита значно обмежує ефективність грохочення, що призводить до зниження якості підготовленої шихти та збільшення енергетичних витрат. Метою дослідження є вивчення впливу віброударної дії просіювальної поверхні на забивання отворів та показники продуктивності грохочення металургійної сировини. Для досягнення цієї мети було розроблено лабораторну модель вібраційного грохота, яка дозволяє імітувати різні режими коливань короба та досліджувати їхній вплив на процес грохочення сировини. Методика дослідження включала серію експериментів зі змінними амплітудою та кутовою частотою коливань короба, аналіз результатів методами математичної статистики та побудову математичних моделей залежності транспортної продуктивності та коефіцієнта забивання від параметрів вібрації. Експерименти проводилися для двох типів просіювальних поверхонь – закріпленої та вільно покладеної, що дозволило оцінити вплив віброударних навантажень на самоочищення отворів сита. Результати показали, що максимальна транспортна продуктивність досягається при амплітуді вимушених коливань  $2 \cdot 10^{-3}$  м та прискоренні  $28 \dots 32$  м/с<sup>2</sup>. Водночас коефіцієнт забивання значно зменшується при амплітуді  $1,8 \dots 2,2 \cdot 10^{-3}$  м та частоті коливань  $94,2 \dots 102$  с<sup>-1</sup>. Побудовані математичні моделі дозволяють прогнозувати зміни технологічних параметрів процесу залежно від динамічних характеристик короба та сприяють вибору оптимальних режимів роботи вібраційних грохотів. Наукова новизна роботи полягає у визначенні впливу віброударної дії на ефективність грохочення металургійної сировини та формуванні нових підходів до зменшення забивання просіювальних поверхонь. Практична значущість дослідження зумовлена можливістю використання отриманих результатів для модернізації існуючих грохотів та розробки нових конструкцій з покращеними технологічними характеристиками, що сприятиме підвищенню ефективності підготовчих процесів у металургійному виробництві.

**Ключові слова:** грохочення, віброударна дія, просіювальна поверхня, продуктивність, забивання, металургійна сировина, математичне моделювання.



## Introduction

Screening is one of the most important technological operations in the preparatory processes of metallurgical production, as it significantly affects the production cost during the sintering or smelting of raw materials. Currently, various types of inertial screeners are widely used for the fractionation of metallurgical raw materials, differing in size as well as dynamic and kinematic parameters. These parameters determine the key technological indicators of the screening process, such as productivity, efficiency in removing unsuitable product fractions, and the degree of clogging of the screening surface with difficult-to-screen particles.

The productivity of screening is determined by the requirements of the technological line in metallurgical production, whereas the efficiency and clogging of the screening surface depend not only on productivity but also on the optimal choice of dynamic and kinematic parameters. However, the efficiency of screening under current conditions remains insufficient, requiring improvement. The main problem is the clogging of the screening surface, which limits the possibility of increasing the efficiency of the process in existing inertial screeners. This is due to the fact that the acceleration of their working elements is limited to the range of  $(1.5...3) \cdot g$ , which is insufficient for modern fractionation requirements of metallurgical raw materials.

Thus, finding ways to intensify the screening process to reduce screening surface clogging and increase fractionation efficiency without losing the necessary productivity is a relevant task. Research in this area is of great importance for optimizing the preparatory processes of metallurgical production.

## Literature review and problem statement

The most commonly used screeners in the mining and metallurgical industry for removing fines are center-of-mass machines with unbalanced vibration exciters operating in the sub-resonant region. These machines are characterized by simple construction, good vibration isolation, and fairly stable operating modes. However, the intensity of the working element's impact on the material in such screeners is low and distributed randomly across stages. Additionally, the kinematic parameters of the working element are chosen independently of the properties of the screened material.

Studies [1-6] provide the main structural and dynamic parameters, as well as technological indicators, of the most common screeners.

According to these studies, oscillation frequency ranges from 73 to 96 s<sup>-1</sup>; oscillation amplitude from 3 to 6 mm; vibration angle from 30° to 50°; sieve inclination angle from 0° to 18°; specific productivity from 40 to 60 t/h·m<sup>2</sup>; specific metal consumption from 400 to 3600 kg/m<sup>2</sup>; and specific power from 2 to 7.2 kW/m<sup>2</sup>.

The analysis of screen surface clogging depending on oscillation accelerations is well-detailed in [7], where it was found that the clogging degree ranges from 58 to 70% at accelerations of 26...32 m/s<sup>2</sup>. Thus, the screening efficiency remains very low – between 28 and 50 %, which does not meet modern requirements and fails to adequately prepare charge materials for sintering and smelting. According to the research in [8], significant improvements in blast furnace performance can be achieved if screening efficiency reaches at least 70...75 %.

This level of efficiency can be achieved by reducing the clogging of screen apertures if sufficient acceleration is applied to the screening surface. According to [9], the required accelerations for sinter fractions of 5 mm should reach 54 m/s<sup>2</sup>, as shown in Fig. 1.

However, the implementation of such accelerations is possible at a vibration machine operating mode coefficient of  $(5.5...6.2) \cdot g$ , which significantly exceeds the recommended value of  $(1.5...3) \cdot g$  when designing vibration machines [10]. Such high dynamic modes lead to a significant reduction in the reliability of the main working elements and result in an increase in the metal and energy intensity of the overall process of screening metallurgical raw materials.

Therefore, conducting research aimed at identifying ways to intensify the screening process of metallurgical raw materials before sintering and melting through the application of vibrational-impact loading is fully justified and represents an important scientific task.

## Research objective and tasks

The objective and tasks of the research involve studying the impact of vibrational-impact action of the screening surface of the screen on its clogging and the performance indicators of screening metallurgical raw materials.

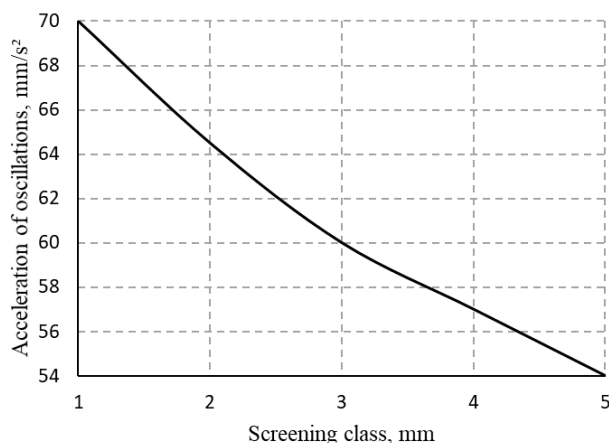


Figure 1. Dependence of the acceleration values ensuring the non-clogging of the screening surface openings on the class of agglomerate screening.

### Materials and research methods

To study the impact of vibrational-impact action on the technological indicators of the screen, a laboratory model was developed, as shown in Fig. 2.

As optimization parameters that most fully reflect the technological efficiency of the vibrating screen, transport capacity and screen surface clogging were selected.

The factors considered were parameters that fully characterize the state of the dynamic system – angular frequency of forced box oscillations ( $\omega = 94.2 \text{ s}^{-1}$ ;  $\omega = 125.6 \text{ s}^{-1}$ ;  $\omega = 157 \text{ s}^{-1}$ ) and their amplitude ( $A = 0.001 \text{ m}$ ;  $A = 0.002 \text{ m}$ ;  $A = 0.003 \text{ m}$ ).

The inclination angle of the screen surface to the horizontal plane and the vibration angle to the normal drawn to the supporting surface of the underscreen frame in the longitudinal plane remained constant across the entire range of factor values and were equal to  $\alpha = 10^\circ$  and  $\beta = 45^\circ$ , respectively.

The studies were conducted with directed box oscillations using both fixed and freely placed screen surfaces.

For the experiments, methods of mathematical processing of the results were applied in accordance with the requirements of the theory of mathematical statistics. [11]

Transport capacity was determined using a solid bottom surface (see item 11 in Fig. 2) without the dividing knife (item 12) by measuring the time required  $t_{fill}$  to fill the receiving hopper (item 13) with a transported

material mass  $m_{mat}$ , according to the formula:

$$Q_{tp} = \frac{m_{mat}}{t_{fill}} \text{ kg/s.} \quad (1)$$

The experiments were conducted with a constant material layer height  $H_{lh} = 60 \text{ mm}$ , varying the angular frequency of forced box oscillations and their amplitude. For each combination of factors, the tests were repeated three times. Limestone with a fraction size of  $1.6 \dots 3 \text{ mm}$  was used as the test material.

The clogging of the screen surface was evaluated using the clogging coefficient, determined by the formula

$$K_{clo} = \frac{S_{cl}}{S_{o.a}} \cdot 100 \%, \quad (2)$$

where  $S_{cl}$  is the area of clogged openings on the screen surface ( $\text{m}^2$ ), and  $S_{o.a}$  is the open area of the screen surface ( $\text{m}^2$ ).

The clogging patterns of the screen surface were assessed by photographing it after each experiment for every pair of dynamic parameters. The box executed directed harmonic stable oscillations with both fixed and freely placed screens.

Screen clogging tests used agglomerate fines with a granulometric composition selected to maximize aperture clogging. For a screen surface with circular apertures of  $5 \text{ mm}$  diameter, a fraction size of  $5 \dots 6 \text{ mm}$  was applied. The experiments were conducted under constant specific loading for the feed input, maintaining a constant layer height of  $60 \text{ mm}$ .

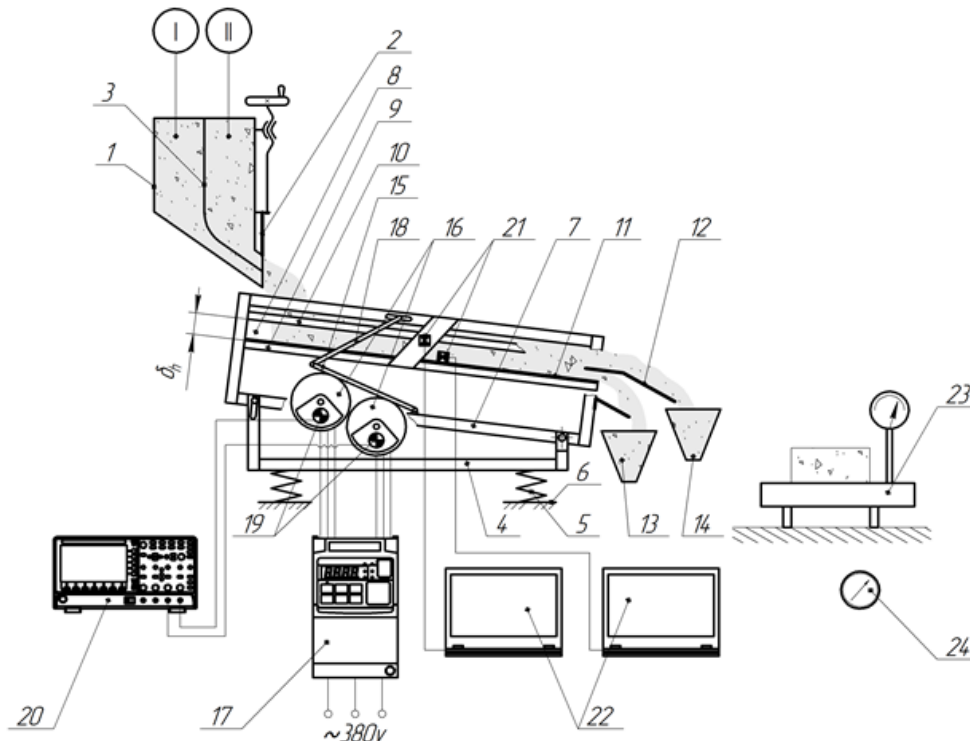


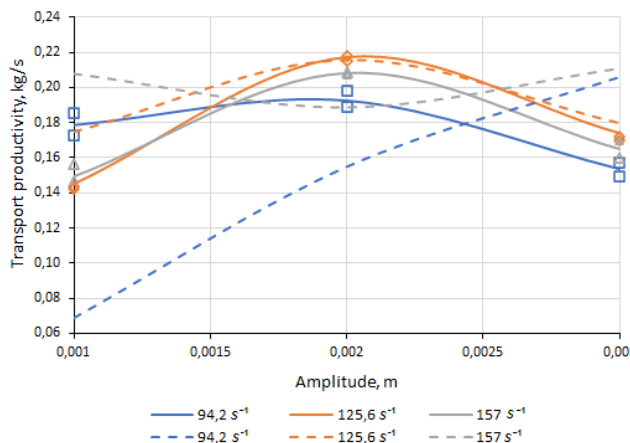
Figure 2. Structural diagram of the laboratory stand: 1 - hopper; 2 - slide gate valve; 3 - partition; 4 - carriage; 5 - spring supports; 6 - foundation; 7 - frame; 8 - box; 9 - fixed support angle bracket; 10 - movable support angle bracket; 11 - screening surface; 12 - dividing knife; 13, 14 - receiving hopper; 15 - sub-vibrator plate; 16 - motor vibrator; 17 - frequency converter; 18 - rod; 19 - phase sensor; 20 - oscilloscope; 21 - acceleration sensor; 22 - laptop; 23 - electronic scales; 24 - stopwatch.



### Research results

Fig. 3 presents the dependencies of transport productivity on the amplitude and angular velocity of box oscillations with both fixed and freely laid sieve surfaces.

The figure shows that, within the studied range, the transport productivity function exhibits a stable dependence on the amplitude of the box oscillations and the angular frequency, with the functional relationship



having an extreme nature. Considering that under identical dynamic parameters of the box, the transport productivity of the screener with a fixed sieve surface exceeds that of the vibratory-impact machine with a non-rigid connection between the box and the sieve, this confirms the necessity of ensuring the required transport speed of the sieved material by increasing the inclination angle of the sieve surface, due to the specifics of its galloping mode.

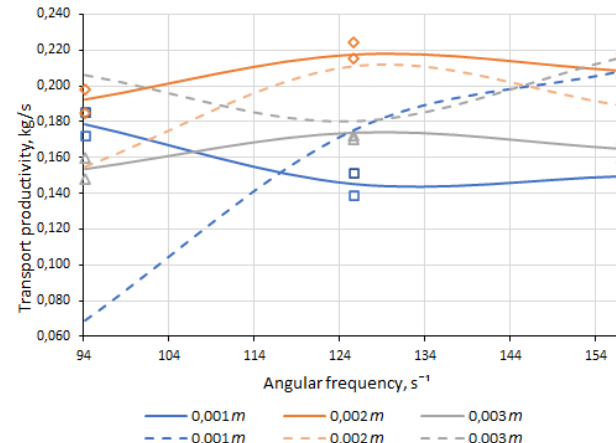


Figure 3. Dependence of transport productivity on the amplitude (a) and angular frequency (b) of box oscillations.

The distinct nature of the functional dependencies of the transport productivity for the screener with fixed and freely laid sieve surfaces indicates the impossibility of adapting existing theoretical models for transport productivity assessment through the determination of corrective coefficients. Therefore, to study the influence of the selected factors on the transport productivity of the vibratory-impact machine with a non-rigid

connection between the box and the sieve, a full factorial experiment was conducted, implementing an orthogonal second-order plan matrix.

The mathematical description of the dependence of transport productivity on the selected factors was performed using a quadratic regression equation, which was verified for adequacy using Fisher's criterion and presented as follows

$$Q_{tr} = 0,0154 + 78 \cdot A + 0,0015 \cdot \omega + 0,5732 \cdot A \cdot \omega - 34000 \cdot A^2 - 9,94 \cdot 10^{-6} \cdot \omega^2 \text{ kg/s}, \quad (3)$$

where  $A$  – amplitude of forced box oscillations, m;  $\omega$  – angular frequency of oscillations,  $s^{-1}$ .

The obtained regression equation (3) represents a mathematical model that demonstrates the influence of the box's dynamic parameters – amplitude (ranging from 0.001 to 0.003 m) and angular frequency (ranging from 94.2 to 157  $s^{-1}$ ) on the transport productivity of the vibratory-impact machine with a non-rigid connection between the box and the sieve, at a 20 % significance level.

The derived mathematical model (3) was subjected to graphical analysis, which allowed determining the extent of each factor's influence on the optimization parameter (Fig. 4).

The obtained surface graph shows that the maximum transport productivity of the vibratory-impact machine with a non-rigid connection between the sieve and the box, which performs directed, harmoniously stable oscillations, is achieved under oscillation conditions with acceleration of 28...32  $m/s^2$  at an amplitude of 0.002 m.

Fig. 5 illustrates the dependence of the clogging coefficient on the amplitude and angular frequency of the box oscillations and includes a photo of the sieve surface from one of the experimental studies of its clogging.

The obtained graphs show that the clogging coefficient of the freely placed sieve surface, unlike the fixed one, is on average 10 times lower under identical dynamic parameters of the box. This indicates a more efficient selfcleaning process of the sieve surface apertures in vibratory-impact machines with a non-rigid connection between the sieve and the box.

The amplitude of box oscillations has the greatest impact on the self-cleaning process, characterized by a decreasing nonlinear dependence with asymptotic convergence. As the amplitude increases to 0.002 m and the box acceleration reaches 32  $m/s^2$ , the clogging coefficient decreases, reaching its minimum of 0.035%. Further increases in amplitude have little effect on it, indicating stabilization of the process and the establishment of a constant level of sieve surface clogging.

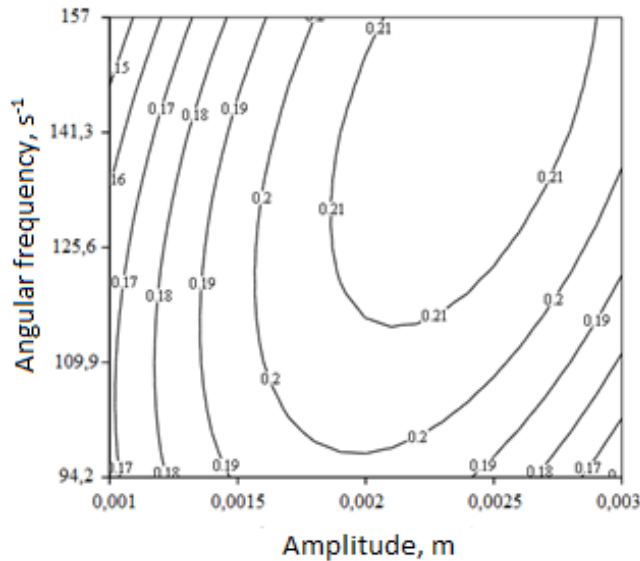


Figure 4. Dependence of transport productivity on the amplitude and angular frequency of box oscillations.

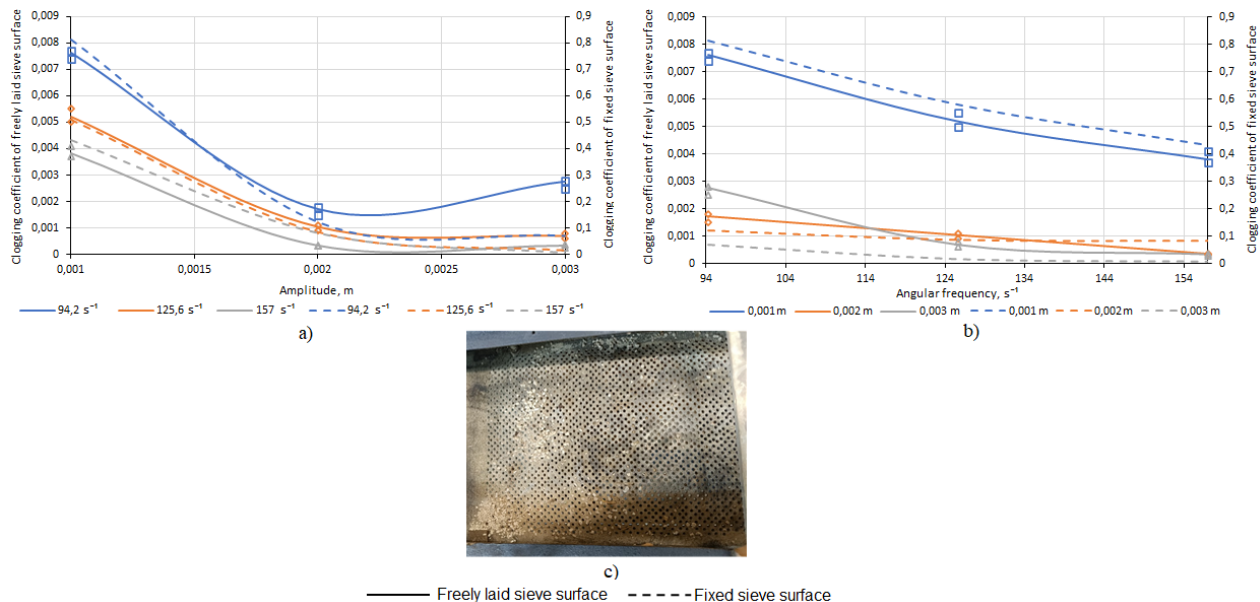


Figure 5. Dependence of the clogging coefficient on the amplitude (a) and angular frequency (b) of box oscillations; c – sieve surface.

To study the interaction between the amplitude of the forced oscillations of the vibratory-impact machine's box with a non-rigid connection and their angular frequency on the clogging coefficient of the sieve surface, a full factorial experiment was conducted using an orthogonal second-order design matrix.

$$K_{clo} = 0,003 - 1610 \cdot A + 0,035 \cdot \omega + 1,115 \cdot A \cdot \omega + 340000 \cdot A^2 - 0,0002 \cdot \omega^2 \% \quad (4)$$

The obtained equation is also a mathematical model demonstrating the influence of the box's dynamic parameters – amplitude (ranging from 0.001 to 0.003 m) and angular frequency (ranging from 94.2 to 157 s<sup>-1</sup>) on the clogging coefficient of the sieve surface in vibratory-impact machines with a non-rigid connection between the box and the sieve, with a significance level of 20 %.

The mathematical description of the dependence of the sieve surface clogging coefficient on the selected factors was performed, as in the case of the screening productivity analysis, using a quadratic regression equation that was verified for adequacy using Fisher's criterion

The resulting mathematical model underwent graphical analysis (Fig. 6), which allowed for determining the degree of influence of each factor on the optimization parameter.

From the obtained graph, it can be seen that the intensification of the cleaning process of the sowing surface in the vibration-impact machine with an uncontrollable connection between the sieve and the box

occurs when both the amplitude of the box oscillations and its frequency are increased. From the perspective of energy efficiency and effectiveness of the cleaning process, the most acceptable value of the clogging coefficient is 0.2 %, which is achieved with the following

dynamic parameters of the box: an oscillation amplitude of 0.0018...0.0022 m at a frequency of 94.2...102 s<sup>-1</sup>, corresponding to accelerations from 16 to 23 m/s<sup>2</sup>, and 0.0022 m at a frequency of 125.6 s<sup>-1</sup>, which is equivalent to an acceleration of 35 m/s<sup>2</sup>.

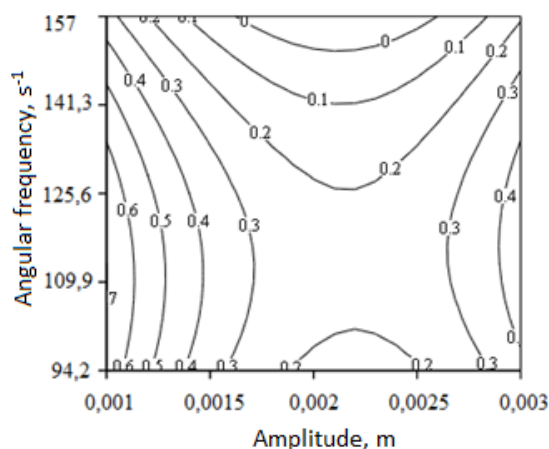


Figure 6. Dependence of the clogging coefficient of the sowing surface on the amplitude and angular frequency of the box oscillations.

### Conclusions

As a result of the conducted studies on the developed laboratory model of the screen with a fixed and freely laid sowing surface, which generates vibration-impact action, its influence on productivity and the process of clogging sieve holes during the sieving of metallurgical raw materials was studied.

Based on the research, a mathematical model was obtained that links transport productivity and the clogging coefficient of the sowing surface of the vibration-

impact machine with an uncontrollable connection between the sieve and its box at a 20% significance level. It was found that the maximum transport productivity is achieved at an oscillation mode with accelerations of 28...32 m/s<sup>2</sup> at an amplitude of  $2 \cdot 10^{-3}$  m, and the most acceptable value of the clogging coefficient at this productivity is 0.2%, which is achieved with an oscillation amplitude in the range of  $(1.8...2.2) \cdot 10^{-3}$  m at a frequency of oscillations of 94.2...102 s<sup>-1</sup>.

### References

1. *Screen agglomerate*. LLC "KVMSH Plus": [Website]. <https://kvmsch-plus.all.biz/uk/gurkit-aglomeratu-j-okatyshiv-41-1-sh-g3011037>
2. *Screens of agglomerates and pellets*. LLC "Progress Industrial Equipment Plant": [Website]. <https://zavodgooprogress.com.ua/g9768701-grohoty-dlya-aglomerata>
3. *Screens*. Scientific and Production Enterprise "Mashprom": [Website]. <https://www.mashprom.ru/competentions/metall/mining/grohot/>
4. *Sandvik Screens*. (2008). Sweden: Sandvik mining and construction
5. *Screens*. Schenck Process: [Website]. <https://www.schenckprocess.com/technologies/screening/screens>
6. *Screens and screening equipment*. Metso: [Website]. <https://www.mogroup.com/products-and-services/plants-and-capital-equipment/screens/>
7. Uchytel, O. D., Vasylyeva, R. A., Zelov, E. O., et al. (1976). *Study and justification of the parameters of high-performance screens with self-cleaning sieves in self-grinding cycles*. Research report (final). Theme code 065275. No. 43221643. Dnipro Metallurgical Institute, Kryvyi Rih
8. Uchytel, O. D., Zaselsky, V. Y., Eltushuler, Ya., et al. (1981). *Study of screen operation to improve sorting efficiency and enhance operational reliability*. Development and research of new screen systems (final). Theme code 082208. No. 80021569. Dnipro Metallurgical Institute, Dnipro
9. Uchytel, S. A., Lyaluk, V. P., & Popolov, D. V. (2014). *Sorting of metallurgical charge on vibrating screens*. Saarbrücken: Palmarium Academic Publishing
10. Reichsfeld, V. O., Shein, V. S., & Ermakov, V. I. (1975). *Reaction equipment and machines of basic organic synthesis and synthetic rubber plants. Textbook for universities*. Khimiya
11. Zaselsky, V. Y., Popolov, D. V. et al. (2019). *Improvement of equipment and processes of coal preparation and coke sorting in metallurgy production*. Litteria

Отримано редколегією / Received by the editorial board: 19.11.2024

Прийнято до друку / Accepted for publication: 20.02.2025

**Proidak Yu.S., Gorobets A.P., Zhadanos O.V., Kamkina L.V., Yaroshenko Ya.O.**  
**Physical and chemical audits and comparative analyses**  
**of scrap remelting technology indicators for high-alloyed steel**  
**with special purposes using the duplex-slag process**  
**and the resource-saving mono-slag process**

**Пройдак Ю.С., Горобець А.П., Жаданос О.В., Камкіна Л.В., Ярошенко Я.О.**  
**Фізико-хімічні аудити та порівняльні аналізи показників**  
**технології переплавки брухту високолегованої сталі спеціального**  
**призначення з використанням дуплекс-шлакового**  
**та ресурсозберігаючого моношлакового процесів**

**Abstract. The goal.** The research purpose is a physicochemical audit and comparative analysis of the indicators of the technologies for remelting scrap of high-alloy special-purpose steels using a two-slag process and a resource-efficient single-slag process to create an innovative technology for the electric steelmaking process. **Methodology.** The research used miscellaneous methods and modern equipment for studying the physical chemistry of metallurgical processes, including optical metallography methods on the "Neophot-24" installation, to assess the microstructure of the metal and the mineralogical composition of the slags. Experimental and industrial smelting was carried out to determine the balance of alloying elements by certified chemical and spectral analysis of the metal and slag. **Results and scientific novelty.** To ensure the rational composition of the slag of reduced basicity during melting, a mixture with the following composition was synthesized from oxides classified as "chemically pure": 50%CaO-35%SiO<sub>2</sub>-5%Al<sub>2</sub>O<sub>3</sub>-5%MgO-5%FeO. This allows for the reduction of the loss of alloying elements and increases the efficiency of remelting. According to the results of the analysis conducted by the requirements of DSTU 8966:2019 regarding the contamination of the metal with non-metallic inclusions and their crystalline and chemical composition, it was found that the vast majority of inclusions are represented by silicates with a size of 7-10 μm. These indicators depend on the size and conditions of crystallization of the ingot. Changes in the content of alloying elements due to the remelting process were analyzed. It was confirmed that the losses of expensive alloying elements (Cr, Mo, W, V) depend not only on their chemical affinity for oxygen but also on the formation of compounds of the type CaO\*MeO in the slag, where MeO oxide has an acidic nature of interaction. New knowledge has been obtained regarding the physical properties and phase composition of lime-iron slag of the CrO-FeO-SiO<sub>2</sub>-(Me)O system where Me-Mn, Cr, V, Mo. The obtained scientific results significantly complement the research of domestic and foreign scientists due to the novelty of the approach and practical orientation to the needs of specific industries. **Practical value.** The developed technological solutions for predicting the optimal composition of the metal dump for metal scraps of alloyed special-purpose steels will increase the technical and economic performance of steelmaking in electric furnaces and promote the reuse of valuable materials. This is important in the context of the constant increase in the cost of raw materials and efforts aimed at reducing the impact on the environment, as well as on the sustainable development of Ukraine (solving environmental problems, reducing greenhouse gas emissions, reducing the consumption of ferroalloys, etc.).

**Keywords.** high-alloy steel, scrap, single-slag process, remelting, model slags of the CaO-FeO-SiO<sub>2</sub>-MeO system.

**Анотація. Мета.** Метою дослідження є фізико-хімічний аудит та порівняльний аналіз показників технології переплавки брухту високолегованих сталей спеціального призначення із застосуванням двошлакового процесу та ресурсоефективного одношлакового процесу для створення інноваційної технології електрометалургійного процесу. **Методологія.** У дослідженні використано різноманітні методи та сучасне обладнання для вивчення фізико-хімії металургійних процесів, включаючи методи оптичної металографії на установці "Neophot-24" для оцінки мікроструктури металу та мінералогічного складу шлаків. Проведено експериментальні та промислові плавки для визначення балансу легуючих елементів шляхом сертифікованого хімічного та спектрального аналізу металу та шлаку. **Результати та наукова новизна.** Для забезпечення раціонального складу шлаку зниженої основності під час плавки синтезовано суміш із наступним складом з оксидів, класифікованих як "хімічно чисті": 50%CaO-35%SiO<sub>2</sub>-5%Al<sub>2</sub>O<sub>3</sub>-5%MgO-5%FeO. Це дозволяє зменшити втрати легуючих елементів та підвищити ефективність переплавки. За результатами проведеного аналізу за вимогами ДСТУ 8966:2019 щодо забруднення металу неметалевими включеннями та їх кристалічного та хімічного складу встановлено, що переважна більшість включень представлена силікатами розміром 7-10 мкм. Ці

© Proidak Yu.S. – Vice-Rector for Scientific Work, Doctor of Technical Sciences, Professor, Ukrainian State University of Science and Technologies;  
 Gorobets A.P. – Candidate of Technical Sciences, Associate professor, Ukrainian State University of Science and Technologies;  
 Zhadanos O.V. – Candidate of Technical Sciences, Associate professor, Ukrainian State University of Science and Technologies;  
 Kamkina L.V. – Doctor of Technical Sciences, Professor, Ukrainian State University of Science and Technologies;  
 Yaroshenko Ya.O. – Postgraduate student, Ukrainian State University of Science and Technologies.



This is an Open Access article under the CC BY 4.0 license <https://creativecommons.org/licenses/by/4.0/>

показники залежать від розміру та умов кристалізації зливка. Проаналізовано зміни вмісту легуючих елементів внаслідок процесу переплавки. Підтверджено, що втрати дорогих легуючих елементів (Cr, Mo, W, V) залежать не тільки від їхньої хімічної спорідненості з киснем, а й від утворення сполук типу  $\text{CaO} \cdot \text{MeO}$  у шлаку, де оксид  $\text{MeO}$  має кислу природу взаємодії. Отримано нові знання щодо фізичних властивостей та фазового складу вапняно-залізного шлаку системи  $\text{CrO-FeO-SiO}_2\text{-(Me)O}$ , де Me-Mn, Cr, V, Mo. Отримані наукові результати значно доповнюють дослідження вітчизняних та зарубіжних вчених завдяки новизні підходу та практичній спрямованості на потреби конкретних галузей. **Практична цінність.** Розроблені технологічні рішення для прогнозування оптимального складу металевої шихти для металобрухту легованих сталей спеціального призначення дозволяють підвищити техніко-економічні показники виробництва сталі в електропечах та сприятимуть повторному використанню цінних матеріалів. Це важливо в контексті постійного зростання вартості сировини та зусиль, спрямованих на зменшення впливу на навколишнє середовище, а також на сталий розвиток України (вирішення екологічних проблем, зменшення викидів парникових газів, зменшення споживання феросплавів тощо).

**Ключові слова:** високолегована сталь, брухт, моношлаковий процес, переплавка, модельні шлаки системи  $\text{CaO-FeO-SiO}_2\text{-MeO}$ .

**Introduction.** The global trend in the development of steelmaking metallurgy focuses on steel production in basic oxygen converters and electric arc furnaces. From a metal recycling perspective, the electric steelmaking process has a clear advantage, as it is designed for remelting 100% scrap, whereas, in basic oxygen furnace (BOF) production, this figure is only 30%. An important techno-economic indicator for both steelmaking processes is the increase in unit productivity, so oxygen is used to introduce thermal energy through the oxidation of elements [1].

The strategy of electric steelmaking in Ukraine's ferrous metallurgy enterprises and machine-building foundry complexes is based on the remelting of common and alloyed steel scraps using a wide range of ferroalloys [2]. In both the classical two-slag refining process and modern melting technologies with alternative energy sources, oxygen is essential for oxidation and refining operations. However, this leads to the almost complete oxidation of highly reactive elements in the charge, such as silicon, vanadium, chromium, and molybdenum. During the melting of the metal charge in an electric arc furnace, significant losses occur of silicon (95%), vanadium (100%), manganese (50%), and chromium (50%). The ferroalloys containing these elements belong to the category of import-dependent metallurgical products with extremely high costs: Ferrovandium: \$9.1–9.7 per kg, Ferrochrome: \$0.9–1.2 per kg, Ferromolybdenum: \$6.9–7.1 per kg [3].

The presented data highlights the necessity for developing technological solutions for the remelting of special-purpose steels alloyed with high-cost elements. The solution to this issue will significantly reduce the consumption of imported ferroalloys and improve both the technical and economic efficiency of alloy steel electric melting. At the same time, it will enable the maximum possible reduction of material and energy costs in metal production, ultimately lowering production costs and increasing profitability.

#### Literature Analysis and Problem Statement.

Taking into account that a significant amount of high- and medium-alloy steel scrap is generated worldwide each year (exceeding 10 million tons, according to [4]), finding efficient solutions for its rational utilization is of great scientific interest on a global scale. Among the studies of the secondary utilization of high-alloy scrap, the next notable scientific works should be

highlighted. In [4], a scheme for induction melting and electrical slag remelting is proposed for scrap processing. Based on this scheme, a pilot experiment and thermodynamic analysis were conducted to investigate the influence of temperature, oxygen content, and element composition on the recovery percentage of alloying elements. In [5], attention is given to metal scrap processing, which is contaminated with oils emitting volatile organic compounds (VOCs) of the benzene series during heating and poses risks to both physical and mental health. The study characterizes VOC emissions and examines the pyrolysis behavior and de-oiling process of contaminated scrap to assess environmental risks. A method for separating the melting process is proposed to enable the economical and environmentally friendly recovery of valuable metals from de-oiled waste. Additionally, the thermodynamics of the  $\text{Al}_2\text{O}_3\text{-SiO}_2$  and  $\text{CaO-Al}_2\text{O}_3\text{-SiO}_2$  systems were calculated to optimize slag formation. Study [6] evaluated the environmental and economic benefits of alternative recycling schemes for end-of-life vehicles. These schemes aim to optimize the utilization of alloying elements found in steel scrap recovered from decommissioned vehicles, enabling more efficient resource use. Article [7] describes a new process for simultaneous preheating and removal of galvanized coatings from scrap surfaces before the melting phase to prevent the formation of harmful dust and hazardous air emissions. The zinc coating is removed in the gas phase through the combustion of chloride-containing syngas and is collected in a specialized recovery system. Two possible innovative process pathways are outlined, incorporating pre-treatment of plastic waste, gasification/pyrolysis of shredded plastic, preheating of steel scrap, and zinc recovery processes. In [8], the authors constructed molecular dynamics models for binary systems  $\text{CaO-FeO}$ ,  $\text{MgO-SiO}_2$ ,  $\text{FeO-SiO}_2$ ,  $\text{CaO-SiO}_2$ , and the ternary system  $\text{CaO-FeO-SiO}_2$  at a temperature of 1873 K using Born-Mayer potential functions. These potentials included effective dipole-dipole interactions for pairs such as Ca-Fe, Mg-Si, Fe-Si, and Ca-Si. The parameters for the dipole-dipole interaction were determined by adjusting the calculated Gibbs free energies of formation for the binary systems  $\text{CaO-FeO}$ ,  $\text{FeO-SiO}_2$ ,  $\text{MgO-SiO}_2$ , and  $\text{CaO-SiO}_2$  to match experimental data. The thermodynamic properties of  $\text{CaO-FeO-SiO}_2$  solutions were studied by converting



several iron ions to calcium ions. This approach allowed the calculation of the changes in Gibbs free energy and the ratio of activity coefficients  $\gamma_{\text{CaO}}/\gamma_{\text{FeO}}$  in the ternary system. The significant scientific interest in modeling the chemical composition of slag during the remelting of high-alloy steel scrap is presented in the study [9], which focuses on predicting the chemical composition of refining slag using an artificial neural network.

Thus, a physicochemical audit and comparative analysis of the indicators of the remelting technologies for high-alloy special-purpose steels - using both the two-slag process and the resource-efficient one-slag process - will provide relevant recommendations and complement existing research.

**Purpose and Objectives of the Research.** The research purpose is to conduct a physicochemical audit and comparative analysis of the indicators of high-alloy special-purpose steel scrap remelting technologies using the two-slag process and the resource-efficient one-slag process to develop an innovative technology for the electric steelmaking process.

**Research Description.** In the classical technology of remelting high-alloy steel scrap in electric arc furnaces, a metal semi-product with a controlled phosphorus content is initially melted under a heavily oxidized slag. Once the oxidation process is complete this slag is removed, and a new slag is created, followed by desulfurization, deoxidation, and alloying with ferroalloys.

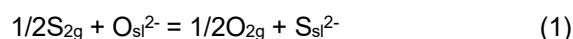
To form slags with a specified composition, before loading the furnace, 10–15 kg/t of lime or 18–23 kg/t of limestone is added. The slags formed during melting ( $B = 1.5\text{--}1.7$ ) are deoxidized and removed. The slag from the melting period is deoxidized using mixtures that consist of 30–40% fresh burnt lime, 5–15% fluorspar, 10–25% electrode scrap, and 15–25% ferrosilicon. After removing the melting-period slag, a new slag is created by adding 20–40 kg/t of lime, 3–10 kg/t of fluorspar, and 2.5–3 kg/t of ferrosilicon to the metal bath. Once the low-viscosity slag is fully formed, the metal is heated to 1500–1540°C and alloyed with ferromanganese. In situations where the carbon content in the metal is between 1.15–1.20%, medium-carbon or low-carbon ferromanganese is used for alloying.

Before tapping the steel from the furnace, the slags from the reduction period are deoxidized with granular aluminum or a deoxidizing mixture. The final deoxidation of the steel is carried out with aluminum in the ladle.

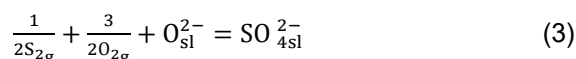
An analysis of changes in the chemical composition of the metal and slag during the melting process shows that the main losses of alloying elements occur during the melting of the charge. Almost 90% of the lost alloying elements transfer into the slag, while 10% transition into the gas phase. The practice of double slag removal, applied at several plants, leads to the loss of a significant portion of alloying elements with the waste slags.

The main idea of the simultaneous process is to use oxidizing slag for phosphorus removal (dephosphorization) and subsequently restore it for desulfurization and other physicochemical operations.

Depending on the degree of oxidation, sulfur in slags can exist in either sulfide (1) or sulfate (2) forms [10]:



$$K_1 = \frac{\alpha_{\text{S}^{2-}} \cdot p_{\text{O}_2}^{1/2}}{\alpha_{\text{O}^{2-}} \cdot p_{\text{S}_2}^{1/2}} \quad (2)$$



$$K_2 = \frac{\alpha_{\text{SO}_4^{2-}}}{\alpha_{\text{O}^{2-}} \cdot p_{\text{S}_2}^{1/2} \cdot p_{\text{O}_2}^{3/2}} \quad (4)$$

For a given temperature and slag composition, the equilibrium sulfur concentration is determined solely by the ratio  $(p_{\text{O}_2}/p_{\text{S}_2})^{1/2}$ , rather than the absolute values of the partial pressures of oxygen and sulfur. At the same time, the partial pressure of oxygen ordains the form in which sulfur is present in the slag melt:

at  $p_{\text{O}_2} \leq 10^{-5}$  atm., sulfur exists in the slag as sulfide ions ( $\text{MeS}$ );

при  $p_{\text{O}_2} \leq 10^{-3}$  atm., sulfur is present as sulfate ions ( $\text{MeSO}_4$ ).

The parameter "sulfide capacity" -  $C_S$  is used to evaluate the properties of desulfurizing slag systems:

$$K_1 \cdot \frac{\alpha_{\text{O}}}{\gamma_{\text{O}}} = C_S = (\text{S}) \cdot \left(\frac{p_{\text{O}_2}}{p_{\text{S}_2}}\right)^{\frac{1}{2}} \quad (5)$$

The characteristics of the sulfide capacity of slags in the ternary  $\text{CaO-Al}_2\text{O}_3\text{-SiO}_2$  system [11], as shown in Figure 1, indicate that the maximum value of the  $C_S$  parameter is found in the  $\text{CaO-Al}_2\text{O}_3$  composition, making it the most suitable slag base for desulfurization. At the same time, according to data presented in E.T. Turkdogan's monograph [10], in the  $\text{CaO-SiO}_2$  slag system, the solubility of  $\text{CaS}$  at temperatures of 1500–1550°C increases from 2.5% to 5% as the basicity ratio  $\text{CaO/SiO}_2$  decreases from 1.5 to 0.5.

Clearly, for optimizing slag composition, the basicity factor of the slag is essential, as is the activity of its components. In  $\text{CaO-CaF}_2$  systems, which act as the fundamental slag-forming system in domestic electrosmelting practices, as well as in slags within the  $\text{CaF}_2\text{-Al}_2\text{O}_3$  system, the calculated activity values of the system's components (Fig. 2) are of practical significance.

Calcium fluoride accelerates the dissolution of lime and increases the fluidity of slags by reducing their viscosity. This enhancement subsequently improves the rate of steel desulfurization. Thus, the effect of  $\text{CaF}_2$  is reflected in the kinetics of the desulfurization process. Some retrospective studies have shown that the presence of  $\text{CaF}_2$  in basic slags can significantly increase their basicity, thereby improving steel desulfurization accordingly.



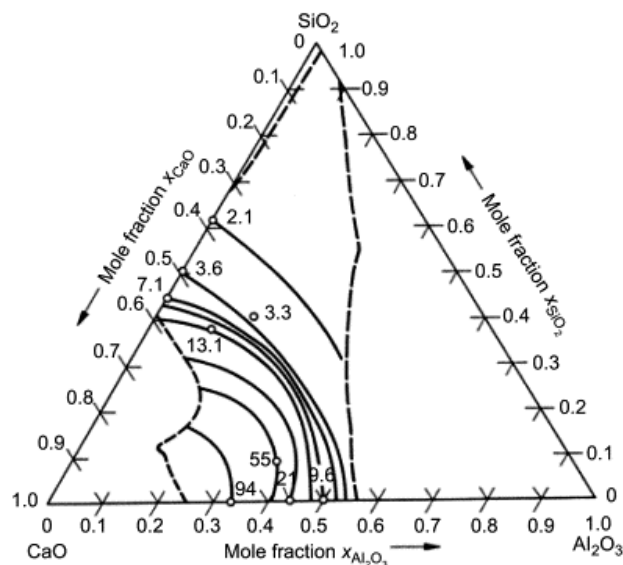


Figure 1. The sulfide capacity  $C_s \cdot 10^6$  of slags in the ternary  $\text{CaO-Al}_2\text{O}_3\text{-SiO}_2$  system at the temperature  $1650^\circ\text{C}$  [12]

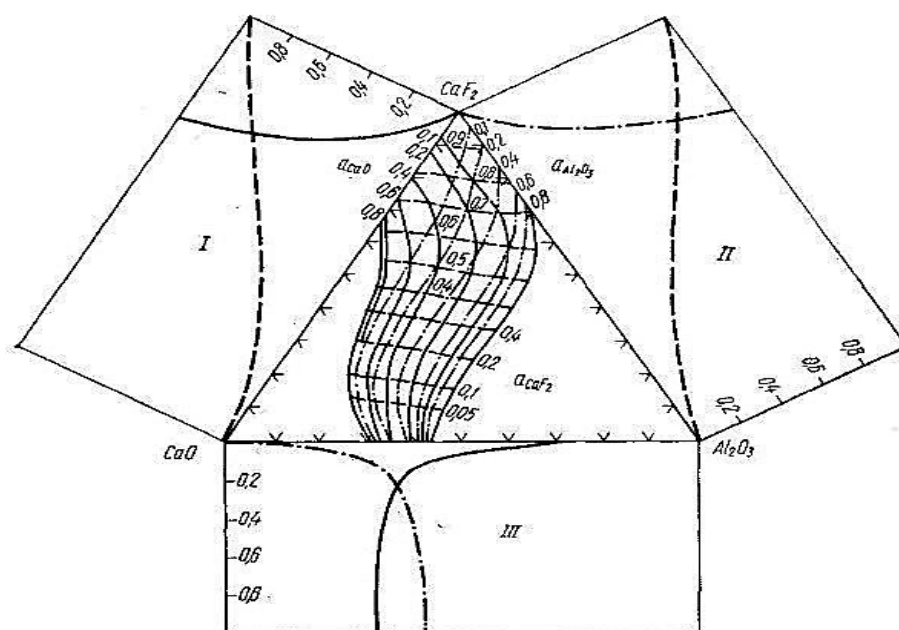


Figure 1. The activities of CO (solid lines),  $\text{CaF}_2$  (dashed lines), and  $\text{Al}_2\text{O}_3$  (dash-dotted lines), determined at  $1500^\circ\text{C}$  in various systems, are as follows: I –  $\text{CaF}_2\text{-CaO}$ ; II –  $\text{CaF}_2\text{-Al}_2\text{O}_3$ ; III –  $\text{CaO-Al}_2\text{O}_3$  [12]

The authors of studies [13, 14] were likely the first in domestic literature to substantiate that the steel desulfurization coefficient  $\Sigma(\text{CaO} + \text{MgO})$  does not

increase but rather decreases when using oxide-fluoride slags with increased  $\text{CaF}_2$  content. This conclusion follows from the data presented below:

CaF <sub>2</sub> content, %	The value of the steel desulfurization coefficient $\left( L_s = \frac{(\%S)}{[\%S]} \right)$	
	$\Sigma(\text{CaO} + \text{MgO}) < 65 \%$	$\Sigma(\text{CaO} + \text{MgO}) > 65 \%$
< 4,0	96 (17 melts)	67 (19 melts)
> 4,0	81 (6 melts)	53,3 (8 melts)

With the same slag fluidity, characterized by the sum of components  $\Sigma(\text{CaO} + \text{MgO})$ , an increase in  $\text{CaF}_2$  content in the slag above 4% reduces the sulfur distribution coefficient by 15%. M.M. Chuyko and V.B.

Rutkovskiy [13, 14] explained the decrease in the desulfurizing ability of furnace oxide-fluoride slags by the increased activity of ferrous oxide, as follows from the expression:

$$L_s = (S)/[S] = K_s a_{(CaO)}/a_{(FeO)}, \quad (6)$$

where  $K_s$  - is the equilibrium constant of the metal desulfurization reaction;  $a_{(CaO)}$  - is the activity of the "free" concentration of calcium oxide, determined by the method of M.M. Chuyko.

The integral assessment of the metal's desulfurization reaction efficiency by slag systems is determined by achieving a balance between the metal and the slag, the oxygen activity in the metal, and the composition of the slag and metal, taking into account the relative weight of the slag.

$$[S]_{fin.} = \frac{\alpha_{[O]}((S)_{sl.} + \frac{[S]_{start.}}{m})}{f_s \cdot C_s + \frac{\alpha_{[O]}}{m}} \quad (7)$$

where  $S_{start, fin.}$  - the sulfur content in the metal before and after desulfurization;  $\alpha_{[O]}$  - oxygen activity in the metal;  $f_s$  - the sulfur activity coefficient;  $C_s$  - the sulfide capacity of the slag;  $m$  - the relative weight of the slag (kg) per kg of steel.

Equation (7) defines the relationship between the activities of oxygen and sulfur and characterizes the desulfurization process as a mass transfer reaction in the "metal-slag" system.

5 laboratory melts were conducted to verify the feasibility of implementing a resource-efficient single-slag technology for remelting high-alloy steel scrap. The chemical composition of the initial metal samples is provided in Table 1.

Table 1. Chemical composition of the metal before remelting, wt. %

No sample	Application	C	Si	Mn	Cr	Ni	Mo	V	P ppm	S ppm
1	Demining roller	0,245	0,272	0,82	2,04	1,05	0,309	0,006	160	90
2	Stainless steel	0,152	0,56	1,30	18,61	9,99	0,10	0,04	220	170
3	Tank armor	0,331	1,49	0,417	1,06	2,31	0,27	0,006	110	56
4	Gun barrel A	0,371	0,316	0,26	1,00	3,12	0,47	0,12	46	37
5	Gun breech B	0,340	0,180	0,61	1,00	2,79	0,49	0,112	37	46

The melts were conducted in a 30 kW Tamman furnace with a graphite heater. Metal samples weighing 120-150 g were melted in alumina crucibles for 30 minutes at a temperature of 1600°C. To ensure a rational composition of the low-basicity slag for the melts, a mixture was synthesized from oxides classified as "chemically pure" with the following composition: 50% CaO, 35% SiO<sub>2</sub>, 5% Al<sub>2</sub>O<sub>3</sub>, 5% MgO, 5% FeO. This mixture was subsequently melted in alumina crucibles to homogenize the slag composition. The slag quantity was 10% of the sample mass.

After remelting the high-alloy steel scrap samples, the prepared metal samples were analyzed using optical metallography on a "Neophot-24" setup, and slag samples were analyzed for X-ray phase analysis of the slag components. This allowed the determination of non-metallic inclusions and their crystal-chemical composition in the metal according to the requirements of DSTU 8966:2019. It was established that the main part of inclusions were silicates, ranging from 7-10 μm, depending on the size and crystallization conditions of the cast. Changes in the content of alloying elements due to the remelting process were analyzed. It was confirmed that the loss of expensive alloying elements (Cr, Mo, W, V) depends not only on their chemical affinity to oxygen but also on the formation of compounds like CaO\*MeO in the slag, where MeO is an oxide with acidic interaction properties.

The results made it possible to conduct an industrial melt for remelting steel 110Г13Л without oxidation at the operating enterprise of PJSC "Dniprovs'kyi strolotchny zavod". The metal charge consisted of 1000 kg of steel scrap and 9000 kg of steel 110Г13Л scrap. The following slag-forming materials were used: limestone 214 kg, fluorite 75 kg, and modifier 39 kg. At the end of the melting period, the slag had the following

composition: FeO - 2.34%, MnO - 25.38%, and its basicity was 1.1. Before the metal was released from the furnace, the slag's basicity was 2.5 with the following chemical composition: FeO - 1.62%, MnO - 10.44%. The metal loss amounted to 954 kg.

Thus, the conducted research enabled the determination of the phase components of the CaO-FeO-SiO<sub>2</sub>-MeO (Me – Cr, Mo, V, Mn) slag systems using physical metallography methods. The viscosity of the slags from the experimental melts was determined using vibration viscosimetry, allowing the prediction of mass transfer reactions in the metal-slag system. The study of the metal from the experimental melt of steel 110Г13Л, following the standards of research control, confirmed the complete compliance of the remelted metal's quality with the DSTU standard

## Conclusions

The conducted research allows the proposal of a new, resource-efficient, one-slag technology for remelting high-alloy special-purpose steel scrap. This technology can be implemented in metallurgical enterprises.

To ensure a rational slag composition with reduced basicity during the melting process, a mixture of oxides classified as "chemically pure" has been synthesized with the following composition: 50% CaO, 35% SiO<sub>2</sub>, 5% Al<sub>2</sub>O<sub>3</sub>, 5% MgO, and 5% FeO. This composition helps reduce the loss of alloying elements and improves the remelting efficiency.

Based on the analysis conducted according to the requirements of DSTU 8966:2019 regarding the contamination of metal by non-metallic inclusions and their crystalline and chemical composition, it was found that the majority of inclusions are represented by silicates, with sizes ranging from 7 to 10 μm. These

indicators depend on the size and crystallization conditions of the ingot. The changes in the content of alloying elements as a result of the remelting process were analyzed. It was confirmed that the losses of expensive alloying elements (Cr, Mo, W, V) depend not only on their chemical affinity to oxygen but also on the formation of compounds in the slag of the type  $\text{CaO} \cdot \text{MeO}$ , where MeO is an oxide with acidic interaction properties.

The newly obtained knowledge regarding the physical properties and phase composition of lime-iron slag in the system  $\text{CrO}-\text{FeO}-\text{SiO}_2-(\text{Me})\text{O}$ , where Me are Mn, Cr, V, and Mo, significantly complements the research of both domestic and international scientists. This is due to the novelty of the approach and its practical orientation towards the needs of specific industries.

The developed technological solutions for predicting the optimal composition of the metal charge for high-alloy special-purpose steel scrap will improve the technical and economic indicators of steel production in electric furnaces and contribute to the reuse of valuable materials. This is crucial in the context of the constant rise in raw material costs and the ongoing efforts to reduce environmental impact, as well as to support Ukraine's sustainable development (addressing environmental issues, reducing greenhouse gas emissions, minimizing ferroalloy consumption, etc.).

Implementing the results obtained at Ukrainian metallurgical enterprises will allow for a reduction in electrical energy consumption within the industry, which in turn will enable this energy to be redirected to other sectors and the needs of the population.

### References

1. Gasik, M. I., Panchenko, A. I., Skripka, L. M., Salnikov, A. S., & Mazuruk, S. L. (2009). Technology of smelting pure ShKh15SH-V electric steel with diversification of ferroalloys. *Steel*, (6), 25-28
2. Panchenko, A. I., Logozinsky, I. N., Salnikov, A. S., Korol, L. N., Kazakov, S. S., Gasik, M. I., & Gorobets, A. P. (2007). Comparative pilot-industrial influence researches of 65% ferrosilicon with different contents of calcium on ShKh15SH-V steel contamination with aluminum-calcium inclusions. *Advances in Electrometallurgy*, (4), 49-55
3. Gasik, M. I., Panchenko, A. I., Skripka, L. M., Salnikov, A. S., & Mazuruk, S. L. (2009). Technology of smelting pure ShKh15SH-V electric steel with diversification of ferroalloys. *Steel*, (6), 25-28
4. Wu, L., Liu, K., Mei, H., Bao, G., Zhou, Y., & Wang, H. (2022). Thermodynamics Analysis and Pilot Study of Reusing Medium and High Alloy Steel Scrap Using Induction Melting and Electroslag Remelting Process. *Metals*, 12, 944. <https://doi.org/10.3390/met12060944>
5. Zhang, L., Su, S. P., Liu, B. B., Han, G. H., Huang, Y. F., Wang, Y. B., & Wang, Y. Z. (2021). Sustainable and high-efficiency recycling of valuable metals from oily honing ferroalloy scrap via de-oiling and smelting separation. *J. Hazard. Mater.*, 413. <https://doi.org/10.1016/j.jhazmat.2021.125399>
6. Ohno, H., Matsubae, K., Nakajima, K., Kondo, Y., Nakamura, S., & Nagasaka, T. (2015). Toward the efficient recycling of alloying elements from end of life vehicle steel scrap. *Resour. Conserv. Recycl.*, 100, 11-20. <https://doi.org/10.1016/j.resconrec.2015.04.001>
7. Porzio, G. F., Colla, V., Fornai, B., Vannucci, M., Larsson, M., & Stripple, H. (2016). Process integration analysis and some economic environmental implications for an innovative environmentally friendly recovery and pre-treatment of steel scrap. *Appl. Energy*, 161, 656-672. <https://doi.org/10.1016/j.apenergy.2015.08.086>
8. Belashchenko, D. K., Ostrovski, O. I., & Skvortsov, L. V. (2001). Molecular dynamics simulation of binary  $\text{CaO}-\text{FeO}$ ,  $\text{MgO}-\text{SiO}_2$ ,  $\text{FeO}-\text{SiO}_2$ ,  $\text{CaO}-\text{SiO}_2$  and ternary  $\text{CaO}-\text{FeO}-\text{SiO}_2$  systems. *Thermochimica Acta*, 372(1-2), 153-163. [https://doi.org/10.1016/S0040-6031\(01\)00451-8](https://doi.org/10.1016/S0040-6031(01)00451-8)
9. Jancíková Z., & Švec P. (2008). Prediction of chemical composition of refining slag with exploitation of artificial neural networks. *Cybernetic letters: informatics, cybernetics and robotics*, (2)
10. Turkdogan E. T. (1980). *Physical Chemistry of High Temperature Technology*. Academic Press
11. Kronievsky, V. N., Panchenko, A. I., Salnikov, A. S., Davidchenko, S. V., Skripka, L. M., Gasik, M. I., & Gorobets, A. P. (2016). Development and investigation of end-to-end technology of bearing steel melting for electroslag remelting and production of section rolled metal of large profile sizes. *Advances in Electrometallurgy*, (3(124)), 9-15. <https://doi.org/doi.org/10.15407/sem2016.03.02>
12. *Schlackenatlas*. (1981). Verein Deutscher Eisenhüttenleute. Ausschuss für Metallurgische Grundlagen. Verlag Stahleisen, p. 282.
13. Chuiko, N. M., & Rutkovsky, V. B. (1960). New technology for smelting roller bearing steel grade ShKh15 under white slag. News of higher educational institutions. *Ferrous metallurgy*, (6), 14-16
14. Rutkovsky, V. B. (1963). On the role of calcium fluoride in deoxidization and desulfurization of steel making in EAF. *Electrometallurgy of steel and ferroalloys*, LI, 30-40



The publication is prepared based on the results of the project 2023.04/0037, "Development of a technology for remelting scrap military equipment in order to preserve valuable alloying elements in the smelting of special functional steels," funded by the National Research Foundation of Ukraine from the state budget.

Отримано редколегією / Received by the editorial board: 18.12.2024

Прийнято до друку / Accepted for publication: 20.02.2025

**Shevchenko D.V., Ovcharuk A.M., Nadtochii A.A., Prikhodko S.V., Shutov V.Yu.**  
**Research on the properties of ferronickel production slags**  
**and development of technological schemes for their enrichment**

**Шевченко Д.В., Овчарук А.М., Надточій А.А., Приходько С.В., Шутов В.Ю.**  
**Дослідження властивостей шлаків феронікелевого виробництва**  
**та розробка технологічних схем їх збагачення**

**Abstract. Objective.** Determination of the physicochemical properties of slags, phase composition, and forms of nickel presence in them, development of enrichment modes and equipment parameters. **Research Methods and Equipment.** X-ray spectral microanalysis (RSMA) on the SELMI REM-106I installation was used to determine the distribution of nickel between the metallic and oxide phases in the presented slag samples. Dry and wet gravity and magnetic separation using modernized magnetic separators established the possibility of slag enrichment and the distribution of nickel between the enrichment products. **Research Results.** This work has conducted research on the gravitational-magnetic separation of electro-furnace and refining slags of ferronickel production in the conditions of the Pobuzhsky ferronickel plant. The efficiency of implementing the developed technological schemes in production was shown, providing additional extraction in the amount of 119 tons or 9.8% of the total annual nickel production at the plant. Slag samples were ground in experimental ball mills to fractions of  $-0.16$ ;  $0.16-1.6$  and  $+1.6$  mm and subjected to enrichment by gravity and magnetic separators with a magnetic induction on the drum surface of  $0.3-0.6$  T (Tesla) of the MBS-300 and MS-500 types with a total metal phase yield of up to 30%. **Scientific Novelty.** RSMA established that nickel, both in electric furnace granulated slags and in refining slags, is in the metallic phase and is represented by metal nuggets in combination with iron of various shapes and sizes. Enrichment of electric furnace and refining slags by a combined method using a high-intensity magnetic field will allow obtaining a metal concentrate containing 0.9-38% nickel. The combined enrichment method using high-intensity magnetic separators is one of the most promising for enriching both primary mineral raw materials and secondary materials of ferrous and non-ferrous metal production. **Practical Significance.** The developed and proposed for implementation technological schemes for enrichment of electric furnace slags using the "wet" technology and refining slags using the "dry" technology allow for the utilization of about 1200 tons of nickel per year or the extraction of 31.6% and 94.65% of nickel from slags, respectively.

**Keywords:** nickel, electric furnace and refining slags, X-ray spectral microanalysis, gravity and magnetic separators, enrichment, metal concentrate, extraction.

**Анотація. Мета.** Визначення фізико-хімічних властивостей шлаків, фазового складу та форм присутності в них нікелю, розробка режимів збагачення та параметрів обладнання. **Методи та обладнання дослідження.** Для визначення розподілу нікелю між металевією та оксидною фазами в представлених зразках шлаку використовувалася рентгеноспектральний мікроаналіз (RSMA) на установці SELMI REM-106I. Суха та мокра гравітаційна і магнітна сепарація з використанням модернізованих магнітних сепараторів встановила можливість збагачення шлаку та розподіл нікелю між продуктами збагачення. **Результати дослідження.** У цій роботі проведено дослідження гравітаційно-магнітної сепарації електропечних та рафінувальних шлаків феронікелевого виробництва в умовах Побузького феронікелевого заводу. Показана ефективність впровадження розроблених технологічних схем у виробництво, що забезпечує додаткове вилучення у кількості 119 тон або 9,8% від загального річного виробництва нікелю на заводі. Зразки шлаку подрібнювалися в експериментальних кульових млинах до фракцій  $-0,16$ ;  $0,16-1,6$  та  $+1,6$  мм і піддавалися збагаченню гравітаційними та магнітними сепараторами з магнітною індукцією на поверхні барабана  $0,3-0,6$  Т (Тесла) типів МБС-300 та МС-500 із загальним виходом металевієї фази до 30%. **Наукова новизна.** RSMA встановлено, що нікель, як у електропечних гранульованих шлаках, так і в рафінувальних шлаках, знаходиться в металевій фазі і представлений металевими самородками в поєднанні із залізом різної форми та розміру. Збагачення електропечних та рафінувальних шлаків комбінованим методом із застосуванням високоінтенсивного магнітного поля дозволить отримувати металевий концентрат, що містить 0.9-38% нікелю. Комбінований метод збагачення із застосуванням високоінтенсивних магнітних сепараторів є одним з найперспективніших для збагачення як первинної мінеральної сировини, так і вторинних матеріалів виробництва чорних та кольорових металів. **Практичне значення.** Розроблені та запропоновані до впровадження технологічні схеми збагачення електропечних шлаків за "мочною" технологією та рафінувальних шлаків за "сухою" технологією дозволяють утилізувати близько 1200 тон нікелю на рік або вилучати 31,6% та 94,65% нікелю зі шлаків відповідно. **Ключові слова:** нікель, електропечні та рафінувальні шлаки, рентгеноспектральний мікроаналіз, гравітаційні та магнітні сепаратори, збагачення, металевий концентрат, вилучення.

© Shevchenko D.V. – Postgraduate student, Ukrainian State University of Science and Technologies;  
 Ovcharuk A.M., Doctor of Technical Sciences, Professor, Ukrainian State University of Science and Technologies;  
 Nadtochii A.A., candidate of technical sciences, associate, Ukrainian State University of Science and Technologies;  
 Prikhodko S.V., Postgraduate student, Ukrainian State University of Science and Technologies;  
 Shutov V.Yu. – Candidate of Technical Sciences, Associate professor, Dnipro University of Technology.



This is an Open Access article under the CC BY 4.0  
 license <https://creativecommons.org/licenses/by/4.0/>

**Introduction.** At the current stage of global industrial production development, special attention is paid to the issues of comprehensive rational use of mineral resources, utilization of secondary material and energy resources, and environmental protection. The production of ferronickel from oxidized nickel ores by the electric thermal method is one of the most material- and energy-intensive processes, due to the low content of the main element - nickel, whose concentration in ores from various deposits is only 1-2.5% [1,2].

With such a nickel content in the raw material, the slag ratio ranges from 6-10 and determines various specific energy consumption values per ton of calcine and finished product, which amounts to 30-55 thousand kWh/ton of nickel, despite the fact that it is an easily reducible element [3]. Therefore, the utilization of the metallic phase of ferronickel allows for the reduction of energy and material costs. The main amount of metal granules is concentrated in both refining and electric furnace slags. The most important aspect in the utilization of slags from ferroalloy production is the separation of their metallic and oxide

components to obtain metal concentrate and slag. Currently, various methods are used worldwide to separate the metallic and oxide components of slags, ranging from manual selection to modern X-ray radiometric separation, although technologies based on gravitational and magnetic methods are the most widespread [4,5].

**Research Goals and Objectives.** Rational and comprehensive use of mineral raw materials in metallurgical production, one of the most material-intensive industries, is an important and urgent problem, the solution of which allows for increased production efficiency, improved economic indicators, and addressing environmental protection issues.

**Theoretical and Experimental Research.** To conduct research on the physical and chemical properties of electric furnace and refining slags, determine the phase composition and forms of nickel in it, and develop enrichment modes and equipment parameters, 5 slag samples (Table 1) from ferronickel production were studied at the Pobuzhsky Ferronickel Plant.

Table 1. Chemical Composition of Slag Samples\*.

Sample	Chemical Composition, %					
	Ni	Fe	MgO	SiO <sub>2</sub>	CaO	Al <sub>2</sub> O <sub>3</sub>
1	0,28	13,02	34,69	47,24	0,297	2,248
2	0,26	12,45	31,48	43,80	0,285	2,056
3	10,95	17,60	7,29	16,30	42,66	6,590
4	9,90	17,75	7,26	16,32	42,68	6,62
5	9,33	17,14	7,34	16,42	42,65	6,61

\*Samples 1-2 – granulated electric furnace slag

Samples 3-5 – refining slags

A distinctive feature of the technological scheme for ferronickel production at PRONICO S.A. is that the refining process of crude ferronickel is carried out in a modern unit - a ladle furnace, while at PFK this process is conducted in oxygen converters. The research on the distribution of nickel in slags was conducted using the RSMA (SELMi REM-106I) setup at the National Technical University of Ukraine (Igor Sikorsky Kyiv Polytechnic Institute) in Kyiv. Based on the results of studies of five slag samples on the SELMi REM-106I installation using the X-ray spectral microanalysis method, it was found that nickel, both in electric furnace (Figures 1-2) and refining (Figures 3-10) slags, is present in compounds with iron in the metallic phase, while no nickel was found in the oxide phase.

Sulfur in electric furnace slags is concentrated in metal granules in compounds with nickel and iron, while in refining slags, it is mainly in compounds with CaO. Metal granules are mostly spherical or represented by aggregates of various shapes and sizes. In some areas of the samples, their significant amount reaches up to 47% (see Figure 1), and the nickel content in some granules reaches ~72%.

In Figure 1, the light spots (point 1) have a high

content of nickel and iron (approximately 70 and 25%), while the dark spots (points 2 and 3) contain silicon and iron oxides (35 and 40%).

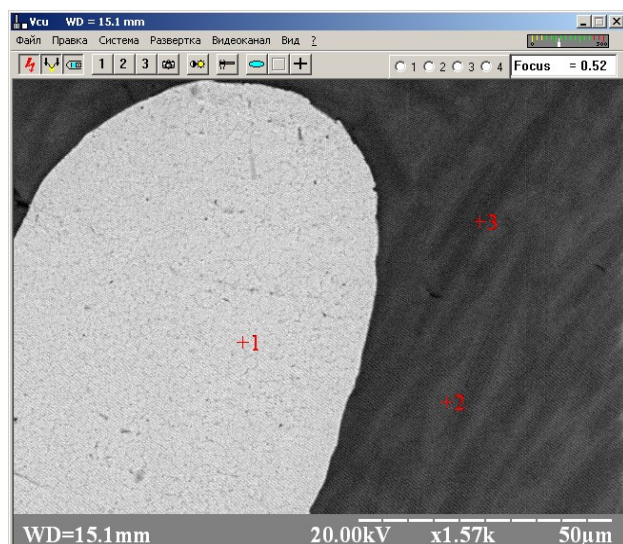
In Figure 2, point 1 contains a large amount of iron and nickel (67% and 30%), while points 2 and 3 mainly contain iron and silicon (40% and 40%) and a small amount of magnesium (11%). Research on samples of electric furnace and refining slags from ferronickel production using nickel-containing ore from the Guatemala deposit by X-ray spectral microanalysis (RSMA) has shown that metal granules are composed of 95-99% iron and nickel in various ratios. The nickel content in some granules of granulated electric furnace slag reaches 72%, which provides some insight into the mechanism of reduction processes occurring in the ore-thermal furnace, indicating the primary reduction of nickel followed by its dilution with iron. The metallic phase also contains the main amount of sulfur, while in refining slags, sulfur is concentrated in compounds with calcium oxide and is inversely related to the content of iron oxides in them.

Currently, various enrichment technologies have been developed and implemented – mechanical, hydrometallurgical, electrolytic, and others, using modern equipment, taking into account the



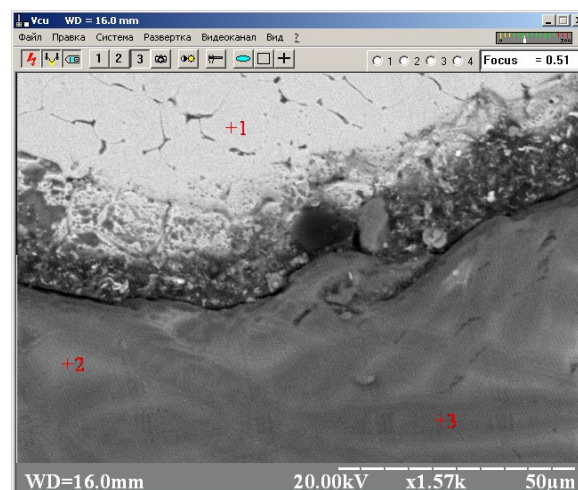
physicochemical and mechanical properties of secondary materials [6-10]. The research conducted in this work is aimed at developing a technological scheme for enriching granulated electric furnace and refining slags from ferronickel production using a high-intensity magnetic field [11-17].

The same five slag samples (Table 1) from ferro-nickel production were studied. To more fully disclose the slags and extract metal from them, they were crushed from the initial fraction (Table 2) to size classes  $-0.16$  mm;  $0.16-0.4$  mm;  $0.4-1.6$  mm and  $+1.6$  mm.



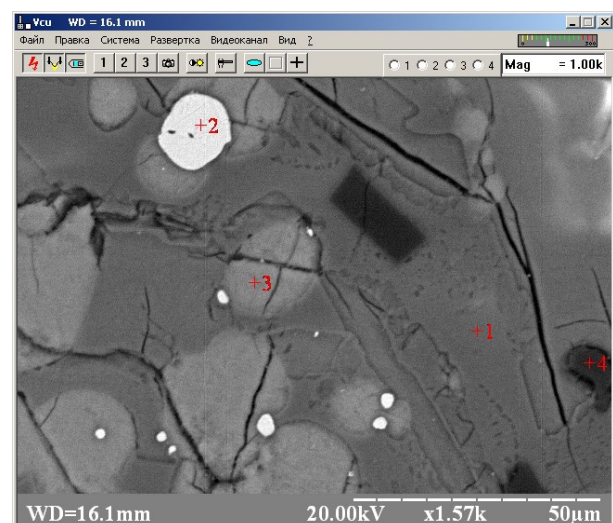
No.	Chemical Composition, %					
	Ni	Fe	S	Ca	Si	Mg
1	71,80	25,88	0,18	0,19	1,29	0,00
2	3,08	45,19	0,00	1,16	39,86	7,11
3	1,25	36,74	0,00	1,58	40,92	15,25

Figure 1. RSMA Results of Electric Furnace Slag (Sample No. 1).



No.	Chemical Composition, %					
	Ni	Fe	S	Ca	Si	Mg
1	31,46	67,21	0,00	0,15	0,29	0,00
2	1,88	51,68	0,00	0,92	36,53	5,01
3	2,34	42,04	0,00	0,34	43,07	10,92

Figure 2. RSMA Results of Electric Furnace Slag (Sample No. 2).

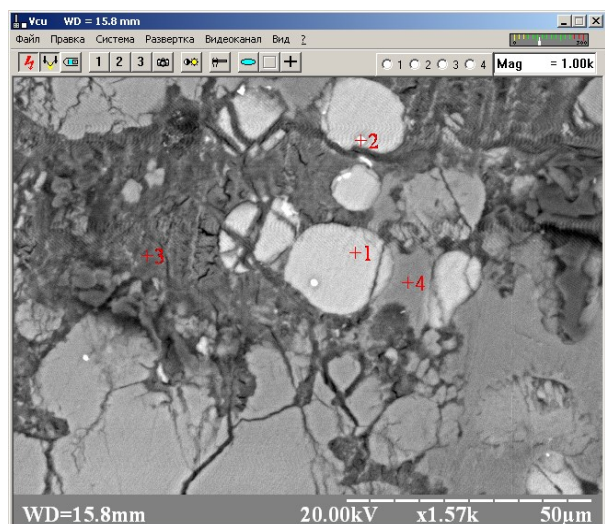


No.	Chemical Composition, %					
	Ni	Fe	S	Ca	Si	Mg
1	0,00	0,00	0,00	88,61	1,49	0,00
2	42,61	56,80	0,11	0,49	0,00	0,00
3	0,00	0,13	34,39	65,29	0,08	0,00

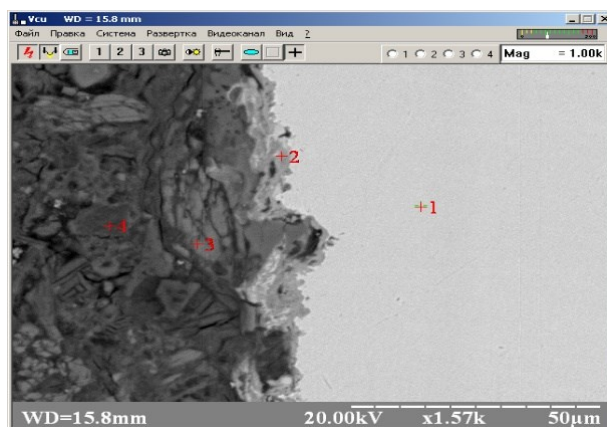
Figure 3. RSMA Results of Electric Furnace Slag (Sample No. 3).



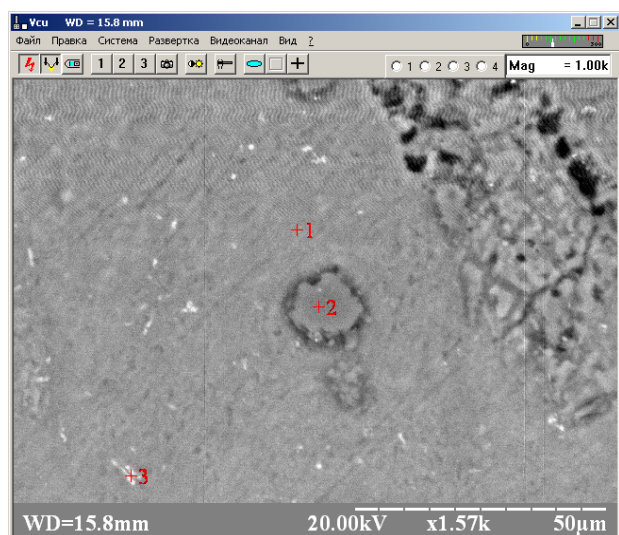
No.	Chemical Composition, %					
	Ni	Fe	S	Ca	Si	Mg
1	0,14	78,46	0,00	1,85	2,28	0,58
2	0,00	88,98	0,19	4,53	4,86	0,00



No.	Chemical Composition, %					
	Ni	Fe	S	Ca	Si	Mg
1	0,33	0,23	34,68	63,89	0,19	0,00
2	25,04	30,42	14,11	29,63	0,07	0,00
3	0,00	3,16	13,07	74,28	4,96	0,00
4	0,45	2,44	3,25	77,44	2,98	0,00



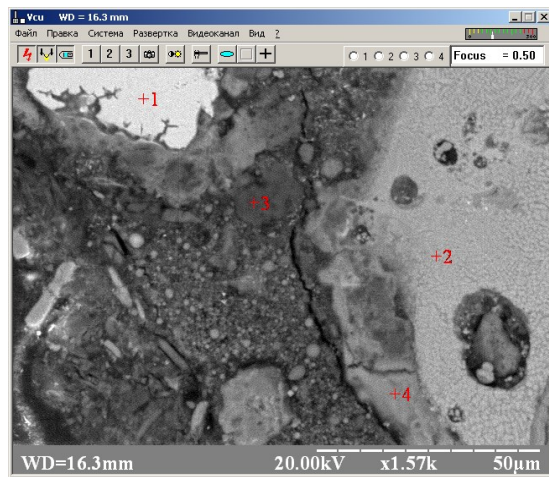
No.	Chemical Composition, %					
	Ni	Fe	S	Ca	Si	Mg
1	30,84	68,00	0,11	0,54	0,00	0,00
2	6,38	83,31	1,17	3,10	0,02	0,00
3	2,31	5,48	1,19	78,60	11,70	0,00
4	4,38	7,88	3,19	70,28	11,46	0,00



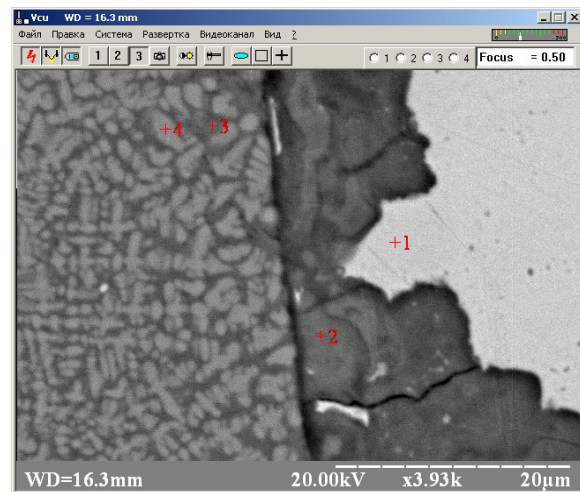
No.	Chemical Composition, %					
	Ni	Fe	S	Ca	Si	Mg
1	2,05	3,72	1,25	55,28	31,14	0,00
2	1,24	1,08	0,40	8,73	86,61	0,00
3	1,05	5,98	2,37	45,21	25,30	0,00

Figure 4. RSMA Results of Electric Furnace Slag (Sample No. 4).

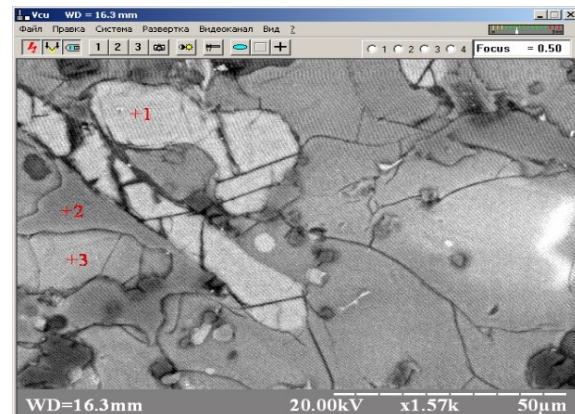




No.	Chemical Composition, %					
	Ni	Fe	S	Ca	Si	Mg
1	23,73	75,69	0,00	0,33	0,25	0,00
2	0,48	96,71	0,00	0,36	2,23	0,00
3	2,83	8,29	0,00	4,26	57,04	0,50
4	21,06	65,42	2,72	7,03	3,19	0,11



No.	Chemical Composition, %					
	Ni	Fe	S	Ca	Si	Mg
1	46,10	53,26	0,34	0,21	0,02	0,00
2	24,29	70,66	1,69	3,02	0,34	0,00
3	2,26	91,57	0,00	0,59	5,02	0,00
4	0,85	97,95	0,38	0,20	0,45	0,00



No.	Chemical Composition, %					
	Ni	Fe	S	Ca	Si	Mg
1	0,00	0,08	36,65	63,26	0,00	0,00
2	0,00	0,97	2,07	78,11	1,26	0,00
3	0,41	0,06	3,61	88,60	7,01	0,04

Figure 5. RSMA Results of Electric Furnace Slag (Sample No. 5).

Table 2. Granulometric Composition of Electric Furnace and Refining Slag Samples.

Size Class, mm	Yield, %	
	Electric Furnace	Refining Slag
+ 5	3,68	3,17
3 – 5	11,58	11,61
1 – 3	73,55	40,22
0,5 – 1	6,36	6,25
0,25 – 0,5	4,4	18,34
0,16 – 0,25	0,3	2,82
– 0,16	0,13	17,59
	100	100

The results of determining the granulometric composition of the samples show that the yield of classes +1 mm for electric furnace slags is more than 88%, and for refining slags – about 55%. It should be noted that in these size classes, there is not enough disclosure of

the initial products, and therefore, preparation operations (crushing, grinding) are necessary for the subsequent enrichment processes of the presented samples.

In the process of developing the technological

scheme for preparing the initial materials and their enrichment, more than 50 experiments were conducted, and more than 70 chemical analyses of enrichment products – metal concentrate, slags, and sludges – were performed.

The slag preparation schemes include: crushing the initial materials on a roll crusher, classification, grinding in a ball mill with subsequent classification – for electric furnace slags, and classification and double grinding for refining slags.

Analyzing the +1.6 mm size class in refining slag samples, it was found that there are metal granules and a non-metallic light product (practically slag fraction). Chemical analysis showed that in this size class, the nickel content in the metal phase is within 26-33%, and in the slag phase, the nickel content is about 0.5%. The +1.6 mm fraction was sent for re-crushing to isolate a purer metal phase. Chemical analysis of the purified metal product showed an increase in nickel content to 38%. The yield of these size fractions for samples No. 3, 4, and 5 is about 10-4.5%.

For the 0.16-0.4 mm size fraction, a metal product with a nickel content of about 9.7% was obtained in the magnetic separation process, with a yield of this product of 15.34%.

For the 0.4-1.6 mm size fraction, a metal product with a nickel content of about 25% was obtained by magnetic separation, with a yield of 18.27%.

Thus, metal products of size fractions 0.16-0.4 mm, 0.4-1.6 mm, and +1.6 mm were obtained with a total nickel content of about 21.94% and a total yield of fractions of 43.6%. The slag fractions of refining slags contain no more than 0.5% nickel.

When working with electric furnace slags, sample

preparation also included the production of size classes -0.16 mm, 0.16-0.4 mm, 0.4-1.6 mm, and +1.6 mm. The prepared size classes were sent both to the magnetic separation stage and to the gravity separation stage.

It was found that repeated crushing and grinding operations of the initial raw material particles lead to the fact that the obtained slag particles acquire a rounded and spherical shape. In further separation processes, especially gravity separation methods, this improves the separation process of the metal phase and the slag fraction.

The yield of magnetic fractions (metal phase) in the magnetic separation process and the yield of heavy fractions (mainly metal granules and aggregates with granules) during wet gravity separation in the studied electric furnace slag samples is about 8-11.6%.

Chemical analysis data show that the nickel content in the obtained metal products is about 0.9-4.75%.

Since granulated electric furnace slags contain moisture under industrial conditions, an enrichment option was investigated that involves a "wet technology." In this option, the enrichment of crushed electric furnace slags will be carried out on magnetic separators adapted to the properties of the initial raw material. Enrichment of electric furnace slags by "wet" technology allows obtaining a metal concentrate with a nickel concentration of 0.9 to 4.75% with a yield of 2-5%. The nickel content in the slag phase is 0.12-0.25%.

The proposed technological line for enriching electric furnace slags (Figure 6) consists of a hopper with a feeder, a belt conveyor, a ball mill, a spiral classifier, a sump with a pump, magnetic separators, a sludge settler, and a pump.

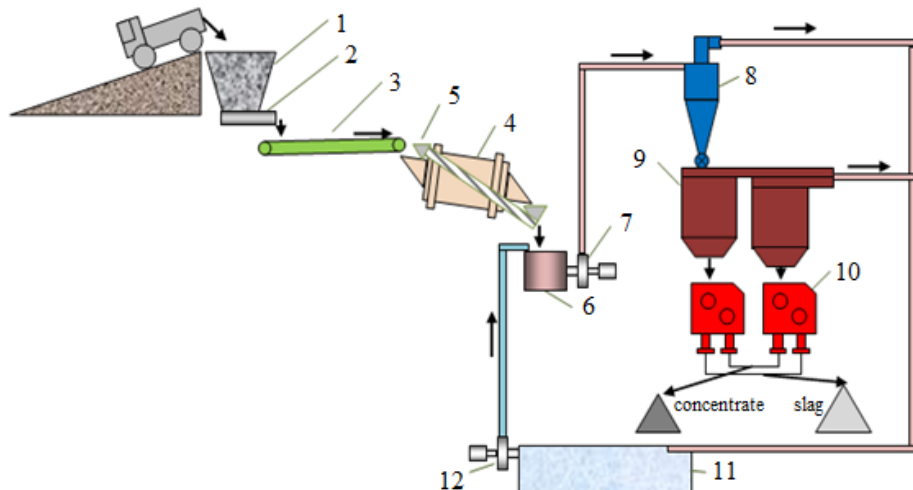


Figure 6. Technological Line for Processing Electric Furnace Slags: 1 – receiving hopper; 2 – feeder; 3 – belt conveyor; 4 – ball mill; 5 – spiral classifier; 6 – sump; 7, 12 – pumps; 8 – hydrocyclone; 9 – hydroclassifiers; 10 – magnetic separators; 11 – sludge settler.

It should be noted that the cost of equipment for the technological line for processing electric furnace slags with an automatic control system will be \$380,000. The installed power of the electrical equipment on the technological line is about 160 kW. The operating

personnel of the technological line is one person.

The refining slag processing scheme includes stages of grinding, air gravity separation, and final product finishing operations of magnetic separation.

The proposed line for processing refining slags,

characterized by a higher nickel content (7.15-10.1%), includes: ball mill MSh1 1500x3000; air gravity separator type VGS-2; magnetic drum separator MBS-300.

The refining slag processing scheme (Figure 7) provides for the supply of slag ground in a ball mill to a gravity separator, where it is separated into size classes. The material of size fractions 0.4-1.6 mm and +1.6 mm is fed to a magnetic separator, where it is

separated into magnetic (metallic) and non-magnetic (slag) fractions.

The cost of the equipment complex for processing refining slags, including an automatic process control system, will be \$280,000, and for processing electric furnace slags – \$380,000, with a payback period of 0.54 months and 0.84 months, respectively.

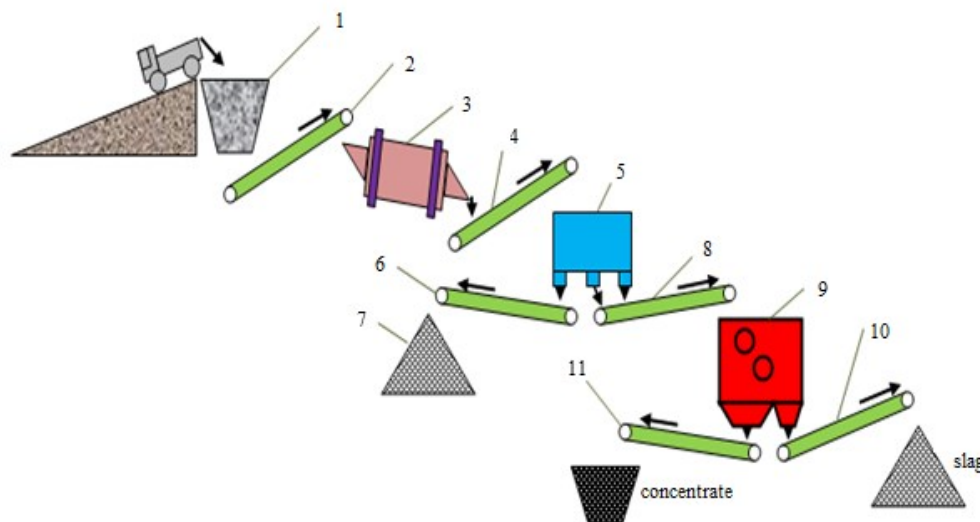


Figure 7. Technological Line for Processing Refining Slags: 1 – receiving hopper with feeder; 2, 4, 6, 8, 10, 11 – belt conveyors; 3 – ball mill; 5 – gravity separator; 7 – storage of fraction -0.16 mm; 9 – magnetic separator.

The developed and proposed technological schemes for enriching electric furnace slags by "wet" technology and refining slags by "dry" technology allow utilizing about 1200 tons of nickel per year or extracting 31.6% and 94.65% of nickel from slags, respectively.

### Conclusions

Based on the results of studies of samples of electric furnace and refining slags from ferronickel production using oxidized nickel ore from the Guatemala deposit at PRONICO S.A. by X-ray spectral microanalysis (RSMA) on the Selmi REM-106I installation, it was determined that the main amount of nickel is concentrated in metal phase granules of various shapes in compounds with iron and sulfur, with a concentration in some cases exceeding 70%.

The studied high-magnesia (31.5-34.7% MgO) acidic ( $\text{CaO} + \text{MgO}/\text{SiO}_2 = 0.72-0.74$ ) granulated electric furnace slags from ferronickel production, containing up to 0.31% Ni, are more than 95% represented by the 0.55 mm fraction, while the highly basic ( $(\text{CaO} + \text{MgO})/\text{SiO}_2$  over 3.0) self-disintegrating refining slags, with a nickel concentration of 9.3 to 10.95%,

are almost 40% represented by the fraction less than 0.5 mm. To more fully disclose the grain, the initial slags were crushed to size classes: -0.16 mm; 0.16-0.4 mm; 0.4-1.6 mm and +1.6 mm in experimental ball mills.

Based on studies of the properties of the initial raw material and its movement in the working zones of separation devices, a new method for enriching ferroalloy slags by the wet method using a modernized magnetic separator adapted to the characteristics of the initial raw material was developed, which allowed for improved nickel extraction from electric furnace slags. The studies on the enrichability of electric furnace slags according to the developed technological scheme allowed obtaining a metal concentrate containing 0.9-4.75% nickel.

The developed and proposed technological schemes for enriching electric furnace slags by "wet" technology and refining slags by "dry" technology allow for the utilization of about 1200 tons of nickel per year, or the extraction of 31.6% and 94.65% of nickel from slags, respectively.

### References

1. Shevchenko, D. V., Prykhodko, S. V., Nadochii, A. A., Shutov, V. Iu., & Ovcharuk, A.M. (2024). Rozvytok tekhnologii vyrobnytstva feronikeliu v Ukraini. *Suchasna elektrometalurhiia*, 2, 5-12. <https://doi.org/10.37434/sem2024.02.01>
2. Prykhodko, S., Shevchenko, D., Akreiev, V. et al. (2023). Plavka skladnykh laterynykh rud ta vybir optymalnoho vidnovnyka. *Modern Eng. and Innovative Technologies*, 1(29-01), 61-70. <https://doi.org/10.30890/2567-5273.2023-29-01-067>
3. Hasyk, M. I., & Liakishev, M. P. (2009). *Fizyko-khimiia i tekhnolohiia ferosplaviv*. (3-ed edition). Systemni tekhnolohii



4. Biletskyi, V. S., & Smyrnov, V. O. (2005). *Pererobka i yakist korysnykh kopalyn*. Skhidnyi vydavnychiy dim
5. Biletskyi, V. S., Oliinyk, T. A., Smyrnov, V. O., & Skliar, L. V. (2019). *Tekhnika ta tekhnolohiia zbahachennia korysnykh kopalyn. Chastyna III. Zakliuchni protsesy*. Kryvorizkyi natsionalnyi universytet
6. Pylov, P. Y., Mostyka, Yu. S., Hrebeniuk, L. Z., Shulte, V. Iu., Zubarev, A. Y., Kutsyn, V. S., Hasyk, M. Y., Poliakov, O. Y., & Tsvetkov, Y. V. (2012). Yssledovanye mahnytnoi vosprymchivosti ferrosylykomarhantsa y vibor metoda mahnytnoi separatsyy otvalnoho shlaka s tseliu yzvecheniya vkluchenyi splava. *Zbahachennia korysnykh kopalyn*, 48 (89), 110-118
7. Mostyka, Yu. S., & Zubarev, A. I. (2012). Analiz sostoyaniya i perspektivy izvecheniya marganecsoederzhashego syrya iz shlamohranilish Nikopolskogo bassejna metodom suhoj magnitnoj separacii. *Naukovi praci DonNTU. Seriya "Girnichno-geologichna"*, 2(19), 227-229
8. Mostyka, Y., Shutov, V., Grebenyuk, L., & Ahmetshina, I. (2013). *Theoretical investigation of dryfrictional separation of materials on rotation cylinder*. Taylor & Francis Group, CRC Press, Leiden, pp. 333-342
9. Shuvaev, S. P., Gasik, M. I., Pilov, P. I., Mostyka, Yu. S., Shutov, V. Yu., & Grebenyuk, L. Z. (2017). Analiz processa i tehnologicheskikh parametrov kinetiki mokroj vysokogradientnoj magnitnoj separacii shlamov obogasheniya margancevih rud i otrabotannyh shlamonakopitelej. *Metallurgicheskaya i gornorudnaya promyshlennost*, 1, 30-35
10. Shuvaev, S. P., Gasik, M. I., Pilov, P. I., Mostyka, Yu. S., Shutov, V. Yu., & Grebenyuk, L. Z. (2017). Kompleksnoe obogashenie margancevykh produktov so stadij vysokointensivnoj magnitnoj separacii i opredelenie magnitnykh svoystv margancevykh koncentratov i aglomerata. *Metallurgicheskaya i gornorudnaya promyshlennost*, 1, 35-44
11. Grishan, D. V., Kulish, A. N., & Kulyk, E. M. (2016). Sensornaya sortirovka shlakov ferosplavnogo proizvodstva. *Suchasni problemi metalurgiyi*, 19(1), 27-34
12. Hrebeniuk, L. Z., Mostyka, Yu. S., & Shutov, V. Iu. (2006). *Sposib mahnitnoi separatsii*. (Patent 19277 Ukraina), Biul. No. 12
13. Mostyka, Yu. S., Shutov, V. Iu., & Mostyka, A. Iu. (2007). *Sposib podilennia materialiv za mahnitnymy vlastyvostiamy*. (Patent 21790 Ukraina), Biul. No. 4
14. Mostyka, Yu. S., Shutov, V. Iu., & Mostyka, A. Iu. (2008). *Elektromahnitnyi valkovyi separator*. (Patent 29966 Ukraina), Biul. No. 3
15. Mostyka, Yu. S., Shutov, V. Iu., & Mostyka, A. Iu. (2008). *Mahnitnyi separator*. (Patent 32106 Ukraina), Biul. No. 9
16. Kulish, A. M., Titenko, S. V., Smolientsev, O. M., Hryshan, D. V., & Voloshyn, S. V. (2008). *Prystrii dlia separatsii tekhnohennoi syrovyny, predstavlenoi metalovmisnymy vidkhodamy abo nekondytsiinymy rudamy*. (Patent 30568 Ukraina), Biul. No. 14
17. Kulish, A. M., Titenko, S. V., Smolientsev, O. M., Hryshan, D. V., Voloshyn, S. V., & Voloshyn, V. M. (2009). *Prystrii dlia separatsii tekhnohennoi syrovyny, predstavlenoi metalovmisnymy vidkhodamy abo nekondytsiinymy rudamy*. (Patent 88221 Ukraina), Biul. No. 18

Отримано редколегією / Received by the editorial board: 29.11.2024

Прийнято до друку / Accepted for publication: 20.02.2025

Grishin O.M., Proidak Yu.S.

## Regularities of solid-phase reduction of iron oxides under conditions of combined chemical-catalytic and energetic influence

Гришин О.М., Пройдак Ю.С.

### Закономірності твердофазного відновлення оксидів заліза в умовах комбінованого хіміко-каталітичного та енергетичного впливу

**Abstract. Purpose.** The purpose of the work is a physicochemical analysis of the intensification of the process of solid-phase iron reduction under the conditions of the joint influence of catalytic additives and an electromagnetic field (EMF). **Methodology.** The experiments were conducted in an alternating magnetic field with a frequency from industrial to ultrasonic using the thermogravimetric method. The process of reduction of various iron ore materials was studied in the temperature range of 873–1373 K. **Results.** The results of laboratory experiments indicate the influence of the electromagnetic field and intensifying catalytic additives on the process of solid-phase reduction of various iron ore materials. The non-additivity of the results of the joint influence of additives and an intensifying EMF is shown. The study of the influence of various process parameters on the rate and degree of reduction of iron ore materials is carried out. **Scientific novelty.** The joint intensifying effect of catalytic additives and EMF on the process of solid-phase iron reduction is experimentally shown. A physicochemical justification of the non-additivity of the joint influence on the kinetics of the reduction process is proposed. **Practical significance.** Intensification of the processes of solid-phase reduction of iron ore raw materials provides a significant increase in the productivity of direct iron production technologies - process intensification and process productivity. **Keywords:** solid-phase reduction, intensification, kinetics, iron oxides, alternating electromagnetic field, mechanism, catalytic additive.

**Анотація. Мета.** Метою роботи є фізико-хімічний аналіз інтенсифікації процесу твердофазного відновлення заліза в умовах сумісного впливу каталітичних добавок та електромагнітного поля (ЕМП). **Методологія.** Експерименти проводились у змінному магнітному полі з частотою від промислової до ультразвукової за допомогою термогравіметричного методу. Процес відновлення різних залізородних матеріалів вивчався в температурному діапазоні 873–1373 К. **Результати.** Результати лабораторних експериментів свідчать про вплив електромагнітного поля та інтенсифікуючих каталітичних добавок на процес твердофазного відновлення різних залізородних матеріалів. Показано неадитивність результатів спільного впливу добавок та інтенсифікуючого ЕМП. Проведено дослідження впливу різних параметрів процесу на швидкість та ступінь відновлення залізородних матеріалів. **Наукова новизна.** Експериментально показано спільний інтенсифікуючий вплив каталітичних добавок та ЕМП на процес твердофазного відновлення заліза. Запропоновано фізико-хімічне обґрунтування неадитивності спільного впливу на кінетику процесу відновлення. **Практичне значення.** Інтенсифікація процесів твердофазного відновлення залізородної сировини забезпечує значне підвищення продуктивності технологій прямого отримання заліза – інтенсифікацію процесу та продуктивність процесу. **Ключові слова:** твердофазне відновлення, інтенсифікація, кінетика, оксиди заліза, змінне електромагнітне поле, механізм, каталітична добавка.

**Introduction.** The processes of solid-phase iron reduction are usually carried out at moderate temperatures (up to 1373 K) [1-4], which makes the productivity and efficiency of the units directly dependent on the rate of iron ore charge reduction and the possibility of its intensification. This, in turn, requires an in-depth study of the kinetic laws and mechanism of the recovery processes, as well as the identification of limiting links to scientifically select ways to accelerate the process.

Various chemical-catalytic and energy (physical) influences as possible regulators of physical and chemical processes are attracting the attention of

researchers for a long time. Thanks to numerous studies, the most significant successes in this area have been achieved by using electromagnetic and corpuscular radiation [5-11] and alkali metal salts.

The possibility of targeted control of the concentration of electronic and structural defects in crystalline phases by introducing impurity ions and energetic influence on the reacting system opens new ways to intensify the reduction of metals from oxides. At the same time, the simultaneous effect of these methods on the solid-phase reduction of iron-containing materials appears to be of interest.



**Research results and their analysis.** Experimental studies of the kinetics of the process of solid-phase reduction of iron oxides under conditions of chemical catalytic and energy impact were performed using the thermogravimetric method, with the registration of changes in the mass of the sample and the composition of the waste gases.

Hematite was reduced at a high rate (Fig. 1), with ~95 % of the oxygen containing iron oxide being removed within 40 min. Increasing the temperature from 1073 to 1173 K accelerated only the first stage, the final stage of reduction proceeded somewhat slower, which is probably due to the increased difficulty of inner diffusion gas exchange due to sintering of iron crystals. The application of EMF slightly intensifies the process (Fig. 1).

The rate of magnetite reduction was lower, with ~90% of the oxygen bound to iron being removed within 40 min (Fig. 2). The transition from 1073 to 1173 K did not cause a significant inhibition at the final stage, which can be attributed to the slow sintering process of iron particles obtained from less active  $\text{Fe}_3\text{O}_4$ . The intensifying effect of EMF is approximately the same as in the case of  $\text{Fe}_2\text{O}_3$  reduction.

The recovery of magnetite concentrate (MC) was slower, with the degree of recovery ( $\omega_B$ ) reaching 63 and 70% in 40 min at 1073 and 1173 K, respectively (Fig. 3). The nature of the effect of temperature on the process kinetics indicates that sintering and recrystallisation do not develop significantly during the experiment. The alternating EMF intensified approximately in the same way as for other iron ore materials (Fig. 3). A similar pattern was observed when the reacting system was chemically catalysed by the introduction of KCl into the charge (Figs. 1-3).

A more significant intensification of iron reduction was observed under the combined effect of EMF and potassium chloride (Fig. 1-3). Lithium chloride had the opposite effect in the process of indirect reduction. Adding it to the charge significantly inhibited the reaction, so that in the presence of 1% LiCl,  $\omega_B$  decreased

by 3-4% (Fig. 1-3). The inhibitory effect of lithium chloride was almost the same for all tested iron ore materials.

The same set of studies was used for the carbon-thermal reduction at 1373 K. Without catalytic influence, the complete carbon-thermal reduction of hematite was completed in 20 min, and of magnetite in 30 min. The last stage of the  $\text{FeO}_{\text{minO}} \rightarrow \text{Fe}$  process was characterized by autocatalysis (Fig. 4), which is due to the catalytic intensification of the gasification step ( $\text{CO}_2 + \text{C} = 2\text{CO}$ ) by metallic iron.

Under these conditions, the catalytic effect of  $\text{Fe}_{\text{Met}}$  was not fully manifested, the process was relatively slow and was completed in 45 min. The chemical-catalytic and energy (EMF) effects had a positive effect on the rate of carbon-thermal reduction (Fig. 4, 5). Lithium chloride, which inhibited the gas reduction process, significantly accelerated the carbon-thermal reduction. The intensifiers were ranked by their effectiveness: EMP, 1% LiCl, 1% KCl, 1% KCl together with the field. Their effect is much higher than in gas reduction. For example, the presence of 1% KCl in the charge provided a relative acceleration of ~30%.

In the experiments with  $\text{Fe}_2\text{O}_3$  and  $\text{Fe}_3\text{O}_4$ , these effects do not change the general appearance of the kinetic curves, however, during the carbon-thermal reduction of magnetite concentrate, catalytic additives led to a clearly expressed autocatalysis at the  $\text{FeO}_{\text{minO}} \rightarrow \text{Fe}$  stage (Fig. 5).

The complex reduction of iron ore materials was carried out by graphite together with CO at 1173 and 1273 K, proceeded at a high rate and complete oxygen removal was completed in 25 min at 1173 K and 16 min at 1273 K. The kinetic curves, as in the case of carbon-thermal reduction, were accompanied by the development of autocatalysis at the  $\text{FeO}_{\text{minO}} \rightarrow \text{Fe}$  stage (Fig. 6).

During the reduction of magnetite concentrate, there were no clear kinks in the kinetic curve (Fig. 5), which may be due to the relatively poor contact between carbon and concentrate.

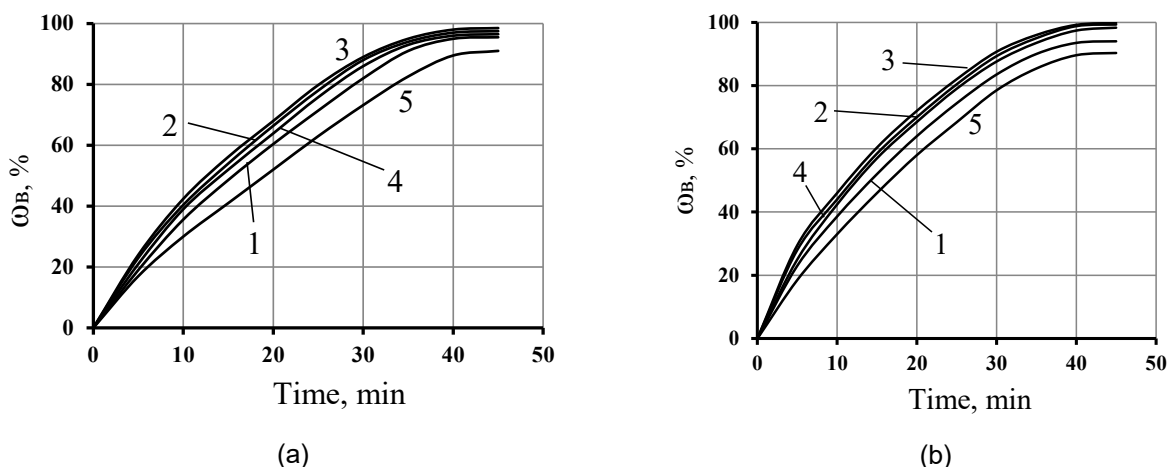
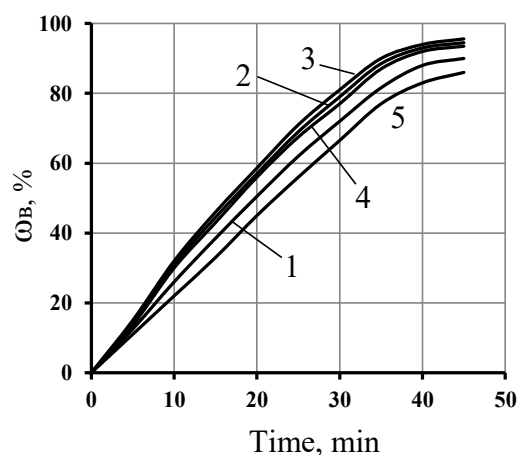
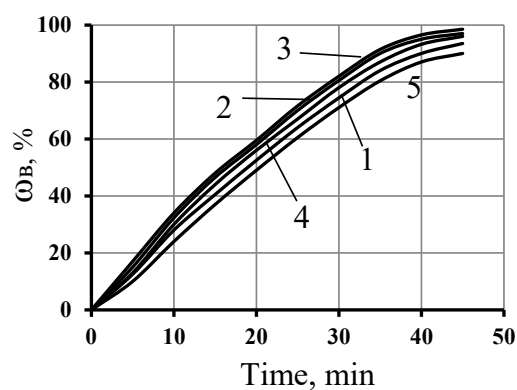


Fig. 1. Kinetics of  $\text{Fe}_2\text{O}_3$  reduction by carbon monoxide at a) 1073 K, b) 1173 K: 1 - no additive; 2 - 1% KCl; 3 - EMF + 1% KCl; 4 - EMF; 5 - 1% LiCl

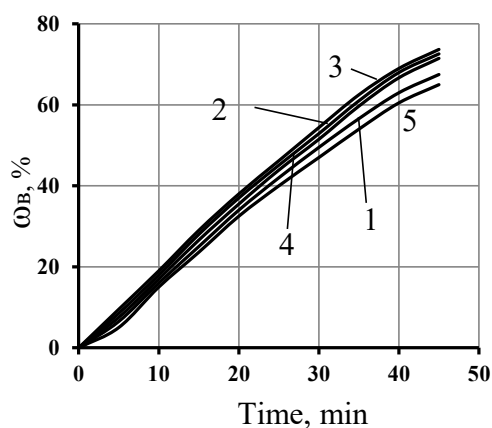


(a)

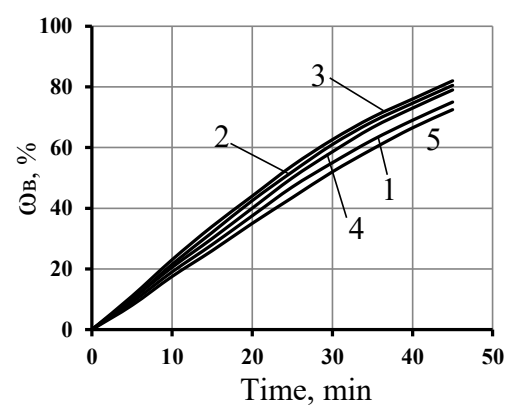


(b)

Fig. 2. Kinetics of  $\text{Fe}_3\text{O}_4$  reduction by carbon monoxide at a) 1073 K, b) 1173 K: 1 - no additive; 2 - 1% KCl; 3 - EMF + 1% KCl; 4 - EMF; 5 - 1% LiCl

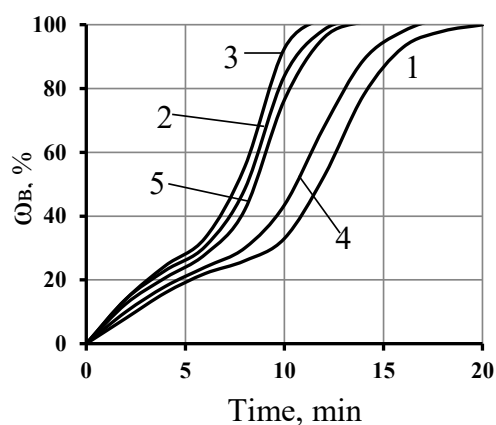


(a)

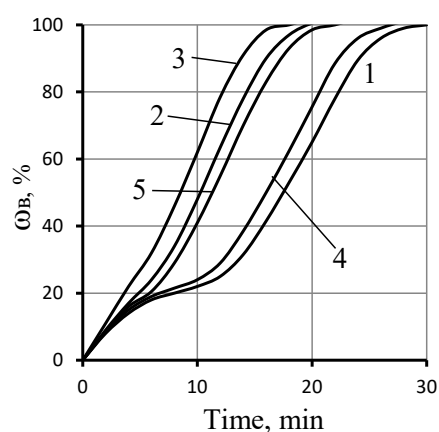


(b)

Fig. 3. Kinetics of MC reduction by carbon monoxide at a) 1073 K, b) 1173 K: 1 - no additive; 2 - 1% KCl; 3 - EMF + 1% KCl; 4 - EMF; 5 - 1% LiCl



(a)



(b)

Fig. 4. Kinetics of carbon-thermal reduction at 1373 K a)  $\text{Fe}_2\text{O}_3$  and б)  $\text{Fe}_3\text{O}_4$ : 1 - no additive; 2 - 1% KCl; 3 - EMF + 1% KCl; 4 - EMF; 5 - 1% LiCl.

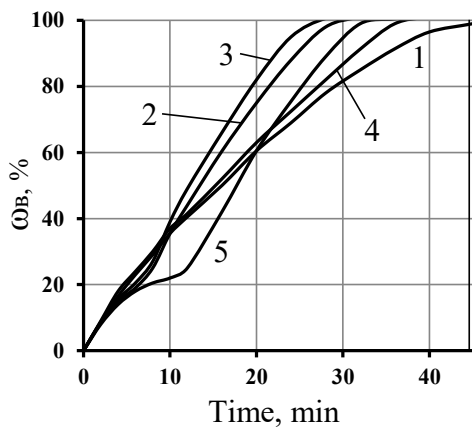


Fig. 5. Kinetics of MC reduction by carbon at 1373 K: 1 - no additive; 2 - 1% KCl; 3 - EMF + 1% KCl; 4 - EMF; 5 - 1% LiCl

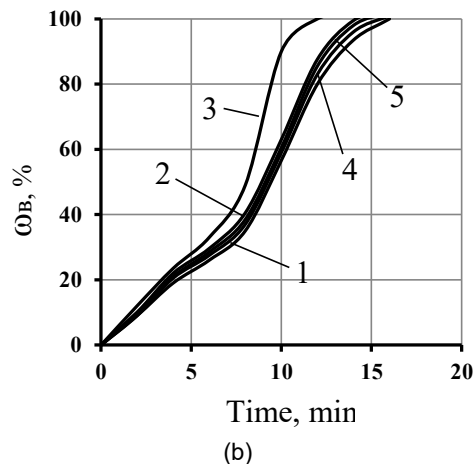
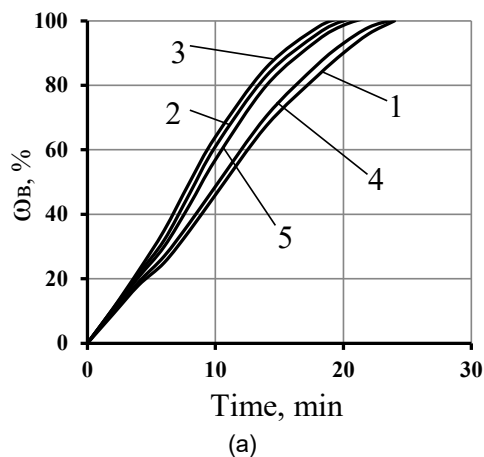


Fig. 6. Kinetics of complex reduction of  $\text{Fe}_2\text{O}_3$  at a) 1173 K, b) 1273 K: 1 - no additive; 2 - 1% KCl; 3 - EMF + 1% KCl; 4 - EMF; 5 - 1% LiCl

The complex reduction of the magnetite concentrate was characterised by a monotonous decrease in the rate (Fig. 7), the reaction proceeded relatively slowly, the time for complete oxygen removal was 75 and 50 min for 1173 and 1273 K, respectively. The degree of influence of the intensifiers was characterised

by the same sequence as in carbon thermal treatment (Figs. 6, 7). The kinetic curves did not undergo serious changes under the influence of the intensifiers. Only in the complex reduction of MC were signs of autocatalysis observed at the last stage if KCl and especially LiCl were introduced into the charge.

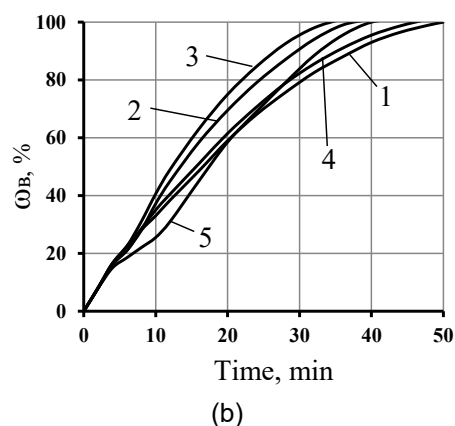
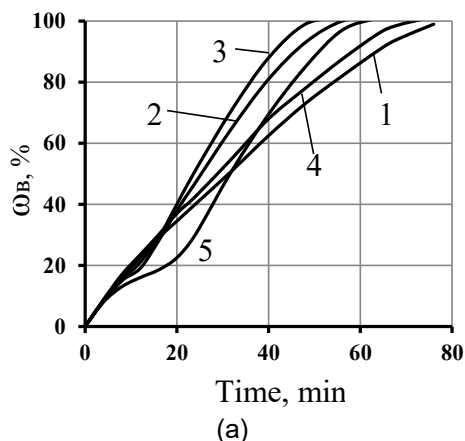


Fig. 7. Kinetics of complex reduction of MC at a) 1173 K, b) 1273 K: 1 - no additive; 2 - 1% KCl; 3 - EMF + 1% KCl; 4 - EMF; 5 - 1% LiCl

In addition to the industrial frequency EMF, the recovery of magnetite concentrate was studied under the application of ultrasonic exposure at 773 K in a

hydrogen flow. This effect had a higher efficiency compared to the industrial frequency field.

Separately, a series of experiments was performed



to study the joint intensifying effect on the process of direct iron reduction in the fluidised bed mode using conical and cylindrical reactors. The temperature and EMF parameters (frequency and intensity) were varied. Table 1 shows some of the experimental results.

The data shows that at 973 K, the effect of additives on the metallisation process occurring under conditions of periodic exposure to a magnetic field was approximately the same as in experiments without a field.

At  $W_{H_2} = 1$  l/min, the value of the degree of metallisation ( $\alpha$ ) because of the introduction of 1% KCl increased significantly (from 46.5 to 63.0%). the reduction in the fluidised bed ( $W_{H_2} = 2$  l/min) was almost doubled. However, at 873 K, additives under these conditions did not produce the expected effect. Moreover, the process even slowed down, which was reflected in a decrease in the amount of metallised iron from 72% to 62.5%.

Table 1. Concentrate metallisation in hydrogen flow under different external influences (conical reactor),  $\tau = 40$  min, EMF:  $f = 0.5$  Hz,  $H = 400$  Oe

T, K	$W_{H_2}$ , l/min	Degree of metallisation ( $\alpha$ ), %		
		No additives and EMF	EMF	1 % KCl + EMF
873	2	46,4	72,2	62,5
973	1	47,5	46,5	63,0
973	2	49,1	55,2	100

The high values of  $\alpha$  observed when the field was applied in a conical reactor in the absence of additives are explained by the specific conditions of the charge particle movement, which was accompanied by alternating cycles of 'deposition' and 'swelling' of the concentrate layer. With such a layer organisation, particle sintering is difficult and does not significantly affect the

process of oxygen removal from the oxide lattice. The weakening of this effect in the presence of salts is difficult to attribute to the influence of their layer structure and the nature of particle movement. Probably, other reasons underlie the observed patterns.

Similar patterns were found in the cylindrical reactor (Table 2).

Table 2. Concentrate metallization under different external influences (cylindrical reactor),  $\tau = 40$  min; EMF:  $f = 0.5$  Hz,  $H = 400$  Oe

T, K	$W_{H_2}$ , l/min	Degree of metallisation ( $\alpha$ ), %		
		No additives and EMF	EMF	1 % KCl + EMF
873	2	42,2	41,6	70,5
973	1	43,5	46,8	93,0
973	2	44,2	45,2	100

At 973 K, KCl additives during the metallisation of the concentrate in a magnetic field had a significant accelerating effect, contributing to an increase in  $\alpha$  from 45-47% to 93-100%. However, in contrast to previous experiments, the positive effect of the additives at a temperature decrease from 973 to 873 K was preserved, albeit in a weaker form: the  $\alpha$  values increased from 41.6 to 70.5%.

It should be noted that the efficiency of salt introduction at 873 K was significantly lower than the observed acceleration of processes without the field. Tables 3 and 4 compare the results of the metallisation of the concentrate with KCl additives under the conditions of field application and without it.

As can be seen from the tables, the combined use

of EMF and catalytic additives has a positive effect on the process only at 973 K. In experiments with a stationary bed ( $W_{H_2} = 1$  l/min), the total accelerating effect exceeded that observed under the conditions of separate action of salts and field, which was reflected in the increase in  $\alpha$  from 63.1% and 46.8% to 93% (cylindrical reactor) and from 55.0% and 46.5% to 63.0% (conical reactor).

In the fluidised bed, similar ratios were obtained in experiments lasting 30 min: the  $\alpha$  values increased under the combined effect of the field and catalytic additives in the conical reactor to 100% compared to 95.5% (1% KCl without the field) and 55.2% (in the field without additives,  $\tau = 40$  min), and in the cylindrical reactor - to 100% compared to 98 and 45.2%, respectively.

Table 3. Concentrate metallization in the layer at different methods of process intensification (cylindrical reactor),  $\tau = 40$  min; EMF,  $f=50$  Hz,  $H=400$  Oe

T, K	$W_{H_2}$ , l/min	Degree of metallisation ( $\alpha$ ), %		
		No additives and EMF	EMF	1 % KCl + EMF
873	2	42,2	95,0	70,5
973	1	43,5	63,1	93,0
973	2	44,2	100	100

Table 4. Concentrate metallization in the layer at different methods of process intensification (conical reactor),  $\tau = 40$  min; EMF,  $f=0.5$  Hz,  $H=400$  Oe

T, K	$W_{H_2}$ , l/min	Degree of metallisation ( $\alpha$ ), %		
		No additives and EMF	EMF	1 % KCl + EMF
873	2	46,4	80,0	62,5
973	1	47,5	55,0	63,0
973	2	49,1	98,0	100

At 873 K, a significant weakening of the catalytic effect was observed when a magnetic field was applied along the course (Tables 3 and 4). This trend was observed both in the pulsed magnetic field and in the field of industrial frequency. The reduction of the accelerating effect of the additives was manifested in a decrease in the degree of metallisation in the field by 22-25%.

In a special series of experiments, the effectiveness of the magnetic field on the catalytic activity of salts was evaluated depending on the frequency and intensity of the magnetic field. The obtained values of the degree of metallisation are presented in Table 5 (numerator); the denominator shows the results of concentrate metallisation in the presence of salts, but without a field.

Table 5. Degree of concentrate metallization in a magnetic field of different frequency and intensity ( $W_{H_2} = 2$  l/min; 1% KCl;  $\tau = 40$  min)

T, K	Reactor type	EMF		$\alpha$ , %
		f, Hz	H, Oe	
873	conical	0.5	200	40.6/80.0
873	conical	0.5	400	62.5/80.0
873	conical	50	400	55.0/80.0
973	conical	0.5	200	100/96.0
973	conical	0.5	400	100/98.0
873	cylindrical	50	200	57.5/95.0
873	cylindrical	50	400	70.5/95.0
973	cylindrical	50	400	100/100
973	cylindrical	50	200	100/100

Experiments with the variation of field parameters (frequency and intensity) confirmed the above correlations.

It is well known that the solid-phase reduction process is complex, which is determined by the closely interconnected links of diffusion, crystal-chemical and carbon gasification reactions. In this context, the mechanism of both energetic and chemical-catalytic influence on the reacting system should be considered.

The presented results of the experiments allow us to draw certain conclusions about the mechanism of joint chemical-catalytic and energy intensifying influence on the processes of solid-phase iron reduction. It should be noted that direct experiments have shown a certain disagreement between the total effect of the sum of influences on the rate of reduction of iron oxides, i.e., there is a non-additivity. Moreover, there was a mutual levelling of the chemical-catalytic and energy effects when they were used together. The intensifying effect of the joint action of the additive and EMF differed depending on the type of process and field frequency and was the smallest compared to the separate variants. All the above makes it very difficult to analyse the mechanism of the joint effect of intensifiers on the iron reduction process.

The catalytic effect of alkali metal salts is widely reported in scientific publications and in our research results [12,13]. Based on the fundamental concepts of

heterogeneous catalysis, solid state physics, and the theory of chemisorption on the surface of semiconductors, the mechanism of additives' action was developed through the influence on the adsorption-chemical link and diffusion of iron ions in the crystal lattice [14]. The influence of catalytic additives on the adsorption-chemical link is realised through changes in the structural and electronic defects of oxide crystals and, as a result, the adsorption capacity of the oxide surface. The diffusion processes are affected by the potential difference between the oxide surface and the volume formed during the chemisorption of gases [15,16].

It should be noted that the energy effect affected the indirect reduction and gasification steps. Iron,  $Fe_3O_4$ , and  $Fe_2O_3 \cdot \gamma$  are typical ferromagnets characterised by magnetostriction: size change when magnetised, and this effect plays a significant role in the reduction of iron oxides under alternating magnetic fields, facilitating inner diffusion gas exchange and crystal-chemical transformations.

Along with the diffusion transport of gases, electromagnetic effects, due to the magnetostriction effect, accelerate the crystal-chemical transformation step. The continuous movement of particles forming crystals in an alternating EMF increases their mobility, which leads to an increase in the rate of ion diffusion through the crystal lattice and facilitates phase transformations.

There are other ways in which an alternating field

can affect the indirect reduction of iron oxides. For example, a change in the linear dimensions of ferromagnetic phases due to magnetostriction causes elastic stresses of different signs in them, which affects the rate of ion movement through the crystal lattice [14]. These stresses can also be transmitted to nonferromagnetic materials (FeO) that are in close contact with ferromagnets within the same grain. Consequently, the solid-phase diffusion of ions throughout the grain is accelerated. This is confirmed by the intensification of NiO reduction by hydrogen when an alternating field is applied to the reacting system.

It is known that an external electric field affects the activity of a semiconductor [17], which is associated with a change in the concentration of electrons and holes, which affects the adsorption capacity of the crystal surface. The activity of semiconductors also changes under the influence of EMFs. Chemisorption on the surface of oxides separates the charge into surface and bulk charges, creating an electric field that regulates the transfer of ions in the solid phase. The EMF imposed on the reacting system affects the mobile electric charge (Lorentz force) and can have a favourable effect on solid-phase diffusion processes and crystal transformations in general.

Lastly, carbon gasification is also affected by EMFs. It is likely that the field affects the destruction of carbon-oxygen complexes on the carbon surface, which is accompanied by the release of CO into the gas phase and thus intensifies the carbon-thermal and complex reduction of iron oxides.

Thus, the mechanisms of influence of catalytic additives and EMFs on the recovery process are quite

similar. The non-additivity of the joint effect of these intensifiers may be due to mutual 'competition'. It is known that the catalytic effect of alkali metal salts is attenuated as the weight of the additive increases. This is also true for the power of the EMF. In this case, when the intensifiers act together, the maximum effect is achieved at a lower level compared to the sum of the effects. In the case of carbon-thermal and complex iron reduction, the non-additivity can also be caused by the physicochemical patterns of the intensifying effect on the carbon gasification reaction. Probably, the field affects the process of destruction of carbon-oxygen complexes on the carbon surface, which is accompanied by their release into the gas phase and thus intensifies the carbon-thermal and complex reduction of iron oxides. In this context, the mechanism of both energetic and chemical-catalytic influence on the reacting system should be considered.

An increase in the speed of each of the links should contribute to the intensification of the process, but the maximum effect can be obtained by accelerating the combination of these reactions.

### Conclusions

The fact of the non-additivity of the joint effect of a catalytic additive and an intensifying EMF on the rate of the direct iron reduction process has been experimentally established. A physicochemical model of the mechanism of joint effect of intensifiers on the reduction process has been proposed. The effect of the frequency and intensity of the EMF on the intensification of the solid-phase reduction of iron ore materials was experimentally confirmed.

### References

1. Bohdandy, L., & Enhel, H. (1971). *Vosstanovlenye zheleznykh rud*. Metallurhiya
2. Weeda, M., Kapteijn, F., & Moulijn, J. A. (1992). Advances in the Development of Coke Free Iron Oxide Reduction Processes. In: Yürüm, Y. (Ed.). *Clean Utilization of Coal*. NATO ASI Series, vol 370. Springer, Dordrecht. [https://doi.org/10.1007/978-94-017-1045-9\\_21](https://doi.org/10.1007/978-94-017-1045-9_21)
3. Kozhevnykov, Y. Iu., Manokhyn, A. Y., Okhanov, V. Y. et al. (1977). Perspektivy razvytiya protsessov beskoksovoi metallurhyy zheleza. *Fyzyko-khymiya priamoho polucheniya zheleza*, 5-11
4. Haryna, Y. M. (1981). Razvytye protsessov priamoho polucheniya zheleza za rubezhom v 1976-1980hh. *Biulleten TsNYY ynform. ChM*, (21(905)), 3-13
5. Thomas, J. M., & Thomas, W. J. (2015). *Principles and Practice of Heterogeneous Catalysis* [2nd Edition]. Wiley-VCH
6. Pizzini, S. (2015). *Physical Chemistry of Semiconductor Materials and Processes*. <https://doi.org/10.1002/9781118514610>
7. Lannoo, M., & Bourgoin, J. (2012). *Point Defects in Semiconductors I*. Springer Berlin, Heidelberg. <https://doi.org/10.1007/978-3-642-81574-4>
8. Smart L., E., & Moore, E., A. (2016). *Solid State Chemistry*. CRC Press. <https://doi.org/10.1201/b12047>
9. Ujam, C. J., & Adebayo, A. D. (2021). Temperature Dependence of Electrical Conductivity in Semiconductors. *Journal of Engineering Research and Reports*. <https://doi.org/10.9734/jerr/2021/v21i1117501>
10. Stiegler, J. O., & Mansur, L. K. Radiation Effects in Structural Materials. *Annual Review of Materials Science*, 9(1), 405-454. <https://doi.org/10.1146/annurev.ms.09.080179.002201>
11. Zhao, C, et al. (2007). *Radiation Physics and Chemistry*, 76, 37-45
12. Hryshyn, A. M., & Symonov, V. K. (2004). Yssledovanye adsorbtsyonno-khymicheskoykh vzaymodeistviy v protsessakh uhletermicheskoho y kompleksnoho vosstanovleniya oksydov zheleza. In *Trudy mezhdunarodnoi konferentsyy "Stalyi rozvytok hirnycho-metallurhiinoi promyslovosti"*. Vol. 2. (pp. 36-41). Tekhnicheskyy unyversytet
13. Symonov, V. K., Hryshyn, A. M., & Rudenko, L. N. (2004). Vlyaniye khymiko-katalyticheskoykh vozdeistviy na razvytye adsorbtsyonnykh protsessov pry hazovom vosstanovlenii oksydov zheleza. *Yzvestiya vuzov. Chernaia metallurhiya*, (6), 3-7
14. Belchenko V. H., Symonov V. K., & Rostovtsev S. T. (1971). Vlyaniye nekotorykh katalyticheskoykh dobavok na kynytyku y mekhanizm vosstanovleniya oksydov zheleza hazamy. *Fyzicheskaya khymiya oksydov*, 27-39

15. Su, G., Yang, S., Jiang, Y., Li, J., Li, S., Ren, J.-C., Liu, W. (2019). Modeling chemical reactions on surfaces: The roles of chemical bonding and van der Waals interactions. *Progress in Surface Science*, 94(4), 100561. <https://doi.org/10.1016/j.progsurf.2019.100561>
16. Shamsuddin, M. (2021). *Physical Chemistry of Metallurgical Processes*. (Second Edition). Springer Cham. <https://doi.org/10.1007/978-3-030-58069-8>
17. Wolkenstein, Th. (1960). The Electron Theory of Catalysis on Semiconductors. *Advances in Catalysis*, 12, 189-264. [https://doi.org/10.1016/S0360-0564\(08\)60603-3](https://doi.org/10.1016/S0360-0564(08)60603-3)

Отримано редколегією / Received by the editorial board: 19.11.2024

Прийнято до друку / Accepted for publication: 20.02.2025

Akreiev V.V., Cherenkov D.V., Prykhodko S.V., Melnyk S.O., Ovcharuk A.M.

**Improved heat-insulating products for ingot  
hot-tops in molds without extensions**

Акреев В.В., Черенков Д.В., Приходько С.В., Мельник С.О., Овчарук А.М.

**Поліпшені теплоізоляційні вироби  
для надлишкових частин виливниць без надставок**

**Abstract.** The fundamental principle of proper ingot solidification in metal molds - hop top part of ingot should cool and solidify slowly than the ingot body. To achieve this, typically hop top parts of ingots are insulated with special thermal insulation products. They are mounted either directly on the inner surface of the mold or installed in special hop top extensions of the mold. This approach effectively directs shrinkage defects away from the usable ingot section into hop top cut zone. For different steel grades (alloys), depending of the application, ingot design, and casting method, hop top cut ranges from 8% to 16% of the total ingot mass. This article presents experience in using an advanced thermal insulation insert design, which enables higher part of usable ingot metal, prevents subhead cracks in the ingot, simplify and lighten the lining of ingot hop top.

**Keywords:** thermal insulation insert, ingot, mold, hop top, hop top cut, usable part of ingot metal.

**Анотація.** Фундаментальний принцип правильного затвердіння зливка у металевих формах полягає в тому, що верхня (надлишкова) частина зливка повинна охолоджуватися та твердіти повільніше, ніж його основне тіло. Для досягнення цього, як правило, надлишкові частини зливок ізолюють спеціальними теплоізоляційними виробами. Їх встановлюють або безпосередньо на внутрішню поверхню форми, або у спеціальні надставки форми. Такий підхід ефективно спрямовує усадочні дефекти за межі корисної секції зливка, у зону обрізання надлишку. Для різних марок сталі (сплавів), залежно від застосування, типу зливка та методу лиття, відсоток надлишку коливається від 8% до 16% від загальної маси зливка. Ця стаття представляє досвід використання вдосконаленої конструкції теплоізоляційної вставки, яка дозволяє отримати більшу частку корисного металу зливка, запобігає підголовним тріщинам у зливку, а також спрощує та полегшує футерування надлишкових частин виливниць.

**Ключові слова:** теплоізоляційна вставка, зливков, виливниця, надлишок, відрізка надлишку, корисна частина металевого зливка.

**Introduction.** Steel casting is final and one of the most responsible operations in the steel ingot production process. As a rule, the quality of steel ingot products is subject of highest requirements, which entails the need to develop and implement effective technologies, that help to reduce physical, chemical and structural heterogeneity in solidifying ingots, reduce hop top cut, and increase usable part of ingot metal.

Moreover, it should be noted that steelmaking is a costly process, both in terms of financial, energy and resource components and in terms of personnel labor. In case of defective production, all these expenses may be wasted. Even minor deviations in the casting process technology lead to a reduction of usable part of ingot, due to an in the amount of low-quality products amount, losses from defective ingots and other excessive production waste.

Unstable or unsatisfactory quality of steel ingots is most often associated with the transition of steel and alloys from a liquid to a solid state. This transformation is accompanied by numerous simultaneous physical and chemical processes. At this time during

ingot formation, it is possible to set the conditions for the further defects background, that cannot be eliminated in the future by plastic deformation of the metal. A large number of simultaneously interacting factors makes it difficult to manage effectively of ingot forming processes and, as a result, to produce high-quality products that will meet the highest requirements of customers.

After casting into the mold, the steel transfers its heat to the mold walls and the environment through the upper end surface of the ingot. Solidification of ingot begins around the walls of the mold. The thickness of the ingot part that has crystallized continuously increases, and a transition zone is formed between the liquid core of the ingot and the solid part of metal. Crystals and liquid metal coexist in this transition zone in the interdendritic space. The crystallization of the ingot ends near its longitudinal axis with the formation of columnar crystals. The steel solidifies in the tree-shaped form of dendritic crystals, whose size and shape depend on the solidification conditions and the chemical composition of the melt.

© Akreiev V.V. – postgraduate student, Ukrainian State University of Science and Technologies;  
Cherenkov D. – postgraduate student, Ukrainian State University of Science and Technologies;  
Prykhodko S.V. – postgraduate student, Ukrainian State University of Science and Technologies;  
Melnyk S.O. – postgraduate student, Ukrainian State University of Science and Technologies;  
Ovcharuk A.M. – Doctor of Technical Sciences, Professor, Ukrainian State University of Science and Technologies.



This is an Open Access article under the CC BY 4.0  
license <https://creativecommons.org/licenses/by/4.0/>

Conditions for directional solidification of the metal are created to eliminate shrinkage defects in ingots. This is achieved by increasing the cross-sectional area of the working cavity of the mold with height and by insulating ingot hot top.

The correct choice of design and dimensions of heat-insulating products for the ingot hot top is crucial for the most complete removal of the shrinkage cavity. This article will present design improvement of the heat-insulating insert, which allows to increase the usable part of ingot metal, reduce the percentage of hot top cut from the total mass of the ingot, reduce metal waste, and eliminate possible defects in the ingot.

**Defects and Flaws in Steel Ingots.** Defects and flaws that can be found on ingots and metal billets (blooms, slabs) are divided into groups:

1. Natural (or unavoidable) defects that occur during the cooling and crystallization of liquid steel in a casting mold (crystallizer, mould), as well as during the cooling of an ingot that has already been formed. These include shrinkage cavity, porosity, shrinkage porosity, gas bubble and non-metallic inclusions. It is impossible to completely eliminate natural defects in the ingot, but it is possible to influence the development of natural flaws, limiting them and thereby improving the quality of ingots, steel billets and rolled products [1].

2. Technological defects. They are formed as a result of imperfections or violations of the established operating conditions of steelmaking and casting. Such defects include transverse and longitudinal cracks, pours, belts, metallic and some non-metallic inclusions, subcortical and internal bubbles in steel ingots. Selection of the most rational designs of replaceable equipment (like molds, pallets, and hot tops) and compliance with metal casting technology ensure a sharp reduction of steel ingots technological defects [1].

From the point of view of defects location in the body of ingot, defects are divided into surface and internal. Surface defects are easy to detect and in most cases can be eliminated on cooled ingots and billets by cleaning. Internal defects are detected in ingots by micro- and macro- examinations.

A separate category includes rejected ingots. Ingot rejects are mostly caused by the presence of cracks,

which are divided into internal and external cracks. External cracks are divided into longitudinal and transverse cracks according to the direction of ingot axis. Hot cracks are cracks that formed on the ingot in the hot state and, accordingly, cold cracks are those that formed in the cold state of the ingot [2].

All kinds of cracks are formed during the crystallization and cooling of ingot, as well as when it is heated before rolling or during rolling (internal cracks). These stresses can be different in strength and sign depending on the shape, geometric dimensions, weight, and mode of forming, cooling, or heating of the ingot. Internal cracks called intergranular ("spider") cracks are often observed in alloy steel ingots. They are located along the ingot axis and cause delamination in the fracture. When steel that is not sufficiently refined from hydrogen is cooled, internal cracks called flocs appear [3].

Transverse cracks (Fig. 1) occur at an early stage of ingot crystallization, when the ingot does not receive free longitudinal shrinkage during solidification. Transverse cracks can form anywhere along the height of the ingot. In the upper hot top part of the ingot (Fig. 1, 1) they occur when the metal overflows and in cases where the pours were not removed before the formation of a hard crust or if the lining (patching) of the insulation was poorly performed. In the hot top part of the ingot (Fig. 1, 2) the cause of cracks is the ingot suspension due to the uneven surface of the mold or metal leakage into the gap between the mold and the hot top extension. If expanded upwards ingots are welded to the bottom or walls of the mold and there is no free longitudinal shrinkage, transverse cracks appear in the body (Fig. 1, 3) [1, 3].

The surface layers of the ingot, which cool down much faster than the inner layers, experience greater shrinkage than the inner layers. At the same time, the inner layers prevent the free contraction of the surface layers and it inevitably develop stresses, which in some places can exceed the tensile strength of the metal and lead to the formation of longitudinal cracks in any area along the height of the ingot. Such cracks are most common in ingots of circular cross-section, i.e. when the cross-section of the ingot has the smallest perimeter.

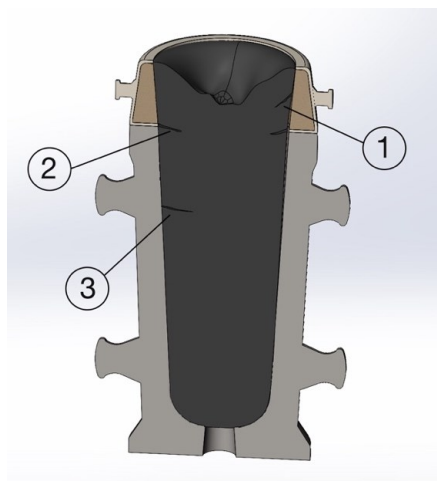


Fig. 1. Transverse cracks in a steel ingot (1 – hot top crack, 2 – "sub" hot top crack, 3 - ingot body crack).



Longitudinal cracks in ingots are formed as a result of a mismatch between the temperature of the poured steel and the speed of ingot mold filling. When the molds are filled with superheated metal at a high speed, a crust of insufficient thickness and strength is formed before the ingot leaves the mold walls, which ruptures when it cannot withstand the pressure of the liquid steel column. Pouring overheated metal at high speed leads to an increase of thermal stress during the ingot cooling process. Numerous studies and factory practice confirm that the formation of longitudinal cracks depends on the poured steel temperature and filling rate of ingot molds. Thus, ingots cast by the casting refractories method, which is characterized by low mold filling rates, always have fewer longitudinal and transverse cracks. It is possible to reduce the number of cracks on the ingots by reducing the pouring rate of overheated steel [4].

When steel is poured from above as a result of metal jet hitting the bottom of the ingot mold, and when it is poured by siphon-casting as a result of metal flowing out of the mold bottom during the initial period of its entry into the mold, metal splashes onto the inner

surface of the ingot mold, which causes the formation of films on the bottom of the ingot. A large number of splashes and droplets lead to formation of a continuous solidified crust on the bottom of the ingot. A continuous crust of the same origin, which extends almost to the entire height of the ingot, is called a "shirt". The formation of continuous pours is only possible when steel is poured from above in a loose jet, when metal splashes continuously hit the walls of the ingot mold [3, 4].

Fig. 2 shows technological defects on ingots (from left to right): films from a sharp lifting of the stopper; films from metal jet splashing; "shirt" as a result of casting the ingot without braking the jet until the end of pouring; line on the ingot and twists of the crust from a long break during pouring; films in the lower part of the ingot from a rupture of the crust during pouring of hot metal.

Fig. 3 shows ingots with surface rejects (from left to right): a bump on ingot caused by incorrect metal jet centering; overflow of a steel ingot; grooves on an ingot caused by a large crack in the casting ingot mold.

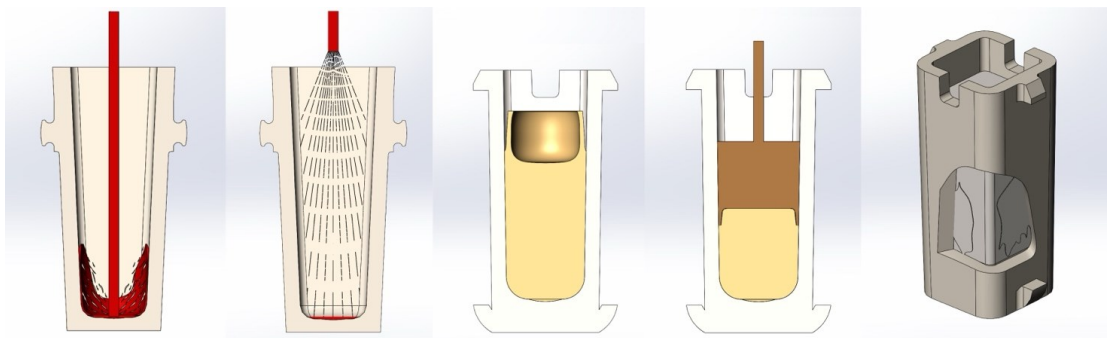


Fig. 2. Technological defects on ingots.

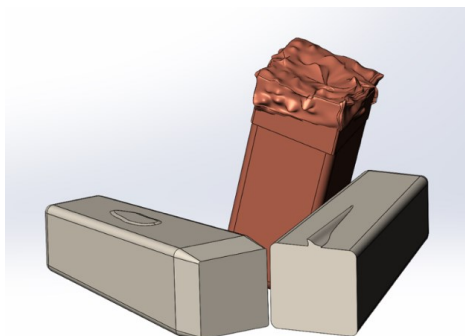


Fig. 3. Ingot surface flaw rejects.

Sulphur, nitrogen, phosphorus, hydrogen and oxygen are in a soluble state in liquid steel and released as solid non-metallic inclusions or as separate gas phases during ingot solidification. Non-metallic inclusions affect the properties of the metal and are often the cause of rejects in ingots and billets. Non-metallic inclusions are natural (endogenous) and extraneous (exogenous) [2]:

1. Endogenous non-metallic inclusions are formed as a result of oxidation and deoxidation reactions of the metal bath, changes in equilibrium constants,

decreasing in the solubility of components with decreasing temperature, and as a result of segregation processes [5, 6].

2. Exogenous inclusions enter the metal from the outside in the form of pieces of refractories, slag particles, etc. Such inclusions amount depends on the condition of the runners, ladles, siphon casting products, hot top margin and the cleanliness of the casting molds. The most effective way to reduce the amount of non-metallic inclusions in steel is to use high-quality refractories and precise adherence to technology [7].

Non-metallic inclusions are found in ingots, billets and finished products as compounds of various metals contained in steel with sulphur (sulphide), carbon (carbide), nitrogen (nitride) and oxygen (oxide). If non-metallic inclusions are located on the surface of the ingot, they are called surface inclusions or edge inclusions; if they are located at some depth in the body of the ingot, they are called internal inclusions. Non-metallic inclusions visible at low magnification, for example, through a magnifying glass, are called macroscopic; inclusions visible only at high magnification (50 times or more) are called microscopic [6].

The form of non-metallic inclusions is mainly determined by their melting point. Non-metallic inclusions with a melting point higher than the melting point of liquid steel solidify in the steel as crystals with sharp edges; these include carbides, nitrides, oxides, and sulfides. Iron oxide, iron and manganese silicates, which have melting point below the solidification point of ingot, usually appear as balls shape, spheres (globules).

Iron sulphides and oxysulphides, having a melting point lower than the melting point of steel, are located along the grain boundaries of the steel and cause a very serious defect – hot shortness. Reducing the sulphur and oxygen content in the finished steel eliminates hot shortness, and adding elements such as manganese, titanium, vanadium, aluminium, zirconium and others that have a higher affinity for sulphur and oxygen than iron to the bath at the end of the melting process helps to produce high quality steel. Non-metallic inclusions in the ingots processing by pressure are drawn in the direction of rolling into lines or strips, resulting in a fibrous structure of metal. Transverse samples of such metal have lower strength than longitudinal samples.

The strength properties of steel products often become worse when ingots contain metal inclusions. All metal inclusions are exogenous. These are either pieces of undissolved decking that have been removed from the nozzle cup and fallen into the mold, or crusts of frozen metal formed in siphon-casting refractories, or plugs and large films [7, 8].

**Metal Shrinkage, Shrinkage Cavity.** When metal is cooled from a temperature of 1600°C to temperature 600°C, it changes from a liquid to a solid state, with a volume reduction of approximately 4-6%. When liquid steel is cooled, its chemical and physical properties change and the ingot structure is formed. As the temperature of steel decreases, the solubility of many chemical elements and gases decreases, and they are released to a greater extent during crystallisation. The density of steel is temperature-dependent and decreases with temperature reduction in the liquid and solid states. As a result of its crystallization decrease in the volume of the metal leads to the formation of shrinkage cavities or pores in metal ingots, which can lead to a decrease of usable part of metal ingot.

Due to the change in ingot volume, the geometric volume of the mold will not be completely filled with metal. A cavity is formed, which is called a shrinkage cavity. This shrinkage cavity is concentrated in the thermal center of the ingot, where the very last portions of the metal solidify. In addition to the shrinkage cavity, small macro voids of shrinkage origin can form in the ingot, which are most often located along the axis (central porosity) [3].

The shape and location of the shrinkage cavity in the ingot, as well as character of central porosity and dispersed shrinkage, depend on the design of the mold and heat dissipation conditions through the mold walls. To reduce the hot top cut, the top of the ingot is often made in the shape of a truncated pyramid. In this case, the lowest heat removal from the ingot head is achieved by reducing the specific cooling surface due to the conical design of the ingot top. Additionally, the hot top part is insulated with refractory materials and insulating plates using corner elements for rectangular moulds (Fig. 4). Under these conditions, the heat centre is located in the hot top part of the ingot, which ensures that liquid metal flows down the ingot throughout the solidification period. The liquid metal fills all the shrinkage cavities, and the ingot body is formed quite densely.



Fig. 4. Rectangular mold lined with heat-insulating boards using corner elements.

Maintaining the metal in the hot top of the ingot in a liquid state is achieved by retaining the internal heat of the metal itself. If this is not enough to produce a high-quality ingot, the hot top is additionally heated. Gas burners, various types of electric heating, heat-insulating mixtures for insulating the metal surface, exothermic masses, exothermic heat-insulating plates and shells are used for this purpose.

The volume and location of the shrinkage cavity largely depends on the casting technology. As the metal temperature increases, the shrinkage cavity increases accordingly and it penetrates deeper into the ingot body. In order to reduce the length of the shrinkage cavity, hot metal is poured slowly whenever possible. All of the above measures should be carried out in an integrated manner to minimize shrinkage cavity or to weld it out during deformation. This will help to increase the usable part of metal ingot [9].

**Designs of the Ingot Hot Top and Their Disadvantages.** This article examines a method for manufacturing a thermal insulation insert that can be used in ingot casting molds with an upwardly expanded or constant cross-section of working cavity. It is suitable for

molds with a round or polygonal cross-sectional shape.

The basic principle of ingots casting in metal molds is that the hot top part should crystallize last. For this purpose, the hot top parts of the molds are equipped with thermal insulation in the form of thermal insulation inserts located on the inner surfaces of the mold end or on the inner surfaces of the hot top extensions to prevent unwanted heat exchange with the environment.

For different steel grades (alloys), depending on the purpose, ingot design and casting method (top or siphon casting), the hot top cut is generally ranges between 8 and 16% of the total ingot weight (Fig. 5). Let us consider the methods of implementation of the ingot hot top section:

Thermal insulation products for molds lining without hot tops, which partially extend beyond the mold cavity and allow partial formation of the hot top outside the mold cavity. The disadvantage of these kind thermal insulating products is highly skilled personnel need in order to perform the lining and increased risk of metal leakage from the hot top area.



Fig. 5. Hot top cut 11% of 6,5 ton ingot 1.4541 (AISI321)

2. Thermal insulation inserts used in molds with hot top extensions lined with such inserts. The use of the hot top mold extensions with these inserts, depending on the design, has several disadvantages, including:

- high cost of the hot top metal body extensions;
- increased risk of ingot cracking;
- high labor intensity for lining;
- large hot top cut of the ingot.

3. Thermal insulation inserts used in molds without hot top extensions, where the upper part is also lined with thermal insulation materials (products). The disadvantages of using such molds include:

- need for highly skilled personnel for lining works with these kind of thermal insulation inserts;
- impossibility to use the entire volume of the mold to produce a usable part of metal ingot;
- necessity to place the hot top part of ingot in the body of the mold.

4. Thermal insulation inserts, used for producing steel ingots, installed as separate elements on the

inner surface of the hot top in the mold, which has an upwardly expanded body with an internal working cavity. The hot top, mounted on the mold, consists of an outer metal body and a dense refractory lining inside. The refractory material is replaceable. The disadvantages of this type of design include:

- low usable part of ingot metal;
- increased maintenance time;
- high labor intensity.

This type of hot top is reusable, but with repeated use, the thermal insulation insert experiences significant wear and requires intermediate repairs. After several repairs, the refractory lining surface becomes distorted, making it impossible to maintain consistent dimensions of the ingot's hot top section. Additionally, the hot top has a significant weight, making installation on the mold impossible without lifting equipment.

**Problem Statement.** With a purpose of ingot casting efficiency improving, it is necessary to modify the thermal insulation insert design to achieve the following objectives:



- increase the usable part of metal ingot;
- reduce the percentage of hot top cut acc. to the total weight of the ingot, thereby minimizing metal losses;
- obtain stable dimensions of the ingot hot top section;
- simplify the lining process of the hot top in molds using thermal insulation products, reducing the risk of liquid metal leakage from the hot top;
- extend the hot top section beyond the mold cavity;
- decrease the labor intensity of the hot top manufacturing and installing;
- reduce maintenance time and overall process costs.

The task is solved by installing a heat-insulating insert on the mold body instead of the add-on to form the ingot hot top part with various options for its installation.

The proposed thermal insulation insert for the ingot hot top forming has a vertical shape with upper and lower end faces, with inner working wall and an outer wall. It is designed as a continuous structure along the perimeter. The horizontal section is shaped as an outer shoulder, corresponding to the contour of the mold's top end. The outer surface of the vertical section matches the shape of the inner surface of the upper

part of the mold, ensuring a precise fit and effective thermal insulation.

The thermal insulation insert is designed as a continuous structure along the perimeter, with the thickness of its horizontal section ranging from 10 mm to 100 mm, and the thickness of its vertical section ranging from 10 mm to 50 mm. The horizontal part of the thermal insulation insert can be made flush with the top of the vertical section or positioned at the midpoint of the vertical section.

Depending on the cross-sectional shape of the mold, the cross-section of the thermal insulation insert can be circular, rectangular, or polygonal. The vertical part of the mold thermal insulation insert may have different shapes - conical, cylindrical, or polyhedral [10].

**Universal Thermal Insulation Product for Molds without Add-ons.** The thermal insulation insert consists of a vertical part (1) and a horizontal part (2), with an inner working wall and an outer wall, both having upper and lower end faces. The horizontal part (2) is designed in the shape of external shoulders, matching the contour of the mold's end face. The vertical part has a shape that matches the upper part of the mold (Fig. 6, Fig. 7).

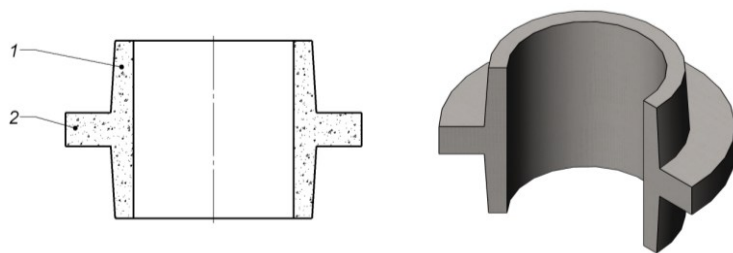


Fig. 6. Example of thermal insulation insert design for a mold with a circular cross-section.

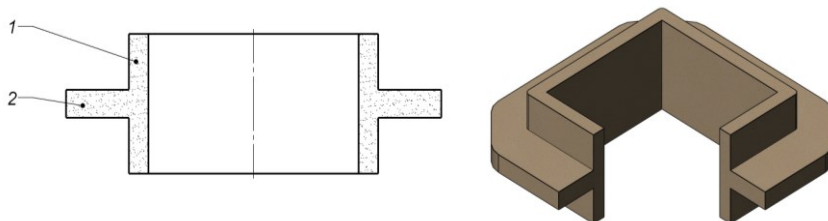


Fig. 7. Example of the thermal insulation insert design for a mold with a square cross-section.

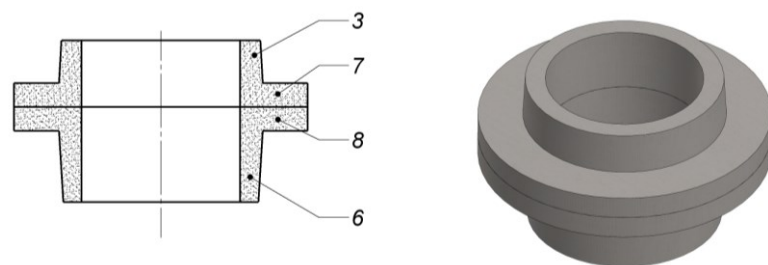


Fig. 8. An example of the proposed design of a composite thermal insulation insert.

The horizontal part of the thermal insulation insert is designed to closely match or be equal to the dimensions and shape of the upper end face of the mold, onto or into which it is installed. The thickness of the horizontal part can range from 10 mm to 100 mm.

The vertical part of the thermal insulation insert is either conical or cylindrical, and its shape and size depend on the required volume of the hot top section and

the taper of the mold cavity. The thickness of the vertical part can range from 10 mm to 50 mm.

The thermal insulation insert can be made as a single piece or composed of two elements — the lower and upper parts (Fig. 8). The insert consists of the following parts: 3 – vertical part of the upper element, 7 – horizontal part of the upper element, 8 – horizontal part of the lower element, 6 – vertical part of the lower

element. The dimensions and shape of the horizontal part of the thermal insulation insert must match or closely resemble the size of the mold upper end face in order to maximize the contact area with it. The lower and upper surfaces of the horizontal part, shaped as an external shoulder of the thermal insulation insert, are designed to be flat and even.

The overall height of the thermal insulation insert (lower and upper elements), its volume, and the shape of its internal cavity are determined based on the mass and shape of the ingot, ensuring the correct removal of the shrinkage volume into the hot top section.

The thermal insulation insert is installed into the mold cavity to a depth of 150 mm and additionally forms a hot top volume of 50 mm outside the mold cavity. For operational convenience, the thermal insulation

insert is pressed against the mold body using a weighting element (7) (Fig. 9).

The shape of the thermal insulation inserts and the ratio of the horizontal and vertical (conical) parts of the product allow them to be used both for partially forming ingot hot top section inside the mold and entirely outside the mold.

The paired use of the proposed thermal insulation inserts enables the formation of the hot top section of the ingot within the mold, with the possibility of increasing the hot top section outside the mold to the required dimensions [10].

An example of the proposed thermal insulation insert design for a mold with a circular cross-section is shown in Fig. 10, where the insulation insert is pressed against the mold body (8) using a weighting element (7).

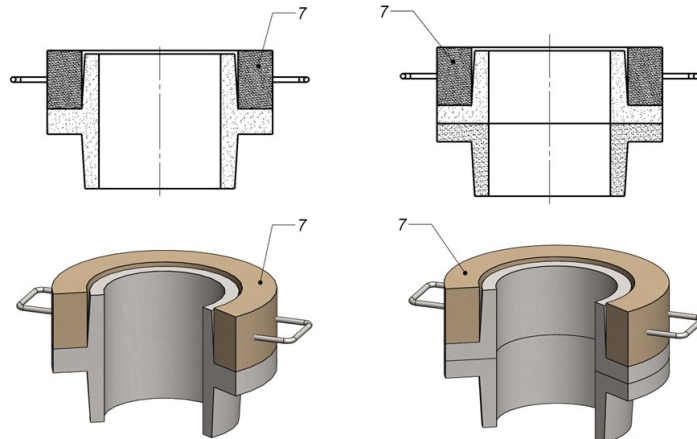


Fig. 9. Example of the weighting device installation method for a solid and assembled thermal insulation insert for a circular cross-section mold.

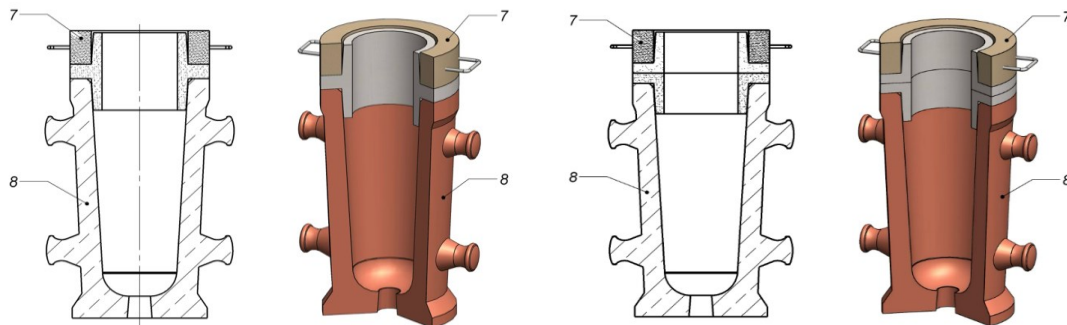


Fig. 10. Installation examples of a solid and assembled insert with a weighting element in a circular cross-section mold.

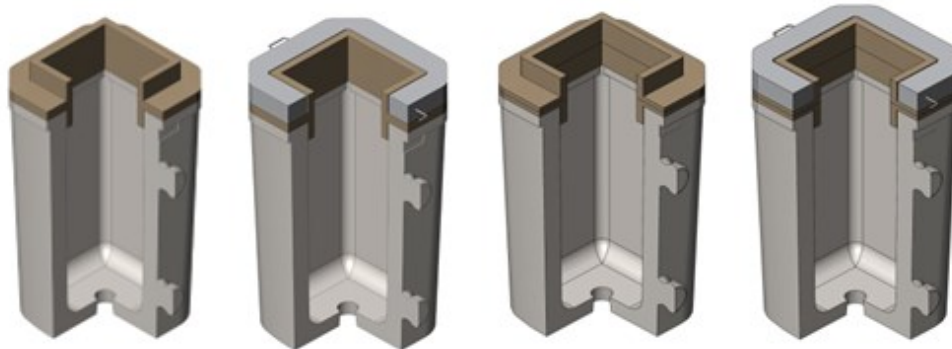


Fig. 11. Installation examples of a solid and assembled insert with a weighting element in a square cross-section mold.

Fig. 11 illustrates the same concept for a mold with a square cross-section. Similar thermal insulation inserts designs are used for rectangular and polygonal molds.

The outer surface of the lower vertical part of the thermal insulation insert follows the geometry of the inner cavity of the upper part of the mold and fits tightly against its surface. Meanwhile, the outer surface of the vertical part of the upper thermal insulation insert can have a variable shape, but must provide the required wall thickness. This design of the thermal insulation insert can be used for installation on molds with a direct taper (where the cross-sectional area of the working cavity increases upward) and a flat upper end face (without projections and slots).

The outer surface of the vertical part follows the geometry of the inner cavity of the upper part of the mold and fits tightly against its surface. The dimensions of the lower and upper vertical parts of the insert (or the vertical parts of the lower and upper components when used in pairs) are selected to extend a significant portion of the hot top section beyond the upper end face of the mold, thereby increasing the ingot body mass.

To prevent the thermal insulation insert from lifting due to the pressure of molten metal and to ensure a tight fit of the insert against the mold surface, as well as proper contact between the surfaces of the upper and lower components when used in pairs, a ring-shaped or custom-shaped weighting element of the required mass is placed on its horizontal section. Molten metal penetration from the mold is prevented by the tight adhesion of the insert to the mold surface, both within the working cavity and along the upper end face. This is achieved through the precision of geometric dimensions, the pressing of the weighting element from above and the extensive total contact area between the insert and the mold.

When using paired inserts, molten metal penetration between the lower and upper parts is prevented by the tight fit of their horizontal surfaces, which is ensured by dimensional accuracy and compression from the weighting element above [10].

The weighting element can be made of either metal or reinforced concrete. During the casting process, the weighting element is not subject of mechanical stress

and does not come into contact with the liquid metal.

When the proposed products replace heat-insulating products that are completely submerged in the working volume of the casting mold, the weight of the ingot increases due to an increase in the size of ingot usable part (with a constant weight of the hot top part), which results in:

- a) reduction of specific costs for the formation of hot top cut;
- b) reduction of specific costs related to mold operation and maintenance.

Replacing hot top extensions lined with reusable refractory materials by proposed insulating inserts allows to reduce the weight of the ingot hot top part. This is ensured by high thermal insulation properties of the product and the absence of a cooling effect on the liquid metal of the extension body.

The fit of the lower vertical part of the insulating product to the wall of the inner surface of the casting mold, combined with the pressing of horizontal part of the insert (product) against its end, minimizes to an insignificant level ingot hanging on the upper end of the mold and for this reason prevents the formation of surface cracks on the ingot.

The installation of the insulating insert and the weighting element on top of the mold is significantly simpler, faster, and more reliable than assembling refractory lining elements inside the mold cavity or hot top extension body. This enables the use less qualified personnel for mold preparation before metal casting.

The average ingot mass when filling the mold with the thermal insulation insert, following the installation scheme shown in Fig. 12, is 0,78 tn. The mass of the solidified hot top head is 67 kgs, which, when converted into percentage terms, accounts for 8,6% compared to 12% with the existing hot top extension. Due to the high thermal insulation properties of the material and the geometric dimensions of the thermal insulation insert, it may even allow for the complete elimination of the ingot's hot top cut in some forging applications [10]. According to the table, the use of a thermal insulation insert increases the usable part of ingot metal by 3% (i.e., by 30 kg per ton). This results in significant cost savings, when casting ingots from high-cost metal.



Fig. 12. Round-section mold (0,78 tn) with composite thermal insulation insert.



Table 1. Example of ingot production and usable part of ingot metal

Ingot production technology	Ingot weight, t	Weight of usable metal, t	Yield of usable metal, %
With known hot top extension	1,0	0,88	88
With improved thermal insulation insert	0,78	0,71	91

The yield of usable metal when casting an ingot with a known hot top extension is 0,88 tons (when casting 1 ton into a mold), while in the case of the developed heat-insulating insert, the yield of usable metal is 0,71 tons (when casting 0,78 tons into a mold). When converted to 1 ton of metal by using the heat-insulating insert, the savings of usable metal is 34 kg per ton in favor of the developed heat-insulating insert. Additionally, when switching to the developed heat-insulating product, there is no need to modify the equipment and change the existing production technology [10].

#### Conclusions

The proposed heat-insulating insert without extension allows combining the advantages of the lined

heat-insulating inserts technology and the technology of mold casting cavity lining with heat-insulating products, while ensuring high technical and economical performance of the ingot, its quality, and simplicity of preparatory operations. The use of improved thermal insulation insert makes it possible to:

- increase the yield of usable metal to 91% of the total ingot weight;
- reduce the hot top cut by 25% of the base value;
- reduce metal waste;
- obtain stable dimensions of the ingot hot top part;
- reduce maintenance time;
- reduce labor intensity.

#### References

1. Zaveryukha, N. V., Volkov, L. A., & Chechetkin, A. V. (1974). *Steel Casting*. Metallurgy [in Russian]
2. Yefimov V. A. (1976) *Casting and Crystallization of Steel*. Metallurgy [in Russian]
3. Dubrov N. F., Vlasov N. N., & Korrol V. V. (1975) *Steel Casting*. Metallurgy [in Russian].
4. *Steel Casting Processes and Ingot Quality: Collection of Scientific Papers*. (1989). Academy of Sciences of the Ukrainian SSR, Institute of Casting Problems, Kyiv [in Russian]
5. Shulte, Yu. A. (1964). *Non-Metallic Inclusions in EAF Steel*, Metallurgy [in Russian]
6. *Non-Metallic Inclusions and Gases in Foundry Alloys*: Proceedings of the 10th International Scientific and Technical Conference, May 12-16, 2003. Zaporizhzhia: ZNTU [in Ukrainian]
7. Levin, B. A., Salnikov, A. S., & Knokhin, V. G. (2004). *Collection of Technological Instructions for Steelmaking in an Open Arc Furnace*, PJSC "Dnipropetsstal", Zaporizhzhia [in Russian]
8. Campbell, J. (2011). *Complete Casting Handbook. Metal Casting Processes, Metallurgy, Techniques and Design*. Butterworth-Heinemann
9. Levada, A. G., Makarov, D. N., Hyakinen, V. I., & Khvastunov, V. D. (2008) Experience in Using Insulating Materials for Steel Casting by Siphon Casting Method. *Science, Technology, Production*, 6, 78-81 [in Ukrainian]
10. Akreiev V. V., Akreiev A. V., & Cherenkov D. V. (2024). Teploizoliatsiina vstavka dlia formuvannia prybutkovoi chastyny zlytka (Patent No. 157426, Ukraina), Biul. No. 42

Отримано редколегією / Received by the editorial board: 23.12.2024  
 Прийнято до друку / Accepted for publication: 20.02.2025

## Ignatiev V.S., Holovachov A.M., Kolbin M.O., Yaroshenko Ya.O., Ovcharuk A.M. Promising metal-thermal technologies for titanium production

### Ігнат'єв В.С., Головачов А.М., Колбін М.О., Ярошенко Я.О., Овчарук А.М. Перспективні металотермічні технології виробництва титану

**Abstract.** This review discusses existing and new titanium production technologies, their advantages and disadvantages. The current global production of titanium metal is based on the production of titanium sponge by reducing titanium tetrachloride with liquid magnesium and then purifying it by electric arc remelting (Kroll's metallothermic method). The Kroll method has some disadvantages: periodicity of the process, low speed, and high cost of raw materials. The paper analyzes a number of fundamentally new technological schemes for titanium production: magnetism in salt melts; magnetism in a liquefied layer of magnesium particles (TIRO process); sodium jet thermionic (Armstrong process); steam process. In the near future, we can expect a breakthrough in titanium technology that will reduce its cost.

**Key words:** titanium, titanium production, metallothermic technologies, Kroll method, magnesium reduction, TIRO process, Armstrong process.

**Анотація.** У цьому огляді обговорюються існуючі та нові технології виробництва титану, їхні переваги та недоліки. Сучасне світове виробництво титану базується на отриманні титанової губки шляхом відновлення тетрахлориду титану рідким магнієм з подальшим очищенням методом електродугової переплавки (металотермічний метод Кролла). Метод Кролла має низку недоліків: періодичність процесу, низьку швидкість та високу вартість сировини. У статті проаналізовано низку принципово нових технологічних схем виробництва титану: магнетизм у сольових розплавах; магнетизм у розрідженому шарі частинок магнію (процес TIRO); натрійтермічний струминний процес (процес Армстронга); паровий процес. У найближчому майбутньому можна очікувати прориву в технології виробництва титану, що дозволить знизити його вартість.

**Ключові слова:** титан, виробництво титану, металотермічні технології, метод Кролла, магнетизм, TIRO процес, процес Армстронга.

#### Introduction

Titanium is considered a light "new" metal that possesses a combination of unique properties: high mechanical strength, corrosion resistance, heat resistance, and low density. These properties make titanium of particular interest as a structural material in aerospace and rocket engineering, machinery, medicine, and other industries.

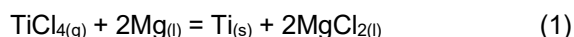
The raw materials for the metallurgical production of titanium can be ore concentrates and titanium slags containing titanium in the form of  $\text{TiO}_2$ . Direct reduction of titanium dioxide to metal is associated with significant challenges. The reason for these difficulties lies in titanium's high reactivity, even at elevated temperatures, particularly with respect to oxygen, nitrogen, and carbon. Even small amounts of these impurities lead to the formation of titanium oxides, nitrides, and carbides.

Therefore, at all stages of titanium production, it is necessary to prevent its contact with these elements. This is achieved by sealing the equipment and creating a neutral atmosphere or vacuum within it.

Today, the largest share of titanium produced worldwide is made through the reduction of titanium tetrachloride with magnesium, sodium, and calcium (metallothermic reduction).

#### Magnesiothermic process of obtaining titanium sponge (Kroll method)

The traditional and most widespread method of obtaining metallic titanium was patented by William Justin Kroll in 1940 [1]. The Kroll method involves the reduction of titanium tetrachloride ( $\text{TiCl}_4$ ) by liquid magnesium to produce titanium sponge, which is then subjected to arc remelting into ingots [1]. The overall reaction of the process is as follows:



Titanium tetrachloride is obtained by carbothermic chlorination of titanium slag. The cost of titanium sponge is 8-10 USD/kg [2]. The cost of raw materials in titanium production by the Kroll method is as follows (USD/kg): titanium slag 0.37;  $\text{TiCl}_4$  – 0.91; Mg – 1.0. The cost breakdown of individual stages in the Kroll process as a percentage of total cost is: preparation of titanium slag 4%, synthesis of  $\text{TiCl}_4$  9%, reduction of  $\text{TiCl}_4$  with magnesium 25%, remelting of sponge 12%.

The Kroll method has the following drawbacks [3]: 1) The process is batch-based, with component loading done in doses; 2) Low reaction kinetics of the magnesiothermic process; 3) The use of expensive raw materials (rutile or titanium slag) to obtain  $\text{TiCl}_4$ ; 4) The need for regeneration of magnesium and chlorine from

© Ignatiev V.S. – Candidate of Technical Sciences, Associate Professor, Ukrainian State University of Science and Technologies;  
Holovachov A.M. – Candidate of Technical Sciences, Associate Professor, Ukrainian State University of Science and Technologies;  
Kolbin M.O. – Candidate of Technical Sciences, Associate Professor, Ukrainian State University of Science and Technologies;  
Yaroshenko Ya.O. – Postgraduate student, Ukrainian State University of Science and Technologies;  
Ovcharuk A.M. – Doctor of Technical Sciences, Professor, Ukrainian State University of Science and Technologies.



This is an Open Access article under the CC BY 4.0 license <https://creativecommons.org/licenses/by/4.0/>

process products through electrolysis of molten salts; 5) To remove residual oxygen from the ingots of the obtained titanium, vacuum separation or acid leaching of the titanium sponge is required.

In Ukraine, titanium sponge and ingots produced by the Kroll method are manufactured at the Zaporizhzhya Titanium and Magnesium Plant with a capacity of 500 tons per month [4].

The drawbacks of titanium production worldwide and in Ukraine stimulate the search for new technologies for metallothermic production of pure titanium.

#### **Comparison of metallothermy and electrochemistry for titanium production**

Metallothermy of titanium is characterized by high specific productivity of the reactor and the release of a large amount of thermal energy, which serves as potential energy in the reducing metal (Mg, Na). The pure alkali and alkaline earth metals used for reduction can only be obtained through the electrochemical decomposition of their salts. Therefore, the process of obtaining titanium is complicated by the stage of regenerating the reducing metal. As a result, the total electricity consumption per unit of product for metallothermy is higher than for electrochemical processes. In this respect, metallothermy falls behind electrochemistry.

The metallothermic process is most efficiently carried out at temperatures above the melting point of titanium (1668°C). At this temperature, the reduced titanium is able to leave the reaction zone without interfering with the reduction process. At relatively low temperatures (<1000°C), titanium chloride reduction does not yield satisfactory productivity.

However, the reducing metal (Na, Mg) is in liquid form at 1000°C, and the electrolysis of their chlorides does not present significant difficulties. From this point of view, the technological scheme of metallothermy includes both the electrochemical regeneration stage of the reducing metal and the titanium reduction process itself.

The initial reagent for titanium metallothermy is always its chlorides. The reduction of titanium dioxide with an alkali metal is not possible, as they do not form stable oxide compounds and, during reduction, a solid mixture of titanium particles and alkali metal oxide is formed. Separating them is difficult, and heating this mixture to temperatures above the melting point of titanium leads to the oxidation of titanium (TiO) – at such a high temperature, titanium has an oxygen affinity comparable to calcium and magnesium.

During the reduction of chlorides, the equilibrium constant of the metallothermic reaction is very large. Reducing metals form strong salts with chlorine. Leaching these salts from titanium sponge or powder, or their vacuum distillation, can yield a sufficiently pure product. There is another argument in favor of chloride metallothermy. The intermediate product, titanium tetrachloride, is relatively easy to purify from most impurities through rare-phase reactions and distillation, so any reaction for obtaining high-purity metallic titanium or its dioxide involves the synthesis and purification of TiCl<sub>4</sub>. Additionally, reducing the chloride or its

subchlorides requires much lower energy costs than regenerating the reducing metal in the process.

#### **New metallothermic processes in titanium metallurgy**

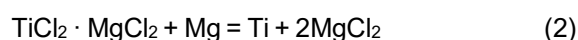
New technologies for obtaining pure metallic titanium can be divided into two groups: metallothermic and electrochemical. Metallothermic processes for titanium reduction include the following: reduction of titanium from chlorides (TiCl<sub>4</sub>) using magnesium or sodium; reduction of titanium from oxides (TiO<sub>2</sub>) using calcium. Depending on the reduction method, titanium is obtained in the form of sponge or powder, which are then used to produce compact billets by electrosmelting and powder metallurgy methods [5]. Below is a critical review of new metallothermic methods for obtaining metallic titanium.

##### **Magnesium thermite in molten salts**

A serious disadvantage of the Kroll process is the heterogeneity of the titanium reduction reaction. In the Kroll method, gaseous TiCl<sub>4</sub> interacts with the surface of molten magnesium. The strong exothermic reduction reaction is localized at the interface. The release of a large amount of heat in a relatively small volume of space leads to a disturbance in the optimal thermal regime when the reactant supply rate is high. Reducing this rate causes low reactor productivity [3].

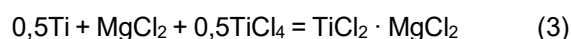
To improve the process, it is necessary to move toward homogeneity in the reduction process. This can be achieved by converting all the reactants into gas or liquid phases. In this case, there are no diffusion limitations, and the reaction takes place throughout the entire reaction volume, which allows for an even distribution of thermal load throughout the reactor and a significant increase in its productivity.

To implement this idea, the work [6] proposed magnesium thermite in a molten salt. The process is based on the reduction of a molten double salt TiCl<sub>2</sub> - MgCl<sub>2</sub> by liquid magnesium according to the reaction:



The feature of the process is that all the reactants are in the liquid phase. MgCl<sub>2</sub> acts as an inert diluent-thermostat, which protects the reaction zone from overheating during the heat release of the reaction.

TiCl<sub>2</sub> is obtained in the same reduction reactor but in a different reaction zone by passing TiCl<sub>4</sub> through titanium powder (sponge) according to the reaction:



Unlike reaction (2), in reaction (3) the initial charge mixture is heterogeneous. Reaction (3) is endothermic and does not cause local overheating. The heat of the reaction is supplied by the liquid MgCl<sub>2</sub>. The double salt is the product of the titanium sponge synthesis with the MgCl<sub>2</sub> thermostat. The titanium sponge acts as a reducer for TiCl<sub>4</sub> to TiCl<sub>2</sub> in the reaction:



Pieces of titanium sponge are placed in a basket made of corrosion-resistant steel, where they surround a tube for the supply of TiCl<sub>4</sub>. After loading a specific

amount of  $\text{MgCl}_2$ , the temperature in the reaction zone rises to 850-900°C, and  $\text{TiCl}_4$  is blown through the titanium sponge via the tube until the molar concentration of  $\text{TiCl}_2$  in the double salt melt reaches 18-24%.

Figure 1 shows a diagram of the combined reactor for the magnesium thermal reduction of  $\text{TiCl}_4$  in the salt melt  $\text{TiCl}_2 - \text{MgCl}_2$ .

The reduced titanium is obtained in the reduction reactor in the form of dispersed metal droplets, which partially combine into a sponge upon cooling. Non-consolidated titanium droplets can be continuously removed from the reactor, which is a significant advantage of the proposed method for obtaining titanium

over the traditional one.

The magnesium-thermic scheme for obtaining metallic titanium by reducing the molten double salt  $\text{TiCl}_2 - \text{MgCl}_2$ , which is mixed with liquid magnesium, has an advantage over the Kroll process – better macrokinetics of the reduction reaction, manifested in a shorter time for filling the reactor with sponge.

However, molten magnesium and its chloride do not form a homogeneous solution, which provokes metal coagulation in the salt melt into large droplets due to differences in surface tension. This leads to the formation of interfacial boundaries and a decrease in the volumetric productivity of the reactor.

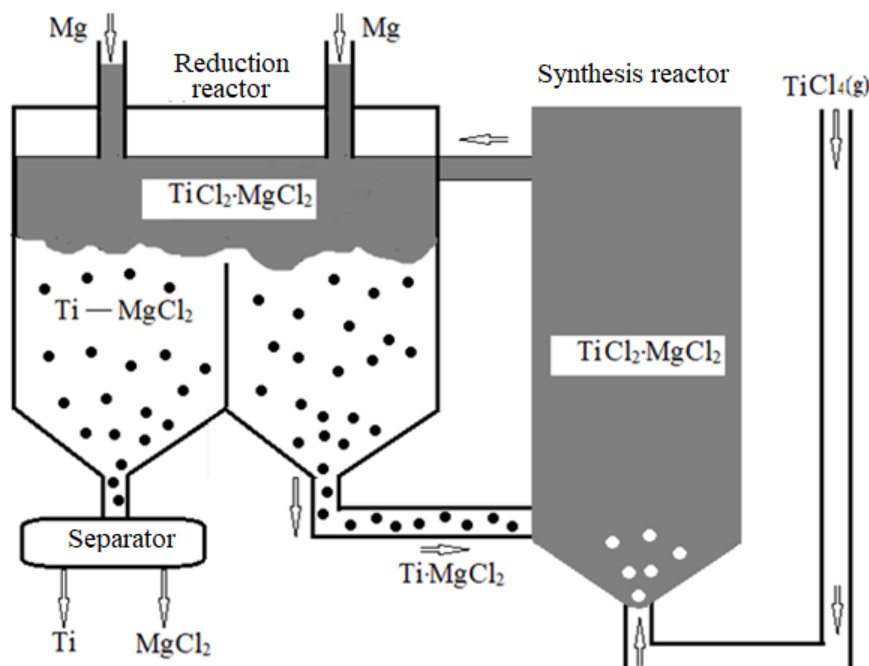


Figure 1. Diagram of the combined reactor for magnesium-thermic reduction of  $\text{TiCl}_4$  in the molten salt mixture  $\text{TiCl}_2 - \text{MgCl}_2$ .

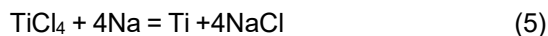
#### Magnesiothermal reduction in a fluidized bed of magnesium particles (TIRO process)

A new method for obtaining titanium has been developed in Australia with the aim of halving the cost of titanium products, known as the TIRO process [7]. This is proposed to be done in two ways: 1) replacing the periodic Kroll method with continuous reduction of titanium tetrachloride in a fluidized bed of magnesium particles; 2) producing titanium powder directly, bypassing several expensive stages in the traditional titanium production technology.

The TIRO process includes two stages: 1) in a reactor with a pseudofluidized bed,  $\text{TiCl}_4$  interacts with magnesium powder, forming solid magnesium chloride particles approximately 350  $\mu\text{m}$  in diameter, in which micron-sized titanium particles are dispersed; 2) titanium is extracted in the form of needles from the  $\text{MgCl}_2$  granules. Figure 2 shows the product of the process as titanium needles mixed with  $\text{MgCl}_2$  granules. The resulting titanium crystals can be given any shape, including needle-like, which is optimal for producing titanium rolling products. The features of the reactor's design and operating conditions are outlined in the work.

#### Jet sodium thermic (Armstrong process)

The Armstrong process is jet sodium thermic, where a continuous process of reduction of gaseous  $\text{TiCl}_4$  by liquid sodium takes place, followed by leaching of sodium chloride ( $\text{NaCl}$ ) that forms, from the titanium powder by the reaction:



The technological diagram of the Armstrong process is shown in Figure 3 [8].

Liquid sodium flows through the chamber.  $\text{TiCl}_4$  vapors are injected into the sodium through a nozzle. The reduction reaction begins immediately after the nozzle. The resulting titanium powder is carried out of the chamber by the liquid sodium. The  $\text{NaCl}$  salt is separated from the titanium by aqueous leaching. The initial reduction of several metal chlorides allows the production of almost any required alloy. The titanium powders and its alloys obtained in the Armstrong process are subjected to hot vacuum pressing and wave rolling to produce large sheets. The cost of titanium powder is 5-10 times lower than the cost of powder obtained by the Kroll process.



Figure 2. Product of the TIRO process – titanium needles in a mixture with  $\text{MgCl}_2$  granules.

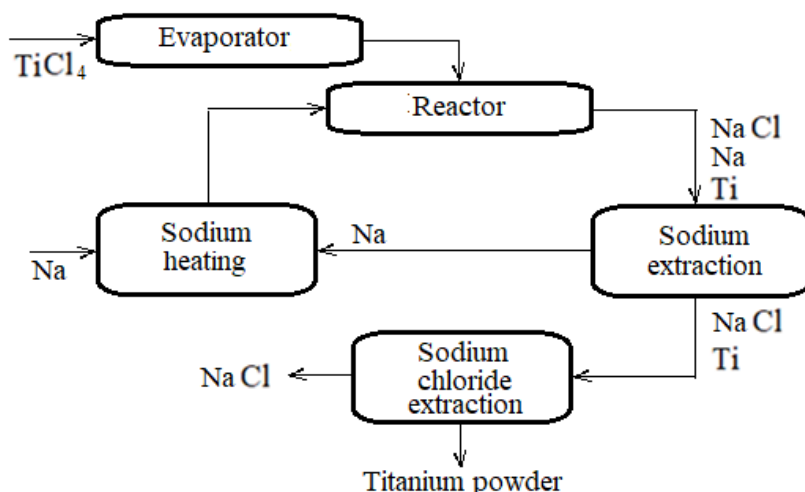


Figure 3. Diagram of the Armstrong process for obtaining titanium powder.

The products of the process – Ti, Na, NaCl are separated by filtration, distillation, and washing. A disadvantage of the Armstrong process is the use of expensive liquid sodium. Returning sodium and chlorine to the technological process requires the use of NaCl electrolysis in a melt and demands high energy costs and complex equipment design.

#### Vapor-phase process of titanium production

The goal of the vapor-phase process is the continuous production of titanium powder in the gas phase using magnesium or sodium vapor. Titanium tetrachloride and the metal reducer interact in the gas phase at high speed at  $850^\circ\text{C}$ .

The separation of the produced powder from  $\text{MgCl}_2$  is accompanied by significant difficulties, and the solution in titanium has an unacceptably high level of impurities – oxygen. This is because, at the specified temperature, magnesium chloride has a low vapor pressure, condenses on the surface of the forming titanium particles, and prevents their further growth. Due to the high dispersion of the powder, the salt process is used for sodium thermite. The molten salt serves as an inert ballast medium.

Ballasting the reaction mixture ( $\text{TiCl}_4 + \text{Na}$ ) with salt allows for better control of the reduction reaction. During mixing, the reagents in the solution are homogenized. In this process, the growth of titanium particles is not hindered as long as they remain within the reaction zone. Intensive mixing prevents small particles from falling out of the reactive zone and allows only large particles to be removed.

#### Conclusions and recommendations

The current global production of metallic titanium is based on the production of titanium sponge using the Kroll method. The process consists of the metal-thermic reduction of titanium tetrachloride with liquid magnesium, followed by purification of the resulting titanium sponge through electric arc remelting.

The Kroll method has the following disadvantages:

The process is periodic with a dosed loading of components;

Low reaction kinetics of magnesium thermite;

The use of expensive rutile or titanium slag to obtain  $\text{TiCl}_4$ ;

The need to regenerate magnesium and chlorine from the process products through the electrolysis of molten salts;

Vacuum separation or acid leaching of the titanium sponge is required to remove residual oxygen in the titanium ingots.

New metal-thermic titanium production processes include magnesium thermite in molten salts, magnesium thermite in a fluidized bed of magnesium particles, and jet sodium thermite.

Magnesium thermite in molten salts is proposed for obtaining metallic titanium by reducing a double salt melt of  $\text{TiCl}_2 - \text{MgCl}_2$  with liquid magnesium. Unlike the Kroll process, where  $\text{TiCl}_4$  vapor is introduced to the surface of liquid magnesium, in the proposed process, all reactants are in the liquid phase.

$\text{MgCl}_2$  acts as an inert diluent, protecting the reaction zone from overheating.  $\text{TiCl}_2$  is obtained by



passing  $\text{TiCl}_4$  through titanium powder (sponge) until the molar concentration of  $\text{TiCl}_4$  in the double salt melt reaches 18–24%. This reaction is endothermic.

The steel reduction reactor can be used in two variants: the double salt is introduced into the molten magnesium, and magnesium granules are introduced into the slurry melt. Titanium sponge forms in about 30 minutes, filling the reactor. Unbound titanium particles can be continuously removed from the reactor.

Magnesium thermite in a fluidized bed of magnesium particles (TIRO process) produces titanium embedded in  $\text{MgCl}_2$  granules. This eliminates the formation of titanium sponge. The resulting titanium

crystals can be given any shape, including needle-like, which is optimal for titanium rolling.

The Armstrong process is a jet sodium thermite process, where continuous reduction of gaseous titanium tetrachloride ( $\text{TiCl}_4$ ) with liquid sodium takes place, followed by leaching of the formed sodium chloride from the titanium powder.

The vapor (salt) process is sodium-thermic, where a salt melt ( $\text{TiCl}_4 + \text{Na}$ ) is used as an inert ballast medium, allowing better control of the reduction reaction. Intensive mixing removes only large particles from the melt.

### References

1. Kroll, W. J. (1940). The production of ductile titanium. *Trans. Am. Electrochem. Soc.*, 78, 35–47
2. *Analiz rynku tytanovoi hubky ta prohnoz na maibutnie*. Website ua.hstmetal.com. <https://ua.hstmetal.com/news/titanium-sponge-market-analysis-and-future-for-75833904.html>.
3. Zelikman, A. N. (1986). *Metallurgy of refractory rare metals*. Metallurgy
4. Proydak, Yu. S., Ignatyev, V. S., Pidgorny, S. M., & Holovachov, A. M. (2023). *Metallurgy of color metals*. PBP "Economy"
5. Parfenov, O. G., & Pashkov, G. P. (2008). *Problems of modern titanium metallurgy*. Publishing house SO RAN
6. Akio, F., & Satoru, T. (2005). Producing titanium by reducing  $\text{TiCl}_2 - \text{MgCl}_2$  mixed salt with magnesium in the molten state. *Ibid.*, 57(10), 56–60
7. Doblin, C., Freeman, D., & Richards, M. (2013). The TiRO™ Process for the Continuous Direct Production of Titanium Powder. In *Key Engineering Materials* (Vol. 551, pp. 37–43). Trans Tech Publications, Ltd. <https://doi.org/10.4028/www.scientific.net/kem.551.37>
8. Matsanga N, Wa Kalenga M, Nheta W. An Overview of Thermochemical Reduction Processes for Titanium Production. *Minerals*. 2025; 15(1):17. <https://doi.org/10.3390/min15010017>

Отримано редколегією / Received by the editorial board: 05.12.2024

Прийнято до друку / Accepted for publication: 20.02.2025

*Starovoi A.G., Maliy Ye.I., Sorokin Ye.L., Starovoi M.A., Popova O.Yu.*  
**Adjusting properties of electrode pitch with fractions of coal tar**

*Старовойт А.Г., Малий Є.І., Сорокін Є.Л., Старовойт М.А., Попова О.Ю.*  
**Регулювання властивостей електродного пеку фракціями кам'яновугільної смоли**

**Abstract.** The paper presents the investigation results of the organic mass modification of the impregnating pitch of coal tar with low pyrolysis degree. The processes that form the pitch operational properties in the impregnation technology of graphitized electrodes were studied. Specific features of the modifying additive effect on the quality characteristics of the pitch and its group composition were established. Such technological approach makes it possible to intensify the impregnation process of blanks for graphitized electrodes.

**Key words:** impregnating pitch phenolic fraction, modification, group composition, low-pyrolyzed coal tar.

**Анонція.** У роботі представлено результати дослідження модифікації органічної маси імпрегнующого пеку кам'яновугільної смоли низького ступеня піролізу. Вивчено процеси, що формують експлуатаційні властивості пеку в технології імпрегнування графітованих електродів. Встановлено специфічні особливості впливу модифікуючої добавки на якісні характеристики пеку та його груповий склад. Такий технологічний підхід дає змогу інтенсифікувати процес імпрегнування заготовок для графітованих електродів.

**Ключові слова:** імпрегнующий пек, фенольна фракція, модифікація, груповий склад, низькопіролізна кам'яновугільна смола.

## 1. Introduction

The graphitized electrodes are carbonaceous current-carrying elements for electric arc furnaces. The production of dense electrodes significantly improves their operational conditions and increases the technical and economic parameters of the process. The impregnation of electrode products with organic substances essentially affects the reduction of the total porosity and the redistribution of the pore volume according to their equivalent radii.

The processes occurring at the boundary of the solid and liquid phases play an important role in the impregnation process of graphitized electrodes. It has been established [1] that the impregnation volumetric rate, calculated according to Darcy's law, is inversely proportional to the viscosity of the impregnating pitch. The correctness of the macrokinetic impregnation model chosen by the authors was confirmed by experiments [2].

The theory of the impregnating pitch (impregnate) motion in porous media due to capillary absorption is rather widely discussed in the literature [3, 4]. In this connection the purpose of the research was to improve the performance characteristics of the impregnating pitch using a phenolic fraction of low-pyrolyzed coal tar.

The values of fluidity and viscosity of the pitch are directly proportional to the temperature and group composition, and even a small difference in the

fractions ratio leads to the significant changes in the impregnate penetration into the pores of the graphitized billet [5].

One of the most important parameters of impregnating pitch properties is  $\alpha_1$ -fraction (substances insoluble in quinoline), which affects the rheological properties of the system, and, consequently, its applicability to be an impregnate. Moreover, a significant content of substances insoluble in quinoline (~6 %) causes adsorption of some high-molecular components of the pitch on the billet surface in the form of 1-5 mm layer [6]. This explains the severe restrictions relative to the "mass fraction of insoluble substances in toluene", which are claimed by consumers to the impregnating pitch. The analysis of publications allows to establish general trends and ranges of individual quality indicators of impregnate used for carbonaceous materials impregnation (Table 1).

So for all the variety of quality indicators of impregnating materials, the main one is the low content of substances insoluble in quinoline (2-4 wt %).

A special electrode pitch- impregnate is not produced in Ukraine as a marketable product due to the lack of appropriate technologies. In this regard, it is very important to develop technological methods of high-quality impregnating pitch production, taking into account the instability of the raw materials quality.

The phenolic fraction of the coal tar was used as a modifying additive due to the significant amount of

© Starovoi A.G. – Doctor of Technical Sciences, Professor, Ukrainian State University of Science and Technologies;  
Maliy E.I. – Doctor of Technical Sciences, Professor, Ukrainian State University of Science and Technologies;  
Sorokin E.L. – Doctor of Technical Sciences, Professor, Ukrainian State University of Science and Technologies;  
Starovoi M.A. – Candidate of Technical Sciences, Associate Professor, Ukrainian State University of Science and Technologies;  
Popova O.Yu. – Head of laboratory, Ukrainian State University of Science and Technologies



This is an Open Access article under the CC BY 4.0 license <https://creativecommons.org/licenses/by/4.0/>

phenols, which take part in the formation of complex molecular complexes - azeotropic compounds. A molecular azeotropic complex is a mixture of two or more liquids the composition of which does not change while boiling. It is a good plasticizer which cannot be separated by thermal fractionation.

## 2. Experimental

Impregnating pitch with 4 wt % of insoluble in quinoline compounds was used as an initial raw material (Table 2).

Peck was heat-treated at 403-413 K, and then the phenolic fraction of coal tar preheated to 333 K (Table 3) was added; after stirring for 30-40 min the mixture was cooled to 293 K.

When choosing the additive to the initial pitch, its operational characteristics, namely the softening temperature ( $T_{soft}$ ) and flash point ( $T_f$ ) were taken into account. The assessment was carried out in accordance with the requirements of PJSC "Ukrainian Graphite". The obtained results were processed by the simplex-lattice planing method [7].

The following stages were used to prepare electrode billets:

Preparation of charge (composition, wt %): calcined petroleum coke 50; calcined oil shale coke 27-30; needle coke 13-20.

Mixing of cokes with a binder pitch: a preheated mixture of cokes is mixed with a pitch melt in a mixer at 393-413 K.

Billets pressing: the blank is pressed through the die carrier and cut at the necessary length.

Billets baking: in a furnace at 1523-1723 K.

Impregnation of billets: in an autoclave for 4-5 h at the temperature of  $473 \pm 10$  K.

Baking of impregnated billets.

Graphitization at 2273-2773 K.

A specific electrical resistivity, bulk density, coefficient of thermal expansion, modulus of elasticity and mechanical tensile strength were determined for the obtained samples according to the standard procedures.

Table 1. Characteristics of industrial indices of impregnating pitch

Raw material	Softening temperature ( $T_{soft}$ ), K	Ignition temperature ( $T_{ign}$ ), K	The content of substances insoluble in		Technical indicators, %			Viscosity		Cok yield, %
			toluene, wt %	quinoline, wt %	ash content	volatiles yield	sulphur content	dynamic, mPas	specific	
Impregnating pitch	333-338	$\leq 483$	$\geq 17$	$\leq 4.0$	$\leq 0.3$	$\leq 68$	$\leq 0.5$	$\leq 150$	$\leq 50$	$\geq 50$

Table 2. Characteristics of the initial coal tar pitch for impregnation

Indicators	Values
Softening temperature, K	338
Volatiles yield, %	64
Ash content, %	0.3
Mass fraction of substances insoluble in:	
toluene, wt %	24
quinoline, wt %	4

Table 3. Composition of two samples of phenolic fraction of low-pyrolyzed coal tar

Fraction composition	Mass fraction, wt %	
Phenol	21.9	22.1
<i>o</i> -Cresol	8.6	8.8
<i>m</i> -Cresol	11.0	12.0
<i>p</i> -Cresol	7.7	8.0
<i>o</i> -Ethylphenol	0.4	0.7
2,5-Xylenol	2.8	3.0
2,4-Xylenol, 3,5-Xylenol, 3-Ethylphenol	11.0	11.2
2,6-Xylenol	3.0	2.5
2,3-Xylenol	0.9	0.9
2,3,5-; 2,4,5-; 2,4,6-Trimethylphenols	1.5	1.7
$\alpha$ -Naphthol	1.0	0.9
$\beta$ -Naphthol	0.5	1.0
Unidentified	29.7	27.1

### 3. Results and Discussion

The components content (wt %) in the mixtures was varied: pitch - from 94 to 98, FF (phenolic fraction of low-pyrolyzed coal tar) - from 2 to 6 and F (phenol) - the rest. The artificial variables were introduced, as shown in Table 4.

$$Y(T_{\text{soft}}) = 113.33X_1 + 113.33X_2 + 73.5 - 36X_1X_2 - 24.33X_1X_3 + 1.33X_2X_3 \quad (1)$$

$$Y(T_f) = 214.33X_1 + 211.33X_2 + 203.5 - 6X_1X_2 - 0.66X_1X_3 + 8X_2X_3 \quad (2)$$

Based on the obtained models, it can be expected that the phenolic fraction in the amount of 2-6 %, reduces the softening temperature of the impregnating pitch but does not change its flash point. However, with an increase of the additive content in the impregnate up to 8 % or higher we observed significant changes. The process is accompanied by low-molecular, light-boiling components which action can be considered as a positive one until the conditions for the fractions thermochemical transformations are created in the pitch.

The matrix of the simplex-lattice plan of the second order is shown in Table 5. The matrix contains the code values of pseudofactors  $X_1$ ,  $X_2$  and  $X_3$ .

After the implementation of the plan (Figs. 1 and 2), the following polynomial relationships were established:

The analysis of the obtained modified impregnating pitch showed (Table 6) that the contents of ash, sulfur and moisture of the pitch do not actually change and stay at the required level. After the pitch treatment with 4 and 6 wt % of phenolic fraction the mass fraction of substances insoluble in toluene was 22 and 21 wt %, respectively, and the mass fraction of substances insoluble in quinoline - 3.0 and 2.5 wt %, respectively. The amount of coke residues from the impregnating pitch and the modified one remained virtually unchanged.

Table 4. Pseudocomponents of the system.

Pseudofactors	Content of components in the mixtures, wt %		
	Pitch	FF	F
$X_1$	94	6	0
$X_2$	98	2	0
$X_3$	94	4	2

Table 5. Conditions and results of the experiments.

Design matrix			Softening temperature ( $T_{\text{soft}}$ ), K			Flash point ( $T_f$ ), K		
$X_1$	$X_2$	$X_3$	$T_{\text{soft}1}$	$T_{\text{soft}2}$	$T_{\text{soft}3}$	$T_{f1}$	$T_{f2}$	$T_{f3}$
1	0	0	336	336	335	488	487	487
0	1	0	338	338	337	485	483	485
0	0	1	326	327	328	473	478	478
0.5	0.5	0	337	337	336	485	483	485
0.5	0	0.5	330	332	333	482	483	480
0	0.5	0.5	331	332	333	483	482	482
1/3	1/3	1/3	334	334	333	481	483	481

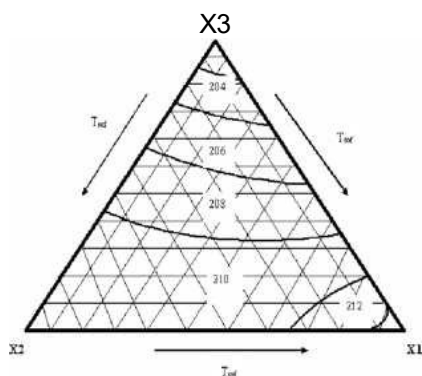


Fig. 1. Mathematical model of the impregnating pitch flash point dependence on FF mass fraction.

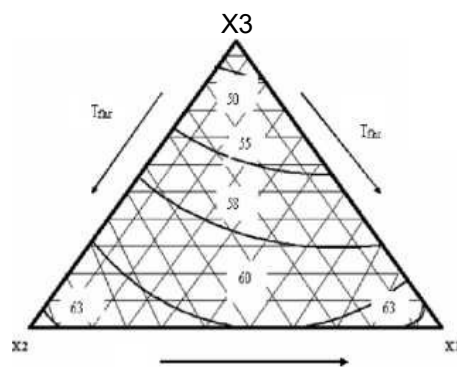


Fig. 2. Mathematical model of the of the impregnating pitch softening temperature dependence on the FF mass fraction.

Table 6. Impregnate quality indices.

Raw material	Coke residue, wt %	Dynamic viscosity at 433 K (Brookfield method), mPas	Technical indices, %			Content of substances insoluble in	
			ash content	volatiles yield	sulphur content	toluene, wt %	quinoline, wt %
Impregnating pitch	53	108	0.1	65	0.5	24	4.0
Impregnating pitch + 4 wt % of phenolic fraction	52	65	0.1	65	0.5	22	3.0
Impregnating pitch + 6 wt % of phenolic fraction	52	60	0.1	66	0.5	21	2.5



Fig. 3. Photos of two electrode billets with a diameter of 400 mm impregnated with a modified pitch.

Table 7. Physico-chemical properties of electrode billets with a diameter of 400 mm impregnated with a modified pitch.

Electrode billets	Indices				
	Modulus of elasticity, MPa	Coefficient of thermal expansion, K <sup>-1</sup>	Bulk density, g/cm <sup>3</sup>	Specific electrical resistance, Ohmm <sup>2</sup> /m	Mechanical tensile strength, MPa
Initial	65	$3.2 \cdot 10^{-63}$	1560	8.0	4.7
Investigated	66	$3.0 \cdot 10^{-6}$	1600	7.5	5.0

To clarify the change in the fractional composition of the impregnating pitch, we additionally estimate the  $\gamma$ -fraction of the impregnate, which was 37.7 wt % in the initial pitch; 39.0 wt % in the pitch modified with 4 wt % of FF and 40.5 wt % in the pitch modified with 6 wt % of FF. The given and previously obtained data [8] reveal that during modification the phenolic fraction plays the role of an auto-plasticizer. It means that the process is accompanied by the formation of azeotropic complex compounds providing a plastic and highly elastic state the impregnating pitch. This, in turn, promotes a better penetration of the pitch into the billet pores (Fig. 3).

Due to the use of phenolic fraction of low-pyrolyzed coal tar as a modifier, redistribution of the group components of the modified pitch occurs (Table 6), which contributes to a change in the physico-chemical properties of the obtained billets (Table 7). During impregnation with a modified pitch, its sticking on the billet surface was not observed (Fig. 3). Also, due to this technological approach, there is the possibility of repeated

application of pitch without significant impairment of the impregnation process, which reduces its consumption during the research.

#### 4. Conclusions

Using the phenolic fraction of the low-pyrolyzed coal tar, the dispersion of  $\alpha_1$ -fractions changes, the share of the substances that are insoluble in quinoline and the pitch viscosity decreases, which is in agreement with the literature data. After the destruction of the pitch structure, the mass fractions of  $\gamma$ - and  $\alpha$ -fractions have the predominant influence. Thus, the phenolic fraction of coal tar can be used in industrial conditions as a modifier of the electrode pitch-impregnate during its production. The autoplacticization process takes place with the formation of azeotropic complex compounds, which promote the impregnating pitch to be in a plastic and highly elastic state. This, in turn, improves the pitch penetration into the billet pores and facilitates the repeated application of the pitch as the impregnate without a significant impairment of the impregnation process.

#### References

1. Chemerinskii, M. (2013). Influence of thermally prepared G coal in compacted batch on coke strength. *Coke and Chemistry*, 56, 16-19. <https://doi.org/10.3103/S1068364X1301002X>
2. Malyi, E. I., Chemerinskii, M. S., Holub, I. V., Starovoyt, M. A., & Shmalko, V. M. (2018) Influence of Microwave Radiation on the Pyrogenetic Transformation of Coal Grains. *Coke and Chemistry*, 61, 87-90. <https://doi.org/10.3103/S1068364X18030055>
3. Starovoyt, A. G., Malyi, E. I., Chemerinskii, M. S., Starovoyt, M. A., Krivonos, V. V., Danilov, A. B., & Solov'ev, M. A. (2013). Modified coal batch in coking. *Coke and Chemistry*, 56, 157-160. <https://doi.org/10.3103/S1068364X13050086>
4. Malyi, E. I. (2014). Modification of poorly clinkering coal for use in coking. *Coke and Chemistry*, 57, 87-90. <https://doi.org/10.3103/S1068364X14030028>
5. Malyi, E. I. (2018). Modification of Electrode Pitch. *Coke and Chemistry*, 61, 262-265. <https://doi.org/10.3103/S1068364X18070050>
6. Malyi, E., Chemerinskii, M., Holub, I., & Starovoyt, M. (2018). Chem. Chem. Technol., 12, 533. <https://doi.org/10.23939/chcht12.04.533>
7. Malyi, E., Chemerinskii, M., Holub, I., & Starovoyt, M. (2017). *Coke and Chemistry*, 60, 37. <https://doi.org/10.3103/S1068364X17010069>
8. Starovoyt, A., Chemerinskii, M., & Malyi, E. (2014). Chem. Chem. Technol., 8, 475. <https://doi.org/10.23939/chcht08.04.475>

Отримано редколегією / Received by the editorial board: 02.12.2024

Прийнято до друку / Accepted for publication: 20.02.2025



Danchenko V.M., Dobrov I.V., Semichev A.V.

**Roll drive mechanism with planetary gearbox for cold pilger pipe rolling mills**

Данченко В.М., Добров І.В., Сьомічев А.В.

**Механізм приводу валків з планетарним редуктором для трубопрокатних станів холодної пілігрової прокатки труб**

**Abstract. Purpose.** Creation and study of a roll drive mechanism with a planetary gearbox, which will ensure a reduction in axial forces in the production of thin-walled pipes and it will expand the range of pipes obtained on cold pilger rolling mills. **Methodology.** The work includes research on determining the parameters of the roll drive of cold pilger rolling mills using the graph-analytical method of studying the kinematics of mechanisms. **Results.** The roll drive mechanism with a planetary gearbox will ensure regulation of the angular speed of rotation of the rolls and a reduction in axial forces. **Scientific novelty.** The influence of the geometric parameters of the roll drive on the value of the angular speed of the rolls, which ensure a reduction in axial forces, has been determined. **Practical significance.** The roll drive mechanism with a planetary gearbox allows obtaining high-quality thin-walled pipes with the possibility of expanding the range.

**Keywords:** roll drive, planetary gearbox, cold pilger rolling, axial forces, thin-walled pipes.

**Анотація. Мета.** Створення та дослідження механізму приводу валків з планетарним редуктором, який забезпечить зменшення осьових зусиль при виробництві тонкостінних труб та розширить сортамент труб, що отримуються на станах холодної пілігрової прокатки. **Методологія.** Робота включає дослідження з визначення параметрів приводу валків станів холодної пілігрової прокатки труб з використанням графоаналітичного методу дослідження кінематики механізмів. **Результати.** Механізм приводу валків з планетарним редуктором забезпечить регулювання кутової швидкості обертання валків та зменшення осьових зусиль. **Наукова новизна.** Визначено вплив геометричних параметрів приводу валків на величину кутової швидкості валків, що забезпечують зменшення осьових зусиль. **Практичне значення.** Механізм приводу валків з планетарним редуктором дозволяє отримувати високоякісні тонкостінні труби з можливістю розширення сортаменту. **Ключові слова:** привід валків, планетарний редуктор, холодна пілігрова прокатка, осьові зусилля, тонкостінні труби.

**Introduction.** The use of various methods and technologies for metal processing using plastic deformation has ensured the production of a wide range of metal products.

At the present stage of development of production technology of thin-walled long metal products are in greatest demand, in particular thin-walled and especially thin-walled pipes. Thin-walled cold-deformed long pipes are the basis for further technical progress.

Analysis of published data and problem statement. The existing mechanism for driving rolls on cold pilger rolling mills leads to the appearance of axial forces, which is the cause of corrugations and other defects. When rolling thin-walled pipes, these defects are more significant. Obtaining high-quality thin-walled pipes is impossible without reducing the magnitude of axial forces [1-2].

To reduce axial forces, it is proposed to use replaceable parts for each rolling route. Adjusting the angular speed of rotation of the rolls will allow for each range of pipes to ensure compliance between the forced rolling radius and the natural one [1-5].

The purpose of the development is to create and study a mechanism for driving rolls with a planetary

gearbox, which will ensure a reduction in axial forces in the production of thin-walled pipes and expand the range of pipes produced on cold pilger rolling mills.

**Materials and methods.** A mechanism for driving rolls of cold pilger rolling mills with a planetary gearbox is proposed. The kinematic diagram of this roll drive is shown in Fig.1.

Wheel 10 is driven by an electric motor. Wheel 8, which is engaged with wheel 10, rotates. Wheel 7 drives connecting rod 5, which is fixed to the roller. The electric motor for driving the working stand rotates crank 2.

To determine the number of degrees of mobility of the mechanism, a structural diagram was constructed (Fig. 2). The structural diagram indicates the links of the mechanism consisting of the working stand mechanism and the roller drive. Crank 1 and wheel 10 are driving, therefore they are indicated by solid lines. Other links have the form of various geometric figures with corners in the form of a circle. For example, a stationary frame contains four vertices. The first circle (from left to right) means the connection of the frame with the gear wheel 10 using a rotational kinematic pair of the first kind (fifth class), the second - the connection



with the carrier 9 using a kinematic pair of the fifth class, the third - with the gear wheel 7 (pair of the 5th class), the fourth - the connection with the working stand 4 (pair of the 5th class), the fifth - the connection with the crank of the roller drive 2. The class of the pair indicates the number of connection conditions that are determined by it. That is, a pair of the fifth class provides one degree of mobility. The working cage 4 contains four vertices. The first circle (from left to right) connects the working cage with the connecting rod 5, the second - connects with the roller 6, the third - connects with the fixed frame 1, the fourth - with the connecting rod 3. All kinematic pairs that connect the working cage with other links are of the fifth class and provide one degree of mobility. The crank 2 is connected by means of kinematic pairs of the fifth class with the fixed frame 1 and the connecting rod 3. The connecting rod 5 is connected by only two kinematic pairs of the fifth class with the working cage 4, the wheel 7 and by

means of a kinematic pair of the fourth class with the roller (one link with a gear wheel) 6.

On the upper and lower rollers there are synchronizing gears. The lower roller forms one link with the synchronizing gear (the link is designated by the number 6 and conventionally called the roller). The upper roller forms one link with the synchronizing gear and the connecting rod (the link is shown by the number 5 and it is called the connecting rod). The roller 6 and the working stand 4 are interconnected by a kinematic pair of the fifth class. The wheel 10 is connected to the frame using a kinematic pair of the fifth class, and to the wheel 8 using a gear pair of the fourth class. The wheel 8 is connected to the carrier 5 using a kinematic pair of the fifth class, and to the wheel 7 using a pair of the fourth class. The wheel 7 is connected to the frame using a kinematic pair of the fifth class, and to the wheel 8 using a pair of the fourth class.

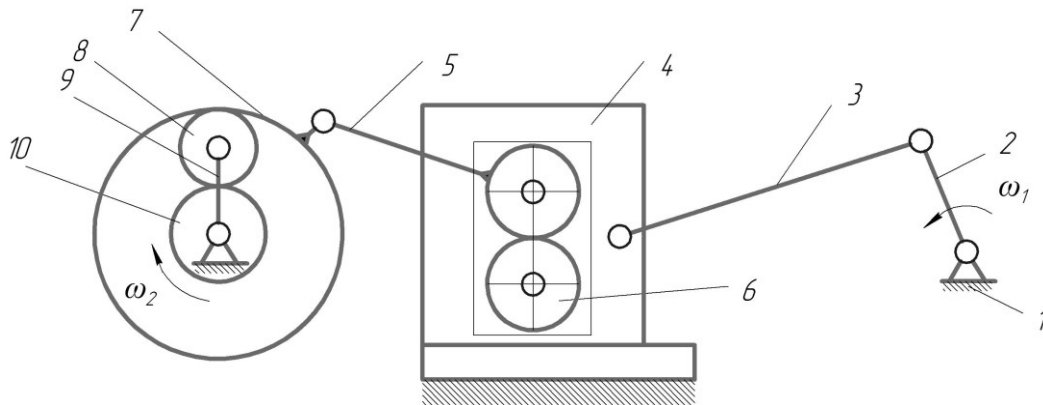


Fig. 1. Roller drive mechanism with planetary gearbox: 1 - fixed frame; 2 - crank drive of the working stand; 3 - connecting rod; 4 - working stand; 5 - connecting rod, upper roller, gear wheel (one link); 6 - roller; 7, 8, 10 - gears; 9 - carrier.

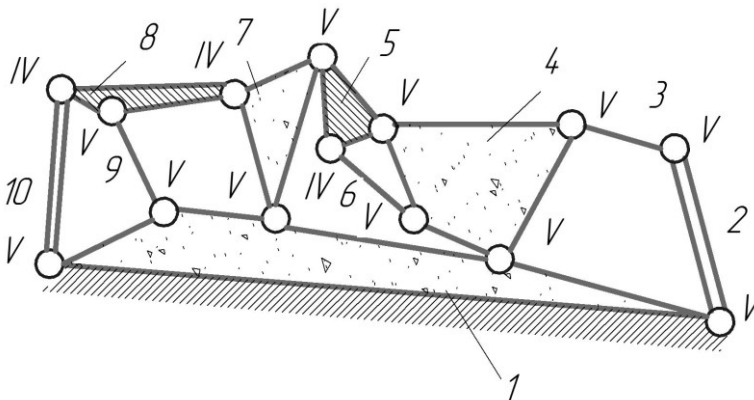


Fig. 2. Structural diagram of the roller drive mechanism with planetary gearbox.

Using the structural diagram, the number of kinematic pairs and their class, as well as the number of links, were obtained. The number of degrees of

mobility of the mechanism (consists of the working stand drive mechanism and the roll drive mechanism) [1]:

$$W = 3(n - 1) - 2p_1 - p_2 = 3 \cdot 10 - 2 \cdot 11 - 3 = 2 \quad (1)$$

where  $n$  - total number of mechanism links;  
 $p_1$  - number of single-moving links of the mechanism,  
 $p_2$  - number of two-moving links of the mechanism.

The number of mobility degrees corresponds to the number of engines (one for the stand drive, the other for the roll drive). This will provide the ability to adjust

the angular speed of the roll depending on the rolling route.

So, it is possible to formulate requirements for the drive of the rolls of cold pilger rolling mills. The drive mechanism must provide the required angle of rotation of the roll, and the angular speed must change

according to the law that ensures the maximum reduction of axial forces.

Using kinematic analysis, it is shown the change in the angle of rotation of the rolls depending on the time of rotation of the crank of the working stand drive (Fig. 4).

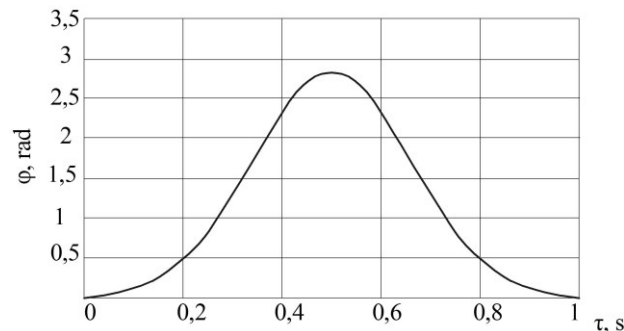


Fig. 4. Change in the angle of rotation of the roll depending on the time of rotation of the crank drive of the working stand

The simulation shows that the nature of the change in torque on the electric motor shaft corresponds to the change in torque on the roll.

It is also important that the direction of rotation of the rotor of the gear drive motor 10 does not change when the direction of movement of the working cage changes. This has a positive effect on the efficiency of the mechanism.

### Conclusions

1. A roller drive mechanism with a planetary gearbox has been developed. Based on the structural analysis of the mechanisms, it was shown that this

mechanism can work.

2. A separate roller drive mechanism with a planetary gearbox allows you to adjust the speed of rotation of the rollers regardless of the speed of the working stand. The parameters of this drive can be determined using kinematic analysis.

3. The roller drive mechanism with a planetary gearbox will provide adjustment of the angular speed of rotation of the rollers and reduce axial forces. This will allow you to obtain high-quality thin-walled pipes with the possibility of expanding the range of pipes produced by these mills.

### References

1. Kinitsky, Ya.T. (2002). *Theory of mechanisms and machines*. Publishing house "Naukova Dumka"
2. Titov, V. A., Shamarin, Yu. E., Dolmatov, A. I., Borysevich, V. K., Makovey, V. O., & Alekseenko V. M. (2010). *High-speed methods of metal processing by pressure*. KVITs
3. Semychev, A.V., Vyshinsky, V.T., Frolov, Ya.V., & Danchenko, V.M. (2007). Determination of axial forces acting in the deformation center during cold pilger rolling. *Bulletin of the Donbass State Machine-Building Academy*, (1(7)), 149-151
4. Semichev, A. V., Danchenko, V. M., Vyshinsky, V. T., & Frolov, Ya. V. (2009). Development of a rocker mechanism with adjustable rocker length. *Theory and practice of metallurgy*, (1-2), 122-124
5. Semychev, A. V., Vyshinsky, V. T., & Danchenko, V. M. (2010). Development of a gear-lever drive mechanism for rolls of cold pilger pipe rolling mills. *Bulletin of the Donbass State Machine-Building Academy*, (1(18)), 149-301

Отримано редколегією / Received by the editorial board: 08.11.2024  
Прийнято до друку / Accepted for publication: 20.02.2025

*Taran O.Yu., Ovcharuk A.M., Malyi E.D.*

## Research into the possibility of producing ferrosilicoaluminum from recycled materials

*Таран О.Ю., Овчарук А.М., Малий Є.Д.*

## Дослідження можливості виробництва феросилікоалюмінію з вторинної сировини

**Abstract.** The technology of electrothermal production of ferrosilicoaluminum using recyclable material from abrasive production has been developed, studied and tested in laboratory and semi-industrial conditions. The following were used as burden components: "old charge" from silicon carbide production, sludge from abrasive electrocorundum and silicon carbide, magnetic fraction from electrocorundum production and gas coal. As a result, an alloy containing 61–69% Al+Si was obtained.

**Key words:** ferrosilicoaluminum, recycled materials, recycling, electrothermal production, abrasive production.

**Аноатація.** Розроблено, досліджено та випробувано в лабораторних і напівпромислових умовах технологію електротермічного виробництва феросилікоалюмінію з використанням вторинної сировини абразивного виробництва. Як шихтові компоненти використовувалися: "стара шихта" з виробництва карбіду кремнію, шлами абразивного електрокорунду та карбіду кремнію, магнітна фракція з виробництва електрокорунду та газове вугілля. В результаті отримано сплав, що містить 61–69% Al+Si.

**Ключові слова:** феросилікоалюміній, вторинна сировина, переробка, електротермічне виробництво, абразивне виробництво.

Being one of the most effective deoxidizers, aluminum is widely used in steelmaking for final metal deoxidation. [1] Aluminum is used in the form of ingots of pure or secondary metal. In the first case, the high cost of the deoxidizer significantly affects the cost of production, and in the second case, a considerable amount of non-ferrous metal impurities (Zn, Sn, Cu, Pb, As) gets into the steel, ultimately worsening its quality [2]. In addition, when added into steel, 70–90% of aluminum is oxidized under the influence of air and slag, and the amount that gets into the metal and performs its direct function is difficult to predict. Despite the disadvantages, it is not advisable to reject aluminum for a number of reasons, so research aimed at replacing primary and secondary aluminum with its alloys with other elements is becoming relevant. Performing steel finishing operations using complex deoxidizers allows reducing their consumption, improving the kinetics of deoxidation, reducing heat consumption for their dissolution, and improving the quality of the processed metal [3]. The most universal and promising in this regard may be a complex deoxidizer – ferrosilicoaluminum (FeSiAl).

Ferrosilicoaluminum can be produced in industrial quantities in two ways: by mixing and by joint reduction of aluminum and silicon oxides with carbon in ore-reducing furnaces [1]. Although the mixing method allows for the production of complex alloys of complex composition, it is not economically viable due to the

high loss of elements. In addition, the problem of using metallic aluminum remains.

In light of the above, the most promising appears to be the electrothermal technology for the production of complex aluminum and aluminum-silicon ferroalloys, developed and improved by the Department of Electrometallurgy of the Dnipro Metallurgical Institute over many years.

### Raw materials

Despite the obvious advantages, this technology is not well developed in Ukraine. The main reason for that is the lack of a reliable raw material base. In Kazakhstan, for instance, the production of FeSiAl is actively expanding [4] due to the use of high-ash coals from the Ekibastuz deposit, which are practically a ready-made mono-charge for production of FeSiAl [5].

Studies of the domestic mineral resource base has shown that aluminosilicate rocks can be used as the ore part of the burden charge for the electrothermal production of ferrosilicon aluminum: bauxites, clays, primary and secondary kaolins, kyanites, sillimanites, etc. The existing deposits of these types of raw materials [6] are either not developed or are used for the production of electrolytic aluminum, electrocorundum, refractories, ceramics, etc.

The most promising natural raw material for smelting FeAl and FeSiAl in Ukraine is bauxite. The largest deposit in Ukraine is Vysokopolske, represented by gibbsite bauxites (33–45% Al<sub>2</sub>O<sub>3</sub>, 5–9% SiO<sub>2</sub>, 26–32%



Fe<sub>2</sub>O<sub>3</sub>, 1.9–2.3% TiO<sub>2</sub>, 0.1–0.18 CaO), explored reserves are 19 million tons. [7] Vysokopolske bauxite has low content of Al<sub>2</sub>O<sub>3</sub>, low silicon and calcium modules, so domestic producers do not use it directly for obtaining alumina, especially when there is an opportunity to purchase high-quality ores abroad. At the same time, there are no restrictions on the use of this raw material for the production of complex ferroalloys. At the same time, studies were conducted on the possibility of production ferrosilicoaluminum from pre-

Al <sub>2</sub> O <sub>3</sub>	SiO <sub>2</sub>	Fe <sub>2</sub> O <sub>3</sub>	TiO <sub>2</sub>	C	K <sub>2</sub> O	Na <sub>2</sub> O	CaO
32–37	15–20	8–10	1–2	40–42	3–4	1–1,5	0,15–0,30

Dust particle size is less than 160 мкм.

During the processing melted abrasive electrocorundum into grinding materials after a whole complex of technological operations (crushing, wet grinding, dehydration, drying) it undergoes primary magnetic enrichment. The magnetic material removed from the technological scheme is represented by a

agglomerated Vysokopolski bauxite [8], but this technology did not receive further development in our country.

To solve the problem of raw material shortage, the possibility of using man-made secondary materials from abrasive production containing compounds of aluminum, silicon and carbon was considered.

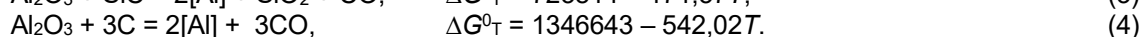
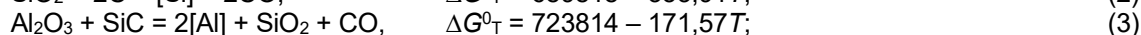
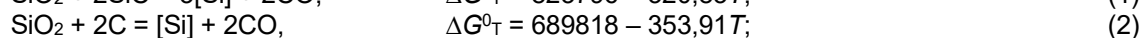
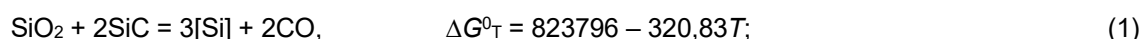
During production of abrasive electrocorundum, electrofilters and a mechanical cleaning system capture dust of following chemical composition, %:

conglomerate consisting of associated low-silicon ferrosilicon and abrasive electrocorundum. The content of each material depends on the technology conditions, the selected crushing scheme and can vary significantly: the content of corundum, for example, can vary from 50 to 70%. The most probable composition of the magnetic material is presented in Table 1.

Table 1. Fractional and chemical composition of magnetic material of electrocorundum production.

Size, mcm/%										
1250	1000	800	630	500	400	315	250	200	160	–160
12,2	8,0	12,5	9,0	12,0	7,0	9,0	7,0	6,1	7,4	9,8
Composition, %mac.										
Al <sub>2</sub> O <sub>3</sub>	SiO <sub>2</sub>	Fe <sub>2</sub> O <sub>3</sub>	TiO <sub>2</sub>	Al	Ti	Si	Fe	C		
51,4	0,6	0,5	3,1	0,4	0,6	5,1	34,9	0,7		

In the production of silicon carbide grinding materials, wet grinding of the original piece in ball mills produces sludge containing at least 80% SiC, about 5% free carbon, up to 14% SiO<sub>2</sub> and 2–3% Fe. In the same production, the so-called "old charge" that is regularly removed from the process flow chart, containing up to 20% SiC, about 50% SiO<sub>2</sub>, more than 25% C and 3–4% Fe<sub>2</sub>O<sub>3</sub>, 1.5–2.0% Al<sub>2</sub>O<sub>3</sub>, up to 1% CaO, which are harmful to abrasive production. In winter, the sludge generated during the production of grinding materials from abrasive electrocorundum and silicon carbide is mixed during transportation to filter treatment facilities and has the following composition: 50–58% Al<sub>2</sub>O<sub>3</sub>, 4–5% Fe<sub>2</sub>O<sub>3</sub>, 20–25% SiO<sub>2</sub>, 5–6% SiC, 5–6% C.



The reactions proceed with the absorption of heat, and the specific heat consumption per unit of silicon and aluminum is:

	1	2	3	4
kJ/mole Si(Al)	274,6	689,8	361,9	673,3
MJ/kg Si(Al)	9,81	24,64	13,40	24,94

As can be seen from the calculations, in the case of using SiC as a reducing agent instead of carbon, a reduction in heat consumption is expected for reducing silicon by 2.5 times, and aluminum by 1.8 times. Thus, using silicon carbide as a reducing agent can significantly reduce energy consumption for smelting ferrosilicon aluminum. Metallurgical silicon carbide itself is a very valuable and expensive material, which once again indicates the feasibility of its use in the

composition of technogenic raw materials for abrasive production, which in its current form is not used in industry.

**Experimental production of FeSiAl.** In order to develop a rational technology for producing FeSiAl, experimental production was carried out in a Tamman furnace using various combinations of burden materials. The characteristics of the initial raw materials are given in Table 2. The burden charge under study was



heated at the same rate, while the temperature and mass of the burden charge were recorded. Each composition was heated to 1800°C. Based on the lost

mass, the degree of reduction of a particular burden charge was calculated. The results of the experimental smelting are given in Table 3.

Table 2. Chemical composition of burden materials for the production of FeSiAl.

Material	Composition, %									
	Al <sub>2</sub> O <sub>3</sub>	SiO <sub>2</sub>	Fe <sub>2</sub> O <sub>3</sub>	TiO <sub>2</sub>	CaO	Si	Fe	SiC	C	ППП
Bauxite	38,4	4,7	32,4	3,5	–	–	–	–	–	21
Quartzite	0,52	97,5	0,63	–	0,9	–	–	–	–	–
Anthracite	1,329	2,528	0,475	–	0,147	–	–	–	95	–
Sludge from the abrasive production	56,82	1,9	4,4	1,57	–	–	–	25,51	8,4	–
SiC "old charge"	2,7	50,57	2,6	–	–	–	0,03	21,4	22	–
Electrocorundum magnetic fraction	54,1	0,6	0,5	3,1	–	5,1	34,9	–	0,7	–

Table 3. Experimental results.

Indicator	Charge		
	1	2	3
Charge composition, %			
Bauxite	44,3	–	47,75
Quartzite	36,25	–	–
Anthracite	19,45	–	2,55
Sludge	–	10	–
SiC "old charge"	–	55	49,7
magnetic fraction	–	35	–
Duration, min	25	28	27
Mass of the metal (calculated), g	13,35	20,53	16,55
Mass of the metal (real), g	9,31	19,57	13,49
Metal reduction degree, %	69,74	95,32	81,51
Metal composition, %:			
Al	14,97	17,12	12,13
Si	28,65	45,97	42,47
Ti	1,07	1,18	0,83
Al+Si	43,62	63,09	54,6

The degree of reduction of burden containing secondary materials turned out to be significantly higher, which is due to the presence of both already reduced metallic phases and a complex reducing agent – silicon carbide. This raw material is of considerable interest and is currently widely used in metallurgical and foundry production. The study of the physicochemical and metallurgical properties of silicon carbide materials as reducing agents, especially in electrometallurgy of ferroalloys, is an urgent task for increasing the efficiency of production.

#### Experimental studies of FeSiAl production using silicon carbide as a reducing agent

The alloy was produced in a laboratory electric furnace with a capacity of 250 kVA and electrodes with a

diameter of 100 mm. The furnace bath had a diameter of 450 mm and a depth of 240 mm. The production was carried out at a voltage level of 49 V and a current of 1–2 kA. 37 experiments were completed and, in total, 399 kg of alloy were produced for the series. The FeSiAl production process was assessed based on 10 experiments (No. 10–19), during which there were minimal violations of the process mode. Based on the results of these experiments, the furnace productivity, specific energy consumption and other process indicators were calculated. The results of the experiments are presented in Table 5.

During the entire series of experiments, no adjustment of the charge was made. 50 kg of briquetted charge was loaded into the furnace, and the process duration, on average, did not exceed two hours.

Table 5. Experiments performance.

№	Duration, hours	Charge, kg	Metal mass, kg	Energy of attempt, kW·h	Energy per ton, kW·h/t	Productivity, kg/h
10	1,58	50	11,0	64	5818	6,96
11	1,33	50	10,5	56	5333	7,89
12	1,48	50	7,2	52	7222	4,86
13	1,70	50	6,3	56	8889	3,71
14	2,08	50	16,5	83,2	5042	7,93
15	2,08	50	10,5	67,2	6400	5,05
16	1,92	50	15,0	65,6	4373	7,81
17	1,92	50	14,0	68,8	4914	7,29
18	2,00	50	12,1	72	5950	6,05
19	2,13	50	15,0	84	5600	7,04
Average	1,82	50	11,81	66,9	5954	6,49

With a constant amount of the charge loaded for the experiment, there was a deviation of the average hourly power consumption from the average value for the company (from 32.3 to 40.5 kW·h, with an average value of 36.82 kW·h). Such furnace operation also affected other indicators: the furnace productivity fluctuated from 3.71 kg/h to 7.93 kg/h, the specific power consumption from 4914 to 8889 kW·h/t. For the same reason, the chemical composition of the products fluctuated: the aluminum content changed from 7.92 to 15.14, and silicon from 58.77 to 51.42% (Table 6). At the same time, the sum of aluminum and silicon in the

alloy fluctuated insignificantly. The indicated instability of the average hourly power output is caused mainly by the design feature of the furnace unit: different distances between the electrodes, imperfections of the taphole unit (due to which the taphole opening time was unjustifiably increased), weak contact of the graphite electrode in the electrode holder, led to electrode slippage and forced downtime.

The process was almost slag-free, the aluminum and silicon content were very close to the calculated ones. In some experiments, the aluminum extraction was 79.5%, and silicon 71%.

Table 6. Chemical composition of products.

№	Al	Si	Fe	Ca	C	P	S	Al+Si
10	11,97	53,13	34,31	0,21	0,34	0,044	0,026	65,10
11	13,69	55,24	30,27	0,41	0,35	0,044	0,004	68,93
12	12,03	56,97	30,42	0,21	0,33	0,032	0,003	69,00
13	10,82	58,03	30,71	0,21	0,19	0,027	0,002	68,85
14	7,92	58,77	32,77	0,21	0,25	0,046	0,016	66,69
15	10,03	56,72	32,62	0,11	0,38	0,039	0,102	66,75
16	10,67	50,09	38,63	0,11	0,40	0,035	0,037	60,76
17	10,38	51,48	37,67	0,11	0,29	0,034	0,038	61,86
18	9,16	54,27	36,47	0,06	0,04	0,018	0,003	63,43
19	15,14	51,42	32,71	0,11	0,58	0,008	0,031	66,56

The consumption of briquettes was 4234 kg per ton of alloy, including silicon carbide “old charge” – 2530 kg, abrasive electrocorundum and silicon carbide sludge – 616 kg, magnetic material – 873 kg, gas coal – 215 kg. Energy consumption was 10860 kWh/t.

### Conclusion

The technology of ferrosilicoaluminum production with use of secondary materials from abrasive production has been developed, studied and tested in laboratory and semi-industrial conditions (more than 67 hours of continuous operation of the electric furnace). As a result, the pilot company carried out 37 smeltings and smelted 399 kg of alloy containing 61-69% Al + Si. The

possibility of recycling man-made raw materials that have not yet found application and producing a competitive and high-quality complex deoxidizer has been proven. This scheme, being resource-saving, allows solving issues related to the need for complex use of valuable and scarce mineral raw materials in the national economy and environmental protection. The presence of silicon carbide and metallic iron in the charge made it possible to significantly improve the conditions for the flow of reduction processes, which made it possible, in comparison with the current technological schemes, to reduce the specific energy consumption by 30%.

### References

1. Hasyk, M. Y., & Emlyn, B. Y. (1971). *Elektroplavka aliumosylykatov*. Metallurhyia
2. Kudryn, V. A. (1992). *Vnepechnaia obrabotka chuhuna y staly*. Metallurhyia
3. Kudryn, V. A. (1989). *Metallurhyia staly*. Metallurhyia
4. Tolymbekov, M. Zh. (2011). Perspektivi rasshyreniya proyzvodstva ferrosylykoaliumyniya v Kazakhstane. In. *IV Mezhdunarodnaia nauchno-tekhnicheskaya konferentsiya UkrFA “Kliuchevye voprosy razvytiya elektrometallurhicheskoi otrasly”*. Kyev, 2011 April 20-21. (pp. 42–48)
5. Druynskiy, M. Y., & Zhuchkov, V. Y. (1988). *Poluchenye kompleksnykh ferrosplavov yz myneralnoho siria Kazakhstana*. Nauka
6. Tretiakov, Yu. I., Martyniuk, V. I., Subotin, A. H. et al. (2007). *Mineralni resursy Ukrainy ta svitu na 01.01.2006 r.* Derzhavne naukovo-vyrobnyche pidpriemstvo “Heoinform Ukrainy”
7. Ovcharuk, A. N., Taran, A. Yu., Rudenko, V. K., & Hasyk, M. I. (2008). Kharakterystyka boksytov Visokopolskoho mestorozhdeniya y analiz tradytsionnykh sposobov eho obohashcheniya. *Metallurh. y hornorud. prom-st.* (6), 22–26
8. Emlyn, B. Y., Manko, V. A., Druynskiy, M. Y. et al. (1973). Vyplavka ferrosylykoaliumyniya yz ahlomeryrovannoho boksyt. *Metallurh. y hornorud. prom-st.* (10), 903–904

Отримано редколегією / Received by the editorial board: 26.12.2024  
 Прийнято до друку / Accepted for publication: 20.02.2025

## CONTENT

<b>Sukhyi K.M., Proidak Yu.S.</b> On the 100th Anniversary of the Department of Electrometallurgy	5
<b>Gasik M.M.</b> Microwave processing of materials in metallurgy	10
<b>Jiang ZhouHua , Yang Ce, Zhu HongChun, Lu HongBin</b> The-state-Art of steelmaking technology based on hydrogen metallurgy	16
<b>Gryshchenko S.G., Proidak Yu.S., Ponomarenko R.V., Kravchenko A.P., Kalenkov O.F., Kudriavtsev S.L.</b> Ukrainian steel and ferroalloys in 2022-2024: how russian aggression has impacted on the work of the country's metallurgical industry	31
<b>Karbowniczek M.</b> Some aspects in the electric arc steelmaking production	36
<b>Stovpchenko G.P., Medovar L.B.</b> Decarbonisation challenges for steelmaking and scrap recycling role	42
<b>Shevchenko D.V., Ovcharuk A.M., Gladkih V.A., Bezugliy A.V., Nikolenko A.V.</b> Research of the ore reducing furnaces electrical modes for ferronickel production	49
<b>Zaselskyi V.Y., Popolov D.V.</b> Laboratory studies on the effect of vibro-impact action of the screening surface on the main technological indicators of metallurgical raw material screening	61
<b>Proidak Yu.S., Gorobets A.P., Zhadanos O.V., Kamkina L.V., Yaroshenko Ya.O.</b> Physical and chemical audits and comparative analyses of scrap remelting technology indicators for high-alloyed steel with special purposes using the duplex-slag process and the resource-saving mono-slag process	67
<b>Shevchenko D.V., Ovcharuk A.M., Nadtochii A.A., Prikhodko S.V., Shutov V.Yu.</b> Research on the properties of ferronickel production slags and development of technological schemes for their enrichment	73
<b>Grishin O.M., Proidak Yu.S.</b> Regularities of solid-phase reduction of iron oxides under conditions of combined chemical-catalytic and energetic influence	81
<b>Akreiev V.V., Cherenkov D.V., Prykhodko S.V., Melnyk S.O., Ovcharuk A.M.</b> Improved heat-insulating products for ingot hot-tops in molds without extensions	89
<b>Ignatiev V.S., Holovachov A.M., Kolbin M.O., Yaroshenko Ya.O., Ovcharuk A.M.</b> Promising metal-thermal technologies for titanium production	98
<b>Starovoi A.G., Malyi Ye.I., Sorokin Ye.L., Starovoi M.A., Popova O.Yu.</b> Adjusting properties of electrode pitch with fractions of coal tar	103
<b>Danchenko V.M., Dobrov I.V., Semichev A.V.</b> Roll drive mechanism with planetary gearbox for cold pilger pipe rolling mills	107
<b>Taran O.Yu., Ovcharuk A.M., Malyi E.D.</b> Research into the possibility of producing ferrosilicoaluminum from recycled materials	110
CONTENT	114
ЗМІСТ	115

## ЗМІСТ

<b>Сухий К.М., Пройдак Ю.С.</b> До 100-річчя кафедри електрометалургії	5
<b>Гасик М.М.</b> Мікрохвильова обробка матеріалів у металургії	10
<b>Jiang ZhouHua , Yang Ce, Zhu HongChun, Lu HongBin</b> Сучасний стан технології виробництва сталі на основі водневої металургії	16
<b>Грищенко С.Г., Пройдак Ю.С., Пономаренко Р.В., Кравченко А.П., Каленков О.Ф., Кудрявцев С.Л.</b> Українська сталь та феросплави у 2022-2024 роках: як російська агресія вплинула на роботу металургійної промисловості країни	31
<b>Karbowniczek M.</b> Деякі аспекти у виробництві сталі в електродугових печах	36
<b>Стовпченко Г.П., Медовар Л.Б.</b> Проблеми декарбонізації металургії та роль переробки металобрухту	42
<b>Шевченко Д.В., Овчарук А.М., Гладких В.А., Безуглий А.В., Ніколенко А.В.</b> Дослідження електричних режимів рудовідновлювальних печей для виробництва феронікелю	49
<b>Заселський В.Й., Пополов Д.В.</b> Дослідження впливу віброударної дії просіювальної поверхні на основні технологічні показники грохочення металургійної сировини	61
<b>Пройдак Ю.С., Горобець А.П., Жаданос, О.В., Камкина Л.В., Ярошенко Я.О.</b> Фізико-хімічні аудити та порівняльні аналізи показників технології переплавки брухту високолегованої сталі спеціального призначення з використанням дуплекс-шлакового та ресурсозберігаючого моношлакового процесів	67
<b>Шевченко Д.В., Овчарук А.М., Надточій А.А., Пріходько С.В., Шутков В.Ю.</b> Дослідження властивостей шлаків феронікелевого виробництва та розробка технологічних схем їх збагачення	73
<b>Гришин О.М., Пройдак Ю.С.</b> Закономірності твердофазного відновлення оксидів заліза в умовах комбінованого хіміко-каталітичного та енергетичного впливу	81
<b>Акреєв В.В., Черенков Д.В., Приходько С.В., Мельник С.О., Овчарук А.М.</b> Поліпшені теплоізоляційні вироби для надлишкових частин виливниць без надставок	89
<b>Ігнат'єв В.С., Головачов А.М., Колбін М.О., Ярошенко Я.О., Овчарук А.М.</b> Перспективні металотермічні технології виробництва титану	98
<b>Старовойт А.Г., Малий Є.І., Сорокін Є.Л., Старовойт М.А., Попова О.Ю.</b> Регулювання властивостей електродного пеку фракціями кам'яновугільної смоли	103
<b>Данченко В.М., Добров І.В., Сьомічев А.В.</b> Механізм приводу валків з планетарним редуктором для трубопрокатних станів холодної пілігримової прокатки труб	107
<b>Таран О.Ю., Овчарук А.М., Малий Є.Д.</b> Дослідження можливості виробництва феросилікоаломінію з вторинної сировини	110
CONTENT	114
ЗМІСТ	115

## **ТЕОРІЯ І ПРАКТИКА МЕТАЛУРГІЇ**

науково-виробничий журнал

**Засновники:** Український державний університет науки і технологій  
Відділення матеріалознавства і металургії  
Академії інженерних наук України

**Видавець:** Український державний університет науки і технологій  
Головний редактор – проф. Проїдак Ю.С.  
Заст. головного редактора – д.т.н., проф. Камкіна Л.В.

Комп'ютерна верстка – Безшкурєнко О.Г.

### **Адреса і місцезнаходження видавця:**

Український державний університет науки і технологій,  
вул. Лазаряна, 2, м. Дніпро, 49010, Україна.

**Тел.:** +38-056-373-15-44, **Email:** office@ust.edu.ua

**Сайт наукового видання:** <https://tpm.ust.edu.ua/>

Підписано до друку 21.02.2025 року.  
Формат 60x84 1/8. Тираж 100 примірників.

---

## **THEORY AND PRACTICE OF METALLURGY**

Scientific and Production Journal

**Founders:** Ukrainian State University of Science and Technologies  
Department of Materials Science and Metallurgy  
of the Academy of Engineering Sciences of Ukraine

**Publisher:** Ukrainian State University of Science and Technologies  
Editor-in-Chief – Prof. Proidak Yu.S.  
Deputy Editor-in-Chief – Ph.D., prof. Kamkina L.V.

Page layout by O.H. Bezhkurenko

### **Publisher's address and location:**

Lazariana Str., 2, Dnipro, 49010, Ukraine

**Phone:** +38-056-373-15-44, **Email:** office@ust.edu.ua

**Journal website:** <https://tpm.ust.edu.ua/>

Signed for printing 21/02/2025.  
Format 60x84 1/8. Edition of 100 copies.